Development of Microparticulate Formulations for the Delivery of Therapeutic Antibodies to the Respiratory Tract

Thesis submitted in accordance with the requirements of the School of Pharmacy, University of London, for the degree of Doctor of Philosophy

Richard Simon Kaye

Centre for Drug Delivery Research
School of Pharmacy
University of London
29-39 Brunswick Square
London
WC1N 1AX

October 2007

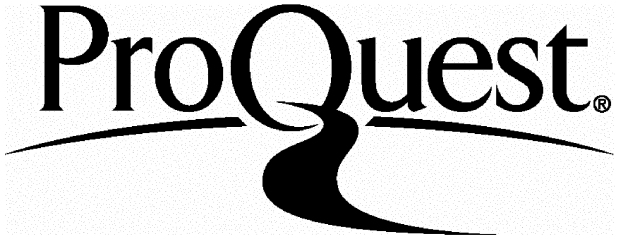

DECLARATION OF PLAGIARISM AND COPYRIGHT

This thesis describes research conducted in the School of Pharmacy, University of London between October 2004 and October 2007 under the supervision of Professor Oya Alpar (School of Pharmacy, University of London) and Dr Tarlochan Singh Purewal (Bespak PLC).

I certify that the research described is original and that any parts of the work that have been conducted by collaboration are clearly indicated. I also certify that I have written all the text herein and have clearly indicated by suitable citation any part of this dissertation that has already appeared in publication.

_____ _____

Signature Date

Copyright

1) Copyright in the text of this thesis rests with the Author. Copies (by any process) either in full, or of extracts, may be made only in accordance with instructions given by the Author and lodged in the School of Pharmacy Library, University of London. Details may be obtained from the librarian. This page must form part of any such copies made. Further copies (by any process) of copies made in accordance with such instructions may not be made without permission (in writing) of the Author.

2) The ownership of any intellectual property rights which may be described in this thesis is vested in the School of Pharmacy, University of London, subject to any prior agreement to the contrary, and may not be made available for use by third parties without written permission of the University, which will prescribe terms and conditions of any agreement.

ABSTRACT

Background

Antibodies are immune proteins that have been developed into therapeutic agents due to their highly specific targeting capabilities. The respiratory delivery of antibodies targeted against inhaled pathogens is desirable, since this would reduce the quantity and inconvenience of dosing that would be required by injection, given that antibodies are not orally bioavailable. Microparticulate formulations have been developed to encapsulate antibodies in order to achieve the stability, modified-release (MR) and the aerodynamic properties required for pulmonary and nasal delivery.

Method

Antibody (IgG)-loaded microparticles were manufactured by the spray-drying of a W/O/W double-emulsion, which contained the bio-compatible, poly(lactide-co-glycolide) (PLGA) as the MR polymer, and the lung delivery-approved excipients dipalmitoylphosphatidylcholine (DPPC) and lactose, for emulsion stability and thermal protection, respectively, having found that these excipients gave an improved encapsulation efficiency (EE) and reduced initial burst-release compared to poly(vinyl alcohol). This IgG formulation was optimised by factorial experimental design, primarily in terms of yield, encapsulation efficiency and initial burst-release. The optimised microparticulate IgG formulation was characterised in terms of particle diameter and morphology by laser diffraction, photon correlation spectroscopy, and both scanning and transmission electron microscopy. The antibody release profile was measured in both pH 7.4 and pH 2.5 release media, comparing various types of PLGA polymers. The released antibody stability was investigated by gel electrophoresis, enzyme-linked immunosorbent assay and field-flow fractionation. The 3-(4,5-dimethyl-thiazol-2-yl)-2,5-diphenyl-tetrazolium bromide (MTT) assay was performed with an *in vitro* epithelial cell line to assess any potential toxicity of the formulation. The powder dispersibility, aerodynamic diameter (MMAD) and fine particle fraction (FPF) of the IgG formulation, with or without 1% m/m additions of leucine and magnesium stearate, were measured by laser diffraction with a 'RODOS' dry-powder feeder, and using an 'Andersen' cascade impactor (ACI), using an Aerolizer® dry-powder inhaler. An intraperitoneal *in vivo* model was used to assess the efficacy of formulated therapeutic F1+V antibodies for the potential treatment of *Yersinia pestis* (plague). Separately, a spray-dried, water-soluble IgG formulation was developed for nasal delivery, using sugars, albumin and sodium chloride as excipients. This formulation, and variations of it containing leucine, Aerosil® and magnesium stearate, were evaluated in terms of nasal deposition by actuating from Uni-Dose DP™ devices into a nasal cast model.

Results

The 'dry' particle median diameter (D50%) of the pulmonary formulation, as measured in cyclohexane, was ~4 μm, and the particles were spherical. However, when measured in water, the lactose component dissolved, producing nanoparticles (~400 nm), which were anticipated to be small enough to avoid phagocytosis within alveoli. The IgG encapsulation efficiency (using a theoretical loading of 3.5% m/m) was close to 100%, with ~30% immediate burst-release. After 35 days ~90% cumulative IgG was achieved using pH 2.5 release media. The IgG released after 2 h was found to be stable in terms of molecular weight and biological activity. The formulation did not affect the viability of *in vitro* epithelial cells, relative to positive and negative controls. The MMAD calculated from the ACI deposition data was ~3-4 μm. The addition of leucine and magnesium stearate to the formulation was found to increase powder dispersibility. Use of these excipients achieved FPFs of up to ~60%. The therapeutic F1+V antibodies were successfully incorporated into the formulation, although, in preliminary *in vivo* studies, the formulated antibody was found not to confer protection against infection. The best of the nasal formulations achieved ~45% dose deposition beyond the nasal vestibule of the cast model.

LIST OF PUBLICATIONS

Sep 2005 "Development of Biocompatible Formulations for the Airway Delivery of Immunoglobulins". Poster presentation and abstract at UK Polymer Showcase, Wakefield.

Dec 2005 Above title and "The Effect of Manufacturing Parameters on the Properties of a Biocompatible Formulation for the Airway Delivery of Immunoglobulins". Poster presentation and extended abstracts at Drug Delivery to the Lungs XVI, Aerosol Society, Edinburgh. Abstract summaries published in the *Journal of Aerosol Medicine* (2006) **19**(2): 221-241.

Mar 2006 "Development of and Optimisation of Biocompatible Formulations for the Airway Delivery of IgG". Podium presentation at 6th European Workshop on Particulate Systems, Geneva.

Sep 2006 "Optimisation and Characterisation of Biocompatible, Microparticulate, Modified-Release Formulations, for the Pulmonary Delivery of Immunoglobulins". Podium and poster presentation at The British Pharmaceutical Conference, Manchester. Abstract published in the *Journal of Pharmacy and Pharmocology* (2006) **58**(S1): A62.

Dec 2006 "Development and Testing of Formulations for the Nasal Delivery of Antibodies". Podium and Poster presentation, and extended abstract at Drug Delivery to the Lungs XVII, Aerosol Society, Edinburgh. Abstract summaries to be published in the *Journal of Aerosol Medicine.*

Jul 2007 "Modified-Release of IgG from Poly(lactide-co-glycolide) Microparticles for Pulmonary Delivery: Comparison of Uncapped and Capped Polymers"/ Poster presented at the annual Controlled Release Society conference, Long Beach, USA.

ACKNOWLEDGEMENTS

I would like to thank my supervisor Professor Oya Alpar for providing me with the opportunity to undertake a doctoral research project in such an interesting field of pharmaceutical science, and for giving me free reign to take the project in my own direction. I would also like to thank Dr Tol Purewal, my supervisor at Bespak, for his keen interest in my work, and his industrial perspective.

I gratefully acknowledge the School of Pharmacy, Bespak and the EPRSC for funding this project, and The Polymer Innovation Network (formerly Faraday Plastics) for arranging this collaboration.

I wish to thank Diane Williamson, Nicky Walker and other staff of the Defence Science and Technology Laboratory (DSTL), Porton Down, for the *in vivo* work, Dave McCarthy and Kate Keen, of the School of Pharmacy for the electron microscopy, and Andy Smith of Sympatec, UK for his help with the RODOS/HELOS work.

Thanks also to Phil, Colin, Dave, Helen, Amy, James and other staff at Bespak, Milton Keynes, who gave up their time and lab space to assist me with my project.

Thank you to members of Lab 341 and the Pharmaceutics Department, past and present, especially: Amr, Claire, Erdal, Helena, Hisham, Jag, Manny, Mike, Pandit, Pei Li, Sally, Soma, Stefan, Sterghios, Xiong-Wei, and particularly to those that trained me on various techniques. A special mention must go to John Frost whose skills with a tool box have saved me weeks of repair time, and probably the Department thousands of pounds.

I would also like to thank my family for their love and support in all of my endeavours. I wish to particularly recognise my father, Dr Clive Kaye, whose passion for science inspired me to follow in his footsteps, and whose common-sense, principled approach, made him a frequent sounding-board for ideas throughout this project.

Finally, thank you to my fiancée Racheli for her devotion and unrelenting faith in me.

TABLE OF CONTENTS

LIST OF FIGURES

LIST OF TABLES

LIST OF ABBREVIATIONS

%	percent
°C	degrees Celsius (centigrade)
µg	microgram(s)
µL	microlitre(s)
µL	microlitre(s)
µM	micromolar
µm	micron(s)
A	adaptor
Å	Angstrom
ACI	'Andersen' cascade impactor
ACT	actuator
Adj	adjusted
ANOVA	analysis of variance
BALT	bronchas-associated lymphoid tissue
BCA	bicinchoninic acid
BDP	beclometasone diproprionate
BSA	bovine serum albumin
c.f.	compared with
CFC	chlorofluoroalkane
CFU	colony forming units
C_H	constant region on the heavy chain
CHO	Chinese hamster ovary
C_L	constant region on the light chain
cm	centimetre(s)
Coef	coefficient
COPD	chronic obstructive pulmonary disease
Cu	copper
D	remaining in device
D10%	diameter that 10% of the measured population volume is smaller than
D50%	median volume diameter
D90%	diameter that 90% of the measured population volume is smaller than
D_a	aerodynamic diameter
Da	dalton(s)
dAb™	domain antibody
DCM	dichloromethane
DF	degrees of freedom
DLVO	Derjaguin - Landau - Verwey – Overbeek (theory)
DMSO	dimethylsulphoxide
DNA	deoxyribonucleic acid
DP	dry powder
DPI	dry powder inhaler

DPPC	dipalmitoylphosphatidylcholine
DSC	differential scanning calorimetry
EDTA	ethylenediamine tetraacetic acid
EE	encapsulation efficiency
e.g.	for example
ELISA	enzyme-linked immunosorbent assay
et al.	and others
F	filter
Fab	antigen binding fragment of antibody
Fc	constant (crystallisable) fragment of antibody
FDA	Food and Drug Administration
FFF	field-flow fractionation
FPF	fine particle fraction
FT	front turbinates
Fv	antibody variable region
g	gram(s)
GRAS	generally regarded as safe
h	hour(s)
H_2SO_4	sulphuric acid
HCl	hydrochloric acid
HELOS	Helium Neon Laser Optical System
HFA	hydrofluoroalkane
HPLC	high performance liquid chromatography
HPMC	hydroxypropylmethylcellulose (hypromellose)
Hz	Hertz
i.e.	that is
Ig	immunoglobulin
i.m.	intramuscular
Inc	incoporated
i.p.	intraperitoneal
IVIVC	*in vitro-in vivo* correlation
kcps	kilocounts per second
kDa	kilodalton(s)
kV	kilovolt(s)
L	litre(s)
Ltd	limited
lys	lysine
m	metre(s)
M	molar
m/m	mass per mass
m/v	mass per volume
mag	magnification
MDI	metered dose inhaler

MDRI	P-glycoprotein efflux transporter gene
Mg	magnesium
mg	milligram(s)
$MgCO_3$	magnesium carbonate
min	minute(s)
mL	millilitre(s)
mM	millimolar
mm	millimeter(s)
MMAD	mass median aerodynamic diameter
mol	mole(s)
MR	modified-release
MTT	[3-(4,5-dimethylthiazol-2-yl)-2,5-diphenyltetrazolium bromide]
mV	millivolt(s)
mW	milliwatt(s)
MW	molecular weight
Na_2CO_3	sodium carbonate
NaCl	sodium chloride
$NaHCO_3$	sodium bicarbonate
NALT	nasal-associated lymphoid tissue
NaOH	sodium hydroxide
ng	nanogram(s)
nm	nanometre(s)
NP	nasal pharynx
NV	nasal vestibule
O/W	oil-in-water
O/W/O/W	oil-in-water-in-oil-in-water
OPD	o-phenylenediamine substrate
OR	olfactory region
P	preseparator
p	probability
PAGE	poly(acrylamide) gel electrophoresis
param	parameter
PBS	phosphate buffered saline
PCS	photon correlation spectroscopy
PEG	poly(ethylene glycol)
PEI	poly(ether imide)
per se	by itself
PGA	poly(glycolic acid)
pH	power of hydrogen
PhD	doctor of philosophy
PLA	poly(lactic acid)
PLGA	poly(lactide-co-glycolide)
PLLA	poly(L-lactic acid)

pMDI	pressurised metered dose inhaler
PVA	poly(vinyl alcohol)
r	recombinant
R^2	correlation coefficient
RI	refractive index
RNA	ribonucleic acid
RODOS	dry powder air-dispersion system
RPM	revolutions per minute
RT	rear turbinates
s	second(s)
S/O/W	solid-in-oil-in-water
s.c.	subcutaneous
SD	standard deviation
SDLM	spray-dried lipid microspheres
SDS	sodium dodecyl sulphate
SEM	scanning electron micrograph/microscopy
T	throat
TEM	transmission electron micrograph/microscopy
TEMED	N,N,N',N'-tetramethylethylenediamine
TF	throat filter
T_g	glass transition temperature
TGA	thermo-gravimetric analysis
TGS	Tris + glycine + sodium dodecyl sulphate (buffer)
TTD	time to death
U	protein unaccounted for
UK	United Kingdom
USA	United States of America
USP	United States Pharmacopoeia
UV	ultraviolet
V	volt(s)
v/v	volume per volume
V_H	variable region on the heavy chain
V_L	variable region on the light chain
Vs	versus
W/O	water in-oil
W/O/W	water in-oil-in water
WHO	World Health Organization
XRPD	x-ray powder diffraction
Y. pestis	*Yersinia pestis*
$Zn(OH)_2$	zinc hydroxide
$ZnCO_3$	zinc carbonate
ρ	density

1 GENERAL INTRODUCTION

1.1 Introduction

Since the beginning of civilisation, the airways have been exploited for the administration of pharmacologically active compounds for both recreational purposes, and as primitive treatments for disease. The earliest form of such treatments were volatile compounds added to boiling water for steam inhalation (Fiel, 2001), and the breathing in of smoke fumes from burning aromatic plants, such as *Atropa belladonna*, which was used for cough suppression (Gonda, 2000). While many of these were for the intention of treating respiratory diseases, the airways were also recognised as a means of administering medicine for systemic conditions. For example, in the Middle Ages, immunity to the bubonic plague was believed to be conferred by inhalation of sulfurous fumes (Newman, 1997). Throughout the same scale of history, the nasal cavity has also been recognised as a site of drug administration, with the systemic effects of psychotropic and hallucinogenic drugs being attained quickly by the snorting of powder preparations (Illum and Fisher, 1997).

In the more recent history of medicine, the pulmonary route has been used to deliver systemic gaseous anaesthetics, and the nasal route for the delivery of toxins for immunisation. However, for most of the last half-century, therapeutic developments in the field of pulmonary and nasal drug delivery have mainly been topical treatments for respiratory diseases. Such treatments were recognised as a basic form of targeted drug delivery to the site of action. The advantage of such topical treatments was the achievement of a rapid onset of action with relatively small drug doses, thus minimising systemic side-effects and toxicities. This form of therapy really became established with the invention of portable inhaler devices in the 1950s, allowing convenient self-medication by patients for diseases such as asthma and chronic obstructive pulmonary disease (COPD). However, it is only in the last 10-20 years or so that these routes of delivery have been once again considered as a means of delivering novel treatments for respiratory conditions, and new systemic therapies.

This revival of investigation of the pulmonary and nasal routes has coincided with the exponential rate of progress in biotechnology. Projects, such as the mapping of the human genome, have led to the identification of numerous new therapeutic targets. This has been coupled with the ability to exploit cell cultures as factories for the biosynthesis of macromolecular drugs, such as peptides, proteins and polynucleotides, which can selectively modulate these new targets. However, despite all of this progress, and the

media hype of the "biotech revolution", relatively few of these biotherapeutics have actually reached the market place. This has led to a growing concern among some groups of the scientific community, who are beginning to doubt if biotechnology will be able to provide any substantial improvement to current healthcare (Nightingale and Martin, 2004). In many cases, these new therapies fail because their promising activity shown in laboratory studies cannot be effectively transferred to humans. This is often due to inadequate delivery of the macromolecular drug to its site of action.

Whilst it is unquestionable that the most patient-acceptable drug delivery route is *via* oral ingestion, for macromolecular drugs this has proved not to be viable in most cases. This is primarily because of high levels of proteolytic enzymes secreted by the gastro-intestinal epithelium. Protease enzymes are designed to efficiently catalyse the degradation of potentially harmful, ingested foreign peptides and proteins, into their constituent amino acids, which are then used by the body. In addition, biological macromolecules are hydrophilic, charged molecules, of high molecular weight. Therefore, even if they had the ability to avoid degradation, passive absorption rates would be extremely slow, since the gastro-intestinal epithelium is most permeable to small, unionised, lipophilic molecules. It seems to be uncommon for macromolecules to be substrates for specific, transmembrane, transporter proteins, whilst such transporters can be involved in the absorption of lower molecular weight compounds. (However, the majority of epithelial transporters are efflux transporters, limiting rather than assisting absorption). In addition to this pre-hepatic hurdle, all compounds that are absorbed into the blood, from the intestine, pass into the hepatic portal vein, which channels them directly to the liver - the body's organ with the highest capacity for the metabolism of exogenous chemicals. This 'first-pass' extraction invariably results in negligible systemic availability of orally administered macromolecules.

As a result of this very effective pre-systemic exclusion of orally administered peptides, proteins and polynucleotides, the majority of macromolecular drugs used clinically today are given subcutaneously or by intravenous injections or infusions. Due to the relatively short elimination half-life of macromolecular drugs in general, parenteral injections are often required to be repeated frequently for optimal efficiency, and even continuous infusions have needed to be employed in some cases. Being large molecules, extravasation from the systemic circulation is usually limited. Thus, when given by these routes, drugs for treating respiratory disease can often only achieve low concentrations in pulmonary tissue, despite high systemic exposure (Gupta and Adjei, 1997). As well as the obvious invasive nature of using these parenteral routes, which

are not favoured by patients, such therapy is a burden to healthcare staff, who have to train patients on how to self-dose by these routes, or be required to administer these injectable preparations to patients. Even in the case of subcutaneous insulin preparations, which with the advent of disposable pens are relatively easy to use, patients still require extensive training. Absorption from subcutaneous sites is usually slow, and in the case of insulin does not achieve a physiological profile (Patton *et al.*, 1999). Also, local irritation can be a problem with subcutaneous injections. These disadvantages of injectable preparations are a particular caveat to the scenario of an acute situation, where a patient may need to be administered a treatment rapidly and/or with a rapid onset of action, outside of a hospital setting, either by themselves or by a non-healthcare professional. This is especially difficult if the therapy is prophylactic, and thus the patient is often quite healthy, and may be extremely reluctant or even unwilling to receive invasive therapy, particularly on a regular basis.

In light of these problems, alternative routes for the administration of macromolecules have been sought. The nasal and pulmonary routes are being extensively researched as a means by which macromolecular drugs could be effectively delivered. For respiratory conditions the advantages are obvious: non-invasive, topical application of the drug, reducing systemic effects. This has proved to be the case with dornase-alpha (Pulmozyme®, Roche) and insulin (Exubera®), the only currently licensed pulmonary formulations of a macromolecular drug. For the treatment of lung diseases using the pulmonary route of administration, molecules can be selected which are very rapidly metabolised in the liver to pharmacologically inactive compounds, and so result in the virtual absence of unwanted side-effects that would arise from notable systemic exposure. On the other hand, lung formulations are now seriously being considered as candidates for the systemic delivery of macromolecules. The lungs have several advantages for this application, including a large surface area for absorption (~75 m^2, for an average adult), and high perfusion by a vascular bed that is in extremely close proximity to the absorption surface. Also, there is a reduced expression of locally secreted proteases, and avoidance of first-pass metabolism (Qui *et al.*, 1997). Efflux transporters, such as P-glycoprotein (MDRI) are present, though, primarily in the alveolar and nasal membranes.

The nasal route has already provided success stories for the effective systemic delivery of macromolecules. There are licensed nasal formulations of desmopressin, calcitonin and buserelin. The nasal cavity offers an easily accessible route to a relatively leaky mucosa, served by a rich blood supply. The nasal cavity also has a tortuous anatomy

that assists the retention of inhaled particles (Illum and Fisher, 1997). As mentioned previously, it is an obvious requirement that nasal formulations are not locally irritant.

In an era where the discovery of new biological targets, and availability of potential drugs to modulate those targets, have become relatively more straightforward, if not semi-automatic, it is now the formulation that is a key factor in determining whether or not a new active compound will be able to reach the clinic as a medicine. In the case of inhaled therapies, the formulator must ensure that for local therapies, the drug is distributed, released and retained effectively, whilst for systemic therapies, the drug reaches absorption sites, and is absorbed effectively in order to achieve adequate systemic concentrations. In both cases, the drug is required to remain stable and active within a suitable delivery device that is able to function accurately at intermittent intervals, time and time again.

1.2 Anatomy and Physiology of the Airways

1.2.1 Structure of the nasal cavity

Being the primary route by which inspired air enters the body, the main functions of the nasal cavity are to clean, warm and humidify the outside air, in preparation for reaching the sensitive tissues of the lung (Hinchcliffe and Illum, 1999). For example, dry inhaled air, at 0°C, is raised to 31°C and 98% humidity during its passage through the nose (Illum and Fisher, 1997). The gross anatomy of the cavity, which is ~12 cm in length, has a volume of ~15 ml, and a total surface area of ~150 cm^2, is depicted in Figure 1.1. The nasal cavity extends from nostrils to the nasal pharynx, and each side of the cavity (separated by the septum) can be considered as three regions, namely, the vestibule, the olfactory region, and the respiratory region. The vestibule is located just inside the nostrils, which then open up into the main chambers, where olfactory tissue lines the cavity roof and wall (Illum and Fisher, 1997). The internal osteum, a length of cartilage at the junction of the vestibular and respiratory regions, causes a 90° bend in the air stream, and causes turbulence that reduces air velocity and causes the impaction of larger particles (Hinchcliffe and Illum, 1999). The respiratory region comprises most of cavity volume and surface area, and contains the three turbinates. The turbinates, which have a rich blood supply, form narrow air channels with a large surface area, and provide the site for air conditioning, and further particle entrapment (Illum and Fisher, 1997). A region of the nasal cavity contains olfactory neurones which connect directly to the central-nervous system (CNS) (Illum, 2003).

Figure 1.1.1 Structure of the nasal cavity. The three red shaded areas represent the turbinates, and the green shaded areas represent the sinuses. Adapted from Illum and Fisher, 1997.

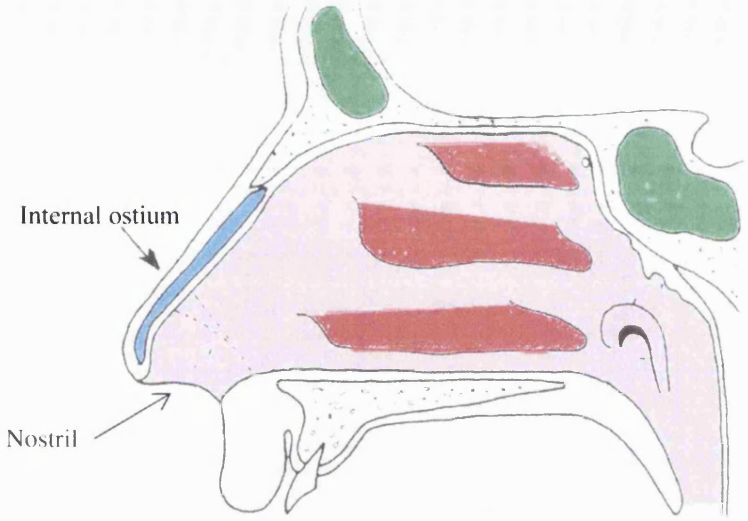

1.2.2 Structure of the lungs

The lungs have evolved to an ideal design for performing their primary function of mediating the rapid exchange of oxygen and carbon dioxide between the body, and the outside world: a huge surface, but compacted into a small space, in uniquely close contact with the blood. While facilitating this intimate contact, the lungs are replete with numerous defence mechanisms to ensure that only the required substances pass through to the blood stream.

The structure of each lung has often been compared to a branching tree. This analogy is most intricately depicted by Patton (1996), who compared the thick-barked branches of the tree, with the thicker walled branching tubes of the upper airway, and the thin, high-surface area leaves, connected to the ends of the finest branches, to the thin-walled alveoli, located where the smallest air tubes terminate. Both the leaves of a tree, and the alveolar sacs of the lung, are the principal sites of gas exchange.

Indeed, physiologically, there are two distinct regions of the airways. The conducting, or central, airways consist of the trachea, bronchi, bronchioles and terminal bronchioles. These vessels branch sequentially and dichotomously, with each airway generation having a reduced diameter, and an increased surface area. Weibel first proposed this model, and an adapted version is illustrated in Figure 1.2. The conducting airways are not involved in gas exchange, but rather provide gas buffering and humidification of inspired air, as it is transported towards the alveoli. This buffering capacity is attributed to the dead space volume of air, not involved in gas exchange, which resides in the conducting airways (Hickey and Thompson, 1992). The repeatedly bifurcating

structure creates a tortuous pathway, inducing turbulence, thereby reducing air velocity. This has the effect of not only increasing gas exchange efficiency, but also allows these airways to act as a particle filter (Kim and Folinsbee, 1997). The conducting airways are supplied with oxygenated blood, from the systemic circulation (Hickey and Thompson, 1992).

The transitional and respiratory airways, or peripheral airways, consisting of the respiratory bronchioles (the transitional zone), the alveolar ducts and the alveolar sacs, account for 95% of each lung's surface area (~75 m^2) (Smith, 1997; Laube, 2005). The presence of thin-walled, alveolar pockets, on these seven terminal generations of the airways, permits gaseous exchange in this region. The respiratory zone is supplied by the pulmonary circulation; deoxygenated blood pumped directly from the right ventricle of the heart, under lower pressure than the systemic circulation (Hickey and Thompson, 1992). However, even in the healthy lung, there is some mismatching of ventilation and perfusion, as there are some deep-seated alveoli that are well perfused but poorly ventilated, and other alveoli that are well ventilated, but poorly perfused. The latter alveoli contribute to the physiological dead space mentioned above in reference to the conducting airways. In lung disease, the degree of mismatching increases, such that gas exchange is not of an adequate efficiency (Hickey and Thompson, 1992).

Figure 1.2 A schematic of Weibel's model of airway branching in the human lung.
Diameters and surface areas of each airway generation are provided. Taken from: Patton, 1996.

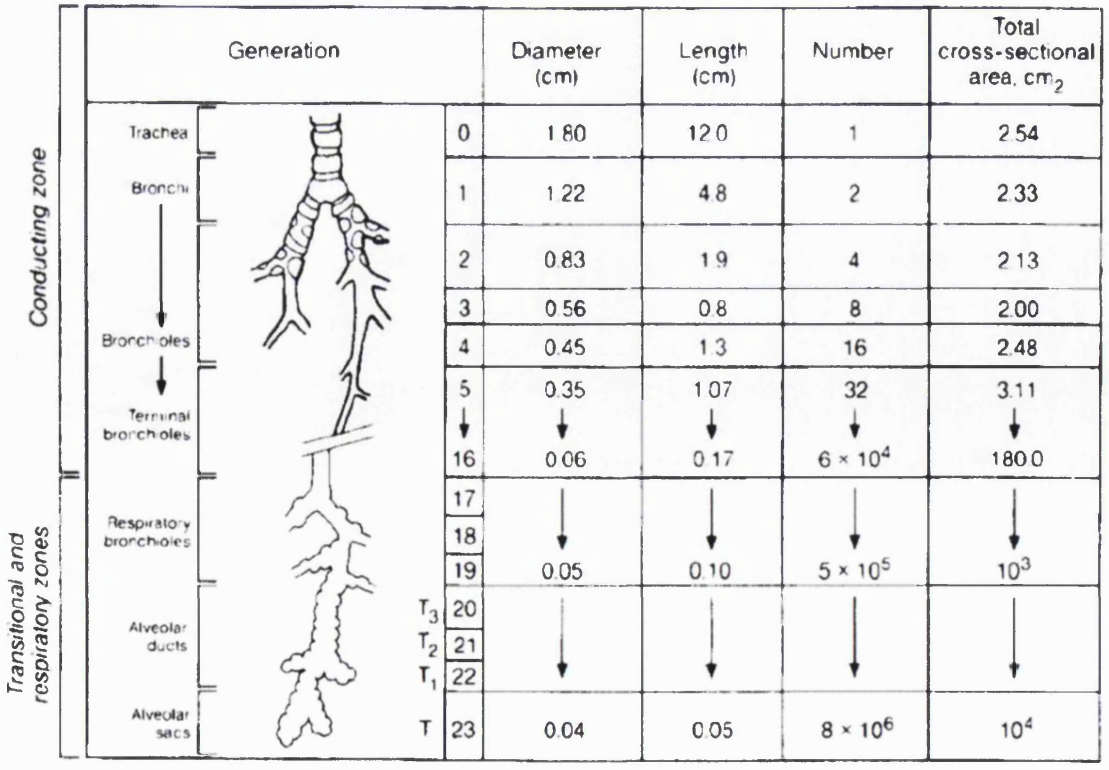

Generation		Diameter (cm)	Length (cm)	Number	Total cross-sectional area, cm_2
0		1.80	12.0	1	2.54
1		1.22	4.8	2	2.33
2		0.83	1.9	4	2.13
3		0.56	0.8	8	2.00
4		0.45	1.3	16	2.48
5 ↓ 16		0.35 ↓ 0.06	1.07 ↓ 0.17	32 ↓ 6×10^4	3.11 ↓ 180.0
17 18 19		↓ 0.05	↓ 0.10	↓ 5×10^5	↓ 10^3
20 21 22	T_3 T_2 T_1	↓	↓	↓	↓
23	T	0.04	0.05	8×10^6	10^4

1.2.3 Characteristics of airway tissues

1.2.3.a) Epithelium

In the nasal cavity, the epithelium gradually shifts from being stratified squamous cells, in the vestibule region, to pseudo-stratified, columnar respiratory epithelial cells. The former occur in overlapping layers, and are non-ciliated, whereas the latter are ciliated and are seated on an underlying, highly vascular, connective tissue (Illum and Fisher, 1997). The cilia form part of the mucociliary clearance system, described in Section 2.4. The respiratory endothelial cells have mucus-secreting goblet cells, interspersed between them. The lateral membrane connections, between these two types of cell, are non-uniform and weak, resulting in a relatively permeable (or "leaky") epithelium (Hinchcliffe and Illum, 1999). The vascular bed underlying the respiratory epithelium consists of highly fenestrated capillaries, and large vascular sinuses, which have the ability to dilate, thereby reducing airflow. The sinuses in each nostril swell alternately, resulting in the phenomenon known as nasal cycling, which is most detectable when the nose is partially blocked by a viral infection (Illum and Fisher, 1997).

The trachea to the terminal bronchioles of the lung is lined with a ciliated, columnar epithelium. These epithelial cells are joined with tight junctions. There are also non-ciliated, clara cells that produce surfactant, and goblet cells that produce mucus. The cartilage present in the walls of these airway vessels confers their rigidity (Hickey and Thompson, 1992).

The alveoli are lined by type I and type II alveolar cells. Type I alveolar cells, which form the majority of the alveolar surface, are broad and thin, providing a short distance for gas exchange with blood across the juxtapositioned vascular endothelium (Hickey and Thompson, 1992; Patton, 1996). Typically, the alveolar walls are an order of magnitude thinner than most other mucosal and epithial membranes. Type II cells are small and compact, and secrete surfactant as well as being progenitors for type I cells. The other cells, which are present on the alveolar surface, are macrophages, which are further described in Section 1.2.4. There are two type II cells, and eight macrophage cells, for every one type I cell (Patton, 1996).

1.2.3.b) Secretions

Goblet cells and gland cells, in the nasal epithelium, trachea and bronchi, produce mucus, which is a viscous solution of glycoproteins and complex carbohydrates (Hickey and Thompson, 1992; Kim and Folinsbee, 1997). The mucus consists of two phases: a viscous gel layer, which floats on a more watery sol layer (Hinchcliffe and Illum, 1999).

Mucus lines the airway wall, keeping the epithelium well hydrated, and also humidifying inspired air. Mucus also forms part of the mucociliary clearance mechanism described in Section 1.2.4. Mucus production is usually quite low, and increases with the inspiration of irritant particulates (which could be dirt, but could also be inhaled drug particles), or increases as a result of infection and disease (Patton, 1996). Alveolar tissue contains a very thin layer of a much less viscous tissue fluid. This liquid contains surfactant-like phospholipids, which reduce the alveolar surface tension (Patton, 1996).

1.2.3.c) Metabolic capacity

After the liver, the nose is the most metabolically active organ. Like the liver it has a cytochrome P450 system, capable of metabolising inhaled exogenous chemicals. This could potentially defeat the object of avoiding first-pass metabolism by delivering *via* the nasal cavity. Whilst the overall drug metabolising capacity of the nasal mucosa is very low, compared to the liver, nasal doses are also usually low, relative to oral doses.

Nasal and lung tissue also secrete small amounts of protease enzymes such as amino- and carboxypeptidases (Illum and Fisher, 1997). Lung tissue also produces elastase, collegenase, chymotrypsin and the membrane bound angiotensin-converting enzyme. These enzymes are involved in the breakdown of both endogenous and exogenous proteins (Qui *et al.*, 1997). Lung Clara cells also have cytochrome P450 activity, but of lower capacity compared to the nose and liver (Hukkanen *et al.,* 2002). Both nasal and lung tissues incorporate efflux transporters, particularly P-glycoprotein.

1.2.3.d) Immune tissues

The airway tissues confer a number of mechanisms of innate immunity that can prevent infection by inhaled pathogens. The very structure of the nasal and respiratory anatomy acts as a barrier, and trapping mechanism, of inhaled antigenic material. The secretions described above, and the clearance mechanisms described below, also contribute to innate immunity (Hinchcliffe and Illum, 1999). The airways are also lined with mast cells that, when triggered by antigens, degranulate to release inflammatory mediators such as histamine (Hickey and Thompson, 1992).

However, when innate immunity proves insufficient, the specialised lymphoreticular tissues are located in the upper airways, beneath the ciliated epithelia, and form part of the mucosal immune system. This bronchus-associated lymphoid tissue (BALT) can capture inhaled antigens, and trigger adaptive humoral and cellular immune responses

(McGhee *et al.*, 1992). Similar nasal-associated lymphoid tissue (NALT) has been found near the entrance to the nasopharynx, at the site of the nasopharyngeal and palatine tonsils, as shown in Figure 1.3. One of the major safety concerns about delivering proteinaceous drugs, *via* the airways, is the triggering of these immune responses, which can result in fever-like symptoms. These immune responses are particularly sensitive to aggregated proteins, which can result from an inadequate formulation or formulation process (Arvinte, 2005). Also, once antibodies are produced against a proteinaceous drug, the drug will rapidly become pharmacologically inctive.

1.2.4 Clearance mechanisms

The above description of the airways demonstrates how the anatomy is designed to trap inhaled particles (the detailed mechanism by which particles can settle in the airways is discussed in Section 1.3). However, in order to prevent the nasal and pulmonary passages from becoming occluded by particulate matter, clearance mechanisms exist to "clean" the airways. This service is provided by two very different methods: mucociliary clearance and phagocytic degradation by macrophages.

1.2.4.a) Mucociliary apparatus

In the nose, the cilia on the respiratory epithelium beat symmetrically, ~60 times/min, propelling the gel layer of mucus (pH 5.5-6.5) towards nasopharynx, at a rate of ~5-6 mm/min (resulting in a clearance half-life of ~15-20 min) (Maggio, 2006). Thus, particles that become adhered to, or dissolved in, the mucus are pushed to the back of the throat, *via* the wave-like motion of the cilia, and are ultimately swallowed into the stomach. Mucus can also be transported to the anterior nasal cavity, from where it exits *via* the nostrils, with large amounts, or very irritant particles, triggering the sneeze reflex (Hinchcliffe and Illum, 1999). Inadequate or excessive mucus, or mucus of the incorrect composition, can result in reduced clearance rates (Illum and Fisher, 1997).

Figure1.3 Locations of the human tonsils. The nasopharangeal tonsil (1) and the palatine tonsil (2) are the sites of the nasal-associated lymphoid tissue (NALT). The lingual tonsil and the epiglottis are represented by (3) and (4), respectively. Taken from: Healthopedia.com.

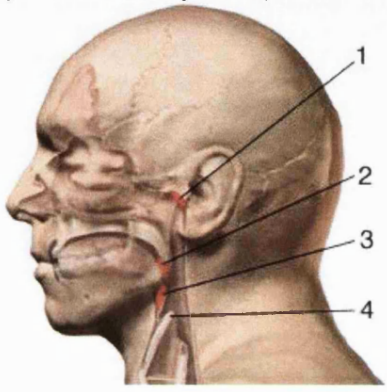

A very similar mucociliary apparatus is present in the conducting airways of the lung. The ciliated epithelium and mucus form what is called the 'mucociliary escalator', since particles trapped in mucus are pushed up the airway, towards the pharynx, where the mucus is swallowed, or ejected. Generally, the cilia beat at higher frequencies than the nasal cilia, with average frequencies being about 1000 beats per minute (Kim and Folinsbee, 1997). The rate of propulsion decreases in the smaller airways, due to the smaller population of ciliated cells, and a slower beat frequency. This allows the larger airways, which receive the combined mucus from the converging lower airways, to efficiently meet the demand. The coughing reflex greatly enhances the effective speed of the escalator (Hickey and Thompson, 1992). However, similar to the nose, pathologies causing mucus hyper-secretion (as with damage to the ciliated cells caused by smoking) can impede clearance. Generally, the process of mucociliary clearance takes ~24 to 48 h.

1.2.4.b) Alveolar macrophages

In the respiratory regions of the lungs, cells are not ciliated, and little mucus is present (Laube, 2005). In these regions, alveolar macrophages act as 'housekeeper' cells, removing inhaled particles principally by phagocytosis. Engulfed matter, if digestible, is degraded within the lysosyme of the macrophage. Indigestible matter, such as asbestos, silica and dusts, deposit on the alveolar surface when the macrophage dies, which is usually after one to five weeks. After engulfing the particle, the macrophage may slowly migrate upwards, towards the central airways, where it joins the bottom of the mucociliary escalator, and is subsequently cleared. Alternatively, the macrophage can possibly pass through the epithelium, and into the lymphatics. The optimum particle size for phagocytosis is 2-3 μm, with larger and smaller particles avoiding recognition by macrophages (Edwards *et al.*, 1998; Patton & Byron 2007). These particles can remain in the alveoli for prolonged periods and may be eventually removed by endocytosis into the epithelium. Often, the entire clearance process by macrophages can require months to years (Kim and Folinsbee, 1997; Qui *et al.*, 1997).

Generally speaking, for an inhaled drug therapy to be able to either persist locally in the airways, or be absorbed into the systemic circulation, these clearance mechanisms need to be taken account of, and possibly avoided. Given the rapid and extensive clearance of material in the nasal cavity, prolonged drug release from a locally resident formulation would appear very difficult to achieve. However, there is more scope for such a formulation in the lungs, provided formulation particles could be deposited beyond the mucociliary region, and were small enough to avoid phagocytosis.

1.3 General principles of inhaled drug delivery

1.3.1 Aerosol deposition

It has been described above how different locations along the airway can have different structures and environments. The functionality of clearance mechanisms that can remove drugs, and the availability of permeable epithelium that can facilitate drug absorption, widely vary according to the site. Therefore, it is likely that the effectiveness of a given therapy will partly depend on which region of the respiratory tract drug particles (or droplets) are deposited. The deposition site of aerosolised drug particles is dependent on both the particle characteristics and patient factors. In addition the delivery device can have a major contribution to particle dispersion.

1.3.1.a) Particle characteristics

The characteristics of an aerosol of drug particles will depend on both the drug formulation as it resides in the delivery device, and the method by which the delivery device propels the formulation into the airways. The primary determinant of particle deposition is the aerodynamic diameter of the particles, usually expressed as the mass median of the aerodynamic diameter (MMAD) (Agu *et al.*, 2001). This function accounts for particle size, density and shape, and for spherical particles it can be expressed as in Equation 1.

Equation 1 Calculation of aerodynamic diameter (D_a), where D = geometric diameter and ρ = particle density (Edwards *et al.*, 1998).

$$D_a = D\sqrt{\rho}$$

For nasal drug delivery, particles of MMAD >~10 μm (but <~30 μm) will only be deposited in the nasal cavity. Particles <~1 μm, will pass straight through the nose to the pulmonary tract. Particles of MMAD between these values will deposit according to the velocity and turbulence of the airflow, with higher velocities increasing the likelihood of deposition. For a given velocity, larger particles will deposit towards the anterior of the nasal cavity, and smaller particles further down, where turbulence increases surface contact (Illum and Fisher, 1997). This initial site of deposition will determine the total deposition area after redistribution by the mucociliary system (Kublik and Vidgren, 1998). The mechanisms by which these particles initially settle in the nasal cavity, are similar to those described below for lung deposition.

When delivering particles to the lung, *via* the mouth, particles of MMAD >~10 μm are

deposited in the oropharynx. However, particles smaller than ~5 μm, generally reach the tracheobronchial region of the lungs, and particles <3 μm may reach the alveolae. Therefore, as a function of particle size, oropharyngeal deposition is less than nasal deposition. Thus, drug particles intended for the lungs are generally given *via* the mouth, rather than the nose, to maximise lung deposition (Lalor and Hickey, 1997). Again, the actual deposition pattern will also depend on the airflow velocity.

There are three main mechanisms by which particles are deposited along the respiratory tract. Particle MMAD governs which of the mechanisms a given particle will be most influenced by.

Inertial impaction arises when particles continue to move in a straight direction, instead of following the path of the air stream that they are being carried in. This results in the particle hitting an airway wall in its trajectory, rather than flowing further down the respiratory tract. Particles with a greater MMAD and initial velocity, will have greater inertia, and thus are more likely to become deposited by this method (Gonda, 1992). For smaller particles, the inertial contribution can be considered negligible, and thus the particle is assumed to rapidly equilibrate with airflow movement (Annapragada *et al.*, 1997).

Sedimentation occurs further down the airway, where airflow velocity is low, and thus is the primary cause of deposition for particles of <~3 μm that are not deposited by impaction. These particles settle due to the effect of gravity. Therefore, as with impaction, sedimentation increases with increasing particle density (Gonda, 1992).

Diffusion becomes appreciable for very small particles (<~0.5 μm), since they are less affected by gravity. Particles diffuse by Brownian motion, and can be deposited by a random collision with an airway wall. Diffusion occurs more rapidly as particle size decreases. Therefore, during normal breathing, only ultrafine particles smaller than ~0.01 μm can diffuse rapidly enough to be deposited (Heyder, 2004). However, particles greater than this size, but <~0.5 μm, are mainly exhaled, since there is not sufficient time for diffusion to occur (Gonda, 1992).

Although different values are quoted, the general result is that inhaled particles, of MMAD >~5-10 μm, deposit in the head region by inertial impaction. Particles between ~3-5 μm will mainly deposit in the tracheobronchial region, again predominantly by impaction. For deposition in the alveolar regions, particles should have an MMAD of <~3 μm, with ~2 μm being an optimum size. Most of these particles will settle by

sedimentation. Particles of MMAD <~0.5-1 μm are mainly exhaled (with exception of those of ultrafine sizes as explained above). Therefore, sizing particles to a range of ~1-5 μm should ensure all areas of the lungs are covered, without too much wastage by oropharyngeal deposition (Gonda, 1992; Lalor and Hickey, 1997; Agu *et al.*, 2001).

There are particle factors, other than size and density, that can also influence deposition. Non-spherical, elongated, particles have a MMAD much more closely related to their shorter dimension, than their length. Therefore, these long fibres (including asbestos) can reach the alveoli. However, rather than being exhaled, as their MMAD would suggest they should, the fibres can be deposited by interception with structures on the airway epithelium (Gonda, 1992).

Charged particles can induce an opposite charge in airway walls, and then become deposited by electrostatic attraction (Gonda, 1992). For most drug particles, this mechanism is probably of little importance, since any charge imparted on them by the delivery device is subsequently neutralised by ions in the air. However, this effect may be more important for proteinaceous drug molecules, as they can have an inherent charge, depending on the surrounding pH.

Another factor is the hygroscopicity of the particle. Particles that can absorb water can undergo hygroscopic growth as they enter the airways (a phenomenon known as "raining out"). The humidfying effects of lung mucus and nasal turbinates can saturate hygroscopic particles, possibly resulting in an increase of density or diameter. This will obviously affect their deposition site (Gonda, 1992; Gupta and Adjei, 1997). Aggregation of particles can lead to them being deposited orally, and being swallowed.

1.3.1.b) Patient factors

Firstly, successful use of the delivery device can often be reliant on the patient. For example, breath-actuated inhalers require the patient to provide the vacuum to draw out the dose, and most metered dose inhalers require the patient to coordinate breathing with triggering the dose release.

Secondly, airway morphology can vary between patients, particularly with age and in pathological circumstances. Although nasal polyps do not appear to alter the deposition of nasal inhalations (Illum and Fisher, 1997), it is believed that chronic lung disease can structurally alter the airways such that deposition patterns are appreciably changed (Gupta and Adjei, 1997). This needs to be taken into account when treating chronic lung disease using the pulmonary route.

Finally, the patient's respiratory pattern can markedly affect aerosol deposition. For example, the optimum particle diameter range for alveolar deposition is reduced from ~2.5-4 μm to ~1.5-2.5 μm, when breath-holding techniques are used (Lalor and Hickey, 1997). This reduction in optimum range may be due to smaller particles having more time to settle by sedimentation or diffusion, before exhalation. Indeed, breath-holding has been suggested as a method to enhance targeted drug delivery to only the alveolar regions. Particles of MMAD <~0.5 μm have a negligible probability of being deposited in the oropharyngeal and bronchial regions. Although particles of this size would normally be exhaled, by breath-holding these particles can selectively settle in the alveolar regions (Gonda, 1992). In addition, it has already been described how the velocity of the patient's inspiration may affect particle deposition. Higher velocities increase inertial impaction, thereby reducing pulmonary deposition due to increased oropharyngeal deposition. However, increased inertial impaction in the nose can allow smaller particles to be deposition nasally that would otherwise pass through into the lungs.

1.3.2 Delivery Devices

A suitable delivery device is required in order to produce, and deliver, drug particles with the appropriate characteristics described above. The device should be able to generate reproducible doses of drug particles, independent of the administrator. These particles should be of the required diameter range (i.e. <~10 μm for pulmonary delivery). The device should also be a storage unit for multiple doses, and thus must be capable of keeping the drug and formulation stable for a realistic shelf-life. In addition, the ideal delivery device should be portable and easy to use for self-administration. There are many types of nasal and pulmonary delivery devices commercially available, for the delivery of drugs for pulmonary disease. However, generally speaking, their efficiencies are variable, and highly dependent upon the individual patient. For the drugs currently used in these devices, this is not too much of a problem, since the drugs are cheap, potent and have a large therapeutic window. For macromolecular drugs, more precise dosing is required, and product wastage is more important due to economical considerations. The different classes of currently available delivery devices are described below, including some of the formulation requirements of the delivery vehicle. Note, that where excipients are discussed, this is referring to components used with drug particles for their use in delivery devices, and not the formulation of drug particles themselves, which is discussed in Section 1.3.3.

1.3.2.a) Nasal delivery devices

There are a number of delivery devices that have been used for nasal drug delivery, but cannot be used for pulmonary delivery. This may be due to the fact that the entrance of the nose is within a convenient tactile range compared to the lungs, and because particles need not be so small as to penetrate the nasal cavity. Most of these nasal devices deliver aqueous solutions, or suspensions of drug. Whilst these can hydrate the nose, which is beneficial in many nasal pathologies, their formulations require preservatives for microbiological and chemical stability. These preservatives can arrest mucociliary clearance (which could be exploited to prolong drug effects), and possibly cause irritation of the mucosa (Kublik and Vidgren, 1998).

Dropper bottles are one of the oldest methods of nasal delivery. Although they are inexpensive and simple to manufacture, they cannot deliver accurate, reproducible doses. Even if drop sizes were consistent, depending on the patient's head position, during administration of such a large bolus of fluid can quickly drain through the nasal cavity and down to the laryngeal pharynx. Stability is a particular problem, because micro-organisms can adhere to the pipette, especially with squeezable bottles, since these generate a vacuum (Kublik and Vidgren, 1998).

Most nasal pharmaceuticals currently on the market are delivered by metered-dose, aqueous pump sprays. These devices can deliver defined volumes of between ~25-200 μL, thus improving dose reproducibility. It has been shown that delivering a dose by two half-volume sprays reduces clearance, and increases bioavailability, compared with one spray of full volume. This is due to less spreading in the deposition (Illum and Fisher, 1992; Kublik and Vidgren, 1998). Some systems are designed with microbial filters, or as an airless pump, negating the need for preservatives. Also, the latter type of device is capable of delivering uniform doses, when held in any position. Figure 1.4 illustrates two designs for an airless pump system. Spray characteristics can be somewhat varied by the compression, pump and valve employed. However, the physical properties of the liquid will determine the spray pattern and particle size of the aerosol (Kublik and Vidgren, 1998).

Figure 1.4. (a) Airless nasal device with collapsible bag (Nasal 360®,Valois S.A., Le Neubourg, France). **(b) Airless nasal device with sliding piston** (PAS 27®, Valois S.A., Le Neubourg, France). Taken from Kublik and Vidgren, 1998.

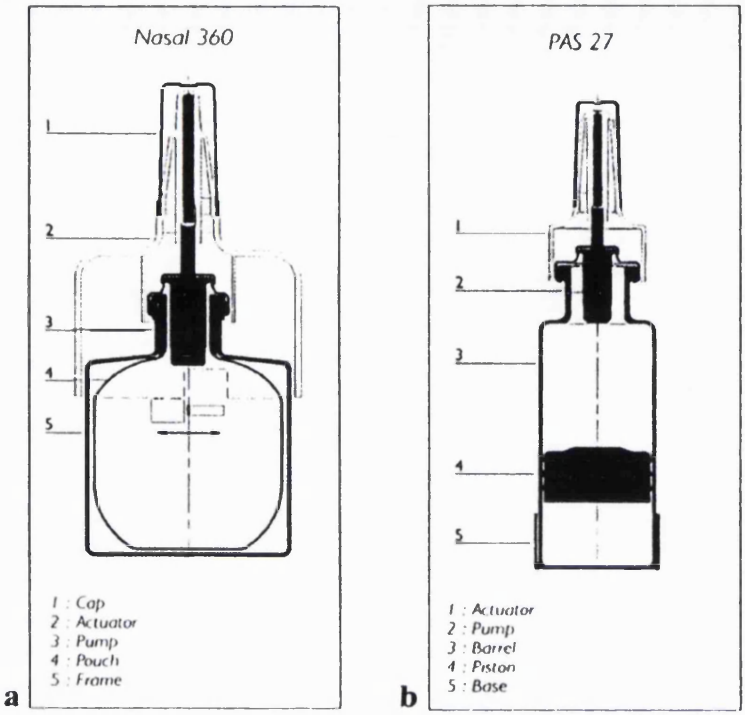

OptiNose has developed a bi-directional nasal delivery device (illustrated in Figure 1.5), where users blow into a mouthpiece to release drug *via* a sealing nozzle into their nose. This propels the drug to more distal, olfactory, parts of the nasal cavity, while reducing drug loss into the throat. The latter effect is achieved because the blowing action closes the soft palate, forcing drug to U-turn into the other nostril. Reaching the olfactory area, allows targeting of drugs across the blood-brain barrier, *via* the olfactory nerves (Illum, 2003; Bryan, 2004; Graff and Pollack, 2005). However, in a clinical trial, there was no improvement in midazolam bioavailability when delivered by a bi-directional device, compared to a traditional spray (Dale *et al.*, 2006).

Figure 1.5. The bi-directional nasal delivery devise by Optinose. Taken from: Bryan, 2004.

Pre-compression pumps have been used for the delivery of nasal gels, which are viscous solutions employed to increase systemic absorption of nasally-applied drugs, by increasing contact time with the mucosa. For this type of vehicle, a specifically designed delivery device is essential to ensure the gel is deposited over a wide distribution area (Kublik and Vidgren, 1998).

The other types of delivery device, discussed below, have been used for both nasal and pulmonary delivery. Most of these devices were originally designed for delivery of locally acting drugs to the conducting airways, and are currently being adapted for systemic delivery, *via* deeper regions of the lung, or *via* the nasal cavity.

1.3.2.b) Nebuliser solutions

Nebulisation is the only available method to achieve pulmonary delivery of aqueous solutions. Air-jet nebulisers atomise the liquid formulation by drawing it into an area of low pressure generated by a source of compressed air. Ultrasonic nebulisers generate aerosols using high frequency ultrasonic waves. Nebulisers can administer much higher doses than other delivery devices, and are still effective in breathless patients, who would be unable to take a deep inspiration, as required for other types of device. However, due to their lack of portability, nebulisers are usually confined to use in hospitalised patients (Lalor and Hickey, 1997).

Nebulisers are unlikely to be suitable candidates to deliver systemic macromolecular drugs. Such molecules are relatively unstable in any type of aqueous formulation since they are prone to hydrolysis. In addition, jet nebulisation exerts a high shear stress on the formulation, which can denature macromolecular compounds (Garcia-Contreras and Smyth, 2005). Also, since the droplets produced are a wide range of sizes, generally above ~2 μm, effective deposition in alveolar regions may not be achieved (Agu *et al.*, 2001), and as a result this method of administration may be too inefficient for expensive or narrow-therapeutic window drugs (Garcia-Contreras and Smyth, 2005). Nevertheless, dornase alpha (Pulmozyme®, Roche), the only currently licensed pulmonary formulation of a macromolecular drug, is formulated as a nebuliser solution. However, firstly, dornase alpha is only required to work on mucus secretions in the upper airways, and secondly, the nebuliser solutions have to be refrigerated for stability.

However, the new generation of vibrating mesh nebulisers have reduced the portability issues associated with nebulisers, and may be more applicable for the delivery of biopharmaceuticals. Also, the AKITA system (Inamed GmbH, Germany), improved dosing consistency by electronically controlling the exact amount of drug released in

accordance with specific patient parameters (Agu *et al.*, 2001).

1.3.2.c) Dry-powder inhalers

There have been many designs of a dry-powder inhaler (DPI), for both nasal and pulmonary use, with the earliest versions using single-dose, gelatin capsules, which were pierced by the device, allowing the patient to inhale the powder contents, *via* a mouth piece. More recent models, such as the Diskhaler®, can hold multiple doses, stored in discrete blisters. However, the more contemporary designs, such as the Turbohaler®, are multi-dose units that can deliver fixed doses from a powder reservoir (Atkins *et al.*, 1992). Although this type of device has superior capacity, there are concerns that there is increased susceptibility for powder reservoirs to be affected by moisture, and that dose-to-dose variations are greater (Agu *et al.*, 2001). Figure 1.6 is a diagram of the Turbohaler®. One major advantage over nebulised systems is the relative portability of dry-powder devices. This is best exemplified by the credit-card form factor device currently being developed by Aespira Ltd., Israel (winner of the 2007 'outstanding new venture of the year' award). This wallet-sized device uses the patient's inspiration to drive a turbine, which scrapes micronised particles into the airflow (Figure 1.7). This method results in high fine particle fractions as well as accurate dosing, and the device is both cheap to produce and discrete (Aespira, 2007).

Unlike pressurised metered-dose inhalers, DPIs require no co-ordination technique by the user, since the patient's breath activates the device. However, this is a "double-edged sword", because the energy to deaggregate and aerosolize the powder comes from the patient's inspiratory airflow (Lalor and Hickey, 1997). Therefore, the distribution pattern from these devices is dependent on the airflow velocity that a given patient can achieve. As a result, children and elderly patients, or those with severe respiratory disease, may not be able to administer reproducible doses, particularly where deep-lung deposition is required. Future devices may incorporate motors, compressed air, or supercritical carbon dioxide to disperse powder into fine, low velocity particles, without depending on the patient's inspiratory ability (Gonda, 2000).

Nasal deposition of dry powders requires less inhalation power from the patient. Because of the lower force required, Bespak has designed a nasal dry-powder device (Uni-Dose DP™), where the dose is ejected from the device by depressing a pressurised air sac, rather than relying on inspiratory force. The use of DPIs for nasal delivery has other advantages over liquid formulations, including increased retention, and less leakage beyond the nasopharynx, which often is the cause of an unpleasant taste (Kublik and Vidgren, 1998).

Figure 1.6. The Turbohaler® (Astra Draco, Sweden). Taken from: Kublik and Vidgren, 1998.

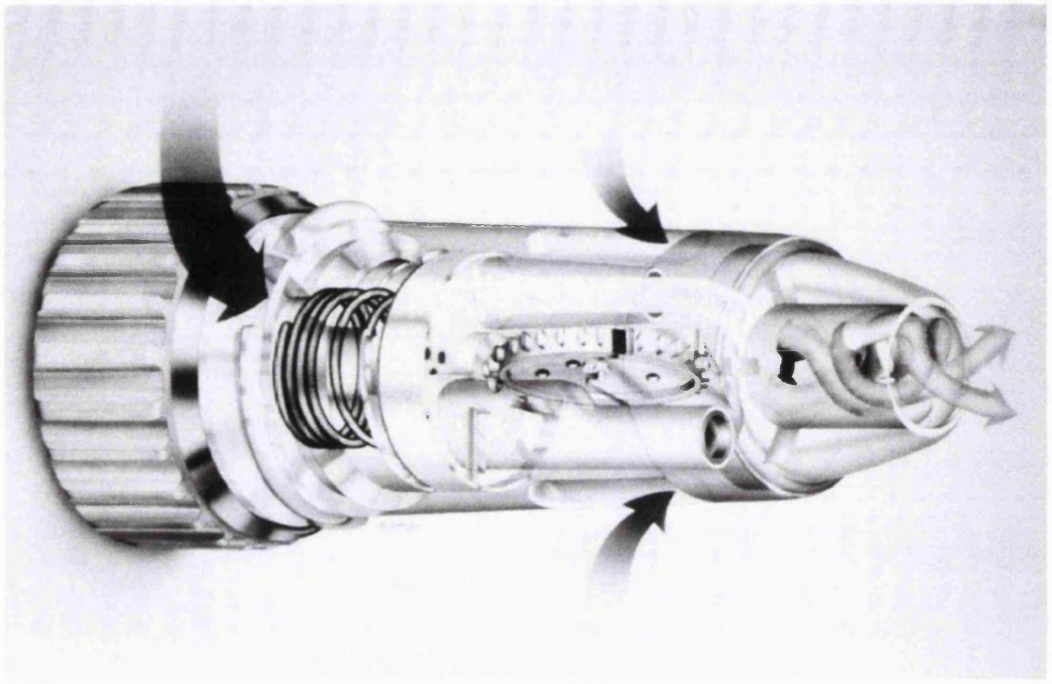

Figure 1.7 Schematic of the credit-card sized dry-powder inhaler device by Aespira Ltd., Israel. Taken from: www.aespira.com.

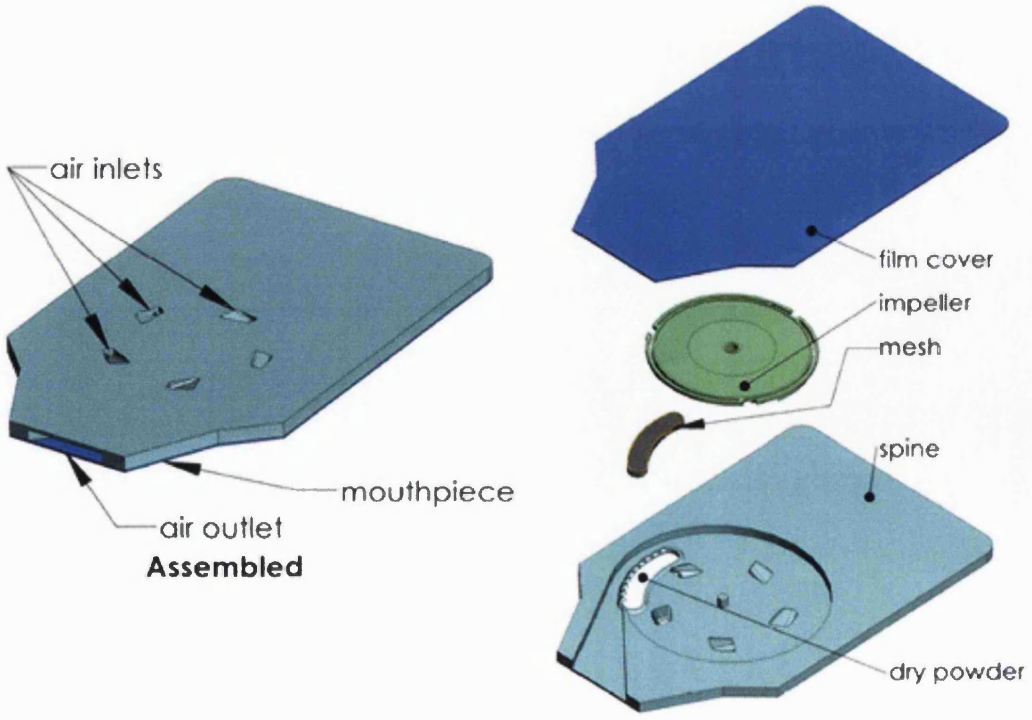

The powder formulation of DPIs reduces the instability observed with aqueous preparations, and the potential instability and environmental hazards associated with propellants used in metered-dose inhalers (see below). However, the micron-sized drug particles required for deep-lung deposition do not flow or disperse evenly due to electrostatic forces, and so the powder formulation of a DPI is critical for the reliability of the device. Usually, drug particles are formulated with α-lactose monohydrate, which is a well characterised inert carrier. These carrier particles are sized larger (tens of microns) than the drug particles, such that they can regulate the overall flow of the formulation, but are then impacted in the head region, without entering the lungs (Lalor and Hickey, 1997). However, drug delivery by this method tends to be inefficient, since very fine drug particles tend not to detach from the carrier molecule, due to high adhesive forces. For the systemic delivery of macromolecular drugs, this may pose a particular barrier, as precise, reproducible doses are likely to be necessary. Lucas *et al.* (1998) have shown that, for a dry-powder protein formulation, the addition of fine particle lactose or micronised polyethylene glycol (PEG 6000), to the usual coarse lactose carrier, improved delivery performance. The addition of these excipients, which are both regarded as safe for inhalation, was believed to cause a redistribution of protein particles, such that multiplets were formed with the fine carrier. These fine multiplets either had a low enough MMAD to result in improved distribution, or the cohesion between the protein particle and the smaller carrier was less than with the coarse carrier.

The first pulmonary-delivered macromolecular drug for systemic treatment was formulated in a dry-powder inhaler. The Exubera® inhaled insulin formulation, developed by Pfizer and Nektar consists, of spray-dried microparticles containing insulin and other excipients to aid dispersion and stability (see the following sections for further details of the formulation), thereby avoiding the need for a lactose carrier (Fineberg *et al.,* 2007). The device itself (illustrated in Figure 1.8) contains a chamber to allow particle dispersion prior to inhalation, which by this means increases dose accuracy and efficiency. However, this somewhat reduces the portability of the device compared to some of the aforementioned examples.

Figure 1.8 Exubera® dry-powder insulin inhaler device (Pfizer and Nektar). This was the first marketed pulmonary formulation of a macromolecular drug for systemic therapy. When in use (right hand image) the device contains a chamber for powder dispersion.

1.3.2.d) Pressurised metered-dose inhalers

The pressurised metered-dose inhaler (pMDI) has become the most widely used type of pulmonary delivery device following its invention in the 1950s. This is due to its convenience of use, ability to deliver reproducible doses and to its cost-effectiveness. The pMDIs utilise the vapour pressure of organic propellants to generate a fine particle aerosol, as they evaporate when the dose is expelled.

1.3.2.d.1 Device components of a pMDI

Figure 1.9 is a schematic diagram of the components of a pMDI. Canisters are typically made out of aluminium, and are required to contain the formulation under pressurised conditions. The canisters usually have a capacity of ~15-30 mL, thus providing ~200 actuations of ~25-100 µL (Atkins *et al.*, 1992). Most designs enable the canister and metering-valve to be replaced, although this is rarely enacted, and the whole device is invariably re-dispensed.

Figure 1.9 The components of a metred-dose inhaler.
Taken from: Stein and Stefely, 2003.

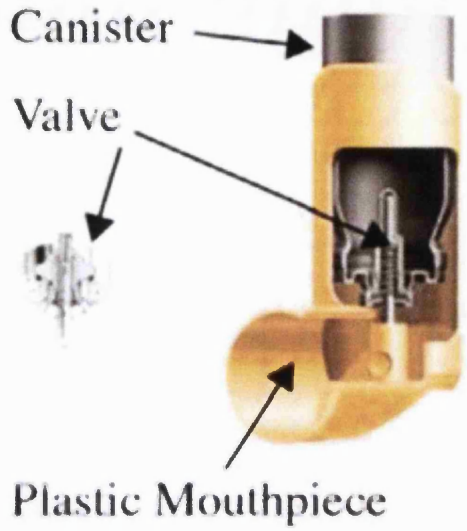

The metering-valve (illustrated in Figure 1.10) provides both accurately measured doses for each actuation, and a vapour seal to prevent loss of the pressurised contents. When the valve is closed, the metering-chamber, which is made to a specified capacity, is filled with a dose of the formulation. Pushing down on the canister opens the valve, thereby allowing the measured quantity to escape *via* the nozzle, while preventing further chamber filling from the canister. Therefore, because the defined dose is based on volume, it is important to consider the formulation density, and so to ensure the formulation is homogenous. It is also important to ensure that the valve is comprised of materials that are durable, and have the necessary deformation and swelling characteristics, while being compatible with the drug and formulation (Atkins *et al.*, 1992).

Figure 1.10. Schematic of the metering valve of a metered-dose inhaler.
Taken from: Ng *et al.*, 2003

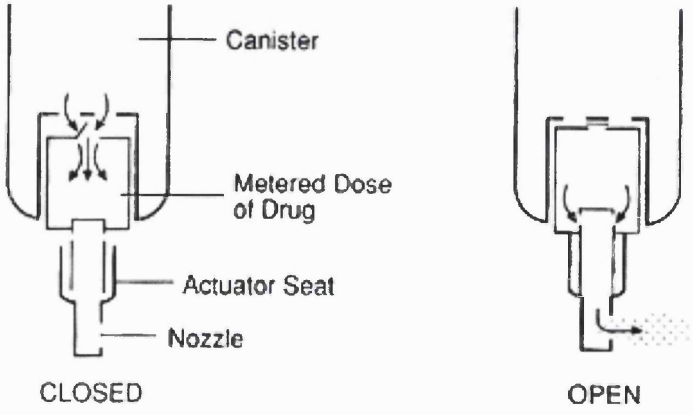

The actuator is generally made from injection moulded polyethylene or polypropylene. The actuator serves the purpose of being both a hand-held dose-trigger, in which the canister is seated, and as a mouthpiece. The orifice diameter of the mouthpiece affects the aerosol cloud generated, and the rate of spray formation (Atkins *et al.*, 1992). As explained below, particles leaving the actuator are still relatively large, and travel at high velocity. Thus, they are susceptible to impaction within the mouthpiece (Lalor and Hickey, 1997). In fact, for some formulations, this can be the fate for up to 80% of the dose! Therefore, optimal mouthpiece design can reduce particle deposition in the actuator, and increase delivery efficiency.

1.3.2.d.2 Propellants for pMDIs

Formulations of pMDIs rely on the use of propellants to generate a fine particle aerosol. Propellants have a high vapour pressure within the airtight canister, and thus, when released into the low pressure of the atmosphere, energy is released by their latent heat of vaporisation. The propellant generally evaporates in two stages, with the first ~10-20% occurring violently, immediately after release from the nozzle. This primary evaporation is known as "flash-off", and causes the initial break up of the formulation into propellant-coated drug particles or droplets. The remainder of the propellant evaporates more steadily during the ensuing moments, as the aerosol traverses the mouth. During this period, further reduction in particle size occurs as the propellant layer reduces (Gupta and Adjei, 1997). Therefore, choosing propellants with high vapour pressures, and thus fast evaporation times, will aid the rapid generation of fine particles, thereby reducing impaction in the oropharynx, and increasing the efficiencies of delivery to the lungs.

Until recently, the propellants used in pMDI formulations were mixtures of chlorofluorocarbons (CFCs), commonly including trichlorofluoromethane (CFC-11), dichlorodifluoromethane (CFC-12) and dichlorotetrafluoroethane (CFC-114) (chemical structures are given in Figure 1.11). Mixtures were based on their various vapour pressures (or boiling points), dielectric constants and densities. These properties are important determinants of a propellant's ability to produce aerosols, solubilise drugs and suspend ingredients, respectively (Lalor and Hickey, 1997; Noakes, 2002).

However, in 1974, Molina and Rowlands published findings that chlorine atoms from CFCs were potentially at least partly responsible for causing catalytic destruction of the Earth's ozone layer. As a consequence of these findings, and general concerns

regarding the possible contribution to the 'greenhouse effect', the Montreal Protocol in 1987 stipulated that all products using CFC propellants had to be reformulated, to gradually phase-out the use of CFCs (Gonda, 2000). This legislation included medicinal pMDIs, despite these accounting for only 0.4% of the world's total CFC emissions! (Atkins *et al.*, 1992).

Pharmaceutical research identified hydrofluoroalkanes (HFAs) as potential replacements for CFCs. In particular, tetrafluoroethane (HFA 134a) and heptafluoropropane (HFA 227) were identified as having properties most suitable for application as a pMDI propellant (chemical structures as depicted in Figure 1.11) (Leach, 2005). However, these compounds are not free from environmental consequences, as they too contribute to greenhouse gases (although to a lesser extent than CFCs), and possibly result in the deposition of toxic breakdown products in the soil (McDonald and Martin, 2000). Also, HFAs have reduced solvency properties compared with CFCs, and so the use of some of the other formulation ingredients in pMDIs had to be rethought (Lalor and Hickey, 1997). Having said this, there are now several CFC-free pMDI products commercially available that utilise HFA 134a as the propellant. In fact, with the Qvar® (3M Healthcare) beclometasone pMDI, a reduction in MMAD and improvements in respiratory fraction have been demonstrated, due to the higher vapour pressure of HFA 134a, compared with CFCs (McDonald and Martin, 2000). This improvement was thought to be the reason for a reduced influence of lung disease state on drug deposition in the lung (Häussermann *et al.*, 2007).

Figure 1.11 Chemical structure of propellants for metered-dose inhalers.
a) trichlorofluoromethane (CFC-11), b) dichlorodifluoromethane (CFC-12),
c) dichlorotetrafluoroethane (CFC-114), d) tetrafluorethane (HFA-134a) and
e) the experimental, heptafluoropropane (HFA-227). Taken from: Lalor and Hickey, 1997.

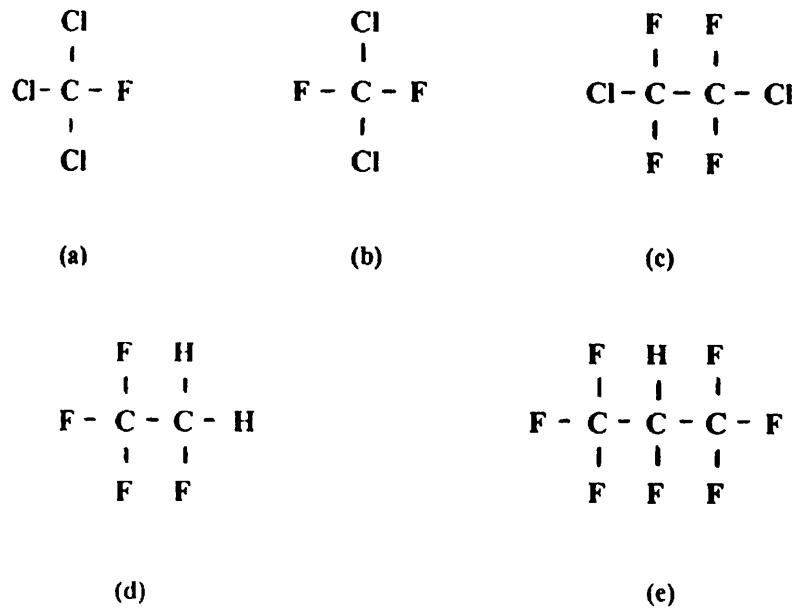

Another approach to replacing the CFC propellant has been to revert to aqueous-based formulations, as seen with nasal products. Here, the energy for vaporisation is provided by a piezo-electric element, rather than the intrinsic properties of the propellant (e.g. the Piezo Electric Actuator, Bespak).

1.3.2.d.3 Suspension formulations in pMDIs

The formulation in a pMDI can either be a solution, or a suspension. Although solutions are more physically stable than suspensions, they are generally chemically less stable. Also, because most drugs have some degree of polarity, they are rarely fully soluble in organic propellants. However, some drugs can be formulated as solutions with the use of co-solvents such as ethanol. This has become easier with HFA propellants, as they are more polar than CFCs. However, the addition of co-solvents results in a decrease in overall vapour pressure (Gupta and Adjei, 1997; Lalor and Hickey, 1997). In the case of Qvar®, which is an HFA/ethanol based solution, redesign of several components of the pMDI was required.

Therefore, suspensions are generally the preferred type of pMDI formulation. Here, microfine drug particles are dispersed in the propellant. This dispersion is required to be as homogeneous and stable as possible, in order to ensure reproducible dosing. The density of the drug particles should be similar to that of the continuous phase (i.e. the propellant). Greater density differences will increase the rate drug particles sink to the bottom, or rise to the top, of the canister. High drug concentrations in the formulation will also decrease suspension stability, and cause aerosolised particles to be larger. However, reducing concentration by increasing dose volume, also results in larger particles, since propellant evaporation rate is reduced (Gupta and Adjei, 1997).

Surfactants are used in pMDI formulations to stabilise suspensions. The three surfactants currently approved for use in inhaled formulations are: oleic acid, sorbitan trioleate (Span 85) and soya-derived lecithin, and in CFC formulations these are used at concentrations of ~0.1-2.0% (McDonald and Martin, 2000). However, the solubilities of these surfactants in HFA are ~100-fold less than those in previously used propellants. Therefore new surfactants, more soluble in HFA, are required for the new generation of pMDIs. Polyethylene glycol, perfluoroalkonic acids and polysorbates, such as Tween 80, have been used experimentally (McDonald and Martin, 2000), as well as polyoxyethylene-ethers and poly(oxyethylene)-poly(propylene oxide) block co-polymers (Ridder *et al.*, 2005). However, they will only be approved for clinical use after their safety profile is clearly demonstrated (McDonald and Martin, 2000).

Drug particles have a tendency to attract one another, over long-distances, due to van der Waals forces. This initially results in particle flocculation, where the particles are in close proximity, but retain their individuality. At this distance, particles experience a repulsive electrostatic force since they carry the same charge. However, if the attractive forces are greater than this, particles will coalesce, and form an aggregate 'cake' on the sides of the container. Caked particles have lost their individuality, and thus cannot be easily re-dispersed. Creaming is the movement of dispersed particles to either the top or the bottom of the propellant phase. This can lead to phase separation, and increase the rate of cake formation. Creaming is accelerated with larger particles, and large density differences between the particle phase and the propellant phase. Creaming is reduced with increased viscosity of the propellant phase (Gupta and Adjei, 1997).

Surfactants are amphiphilic molecules. The hydrophilic end of the molecule adsorbs to the surface of the solid particles, while the hydrophobic tail is dissolved in the propellant. This has the effect of increasing the degree of electrostatic and steric repulsion between particles. The Derjaguin - Landau - Verwey - Overbeek (DLVO) theory predicts that particles can be stabilised at a distance of ~100 Å, when these repulsive forces are increased. This distance is called a secondary minimum, and occurs because the attractive van der Waals forces decrease more slowly with distance than the repulsive forces. This is represented in Figure 1.12. At distances of greater than ~100 Å there is a net attraction. However, once the particles reach a closer proximity the repulsion increases rapidly, mainly due to the presence of the surfactant molecules. The result is a minimum distance that the particles can approach each other before there is a net repulsion, preventing them moving any closer. Therefore, although coalescence would be the lowest energy state for the particles (the primary minimum), this is prevented because the energy barrier is too great to overcome. Rather, the particles remain loosely flocculated at the secondary minimum, and can be easily re-dispersed by shaking the unit (Gupta and Adjei, 1997).

Surfactants also act to lubricate the valve of the pMDI. However, with the invention of new materials for valve components, this function of the surfactant is becoming less necessary. As with co-solvents, excessive use of surfactants can reduce vapour pressure, slowing propellant evaporation, and increasing aerosol particle size (Lalor and Hickey, 1997).

Figure 1.12. DLVO theory (see text) as represented by the force between two colloidal particles when separated by a given distance. At approximately 100 Å separation there is a secondary minimum where the particles are loosely flocculated, but stabilised from caking. Adapted from Gupta and Adjei, 1997.

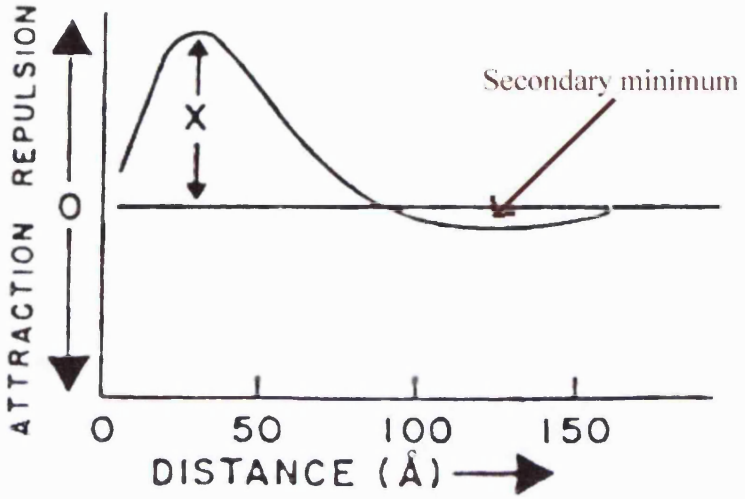

1.3.2.d.4 Advantages and disadvantages of pMDIs

It has already been mentioned that pMDIs offer the advantage of being small, convenient, inexpensive, and yet with the right formulation can offer accurate, reproducible doses. However, many patients do not use them optimally, as they fail to coordinate depressing the actuator, with an appropriate breathing action. Spacer devices, an anti-static air chamber, with openings controlled by one-way valves, can be attached to the pMDI. The dose is then sprayed into the spacer from where it can be inhaled slowly, over several breathing cycles. Even in those patients who can operate a pMDI effectively, the pulmonary delivery efficiency is actually increased with a spacer, since particles are inhaled at lower velocity, and more solvent has evaporated. However, spacers are relatively cumbersome, and reduce the convenience and portability of the pMDI. In order to ensure consistently high delivery efficiencies, the device, rather than the patient, should control the delivery time and velocity (which ideally should be the same as the inhalation velocity). Breath-actuated pMDIs use the patient's inhalation as a trigger to actuate the dose, thereby negating the need for coordination. This also applies to the new piezo electric systems.

The pMDI has also been adapted for nasal delivery. Actuators have been redesigned to include a nose attachment, rather than a mouthpiece. However, the organic propellants can have an irritant and drying effect on the nasal mucosa (Kublik and Vidgren, 1998). Also, given that the distance from the device to the target in the nasal cavity is less, there are probably better options than these pMDIs for a nasal delivery device.

The discontinuation of CFC propellants forced the design of the new types of pMDI formulation, described above. However, because of there is now a requirement for new excipients, which will all need long-term toxicological testing before approval, alternative devices such as the DPI are being intensively re-explored. Therefore, although currently the market leader, the pMDI may eventually lose its status as the pulmonary delivery device of choice.

1.3.3 Excipients for pulmonary formulations

There are a wide variety of excipients currently used in nasal formulations. These include the bulking agent Avicel, the co-solvent phenylethyl alcohol, the preservative benzalkonium chloride and the surfactants Tween, polysorbate 80 and EDTA. However, there are much tighter regulations controlling the inclusion of excipients in pulmonary formulations for the clinic. As a result, there is only a small selection of excipients currently approved for inhalation use by patients. Table 1.1 lists the excipients used in currently licensed medicinal inhalation products. Mannitol, glycine (a dispersibility enhancer), and sodium citrate (an additive of high glass transition temperature), were first used in the recently approved spray-dried insulin formulation Exubera® (Fineberg *et al.*, 2007). Unless the only ingredients of a new formulation (including that of the drug particles, discussed in the next Section) are from the pool of excipients in Table 1.1, toxicology studies on the ingredients, to obtain regulatory agency approval, are likely to be required. However, using biocompatible ingredients is likely to reduce the amount of safety data required.

Table 1.1. Excipients in currently licensed pulmonary drug formulations.
N.B. The marked (*) propellants are chlorofluorocarbons (CFCs), which are being phased-out. Mannitol, glycine and sodium citrate were used in the recently approved spray-dried insulin formulation Exubera®.

Propellants	Co-solvents	Surfactants	Bulking/ protection	Others
Dichlorodifluoromethane*	Ethanol	Soya lecithin	Lactose	Sodium chloride
Dichlorotetrafluoroethane*	Phospho-ric acid	Oleic acid	Mannitol	Calcium chloride
Trichlorofluoromethane*	Sulphuric acid	Sorbitan trioleate		Water for injections
Norflurane (HFA-134a)		Sorbitan laurate		Sodium citrate/ phosphate
		Polysorbate 20		Glycine

1.4 Formulating macromolecular drugs for respiratory delivery

1.4.1 Properties of macromolecular drugs

The main classes of macromolecule used as therapeutic agents are peptides, proteins and polynucleotides. Peptides and proteins are both constructed from sequences of amino acids. Peptides consist of shorter chains of amino acids than do proteins. The physical and chemical properties of peptides can therefore often be predicted from the nature of the individual amino acids, since they primarily exist as a one- or two-dimensional chain. Proteins are larger molecules, with a three-dimensional conformation that results from the hydrogen-bonding and hydrophobic interactions, which cause the organised folding of a much longer amino acid chain. This conformation of a protein is more difficult to predict from the primary amino acid sequence (although in theory this could be possible, if other conditions are known), and is usually important for its activity (Porter, 1997). Changing environmental parameters such as pH, temperature and agitation can cause drastic changes in protein conformation, which can affect its biological activity Daugherty and Mrsny (2006). In some cases this is reversible, provided the chemical structure remains intact, and conditions are returned to normal. However, there are many potential routes for chemical degradation of proteins, including deamidation, oxidation and proteolysis that can lead to permanent conformational changes (Manning *et al.*, 1989). These conformational changes can result in protein aggregation, probably the most reported form of protein damage that can occur during preparation of the formulation (Wang, 2005). Often irreversible, and sometimes insoluble, these aggregates as well as being therapeutically inactive can invoke dangerous immune responses (Arvinte, 2005). Thus, it is essential to provide a stable formulation and suitable manufacturing process.

Peptides and proteins have a vast range of potential therapeutic uses, including hormone replacement, targeting vaccines, enzymatic activity and receptor modulation. Polynucleotides are sequences of deoxyribonucleic acid (DNA) or ribonucleic acid (RNA), and can be used therapeutically for gene therapy, vaccines and antisense therapy. This review focuses on formulating peptides and proteins rather than polynulceotides. However, many of the discussed techniques can be applied to the delivery of RNA- and DNA-like materials.

Several of the amino acids that are contained in peptides and proteins, contain ionisable side chains. The degree of ionisation depends on the solution pH, with the isoelectric point being the pH at which the net charge of the protein is zero. The isoelectric point

varies between proteins, since they contain various amounts of positively or negatively charged side chains. Peptides and proteins are least soluble at their isoelectric point, and their overall solubility will also depend on the presence of other hydrophobic side chains (Porter, 1997). For larger proteins, the degree of hydration will affect their shape, since hydrophilic groups position themselves on the protein surface, while hydrophobic groups position themselves internally. Highly hydrated proteins will aggregate less as protein-protein interactions are minimised. Generally, peptides and proteins are more hydrophilic than small drug molecules, and are often unstable in non-aqueous solvents. These factors will obviously impact on formulation characteristics.

The major difference between peptides and proteins compared with small drug molecules, is molecular weight. Whereas small drug molecules usually weigh <~0.5 kDa, proteins can vary from ~1 kDa, the approximate weight of a small peptide hormone, to ~150 kDa, the weight of an immunoglobulin (Qui *et al.*, 1997). Molecules of this size are only likely to permeate the epithelium at certain sites in the respiratory tract. Therefore, the formulations for systemic therapy may need to target specific sites.

It cannot be assumed that macromolecules have the same pharmacological properties as small drug molecules. Whereas the pharmacological aim for the latter is invariably to achieve a constant plasma level (assumed to correlate with constant drug concentration at the receptor), for the former, optimal therapeutic outcomes may occasionally rely on pulsed release, as with hypothalamic peptide hormones (Dutta *et al.*, 1993). Formulations can be designed to control the drug release profile. However, despite the extensive research (some of which is discussed below) into developing pulmonary modified-release formulations of both small drug molecules and macromolecules, no such systems are currently commercially available. This is likely to be due to the requirement to avoid clearance mechanisms, without the incorporation of potentially toxic excipients, which may accumulate upon repeated administration (Louey, 2004).

The following subsections of this thesis discuss some of the methods that have been used to formulate peptides and proteins for inhalation. Small drug molecules are generally formulated by micronising drug powder, and adding it to the device formulations. For proteins, other techniques have been explored for a number of reasons. Firstly, it is very difficult to obtain a simple protein powder, as proteins are usually kept hydrated, and drying with heat can cause denaturation, as would the shear stresses of a micronising mill. Also, due to their high molecular weight, protein molecules tend to aggregate due to increased van der Waals forces, thus making the control of particle size difficult. Secondly, a protein is unlikely to be stable when

suspended in the other excipients used in the device, such as organic propellants. Finally, as described above, a controlled-release profile may be required.

1.4.2 Polymer-based microparticles

The concept of entrapping a drug molecule in a polymer, in order to protect it or modify its release, has been explored for the past 50 years. Originally these delivery devices were implanted, and then surgically removed. Since the 1970s, the use of biodegradable polymers has negated the requirement for surgical removal, since the device chemically disintegrates over a given period, while in the body (Freiberg and Zhu, 2004). Examples of such polymers are the polyesters poly(lactic acid) (PLA) and poly(lactide-co-glycolide) (PLGA). Microparticles are polymer-based, drug-entrapment, formulations, where the size of the delivery formulation is within the micron range (1-1000 μm). Microparticles have been designed for incorporation into oral capsules, for parenteral administration and for delivery to mucosal surfaces. For each of these applications, the aim of formulating as a microparticle is to either increase the stability of the entrapped drug to the outside and body environments, or to modify the release of drug within the body (Vasir *et al.*, 2003).

With more specific nomenclature, microparticles are often referred to as microspheres or microcapsules. Microspheres are monolithic polymer spheres, where drug is homogeneously dispersed throughout a spherical polymer matrix. Microcapsules have a hollow, central, core, containing high concentrations of drug, which are enveloped by a layer of polymer. For much of the literature reviewed below, the method of producing these two types of microparticles is essentially the same, but with small variations of the method parameters, producing spheres of particle- or capsule-type characteristics. As a result, there is usually some degree of overlap, with microparticles having properties somewhere between the microsphere and microcapsule definitions. However, a nano-coating method has been used to make purely capsule-type PLGA particles, using a very small amount of polymer in an outer layer (Hardy and Chadwick 2000).

Microparticles have generated much interest for use in pulmonary and nasal delivery of proteins. If produced at the lower end of the micron scale (1-5 μm), microparticles would be ideal for delivery to all sections of the airways. Microparticles could potentially allow proteins to be suspended in organic propellants, prolong release of the protein, and enhance the protein's bioavailabilty (Agu *et al.*, 2001).

1.4.3 Manufacturing polymer microparticles by solvent-evaporation

Solvent-evaporation is the most extensively used method for polymer microparticle

production (Vasir *et al.*, 2003). In this method, microparticles are formed from emulsified droplets of a polymer-containing oil phase, dispersed in an aqueous continuous phase. The drug is also dispersed in the oil phase, so that as the solvent in the oil phase evaporates, the polymer precipitates, thereby entrapping the drug. However, because protein drugs are hydrophilic, and thus will not dissolve, or are unstable, in the organic solvents of the oil phase, a double-emulsion method is used. This is where a water-in-oil-in-water (W/O/W) emulsion is employed, such that the drug is in an aqueous phase within the oil dispersed phase. Such emulsions have also been used, without further processing (i.e. without the aim of producing microparticles), for the modified release of drugs such as insulin (Cole and Whateley, 1997). The double-emulsion/solvent-evaporation method was first described by Ogawa *et al.* (1988).

The inner water phase comprises the drug solution with or without an emulsifier. In the case of Ogawa *et al.*, the drug was the peptide leuprolide acetate, and gelatin was the emulsifier. The oil phase contained the encapsulating polymer (PLA or PLGA), dissolved in an organic solvent (dichloromethane, DCM). The primary (W/O) emulsion was formed by slowly adding the oil phase to the inner water phase, under vigorous stirring with a homogeniser or ultrasonicator. The emulsion was then poured through a fine nozzle into the outer water phase (0.5% poly(vinyl alcohol), PVA aqueous solution), again while being homogenised, to generate the double-emulsion. The DCM was then evaporated using a propeller mixer, or rotary evaporator, leading to the formation of hardened microparticles. The microparticles were finally sieved from the outer aqueous phase, and dried into a powder by freeze-drying (Section 1.4.6). The method is illustrated in Figure 1.13. In order to preserve volatile flavours in the food industry, this technique has been taken one step further by preparing particles by the spray-drying of O/W/O/W triple-emulsions (Edris and Bergnaståhl, 2001).

Many other researchers have employed the technique described above. However, variations include the use of different ingredients, such as drug, polymer and emulsifier, drying by vacuum pump rather than lyophilisation (Yang *et al.*, 2000), and using solvent extraction rather than solvent-evaporation (Spiers *et al.*, 2000). Solvent extraction involves a further co-solvent, such as an alcohol, which is added to the W/O/W emulsion before rotary evaporation. The presence of the co-solvent favours the partition of the solvent into the external aqueous phase, from where it evaporates at the water/air interface. The result is a reduced time for solvent evaporation. An alternative to freeze-drying for the final step has been to use spray-drying (Lane *et al.*, 2006). However, as discussed in Section 1.4.4, particle diameter is then primarily controlled by the spray drier atomisation rather than by the properties of the emulsion.

Figure 1.13 A simplified schematic of the water-in-oil-in-water (W/O/W) emulsification method for microsphere production. Taken from: Fu *et al.*, 2002.

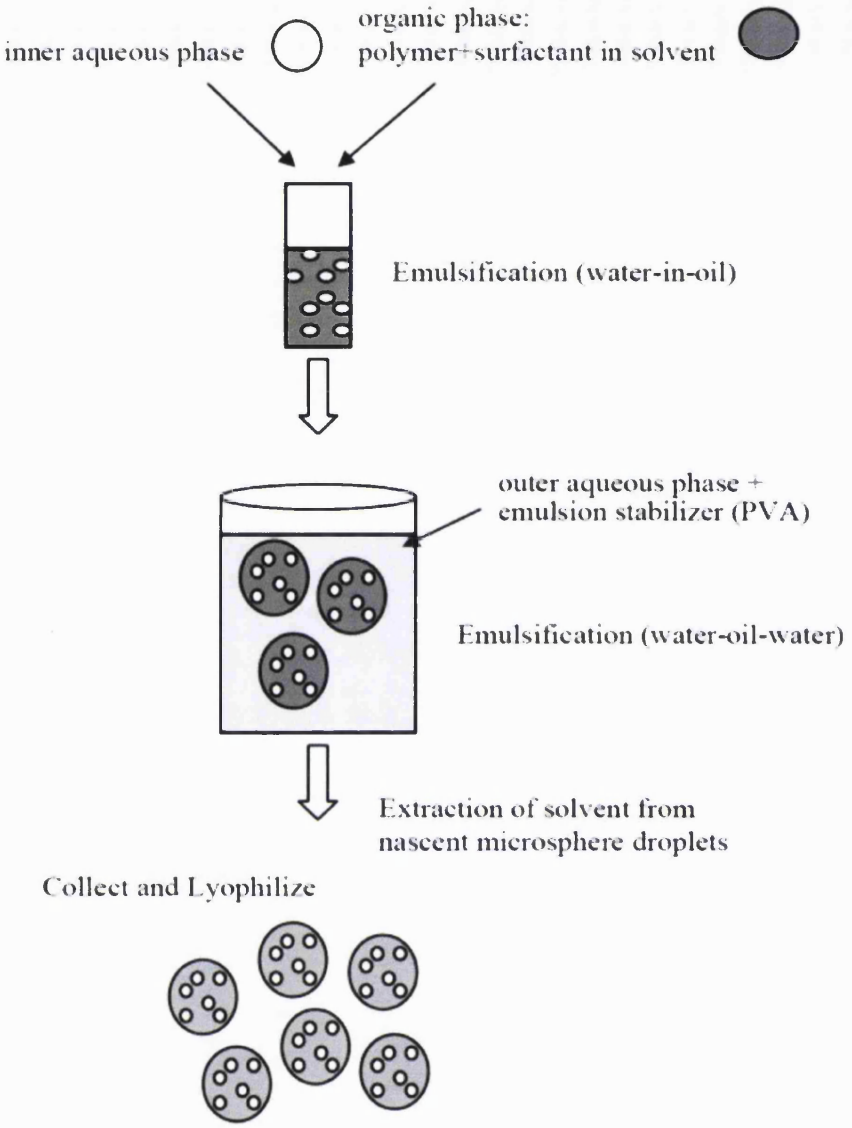

1.4.3.a) Experimental parameters affecting microparticle character

Within the double-emulsion/solvent-evaporation method, there are many parameters that can be altered to produce microparticles of very different specification. Below are described some of the findings published in the literature. Although there were often rational explanations for the findings, prediction of the effects of a technique alteration may not always be intuitive.

The pioneering experiments of Ogawa *et al.* (1988) discovered that the addition of an emulsifier, gelatin, to the inner aqueous phase resulted in a ten-fold increase in drug encapsulation efficiency (EE - this is defined as the actual drug content of the microparticles, as a percentage of the expected content). This was because the gelatin stabilised the primary emulsion, preventing leakage of the drug into the external

aqueous phase. Yang *et al.* (2001), who used PVA rather than gelatin as the internal phase emulsifier, found this also reduced the initial burst-release, since less drug leaked to the surface of the microparticles. Ogawa *et al.* (1988) also found that increasing the viscosity of the phases, by decreasing the volume of inner aqueous and oil phases, relative to the drug and polymer concentrations, resulted in an increased EE. This finding was confirmed by Spiers *et al.* (2000), who explained that increasing the viscosity of the emulsion, resulted in faster microparticle precipitation, thereby reducing the time for drug to diffuse out of the dispersed phase. They also demonstrated that the viscosity of the emulsion could also be increased by decreasing the emulsion temperature, which again increased EE. However, it has been reported that increasing temperature, above a certain critical point (which in that study was 38°C), once again resulted in an increased EE (Yang *et al.*, 2000). This non-linear relationship between temperature and EE was explained as follows. Increasing the rate of polymer precipitation, increased EE. Reducing the temperature increased viscosity, and increasing the temperature accelerated solvent-evaporation, both of which increased the rate of polymer precipitation. Above the critical temperature, the latter effect predominated, such that it more than compensated for the loss of viscosity (Freiberg and Zhu, 2004). Increasing microparticle diameter, by means of employing a slower homogenisation speed, a reduced volume of external aqueous phase, or an increased viscosity, further increased EE. This was because there was more distance between the two aqueous phases preventing drugs diffusing out of the emulsion (Ogawa *et al.*, 1988). However, for the application of pulmonary delivery, smaller particles are likely to be favoured, and so high EEs must be achieved by other means.

Yang *et al.* (2001) further investigated the effects of various experimental conditions on microparticle diameter. They confirmed the observations of Ogawa *et al.* (1988) that stir speed and phase viscosity affected final particle size. Increasing the stir speed caused the emulsion to break up into smaller droplets, thus producing particles of a smaller diameter. Increasing the viscosity of the phases, by increasing their concentration, or reducing temperature, increased the resistance to the break up of the dispersed phases by the homogeniser, thereby resulting in larger particles. Yang *et al.* (2001) also found that increasing the concentration of PVA emulsifier in the external aqueous phase reduced particle size, with an increase in PVA from 0.05% to 0.50%, resulting in a reduction of mean microparticle size from 142 to 104 μm. This was attributed to the PVA preventing coalescence of the disperse phase, thus preserving smaller droplets [in spite of the fact that adding PVA caused an increase in the viscosity (Freitas *et al.*, 2005), which would have been expected to increase microparticle

diameter]. The stability of the protein drug should also be considered, given the shear, surface and thermal stresses occurring during the homogenisation process. In one study, conformational changes to the structure of proteins were reported. However, these were reduced by the addition of trehalose to the internal aqueous phase (Fu *et al.*, 1999).

1.4.4 Manufacturing microparticles by spray-drying

An alternative, but increasingly more popular method for generating microparticles, is the technique of spray-drying. This is where a liquid is fed into the spray drier, which atomises it into a fine mist. The mist is then exposed to high temperatures, thereby drying it into solid particles. A schematic diagram of a lab-scale spray drier is shown in Figure 1.14. The size of the atomised droplets can be controlled, such that particles can be manufactured with a diameter range suitable for inhalation. Because of the high thermal stress, and the stress of storage in the dried state, one cannot successfully spray-dry a simple aqueous solution of a protein. This would result in denaturing of the protein at the gas-liquid interface during drying, and powder aggregation during storage (Andya *et al.*, 1999). Therefore, other liquid protein formulations have been employed for feeding into spray driers.

Figure 1.14 Schematic of a Büchi-191 lab-scale spray drier. Liquid feed of dissolved material is pumped into the nozzle, where compressed air atomises it into fine droplets. Heat is applied in the drying chamber, which evaporates the liquid, resulting in dry particles. These particles are separated from the airflow (generated by the aspirator) by the cyclone, and a powder product is collected in the collecting vessel. Some of the adjustable parameters are listed.

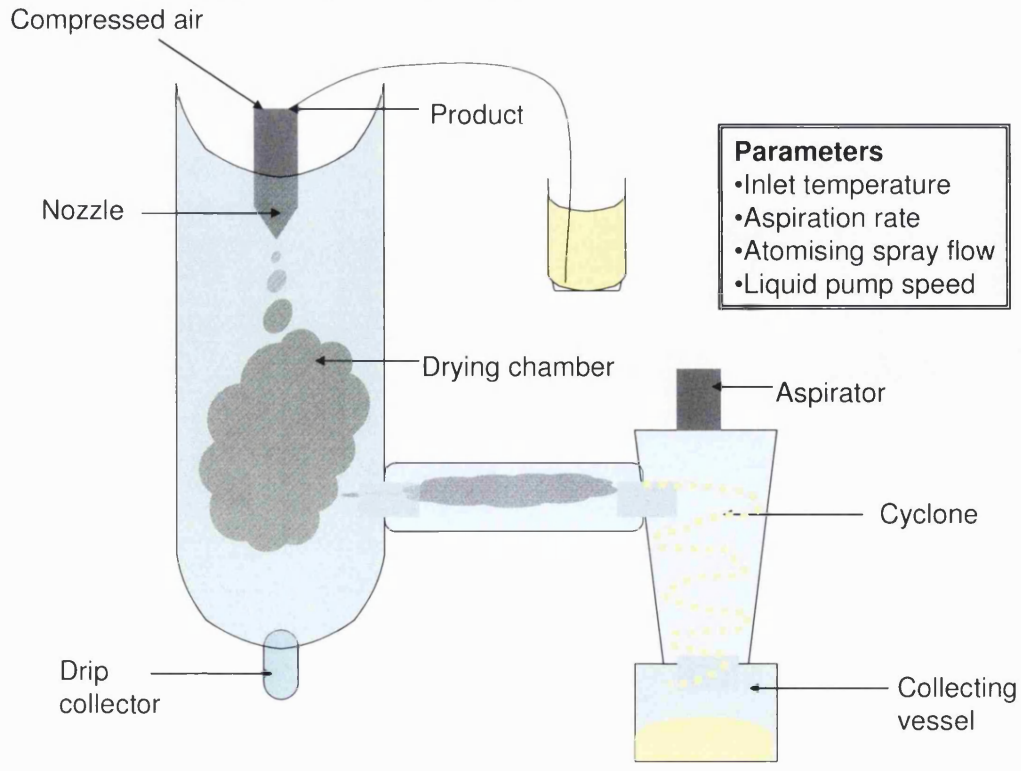

Andya *et al.* (1999) investigated adding various carbohydrates to the protein solution, prior to spray-drying, at molar ratios of 100:1 to 900:1, carbohydrate:protein. Addition of mannitol, trehalose and lactose increased microparticle stability, in terms of preserving protein conformation (measured by circular dichroism), and long-term powder stability. The carbohydrates may have induced this improvement by a number of mechanisms. Firstly, the high glass transition temperature (T_g) of these carbohydrates meant that they remained in the glassy state during the spray-drying process. Therefore, the proteins remained stabilised within a glassy carbohydrate matrix, since their mobility and flexibility were reduced (Michalovic *et al.*, 1995). Secondly, it was also thought that the carbohydrate replaced water, effectively 'hydrating' the protein molecules, by forming hydrogen bonds with surface amino acids. This stabilised the protein conformation, and reduced protein aggregation, since protein-carbohydrate interactions reduced the instance of protein-protein interactions. At higher mannitol and trehalose concentrations, there was a detrimental effect on the size of the aerosolised microparticles, with a reduced proportion being <~7 μm (known as the fine particle fraction, FPF). However, this reduction in FPF was not observed at any lactose concentration. Lactose would also appear a good choice of excipient, since it is approved for use in inhaled formulations. However, unlike trehalose and mannitol, it caused some glycation of the protein, which may have affected its biological activity.

Spray-dried microparticles have also been produced using the polymer, PLGA, which is commonly employed in the double-emulsion/solvent-evaporation method, described above. In direct comparisons between these two methods of PLGA microparticle production, spray-drying was found to be superior to solvent-evaporation. For example, spray-dried particles have been shown to have higher and more consistent EEs, compared to particles produced by solvent-evaporation (Takada *et al.*, 1995; Schwach *et al.*, 2003; Lane *et al.*, 2006) (the last of these three studies directly compared freeze-drying and spray-drying a double-emulsion). One reason for this is that provided optimal drying parameters are selected, all dissolved, solid, material fed into the drier can be potentially dried, compared to solvent-evaporation, where any water soluble component that escapes to the external phase is washed away. In another comparative study (Blanco-Prieto *et al.*, 2004), spray-drying produced PLGA microparticles of a smaller, less widely distributed size of ~1-15 μm, with the majority <~5 μm, whereas solvent-evaporation yielded microparticles of ~10-70 μm diameter. However, other studies have demonstrated that with optimum experimental conditions, solvent-evaporation methods can produce microparticles consistently sized between ~1-10 μm (Spiers *et al.*, 2000).

For spray-drying, parameters such as feed rate, nozzle size, atomisation pressure and liquid feed concentration will determine the size of the microparticles. The range of the particles sizes that can be produced will be limited by the efficiency of the cyclone (the lower limit) and the drying capacity of the drying chamber (upper limit). The smooth, spherical quality of particles can also be improved with addition of a plasticising excipient, such as citric acid (Vasir *et al.*, 2003), and is also determined by the droplet drying rate. For the solvent-evaporation method, the particle size is dependent on the emulsion droplet size, and thus can be controlled by the homogenisation time and speed, and the viscosity of the phases.

Spray-drying is a relatively simple method for the production of microparticles, which is less dependent on the solubility and emulsification properties of the drug and polymer, than are solvent-evaporation methods. Spray-drying can consistently produce microparticles of respirable diameters, and the process is robust on scale-up (Vasir *et al.*, 2003).

1.4.5 Solid/oil/water emulsions and spray-freeze drying

Solid/oil/water (S/O/W) emulsions are another approach that has been employed to improve the limited stability of proteins in W/O/W emulsions. For some unstable proteins, a loss of activity can occur at the water/oil interface, due to breakage of disulfide bridges resulting in conformational changes. The S/O/W method incorporates the use of a solid protein phase rather than an aqueous solution, and thus should reduce the loss of activity. Morita *et al.* (2000) produced a protein powder by freeze-drying a poly(ethylene glycol) (PEG) and protein mixture (freeze-dried protein powders are discussed in more detail in Section 1.4.6). This was then used to produce a S/O/W emulsion, from which microparticles could be produced, as described in Figure 1.15. PEG was able to dissolve in organic solvents used in the emulsion, thus aiding the even dispersion of protein in the O/W emulsion. The microparticles produced by this method were superior in terms of EE and protein functional integrity.

Wang *et al.* (2004) encapsulated immunoglobulin G into microparticles using a S/O/W method. They produced their protein powder by spray-freeze drying. This involves an aqueous protein solution, containing a carbohydrate excipient being atomised by ultrasonication, producing droplets which are frozen and freeze-dried. This avoids the high, potentially degenerating, temperatures of spray-drying. As described previously, the protein powder was then added to a PLGA O/W emulsion to produce a S/O/W emulsion, from which microparticles where produced by solvent evaporation. Wang *et al.* (2004) found that microparticles produced by this method had a smaller size, and a

better protein stability and activity, than microparticles produced by a W/O/W, solvent-evaporation method. This was due to both the lack of presentation of dissolved protein at an O/W interface, and the stabilising effect of the carbohydrate in the solid formulation. If a modified-release formulation is not required, then the spray-freeze drying step could potentially be used alone, in order to produce solid protein microparticles for inhalation.

Figure 1.15. Schematic of the solid-in-oil-in-water (S/O/W) emulsion method of polymer microsparticle production. Other protein solidification techniques such as spray-freeze drying or spray-drying could be used for the first step. Taken from: Morita *et al.*, 2000.

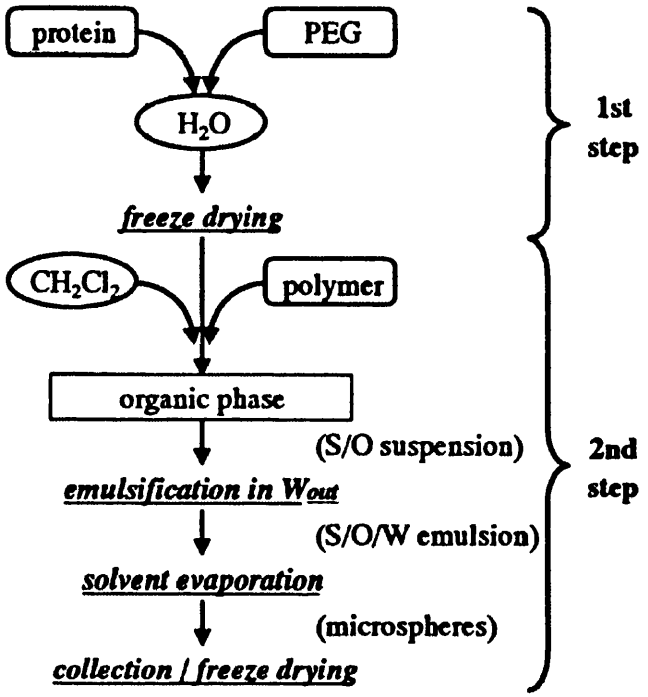

1.4.6 Freeze-drying

Freeze-drying, or lyophilisation, is a technique to generate dry powders from aqueous solutions. Briefly, the aqueous solution is frozen by reduced temperature. Primary drying then occurs by maintaining the low temperature and reducing pressure, such that the ice sublimes directly into water vapour. Secondary drying then occurs as the temperature is slowly increased (Tang and Pikal, 2004). Freeze-drying has already been described for use in the final stage of the double-emulsion/solvent-evaporation method to produce a dry microparticulate powder. However, for more simple formulations, the freeze-drying of an aqueous protein solution is an option for generating an inhalable powder. The process is slow and expensive, but fine, dry powder, suitable for storage is produced, and protein structure is preserved on reconstitution. However, in the case of antibody formulations, at least one additional excipient was required to prevent protein aggregation (Wang *et al.*, 2007a). For example, the percentage of soluble aggregates of a freeze-dried antibody-cytotoxic drug conjugate was reduced when glycine and

mannitol were employed as excipients. Unfortunately, simple protein-only powders are unsuitable for dry-inhalation delivery, because of poor stability and cohesiveness, resulting in unsuitable aerodynamic qualities. However, freeze-drying a protein-surfactant mixture yielded a more stable solid carrier, which could be suspended in an HFA propellant, using ethanol as a wetting agent (Williams III and Liu, 1998). Freeze-dried lipid:polycation:DNA complexes with lactose, produced particles with a more efficient dose emission from a capsule dry-powder device, than when the same formulation was spray-dried. However, of this emitted dose, the spray-dried formulation was superior in terms of the fraction of particles that were of respirable diameter (Li *et al.*, 2003).

1.4.7 Coacervation

Coacervation was one of the original methods of microparticle production. Briefly, this is a phase separation method, where the polymer, for example PLGA, and the drug are dissolved in an organic solvent. The addition of a non-solvent, such as poly(dimethylsiloxane), causes precipitation of the polymer. The precipitated droplets form solid microparticles, potentially in the sub-micron size range, encapsulating a quantity of drug within. However, EEs for this method are low, particularly for hydrophilic molecules. Thus, for proteins, which all exhibit poor solubility and stability in solvents, this method was less favoured than solvent evaporation techniques, with W/O/W emulsions. Nevertheless, there is still some potential to using the coacervation method with proteins. McGee *et al.* (1995) formulated a protein by first producing a W/O emulsion of the protein solution and silicone oil. After addition of dichloromethane, the emulsion was put into a large volume of heptane. Heptane caused phase separation by solvent extraction, and resulted in particle formation. The particles produced using a particular set of parameters, had a zero-order release profile. Carrasquillo *et al.*, (2001), used a stabilised protein-trehalose powder, produced by spray-freeze drying (described in Section 1.4.5). This powder was then suspended in organic solvent, and was encapsulated by polymer, upon the addition of an anti-solvent.

1.4.8 Supercritical fluids

One of the safety concerns regarding the solvent evaporation method is the possibility of residual organic solvents being present in the final product. Supercritical carbon dioxide has been explored as an alternative method to avoid organic solvent use, and has the added advantage of not requiring the high temperatures of spray-drying. Carbon dioxide is used at temperatures and pressures where the liquid and gas forms have the same densities, and therefore simultaneously exist in equilibrium; i.e. above the critical

point, 73.8 bar and a temperature of 31.1°C (McHugh & Krukonis, 1994). At these supercritical conditions, carbon dioxide is a fluid, with solvent-like properties. Unfortunately, proteins are sparingly soluble in carbon dioxide, and so its use as a direct solvent is limited. However, supercritical carbon dioxide has shown promise as a protein anti-solvent. This involves addition of carbon dioxide to a drug solution, thereby reducing solvency and so causing precipitation. The research by Bustami *et al.* (2000) provided an example of how this could be applied to protein microparticle production. They used a modified, ethanol-containing, carbon dioxide anti-solvent to cause precipitation of an aqueous protein solution while it was being finely sprayed into a precipitation chamber. This technique initially produced nano-sized particles, which aggregated to form micron-sized agglomerates, suitable for inhalation. Protein integrity varied with individual proteins, and operating conditions, although many of the structural alterations were reversible on re-solvation. A similar technique has been used to produce particles of the small-molecule drug salmeterol xinafoate. The powders produced were less adhesive than micronised drug powders (Shekunov *et al.*, 2002).

Removal of residual organic solvents is another potential application of supercritical carbon dioxide. Herberger *et al.* (2003) formulated PLGA microparticles by a two-stage spray-drying process, where protein solution was initially spray-dried to form a protein powder, which was subsequently suspended in a PLGA organic solution, and this suspension was then spray-dried. Residual solvents where then removed from the microparticles by carbon dioxide extraction. However, it was found that liquid carbon dioxide had detrimental effects on microparticle morphology and protein integrity, although it was anticipated that with an optimisation of experimental conditions, the process may prove to be successful.

1.4.9 Entirely aqueous systems

Epic therapeutics, a subsidiary of Baxter Healthcare, has developed a method to manufacture microparticles, using only aqueous solutions. The technology, which they have named, PROMAXX®, is actually a collection of different methods to produce microparticles for injection or inhalation that can be used to deliver small molecules, DNA, peptides, or proteins. This has included a method for the pulmonary delivery of insulin. The principle of the technique is the same, irrespective of the actual ingredients. The starting point is an aqueous solution of a macromolecule, which is usually the therapeutic protein drug or DNA. However, for delivery of small drug molecules, a carrier protein such as albumin is used. The solution is pH buffered to the isoelectric point of the protein. A hydrophilic polymer, such as a carbohydrate, is then

added to the solution. Addition of the polymer removes water from the macromolecule as the polymer is hydrated. This "dehydration" of the macromolecule results in the formation of spherical microparticles by volume exclusion. Microparticles can then be stabilised by a number of methods, depending on the particular ingredients used, and the properties required. These stabilising methods include the addition of a cross-linking agent, application of heat and stirring. The end product is microparticles that consist of 70-98% macromolecule (e.g. the therapeutic protein), with the remainder being polymer. The ratio and choice of ingredients, and experimental parameters, can be reproducibly controlled to produce a range of release rates and particle sizes (Scott *et al.*, 2002; Brown *et al.*, 2006; Rashba-Step, 2007).

1.4.10 Liposomes

Liposomes have been one of the most extensively investigated drug delivery systems in recent decades. They exploit the phenomenon observed in cellular membranes, where amphiphilic lipids spontaneously form a bilayer, such that the aqueous intracellular and extracellular environments are separated by a hydrophobic region. Liposomes are usually constructed from the evaporation of solutions of physiological lipids, such as dipalmitoyl phophatidylcholine (DPPC). In an aqueous environment, the lipids form one or more concentric bilayers, denoted as unilamella- and multilamella-liposomes, respectively. Hydrophilic drugs, such as proteins, are retained between the charged, head-regions of the lipids, at the edges of the bilayers (Gupta & Adjei, 1997).

Inhaled liposomal formulations have been delivered by nebulization. A dry powder formulation of liposomes, in a Spinhaler® device, has also been investigated. This would have a portability advantage, as well as potentially reducing the structural damage to the lipid and protein, caused by nebulization (Gupta & Adjei, 1997). Liposomes prolong retention of the protein in the respiratory tract, and provide controlled protein release (Gupta & Adjei, 1997). They may also mediate uptake of biomolecules into cells, by interactions with cellular membranes (Alpar *et al.*, 2005). However, compared to microparticles, liposomes are less physically and chemically stable, and protein encapsulation rates are lower (Gupta & Adjei, 1997). In one study, though, a liposomal formulation of tobramycin prolonged drug residency in the lung compared to a polymer microparticulate formulation (Poyner *et al.*, 1995). The advantage of prolonged drug retention has been achieved while reducing the aforementioned disadvantages by producing an inhalable metered-dose inhaler formulation containing lipids that spontaneously form controlled-release liposome-like colloids upon contact with pulmonary fluid (Alouache *et al.*, 2006).

1.4.11 Crystallisation

A microcrystallisation process has been used for the pulmonary delivery of insulin. Larger, zinc insulin crystals have been used for many years as a long-acting, injectable formulation. However, microcrystals of ~3 μm diameter, suitable for deep-lung delivery, have been produced by a seed zone method. An insulin solution was dissolved in acetic acid, and the pH was raised to 10.5, known as the "seed zone" pH (Kwon *et al.*, 2004). Insulin-protamine-zinc complexes have also been formulated as large porous particles (see Section 1.4.13) by spray-drying an acidified solution. Slow-release insulin complexes then formed *in situ* upon aqueous dispersion of the formulation (Vanbever *et al.*, 1999a). However, whether techniques relying on crystallisation can be applied to other, larger, proteins is questionable, since protein crystals are difficult to prepare.

1.4.12 Protein adsorption onto microparticles

Protein drugs can be adsorbed to the carrier surface, rather than being entrapped within the carrier. Glass, poly(styrene) and latex beads have been used since the 1960s to immobilize proteins. For example, enzymes adsorbed to glass beads are used for laboratory experiments. This allows the enzyme to be recovered, and reused, after completion of a chemical reaction. Antibodies and other proteins adsorbed to latex beads are used for a variety of assays and chromatographic separation methods. Proteins are linked to the bead either by chemical conjugation, or by adsorption due to ionic or physical forces. The protein remains active on the surface of the bead (Rosevear *et al.*, 1987; Liang *et al.*, 2000; Siimon *et al.*, 2001).

Polymer beads can be made by a variety of methods that involve the cross-linking of monomer units. Using a surfactant-stabilised dispersion of a monomer in an organic liquid can result in nanometre-sized beads. By using a water-soluble cross-linking initiator, cross-linking is limited to within the surfactant micelles, thus yielding very small beads. Using an initiator that is soluble in organic solvents, yields beads in the micron-size range (Freiberg & Zhu, 2004). In terms of drug delivery, beads made out of biocompatible polymers such as poly(ethylene glycol) or alginate could be used (Dashevsky, 1998), or indeed protein can be adsorped onto PLGA microparticles fabricated by the double-emulsion method (Section 1.4.3) (Chesko *et al.*, 2005). However, this is likely to have a number of disadvantages compared to microencapsulation. Firstly, the protein capacity of the carrier will be less, since drug is only adhered to the surface, rather than entrapped throughout the carrier. Secondly, proteins may be less stable on the surface of the carrier, since they are more exposed to

the outside environment. Finally, release will depend on how labile the protein-carrier bond/interaction is, rather than on the release from the polymer by diffusion or degradation. Nevertheless, adhering proteins to the surface of a solid carrier may have some applications for drug delivery to specific sites. For example, antibodies or adhesion molecules could be attached to the surface of a drug-containing microparticle for targeting purposes (Yun *et al.*, 2004).

1.4.13 Microparticle porosity

Microparticles can be categorised as being porous or non-porous. Porous microparticles exhibit pores on their surface that can be visualised by microscopy. These pores extend into the internal structure of the microparticle, forming a network of tortuous tunnels that run from the surface to the core (Li *et al.*, 1995). Figure 1.16 is an example microscope image of a visibly porous microparticle.

Porous microparticles have unique characteristics, which are potentially advantageous for pulmonary formulations. Firstly, because a significant proportion of the sphere volume is empty space, filled with the surrounding air, the effective aerodynamic diameter of porous microparticles is substantially smaller than the geometric diameter. For example, porous microparticles produced by Bot *et al.* (2000), had a mean aerodynamic diameter of 4.6 μm, as determined by a time-of-flight method, whereas the mean geometric diameter, measured by laser diffraction, was 7.0 μm. As explained in previous sections, a reduced aerodynamic diameter increases the probability of deep lung deposition, due to reduced particle inertia. Therefore, porous microparticles can potentially enhance the targeting of drugs to alveolar regions of the lung, while having a surface area small enough to reduce particle aggregation, and a geometric diameter large enough to avoid phagocytosis by macrophages (Edwards *et al.*, 1997 and 1998).

Figure 1.16 Scanning-electron microscope image of a porous microparticle. Taken from Wang *et al.*, 2004.

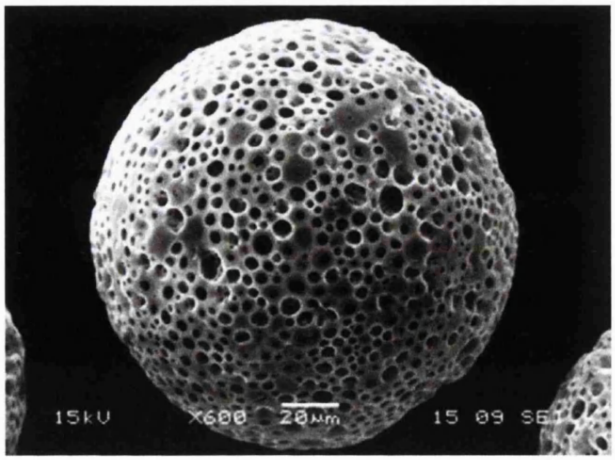

Secondly, porosity can improve the stability of metered-dose inhaler suspensions. Dellamary *et al.* (2000) found that HFA propellant penetrated the pores of their hollow, porous, microparticles, forming, what they termed, a homodispersion. Because the dispersed particles were largely composed of propellant, the density difference between these fluid-filled particles, and the continuous propellant phase, was almost negligible. As described in the previous Section, density differences between the dispersed particles, and the continuous phase, is a driving force for suspension creaming. The authors also proposed that van der Waals forces were reduced in this format, because of a decreased Hamaker constant. The Hamaker constant is proportional to the difference in polarisability of the dispersed and continuous phases. Again, because the dispersed phase of this system was largely composed of continuous phase, this difference was small. The result of reduced van der Waals forces was a reduction in particle aggregation, and thus increased suspension stability.

Finally, porosity can alter the drug release characteristics. Drugs are released from polymer microparticles by several mechanisms. Firstly, drug bound to the surface of the particle is released rapidly, once the particle is placed in a medium that the drug can dissolve into (e.g. saline *in vitro*, blood or secretions *in vivo*). This phenomenon is often termed the 'burst effect' (Huang *et al.*, 1999). Secondly, drug can be released more slowly, from within the microparticle, by diffusion through the polymer matrix. However, for protein drugs, this process is estimated to be negligible, as high molecular weight, hydrophilic molecules cannot partition out of, or permeate through, the polymer matrix. Therefore, the bulk of drug release occurs as a result of polymer degradation. In the case of microparticles made from hydrophobic, bulk-eroding polymers, such as poly(lactic acid) (PLA) and poly(lactide-co-glycolide) (PLGA), complete degradation can take weeks to months, depending on the polymer molecular weight, polymer crystallinity and the conditions of the release media (Fu *et al.*, 2002). However, by introducing porosity, a further mechanism of drug release is introduced. Once an aqueous fluid permeates the pores, protein drugs can diffuse through the pores. Thus, porosity results in an increased rate of protein release from microparticle formulations. This is exemplified in Figure 1.17, where Yang *et al.* (2000) found that introducing porosity resulted in a faster rate of zero-order protein release. Such kinetics may be more appropriate for inhaled drugs. However, porosity may also result in an increased burst effect, which may be undesired (Freiberg and Zhu, 2004). In one example, microparticles produced by a solvent-evaporation method were more porous than the same formulation produced by spray-drying, resulting in a greater initial burst-release (Witschi and Doelker, 1998a).

Figure 1.17 Release of bovine serum albumin from polymer microparticles, formed at different temperatures. The microparticles formed at 38°C had porous characteristics, and thus had a faster release profile. Taken from: Yang *et al.*, 2000.

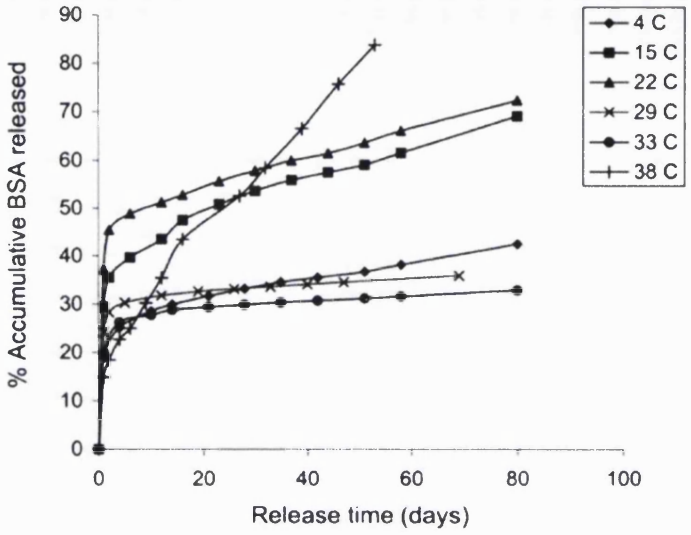

Yang *et al.* (2001) explored the factors controlling the porosity of polymer microparticles produced by the double-emulsion/solvent-evaporation method. Increasing the amount of emulsifier in the internal aqueous phase caused a reduction in porosity, because the inner water droplets were stabilised from coalescence by the emulsifier. When the emulsifier concentration was reduced, however, inner water droplets coalesced, and migrated to the surface of the oil phase, forming pores. During the drying process, the water evaporated to leave pores in the microparticles. In addition, increasing the volume of the internal aqueous phase increased porosity, with the complete removal of an inner aqueous phase, resulting in non-porous, monolithic microparticles (Crotts and Park, 1995). Increasing the viscosity of the oil phase, for example by reducing the oil phase volume, has also been found to increase porosity. This was because the inner water droplets were then less able to migrate out of the inner emulsion, and remained trapped within the oil phase, leading to the formation of pores as they coalesced (Yang *et al.*, 2001). However, increasing viscosity by increasing the polymer concentration, rather than reducing oil phase volume, slightly reduced porosity, possibly because this prevented water droplets coalescing in the internal phase (Yang *et al.*, 2001). Increasing solvent evaporation rate can also increase porosity. In a similar scenario to the paradox of EE described above, moderate increases in temperature reduced porosity, presumably because the viscosity was decreased, allowing water to escape into the continuous phase. However, above a critical temperature, the evaporation rate was so high that the polymer precipitated before the water could escape, thus increasing porosity (Yang *et al.*, 2000). Therefore, the factors controlling porosity were complex, with interplay between many competing mechanisms. However, if porosity is required, it is important to identify those parameters that achieve

porous microparticles without too much compromise on particle diameter range and EE.

Microparticle porosity has also been achieved using a spray-drying method, but by different mechanisms to those described for W/O/W double-emulsions. Vanbever *et al.* (1999b) spray-dried an ethanolic solution of dipalmitoylphosphatidylcholine, lactose, albumin and drug, to produce porous particles. Dellamary *et al.* (2000) produced porous microparticles by spray-drying a mixture of two liquids. The first liquid was an emulsion of a fluorocarbon, perfluorodecalin, in water, stabilised by the emulsifier phosphatidylcholine. Phosphatidylcholine and dipalmitoylphosphatidyl choline are lipids present in both lung surfactant, and in soy lecithin, one of the already approved emulsifiers for inhalation. The emulsion was mixed with an aqueous drug solution, which in this case was Cromolyn®, although this technique has since been applied to protein drugs (Bot *et al.*, 2000). The fluorocarbon acted as a 'blowing agent', creating pores, as it evaporated during spray-drying. This generated hollow, porous microparticles composed 50/50 of the drug and emulsifier. These were known as spray-dried lipid microparticles (SDLM), or Pulmospheres, and in this case had a respirable fraction of 68%. Using flurocarbons of lower boiling points than perfluorodecalin, produced hollow microcapsules, which were non-porous (Dellamary *et al.*, 2000). Dellamary *et al.* (2004) produced SDLM, but without the inclusion of a blowing agent. As expected, this produced non-porous particles. In this study, the lipid was complexed to calcium ions, which resulted in an increased chemical and thermal stability of the microparticles. Hollow particles, with presumably the same aerodynamic advantages as large porous particles, have been prepared by the spray-drying of other materials (Wang *et al.*, 2007b).

1.4.14 Materials used to control drug release from microparticles

1.4.14.a) Polyesters

Many of the microparticle formulations described above, employ a polymer material to encapsulate the active drug, and which constitutes the bulk of the microparticle material, thus controlling drug release. Poly(esters), such as poly(lactic acid) (PLA), poly(glycolic acid) (PGA) and block co-polymers of these two (poly-lactide-co-glycolide, PLGA) (monomer structures given in Figure 1.18), are most commonly used for this purpose due to their accepted bio-compatibility. These polymers, although not endogenous molecules, degrade into lactic acid and glycolic acid, which are products of endogenous metabolism. Therefore, they have been used as biodegradable sutures and biodegradable, injectable drug delivery depots (Ogawa *et al.*, 1988).

Figure 1.18 Chemical monomer structures of poly(lactic acid) PLA and polyglycolic acid (PGA). Taken from: Freiberg and Zhu, 2004

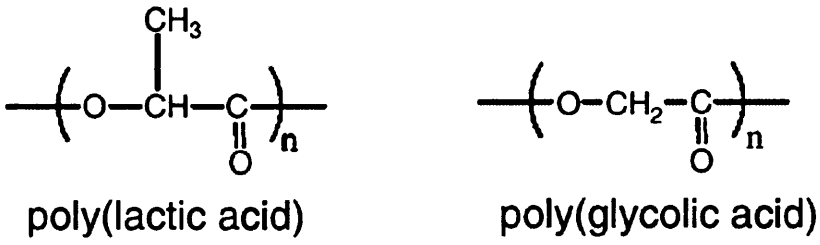

Proteins are poorly soluble in poly(esters), and so their release is controlled by degradation of the polymer. Poly(esters) are generally hydrophobic, and bulk erode. The hydrolysis of poly(esters) is autocatalytic, with the hydrolysis of each bond generating an H^+ ion. This increases the rate of subsequent degradation, due to acid-catalysed hydrolysis. Therefore, the overall degradation and drug-release profile can be difficult to predict. However, there are several factors that can be altered to control drug release from poly(esters). Firstly, degradation rate is slower when polymers of a higher molecular weight are used. There is also evidence to suggest that higher molecular weight polymers provided a less constant, two-stage release profile. Therefore, an optimum release profile may come from mixing a combination of low and high molecular weight polymers (Freiberg and Zhu, 2004). Secondly, degradation is faster in amorphous, rather than crystalline, regions of the polymer. Altering the ratio of PLA and PGA in PLGA block co-polymers can control the degree of crystallinity. Although the glass transition temperature (T_g) marks a change of kinetic state between the glass and rubber forms of an amorphous polymer, a high T_g correlates to a higher polymer melting temperature, and thus indicates a more crystalline polymer (Michalovic *et al.*, 1995). Pure PLA (particularly the pure L-isomer, PLLA) has a higher T_g and is more crystalline than PLGA. Spiers *et al.* (2000) demonstrated that microparticles composed of pure PLLA released drug more slowly than PLGA microparticles. In addition, they showed that incorporating a mixture of PLGA and PLLA resulted in a two-phase release, coinciding with the degradation of the respective polymers. Thirdly, increasing the ratio of PGA to PLA in PLGA increases the hydrophilicity, thus increasing the polymer degradation rate. However, pure PGA cannot be used due to a compromise of solubility in organic solvents, which are usually required for the manufacturing process.

Altering molecular weight and PLA/PGA ratios to their extremes, results in a variation of degradation time from several months to several weeks. However, this may not be appropriate for protein delivery *via* the pulmonary route, where an hours-to-days release profile is likely to be more therapeutically advantageous. Another caveat related to

poly(ester) systems, is the generation of a concentrated acid environment during the degradation process. This may firstly cause chemical hydrolysis of the protein, reducing dosing efficiency, and secondly, damage surrounding tissue (Fu *et al.*, 2002). Therefore, other polymers have been investigated for use in microparticle formulations.

1.4.14.b) Other synthetic polymers

Poly(ether-anhydride)s are examples of synthetic polymers that have been tailor-designed for use in microparticles. They are composed of sebacic acid and poly(ethylene glycol) (PEG), both of which are approved for invasive, human applications, although neither are currently approved for pulmonary delivery. Inclusion of PEG reduces the hydrophobicity, thus reducing particle aggregation in the aqueous environment of the respiratory tract. Also, hydrophilic particles are less detectable by phagocytes. The resultant polymers have a much shorter degradation time than PLGA, providing a protein release profile more suitable to nasal or pulmonary delivery (Fu *et al.*, 2002). Similarly, Huang *et al.* (1999) formed microparticles from a PLA-PEG copolymer. As above, inclusion of PEG increased degradation rate, and it also reduced acidity levels.

At the other end of the spectrum, microparticles have been manufactured with poly(ε-caprolactone), which degrades over periods of greater than one year (Sinha *et al.*, 2004). Whilst this may have applications for parenteral drug therapy, persistence in the respiratory tract for this duration is unlikely to be advantageous.

1.4.14.c) Carbohydrates

The inclusion of sugar monomers such as trehalose and lactose in microparticle formulations have been described above. Although they enhance the stability of proteins, they have little effect on controlling protein release, due to their rapid solubilisation (Dellamary *et al.*, 2004). However, polysaccharides have been explored as release-controlling materials for microparticle formulations.

Starch has been used for microparticle formulations, although its use is limited due to the swelling that occurs when in contact with water. This could be a particular problem for pulmonary delivery, since hygroscopic growth within the respiratory tract could be detrimental to the particle's aerodynamic qualities. Acetylation to form starch acetate increases hydrophobicity, leading to reduced swelling, as well as leading to enzymatic degradation, and therefore may be more appropriate for manufacturing microparticles (Tuovinen *et al.*, 2004).

1.4.15 Other factors for prolonging drug action in the respiratory tract

A modified-release microparticulate formulation will prolong the duration of therapeutic drug levels that would otherwise be reduced by drug-clearance mechanisms. However, as described in Section 1.2.4, in the respiratory system, mechanisms exist that may remove the modified-release formulation itself from the respiratory tract. Therefore, the formulation may require additional properties, such as bioadhesiveness or invisibility to macrophages (both discussed below), in order for drug release to persist to completion.

1.4.15.a) Bioadhesiveness

One method to achieve a persistent drug effect in the lungs or nasal cavity is to increase the residence time of the delivery system at the site of action. Bioadhesion describes the attachment of a delivered macromolecule to a biological tissue (Vasir *et al.*, 2003). The macromolecule in this definition could refer to the active protein drug, such as in the case of small polypeptide drugs, where there are believed to be interactions with membrane phospholipids (McAllister *et al.*, 1996). However, polymers used for structuring and controlled-release in microparticulate systems, could also mediate bioadhesion. Attachment could be to the mucus layer (termed mucoadhesion) on the surface of the nasal and pulmonary epithelium, usually *via* attractive forces, or to actual cellular structures, *via* more specific receptor-mediated interactions (Vasir *et al.*, 2003).

The PLGA polymers and carbohydrates, described above, are considered to have mucoadhesive properties (Vasir *et al.*, 2003). However, carbopol, hyaluronic acid and chitosan, have been highlighted to be particularly mucoadhesive (Alpar *et al.*, 2005). Chitosan also causes a transient inhibition of mucociliary clearance, further prolonging microparticle residence in the nasal cavity (Illum, 2003; Patel, 2007). Additionally, mucoadhesion can be achieved by covalent attachment of ligands to the surface of microspheres. These include anhydride oligomers, positively charged amino acids, mucin and metal cations. Positive charges on divalent metal cations have a strong affinity for negatively charged mucin chains, which are part of mucus composition. Specific cellular bioadhesion can be achieved using bacterial adhesins, specific amino acid sequences and antibodies (Vasir *et al.*, 2003). Hyaluronic acid, mentioned above as a mucoadhesive agent, can also act as a specific ligand for the CD44-receptor on lymphocytes (Alpar *et al.*, 2005), and has been adsorbed onto the surface of hydrophobic drug particles (Rouse *et al.*, 2007).

1.4.15.b) Reducing clearance

The mechanisms of bioadhesion described above will reduce removal by the

mucociliary clearance system, since the particle is attached to the mucosal surface. In addition, some of the bioadhesive agents can actually arrest cilia beating (Illum & Fisher, 1997). However, when targeting the alveolar regions of the lung, the primary mechanism of particle removal is phagocytosis by alveolar macrophages. Clearance by macrophages could be avoided by designing carrier particles that are too large or too small for recognition. It is highly interesting, but unfortunate, that the optimum particle diameter for delivery to alveolar regions of the lung is approximately the same as the optimum particle diameter for macrophage recognition (~1 to 2 μm) (Ahsan *et al.*, 2002). Therefore, although not recognised by macrophages, larger particles would only impact in more central areas of the respiratory tract, and smaller particles would be exhaled before diffusion could occur. However, porous particles (Section 1.4.13) can be physically large enough to avoid phagocytosis, while having a low enough aerosynamic diameter to be inhaled. Manufacturing microparticles from a material indigestible by phagocytosis is another option, although it is unlikely that such a material would still be biodegradable, and therefore, safe.

However, there are some materials that can be added to microparticles to reduce alveolar clearance. Dipalmitoylphophatidylcholine (DPPC), used in the manufacturing of the spray-dried lipid microspheres (SDLMs) described above, is a major component of lung surfactant. When microparticles are coated in DPPC, it acts as a "cloaking-device", hiding the particle from macrophage detection, presumably by camouflage against the surfactant environment (Jones *et al.*, 2002). As well as being used in SDLMs, DPPC has been added to PLGA microparticles, manufactured by solvent evaporation. For these microparticles it was observed that DDPC coats the surface of the microparticle, and its inclusion reduced internalisation by macrophages from 70% to 25% (Evora *et al.*, 1998). Inclusion of poly(ethylene glycol) (PEG) into microparticles, as part of PEG-PLA or poly(sebacic anhydride-co-PEG) coploymers, also reduced macrophage recognition. This is believed to be due to the hydrophilic properties of PEG (Huang *et al.*, 1999; Fu *et al.*, 2002).

In some circumstances, avoiding macrophage recognition may not be beneficial. Rather, the aim might be to actually target the drug to the macrophage, for example to wipe out intracellular infection (Sharma *et al.*, 2001), for vaccination, or for other forms of immunomodulation. In these circumstances, it has been found that macrophage uptake can be improved by using microparticle delivery systems with a high surface charge or containing hydrophobic materials (Ahsan *et al.*, 2002). Of course, the reverse of these findings can be applied to reduce macrophage detection, i.e. hydrophilic microparticles with a low surface charge.

1.4.16 Mechanisms of protein absorption for systemic delivery

Unlike small, hydrophobic drug molecules, which can pass readily through the lipid membranes of epithelial cells, peptides and proteins, being larger and hydrophilic, have lower membrane permeability. It has already been described how the "leakiness" of the nasal epithelium makes it an attractive site for protein delivery. However, the lung epithelium is not particularly permeable to macromolecules; rather its large surface area and low expression of protease enzymes lead to it being a good candidate.

Once a protein has penetrated either the surfactant or mucus, and then the epithelial surface fluid, it can pass through the epithelium *via* two different routes. Either the protein can pass through pores between the cells (paracellular transport), or pass through pores in the cells (transcellular transport). These pores actually represent different mechanisms of protein passage, and therefore vary in size. There are smaller pores that may represent slits within the tight junctions between epithelial cells, or aqueous channels within the cell membrane, allowing passage of the protein into the cell, and out of the other side. Larger pores may represent larger fenestrations between cells, or passage through the epithelial cell within vesicles, known as transcytosis. For some proteins, such as antibodies, transcytosis can be mediated by receptors or influx transporters. Therefore, for larger protein molecules, which cannot penetrate the smaller pores, there are fewer available absorption mechanisms, and hence the absorption rate is inversely proportional to protein size. Generally, ~40 kDa is the protein molecular weight limit for paracellular transport across lung epithelia, and subsequent rapid diffusion into the blood. Above this molecular weight, transcellular transport mechanisms are required, and systemic absorption requires days rather than hours (Patton, 1996).

There are also patient factors that can cause variation in protein absorption. Cellular damage, as a result of smoking or other pathologies, can result in "ultra-large pores", thereby dramatically increasing the absorption of proteins *via* the lungs. Also, there is some evidence that if a patient takes a deep inspiration, the expansion of the lungs causes gaps to open up between cells as the tissue is stretched, thus increasing protein absorption (Patton, 1996). Of course, passage through the epithelium is only one stage in achieving systemic absorption. Similar mechanisms apply to protein absorption through interstitial, connective tissue, and then across the vascular endothelium. In the alveolar regions of the lung, the epithelium lies in close proximity to the very thin endothelia of the pulmonary vascular bed. Therefore, in these regions, systemic absorption of proteins is favoured. The following subsections describe the utility of absorption enhancers and protease inhibitors as possible methods of improving the

systemic bioavailability of inhaled protein drugs.

1.4.16.a) Absorption enhancers

There are many chemicals that can potentially be added to drug formulations to increase the permeability of epithelial cells. A wide variety of compounds have been used in nasal formulations to enhance the absorption of protein drugs. Bile salts, surfactants and chelating agents can disrupt membrane integrity and open up tight junctions, thereby enhancing the nasal absorption of insulin (Hinchcliffe & Illum, 1999). However, their effects on the absorption of larger proteins may be more modest (Arnold *et al.*, 2004). There are concerns over the safety of absorption enhancers, since they may result in irreversible tissue damage, rendering the epithelium permeable to other exogenous allergens or toxins (Illum & Fisher, 1997; Hussain *et al.*, 2004). Also, if the formulation is for lung delivery, there is very strict control over the approval of novel 'excipient' compounds. However, some absorption enhancers appear to have very low toxicity, and thus could be potential candidates for inhaled formulations. These include sodium glycocholate, lauryl-β-D-maltoside, EDTA, and linoleic acid with hydrogenated castor oil (Hussain *et al.*, 2004). Also, group of compounds, collectively designated Intravail™ (including tetradecyl maltoside) are relatively non-toxic nasal absorption enhancers that are metabolised to carbon dioxide and water (Maggio 2006).

Some of the polymers used in microparticle formulations have absorption-enhancing properties, in addition to bioadhesive properties; for example, starch-enhanced nasal insulin absorption. Starch swells as it becomes hydrated, thus opening up tight-junctions as it comes into contact with the aqueous surface of the epithelia (Hinchcliffe & Illum, 1999). A hydrophilic derivative of chitosan, N-trimethyl chitosan chloride, considerably increased peptide permeation across epithelia, and appeared not to cause tissue damage (Alpar *et al.*, 2005).

1.4.16.b) Protease inhibitors

Other compounds, such as bacitracin and bestatin, inhibit protease enzymes, and thus should improve bioavailability of protein drugs. However, experiments with protease inhibitors for the nasal delivery of peptides have only demonstrated modest, if any, benefits (Hinchcliffe & Illum, 1999). Their effects in lungs are less than in subcutaneous formulations, suggesting the low protease activity in lung tissue (Hussain *et al.*, 2004). Given the toxicology profiling that would have to be undertaken for a pulmonary formulation including a protease inhibitor, it seems unlikely that this method would be worth pursuing.

1.5 Inhaled Antibody Formulations

Antibodies, or immunoglobulins, are several classes of proteins that are fundamental for the functioning of the adaptive immune system. The uniqueness of the shape of the targeting region, of a given antibody, allows it to bind selectively to the surface of a specific, foreign protein. Other regions of the antibody protein then allow it to invoke various components of the immune system. As described below, scientists have tried to exploit the highly selective targeting ability of antibodies for the generation of new techniques and therapeutics. However, as with other proteins, formulating antibodies for human delivery poses a number of challenges, and thus pulmonary and nasal routes are being investigated.

1.5.1 Antibody structure

Antibodies are tetrameric proteins comprised of two identical, heavy polypeptide chains, and two identical, light polypeptide chains, which are joined by disulphide bridges. Typically, the simplest class of antibody (IgG) has a molecular weight of ~150 kDa, with an asparagine-linked carbohydrate chain, linked to each of the heavy polypeptide chains (Reff and Heard, 2001). The internal disulphide bridges of each chain, and hydrophobic interactions, result in the folding of the protein into three-dimensional domains, which are designated as either variable or constant domains. The "Y-shaped" configuration of the antibody (illustrated in Figure 1.19) contains the Fab regions at the two prongs of the "Y", with the remainder of the protein comprising the Fc region. The Fc region invokes the immune response, and the Fab region, which varies between specific antibodies, contain the variable domains, which are involved in binding. Therefore, the "Y" shape provides each antibody with two binding sites. This greatly increases binding affinity, since the probability of one of two sites being bound, is much greater than binding occurring at a single site. There are three hypervariable regions within the variable parts of the heavy (V_H) and light (V_L) chains. The folding of the variable domains brings the hypervariable regions into alignment at the tips of the Fab regions of the antibody. It is the shape of these surface tips that provide the unique binding site of the antibody. The antibody's binding site will fit a particular antigen, a small surface on a protein. An antigen is not a specific amino-acid chain, but rather the specific three-dimensional shape of a folded protein surface. A new bioengineering technique has been used to develop single antibody molecules that can simultaneously target two different antigens (Wu *et al.*, 2007).

Figure 1.19 Structure of the IgG antibody.
a) Schematic of domain structures. The shorter light chains are on the outside of the two, longer, heavy chains. b) Three-dimensional, ray-traced image. Red area: heavy chains, yellow area: light chains, purple area: carbohydrate, turquoise area: approximate location of hypervariable region. Adapted from: Google® images.

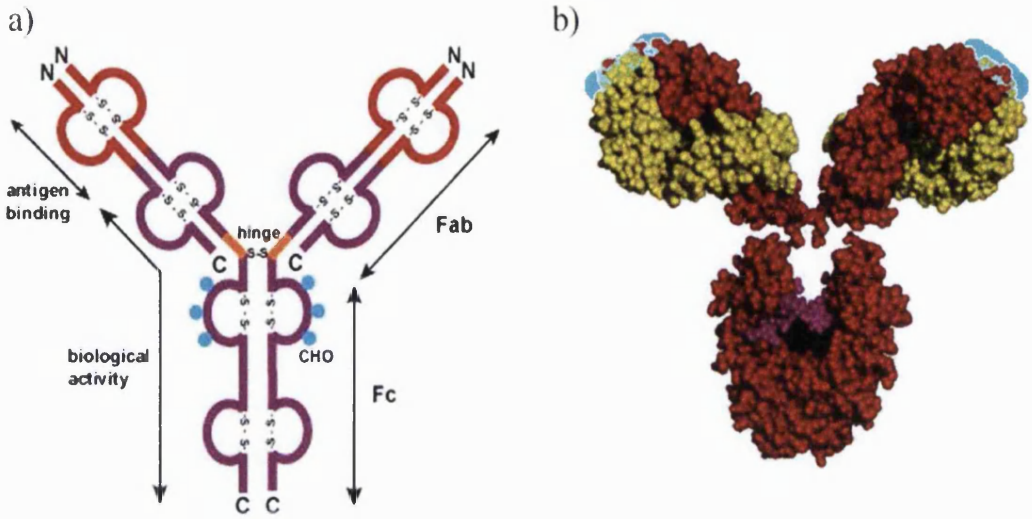

1.5.1.a) Types of antibody

There are five classes of endogenous antibody, which are referred to as IgG, IgM, IgD, IgA and IgE (Reff and Heard, 2001). IgG is the simplest type of antibody, and is the most common type found in blood plasma. IgA antibodies are produced by the mucosal immune system, and thus are the type most often found at mucosal surfaces, such as the lung, nose and gut (McGhee *et al.*, 1992). Therefore, IgA may be the preferred type of antibody to employ when delivering a treatment *via* the inhalation route. IgA, when secreted at mucosal sites, often exists as dimers of two antibody molecules. This increases the number of binding sites, and thus increases binding affinity as described above. IgM exits as five IgG-like structures held together by disulphide bridges, resulting in ten binding sites. Therefore, IgA and IgM antibodies are present earlier in the immune response since less specific interactions are required for binding. IgE antibodies are primarily involved in allergic responses.

1.5.2 Production and function of endogenous antibodies

Antibodies are synthesised within lymphocytes, where it is believed that 10^{15} different variable regions can be produced. Although fewer than 400 genes are involved in the encoding of antibodies, this strikingly huge repertoire of variable regions derives from the ability of the lymphocyte to perform recombination processes that modify the original genes. B-lymphocytes can produce antibodies with a hydrophobic domain, which results in them residing as transmembrane proteins, and thus serving as receptors

for these cells. In addition, B-lymphocytes can produce antibodies without this hydrophobic region. This results in soluble antibodies, which can be secreted from B-lymphocytes into plasma or mucus. In a state of non-infection, there are low levels of millions of different lymphocyte clones, producing low levels of millions of different antibodies. In a simplified version of events, when a lymphocyte uses its antibody receptor to bind to a foreign antigen, such as part of a surface protein on a bacterial cell, or a bacterial toxin, cell division is triggered, to produce clones of lymphocytes that can also target this same antigen. Note that lymphocytes that target "self" antigens are destroyed in the bone marrow or thymus before release, or are suppressed by other components of the immune system (but where these processes fail they can be a cause of auto-immune diseases). In the case of stimulated B-lymphocytes, they also differentiate to become plasma cells, which are factories for the production of soluble antibodies. These soluble antibodies are secreted from the plasma cells, and can bind to this same antigen, if found elsewhere in the body. The binding of a soluble antibody to an antigen, as well as physically immobilising the pathogen, 'flags' (*via* the Fc region) the pathogen to other components of the immune system, such as the complement cascade and phagocytes, which can result in the death of the pathogen (Delves and Roitt, 2000).

1.5.3 Therapeutic use of antibodies

The specificity of antibody-antigen interactions has made them useful tools for a number of applications. Conjugating antibodies with radionuclides or enzymes that produce detectable products, allows them to be used for detection assays (such as the enzyme-linked immunosorbent assay used in the work in this thesis) and diagnostic techniques, *in vitro* and *in vivo*. In terms of therapeutics, there are now several licensed drugs that are antibodies. Examples include infliximab, which targets and disables tumour necrosis factor, a peptide inflammatory mediator over-expressed in rheumatoid and Crohn's disease, and trastuzumab which binds to, and targets for destruction, the human epidermal growth factor receptor 2, present on the surface of certain breast cancer cells (Breedveld, 2000). Prior to these therapies, serum, containing antibodies, has been used for passive immunisation. With particular reference to inhaled therapy, a future application of antibodies could be to use them to target inhaled pathogens or protein toxins, such as pneumonic plague or ricin, respectively (Poli *et al.*, 1996; Hill *et al.*, 2006). This is a particular area of intensive investigation, in light of the current surge in world terrorist activity, and the threat of bio-terrorism (Binder *et al.*, 2003; Newman, 2006). Antibodies themselves can be used as a vaccine using an anti-idiotype network. This involves producing antibodies against an antigen, and then injecting

these antibodies into another organism, which subsequently produces antibodies against the injected antibodies. These anti-ideotype antibodies can have the same binding site shape as the original antigen, and thus can be used as a vaccine.

Other future applications of antibodies as therapeutics, involve using them as targeting moieties for other compounds. This could include conjugating cancer-specific antibodies to either highly potent cytotoxic agents or radiotherapy isotopes. This would provide a means of selectively delivering the drug to the cancer cells, while reducing systemic exposure (the so-called "magic bullet"). However, such approaches are limited by the drug-loading capacity of antibodies, relative to the number of binding sites on the target cell, and the ability of the antibody to reach the target cells, internalise and release the active drug (Reff and Heard, 2001). An alternative approach is to include antibodies in microparticle drug formulations. Antibodies at the surface of the microparticle can act as a targeting moiety to cell surface receptors. The whole microparticle can then be internalised into the cell, and then release the drug. This technique has been shown to increase the uptake of influenza antigens (in a microparticulate formulation) into antigen-presenting cells, thus providing a means of vaccination (Bot *et al.*, 2001).

1.5.4 Producing antibodies for therapeutic use

Traditionally, antibodies for passive immunisations were produced by taking serum from someone previously infected, since this would contain the required antibodies. Indeed, antibodies for any antigen can be produced by inoculating an organism, such as a mouse, rabbit, sheep or monkey, with the antigen, and then collecting the antibodies produced, from the blood. However, the natural body response to a given protein is polyclonal, i.e. many different types of antibody are produced. This is because for a given protein there will be many different binding sites (perhaps overlapping), that different antibodies will be able to bind to, with different degrees of binding affinity. Each of these different clones will go on to be mass-produced, as described above. As a result, the plasma will contain many different antibody clones, all with some ability to bind to the protein. Therefore, from the pool of different antibodies produced some will be highly specific, and others will be less specific. This is not an ideal therapeutic product, since efficacy and side-effects (due to binding to other targets) would be difficult to predict, and quality control hard to ensure. Also, such methods produce a limited quantity based on the size and lifespan of the animal.

Monoclonal antibodies (i.e. a specific clone of antibodies with the same antigen binding

site) can be produced by fusing a spleen plasma cell from an antibody-producing animal, with a plasmacytoma cell, to form an immortal hybridoma. Hybridomas can then be screened to identify a cell which produces antibodies of the required specificity that can then be cloned for bulk culturing. There are also now completely *in vitro* techniques for producing monoclonal antibodies, such as the phage library technique. This utilises recombinant DNA techniques to recombine millions of different antibody genes (similar to the processes undertaken by lymphocytes *in vivo*), with each sequence being expressed on the surface of a bacteriophage. The bacteriophages are screened for binding activity, and the appropriate phage is selected. The DNA can then be cloned and expressed to form monoclonal antibodies (Marks and Marks, 1996).

Antibodies produced in mice, or from mouse cells, can cause an immune response when given to humans, as they are essentially foreign proteins. Also, the Fc region of a mouse antibody may not be physiologically active in a human. This can be a problem if activation of the immune system, against the antibody-bound antigen is required for therapeutic activity. Chimaeric and humanised antibodies are made by fusing the variable regions of monoclonal mouse antibodies with human constant regions. However, phage library techniques, and transgenic mice (Jakobovits *et al.*, 2007) allow purely human antibodies to be made.

Proteins of a lower molecular weight are more stable and more easily absorbed. Therefore, synthesising antibody fragments may improve bioavailability, as well as making production easier. For example, single Fab regions (~57 kDa) or single chains or single domains of the Fab region can be synthesised. Domantis (a subsidiary of GlaxoSmithKline) has developed the smallest type of antibody fragment, domain antibodies (dAbs™) which consist of only the variable region of an antibody light (V_L) or heavy chain (V_H) (illustrated in Figure 1.20), and thereby have a molecular weight of only ~11-15 kDa (Holt *et al.*, 2003). The result are highly potent targeting molecules that are highly stable when freeze-dried or mixed with excipients, making them amenable to formulation for inhaled delivery (Domantis, 2007). However, whilst this approach will produce highly specific binding molecules for targeting receptors, the absence of the Fc region will mean that these molecules cannot replace whole antibodies in cases where therapeutic activity relies on invoking the host's immune system. Taking the example of an antibody therapy against an inhaled toxin, in order for the therapy to be effective, it must be determined if either the binding of the antibody to the toxin is enough to inactive it, or if other components of the immune system are needed to destroy the toxin. In the former case, an antibody fragment may be

enough, provided the steric presence of the Fc region is not required to disable the toxin. However, in the latter case a full antibody with an Fc region will be needed to inactivate the toxin. There are also other problems with antibody fragments, such as reduced circulation half-life, and reduced binding affinity due to the reduced number of binding sites. However, dAbs™ have attempted to overcome these problems by producing dual-binding molecules (incorporating either albumin or PEG into the framework) that can actually simultaneously target two different antigens (Domantis, 2007). Also, PEGylated dAbs™ have been produced to increase their circulation half-life (Holt *et al.*, 2003).

Figure 1.20 Fragment antibodies, including domain antibodies. A human IgG molecule (left-hand side) has both variable (V) regions that confer antigen binding and constant (C and Fc) regions for recruiting the immune system. Domain antibodies, (dAbs ™), of 11–15 kDa either consist of an isolated antibody V_H domain (as shown, right-hand side), or an isolated antibody V_L domain. More conventional recombinant antibody fragments include, Fab fragments (57 kDa) comprising of a V_H–C_{H1} polypeptide disulphide-bonded to a V_L–C_L polypeptide, and scFv fragments (27 kDa) containing only the V_H domain fused to the V_L domain *via* a polypeptide linker. Taken from: Holt *et al.*, 2003.

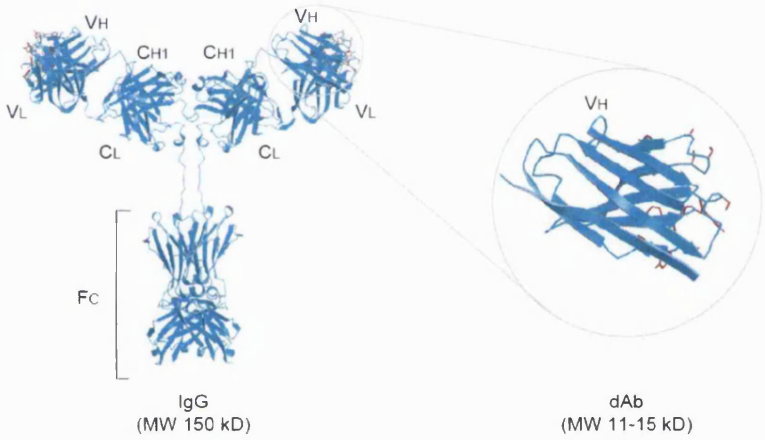

1.5.5 Formulating antibodies for inhalation delivery

The stability concerns associated with formulating macromolecular drugs apply to antibodies. Particular chemical alterations, common to antibodies, include Fc and lys-residue glycosylation, Fc methionine oxidation, aggregation and fragmentation (Daugherty and Mrsny, 2006). Many of the microparticulate delivery systems described in Section 1.3 have been used to formulate antibodies. IgG has been formulated into porous, spray-dried, lipid microspheres (SDLM), where it was found that antibody release from the particles, was slow compared to a small peptide, and also slower than lyophilised antibody powders (Bot *et al.*, 2000). However, these experiments measured release into a large volume of saline. This may not be equivalent to the small volume of surfactant-containing lung fluid. In these formulations, the antibodies remained active, since the Fc region was able to mediate uptake of the microspheres into antigen presenting cells (Bot *et al.*, 2001). Systemic absorption of the antibodies was achieved by nasal and intratracheal instillation, although this was less than for an unformulated antibody (Bot *et al.*, 2000). However, given the rapid decrease in nasal bioavailability

of proteins with molecular weight, it is believed that nasal transmucosal delivery of antibodies is not currently possible (Maggio, 2006). Dellamary *et al.* (2004) also investigated SDLM formulations of an anti-influenza IgG in the lung. This study ascertained that antibodies were absorbed in the lung by Fc-mediated uptake into epithelial cells, avoiding the molecular weight limit for passive diffusion. Antibodies were then released slowly into the bloodstream, with the interstitial tissue acting as a depot. Using an IgG, release-rate controlling polysaccharide in the formulation reduced its efficacy. This was because these particles were cleared by alveolar macrophages, whereas a rapid release of IgG did not saturate Fc-receptors.

Omalizumab (Xolair®), an anti-IgE antibody, has been recently approved for the treatment of the allergic component of asthma. This therapy is currently delivered by injection, where only a small fraction of the administered dose penetrates lung tissue. An inhaled formulation of omalizumab, would obviously be more efficient, since 10-100-fold higher pulmonary concentrations can be achieved compared to injection (Weers *et al.*, 2007). Andya *et al.* (1999) formulated anti-IgE antibodies by spray-drying with carbohydrates. Circular dichroism measurements showed that antibody conformation was well preserved, although when lactose was used rather than trehalose or mannitol, some glycation of the antibodies occurred. Maury *et al.* (2005a) used Fourier transform-infrared spectroscopy to demonstrate that IgG did not undergo secondary structural changes, when re-dissolved after spray-drying, provided the spray-drying feed also contained a disaccharide excipient such as sorbitol. Adding sorbitol to the formulation reduced aggregation of the spray-dried microparticles, although this was not related to a prevention of secondary structural changes in the solid state. The same protection during spray-drying was demonstrated using mannitol (Shüle *et al.*, 2007). Spray-freeze drying of antibody solids, and incorporating these into solid-oil-water emulsions for microparticle production, has also been achieved (Wang *et al.*, 2004).

1.6 Conclusion

In recent years, rapid progress has been made in the field of biotechnology. New biological targets for the treatment of many diseases have been identified, and methods for screening and manufacturing new ligands to modulate these targets have been developed. However, these ligands are generally large biomolecules rather than small, conventional drug molecules, and as a consequence are unstable and poorly bioavailable when given by the preferred, conventional delivery methods. This is a major reason why so few of these biotherapeutic products have become successful medicines, able to achieve marketing authorisation.

The nasal and pulmonary routes have been investigated for the delivery of macromolecules, because of their large surface areas, rich blood supplies and lack of biomolecule-degrading enzymes. These routes have the potential to provide targeted, high concentrations for the treatment of localised, respiratory diseases, as well as a rapid and efficient gateway into the circulation, for systemic treatments. There are a large number of delivery devices already available for delivery to these routes. However, compared to existing inhaled therapies, biomolecular therapies have a narrower therapeutic index, usually need to target specific areas of the lung, and are costly to produce. Therefore, devices are required with more reproducible and higher efficiencies, having less dependence on patient factors.

Formulating a macromolecular drug, such as a protein, for use in an inhalation device, is in itself a huge challenge. As well as ensuring the macromolecule is kept stable in storage, and thus is active when released, the formulation must also have the appropriate aerodynamic properties for inhalation, and the optimum release properties. Microparticulate, protein formulations incorporating lipids or polymers are among the most promising formulation methods, providing many viable material and technique alternatives, to produce microparticles of particular characteristics. Addition of other ingredients, such as those to control release, enhance absorption and inhibit endogenous enzymes, may further optimise the bioavailability of these formulations.

Antibodies have been highlighted as examples of proteins with a wide variety of therapeutic uses. However, their activity critically depends on the ability to preserve structural integrity, and deliver effectively. [Literature available up to end of October 2007 was reviewed].

1.7 Aims of this study

The aim of this project was to develop formulations of a therapeutic antibody, potentially suitable for respiratory delivery. There were a number of key requirements for the formulation:

- It should preserve the antibody activity, during production, storage and use.
- Be composed of biocompatible excipients, suitable for pulmonary delivery.
- To efficiently encapsulate the antibody, and then release it with a profile suitable for the intended clinical application.
- Provide compatibility with a suitable inhaler device.
- Consist of particles of suitable geometric and aerodynamic characteristics for delivery to the respiratory tract.
- Demonstrate *in vivo* activity when used to formulate a therapeutic antibody.

2 MATERIALS AND METHODS

The methods described below were general manufacturing processes, and analysis techniques, which were utilised in the work described in more than one section of this thesis. Specific methods or adaptations that were used within only one section, appear in the Methods for that section.

2.1 Materials

Table 2.1 lists the main materials used in the work described throughout this thesis. All other materials and reagents mentioned in the methods throughout this thesis were of reagent grade, and purchased from Sigma-Aldrich (UK) or VWR International (UK), unless otherwise stated. All water used in the experiments was distilled and deionised using an Option 4 Water Purifier USF ELGA (ELGA Labwater, UK).

Table 2.1. Materials and suppliers

α-Lactose monohydrate	Sigma-Aldrich, Denmark
1,2-Dipalmitoyl-sn-glycerol-3-phosphocholine (DPPC)	Genzyme, Switzerland
Bovine serum albumin (BSA)(fraction V), minimum 98%	Sigma-Aldrich, USA
Flebogamma® 5% human normal immunoglobulin (IgG) for intravenous use (IgG in 1:1 mass ratio with sorbitol)	Grifols, UK
Poly(lactide-co-glycolide) (PLGA) ("Medisorb") 1A 50:50 (7 kDA MW, 2-3 week degradation time)	Lakeshore Biomaterials, USA
Poly(vinyl alcohol) (PVA), 87-89% hydrolysed, average MR 13,000-23,000	Sigma-Aldrich, UK
L-leucine	Sigma-Aldrich, UK

2.2 Manufacturing of particulate IgG formulations

2.2.1 Manufacture of poly(lactide-co-glycolide) microparticles by solvent-evaporation

The method and formulation used initially was a modified version of the double-emulsion, solvent-evaporation technique previously described by Ogawa *et al.*, 1988. The oil phase of the emulsion was formed by dissolving 200 mg poly(lactide-co-glycolide) (PLGA) 1A into 4 mL dichloromethane (DCM). The internal aqueous phase consisted of 10 mg IgG, 10 mg sorbitol (i.e. 200 μL Flebogamma®), and 100 mg (5%

m/v) poly(vinyl alcohol) (PVA), in 2 ml distilled water. The external aqueous phase contained 500 mg lactose and 100 mg (0.1% m/v) PVA in 100 mL distilled water. Solutions of PVA were prepared from a 10% m/v stock solution, where the PVA was dissolved using gentle heat and vigorous stirring. The solutions were cooled in a refrigerator overnight (~ +4°C), and the protein was added to the internal aqueous phase just prior to homogenisation. The internal aqueous phase was added drop-wise to the PLGA solution, while homogenising at 24,000 RPM (Ultra-Turrax T25, IKA-Werke, Germany) for 2 min. This primary emulsion was then added to the external aqueous phase, homogenising at 10,000 RPM (LR4T, Silverson, UK) for 8 min, to produce a W/O/W double-emulsion (see Figure 1.13, Chapter 1, for an outline of the double-emulsion method). The homogenisation process was performed with solutions being kept on water ice, to enhance viscosity, and thus emulsion stability, and to reduce thermal protein damage caused by the shear forces of homogenisation. The excipient quantities and method described above evolved somewhat as the project progressed, in order to accommodate the use of other excipients, and also as a result of optimisation experiments.

Evaporation of the DCM was achieved by leaving the double-emulsions under stirring conditions for at least 4 h, or overnight at room temperature (RT). Generally, 1 h was required to evaporate 1 mL of DCM. The microparticles were washed with distilled water, three times, by centrifugation (Beckman-J20, Beckman-Coulter Instruments Inc., UK) for 20 min at 20,000 RPM, discarding the supernatants and re-suspending the microparticle pellets in fresh distilled water. After the third centrifugation, the pellets were each re-suspended in 4 mL of distilled water, and decanted into pre-weighed glass freeze-drying vials. The microparticles were frozen at -20°C, before freeze-drying (Virtis Advantage, USA) on a 48 h cycle. The shelf temperature was reduced from -15°C to -40°C, and then elevated to +15°C. Upon collection the vials were reweighed to calculate the yield.

2.2.2 Manufacture of microparticles by spray-drying

The double-emulsions were prepared as described above. However, without allowing time for solvent-evaporation, the double-emulsions were immediately fed into the spray drier (Büchi 191, Switzerland), which was pre-heated to the required settings. A small amount of distilled water was fed through the spray drier to stabilise the outlet temperature, prior to commencing feeding of the double-emulsion. After all the material had been fed through, the dry-powder product was collected from the collecting vessel and cyclone into pre-weighed plastic tubes.

2.3 Quantification assays

2.3.1 Bradford assay for the determination of protein concentration

The bicinchoninic acid (BCA) assay, commonly used to measure the protein content of solutions from these type of systems (Smith *et al.*, 1985), could not be employed in this work. Two molecules of bicinchoninic acid chelate one cuprous ion (Cu^{+}) to form a purple coloured complex. In alkaline conditions, the peptide bonds of proteins were capable of reducing Cu^{2+} to Cu^{+}, and therefore could be readily detected. However, lactose, which was used in this work, was a reducing sugar, and thus its presence gave a false positive result, since like protein, it reduced Cu^{2+} ions to Cu^{+}. Therefore, a more protein-specific method was required. The Bradford assay (Bradford, 1976), used the Bradford reagent, which contained a Coomassie Brilliant Blue G-250 stain that was able to bind specifically to tryptophan, tyrosine, histidine, phenylalanine and particularly arginine residues of proteins. The only possible interference may have come from DPPC (used in the formulations described in this thesis) which contained nitrogen. However, given that the nitrogen contribution of DPPC in the formulation was relatively small, this potential problem was overcome by producing blank formulations containing no protein, and subtracting their absorbance values, from the values obtained with the protein containing batches. Binding of the dye shifted it from its cationic form, with an absorption maximum of 470 nm, to the anionic form, which had an absorption maximum of 595 nm, thus giving a blue colour.

2.3.1.a) "Micro-well plate Bradford assay" protocol used for the determination of protein content

This assay was suitable for determining the protein content of solutions with an estimated protein concentration of 10-200 µg/mL. Therefore, where necessary, samples were diluted prior to being used in this assay. The protocol given here was developed as described in the first part of Appendix III of this thesis.

I. Sample preparation

- Sample preparation varied according to the objective of the assay, and the type of sample being analysed. For PLGA-based formulations, powder formulation was either dissolved in 0.5 M sodium hydroxide solution to measure the total protein content, or suspended in phosphate-buffered saline (PBS) pH 7.4 to measure protein modified-release (MR). See the following paragraphs for details. For the instant-release, nasal formulations, the powder formulation was simply dissolved in PBS and

diluted to an appropriate concentration (see Chapter 8 of this thesis for details).

II. Standard preparation

- IgG solution (5 mL, 200 μg/mL) was prepared in either 0.5 M NaOH or PBS.
- This standard solution was diluted with further 0.5 M NaOH or PBS, to produce several standard concentrations, ranging from 200 down to 20 μg/mL. (Details of the dilutions are given in Table I of Appendix I of this thesis).

III. Running the assay

- Each sample, and the seven standards, were plated (50 μL) in quintuplet onto a 96-microwell plate (Fisher Scientific International).
- Bradford reagent (250 μL; warmed to room temperature) was added to each well.
- For a release assay, 50 μL 0.5 M NaOH was added before adding 200 μL Bradford reagent, since the presence of base aided colour development.
- Absorbance was measured at 570 nm using a microplate reader (Opsys MR, Dynex Technologies, USA).

IV. Results analysis

- A calibration curve of concentration versus absorbance was produced, using the standard results (see Appendix II, Figure I for an example). (The values produced by the standard samples fitted a quadratic curve $y = ax^2 + bx + c$). N.B. The Bradford reagent itself had an absorbance of 0.5 units.
- The equation of curve was used to calculate the concentration of samples.
- Values of any non-protein containing (blank) samples were subtracted.

2.3.2 Determination of total protein loading and encapsulation efficiency (EE)

Samples of microparticles (5 mg) were accurately weighed into an Eppendorf tube. The appropriate volume of 0.5 M NaOH was added to give a 5.0 mg/mL solution. Samples were taken from each batch in triplicate. Tubes were gently shaken at room temperature for 2 h. This was found to be the optimal time for digesting microparticles consisting of the lactose and PLGA 1A used in the work described in this thesis (see Appendix III for details). The Bradford assay was performed on the samples and standards as described above, using five microwells for each sample and standard. An average of the five absorbance readings was used to calculate the concentration.

The equation of the standard curve (the data was found to best fit a second order quadratic curve) was used to calculate the concentration of each sample. The apparent concentration of the blank sample was subtracted from each sample concentration. Multiplying this concentration by 20 gave the mass of protein *per* 100 mg, i.e. the percentage protein loading (the original concentration was for a 5 mg sample). Encapsulation efficiency (EE) was calculated by Equation 2, where theoretical protein loading was the percentage of protein in the original formulation ingredients.

Equation 2 Calculation of encapsulation efficiency

$$\text{Encapsulation efficiency (EE) \%} = \frac{\text{Measured protein loading \%}}{\text{Theoretical protein loading \%}} \times 100$$

N.B. This is not the same as the percentage of original protein encapsulated. This would be calculated by dividing the measured concentration by five (i.e. protein *per* milligram of sample), multiplying this by the mass of the collected batch (i.e. how much protein was in the product), and calculating this as a percentage of the amount of protein in the original ingredients. The difference between these was that EE does not take into account the yield of the process. Therefore, a batch can have a 100% EE even if the yield was only 20%. The EE result determined whether the proportion of protein in the final product, was the same as the proportion in which it was added.

2.3.3 Measurement of the instant (2 h) burst-release of protein

Samples (10 mg) of each batch were weighed accurately in triplicate, into Eppendorf tubes. The appropriate volume of PBS was added to give a suspension of 10.0 mg/mL concentration. After vortexing (Cyclone, Clifton, UK) to evenly disperse the powder, the suspensions were shaken in a 37°C incubator for 2 h (Weiss Gallenkamp, UK). Following this, the Eppendorf tubes were centrifuged for 3 min at 13,000 RPM, and the supernatants were analysed for protein concentration by the Bradford assay described above, using PBS for standard dilutions. Blank samples were used, and their apparent concentrations subtracted from the results. The percentage protein released was calculated using data from the total protein loading assay described above. Measurement of the full release profile followed a similar principle. This method is described in Chapter 5 of this thesis.

2.3.4 Poly (vinyl alcohol) assay

For formulations containing poly(vinyl alcohol) (PVA), the residual PVA content was measured by an iodine-based assay, described in Section 3.4 of this thesis.

2.4 Microparticle physical characterisation

2.4.1 Measuring particle mean geometric diameter by laser diffractometry

Laser diffractometry, or low angle light scattering, is a commonly used method for measuring the geometric diameter distribution of particles. Particles diffract light at a different angle depending on their size, with smaller particles diffracting light at larger angles. Monochromatic light from a laser beam was passed through the sample, and the diffracted light was focused on to over 100 detectors. The particle size distribution was calculated using one of two mathematical theorems; Fraunhofer or Mei theory. The latter has been used in the majority of the work described in this thesis, except for the dry-power experiments with the Sympatec HELOS apparatus, in Chapter 6, which used the Fruanhofer theory. Although the difference in the final results output was very subtle, the Mei theory contained mathematical calculations able to handle smaller particles with a degree of transparency, that would add complexity to the laser diffraction pattern (Kippax, 2005).

For the majority of this thesis, laser diffraction was performed in the liquid state (as opposed to measurements on dry powder, detailed in Chapters 6 and 8), using a Malvern Mastersizer (He-Ne gas laser 633 nm wavelength, Malvern Instruments, Malvern, UK). The measurements were taken while the particle suspension was being magnetically stirred around the sample cell. This ensured random orientation of most particles relative to the laser beam, resulting in the calculation of an equivalent spherical diameter (Beuselinck *et al.*, 1998).

Initially, measurements were made by dispersing a small amount (laser diffractometry is not concentration dependent) of powder in an aqueous solution of 0.02% v/v Tween 20, which is a surfactant that acted as a wetting agent, (although later cyclohexane was also used instead of water, see below). Without the presence of the Tween 20, formulations containing DPPC appeared to have a secondary aggregate peak of several hundred microns. After aligning the laser and taking background readings, the sample was added to the measurement cell, which contained the dispersing media, until an obscuration of between 10-20% was achieved. Three measurements were then taken. Where aggregate peaks were present that were clearly separate from the individual particle diameter distribution, they were excluded from the particle size distribution calculations. The modal diameter, the diameter that 50% of particles (by volume) in the sample were less than, D50% and D90% were recorded, as were some distribution peaks.

2.4.1.a) Development of a reliable laser diffraction method

During the factorial formulation optimisation experiments (Chapter 4 of this thesis), it became evident that the laser diffractometry data produced, did not always correlate well with the diameters observed from SEM images. In some cases, sizing was already difficult, because particles were either fused together (perhaps by melting), or aggregated due to moisture effects. However, even for some batches of relatively good particles, the data produced in water were again rather inconsistent.

There were two potential problems with using water as the dispersion media:

a) The particles did not disperse instantly. This was likely to be an effect of DPPC (discussed later).

b) Lactose is slowly soluble in water (20 g/100 mL solubility). Therefore, with the vortexing and sonication conditions required for dispersion, the particles were likely to be partially dissolved by the time of measuring. Thus, an alternative method was sought to achieve reliable diameter distribution data.

A range of other solvents were investigated as possible dispersing media. Many solvents such as dichloromethane, ethyl acetate and acetone were not applicable since PLGA is soluble in these. A range of alcohols were tried such as methanol, ethanol, propan-1-ol, isopropanol and butan-1-ol. However, the particles dispersed poorly in these, despite vortexing for 2 min and sonicating for 5 min. Hexane and cyclohexane were slightly more promising, but large aggregate peaks were still present, often hiding the individual particles' peak. Using cyclohexane with 1% v/v Span 80, appeared to help dispersion in the tube, but in fact increased the amount of aggregation measured.

The apparent lack of dispersion was checked by observing the particles under a light microscope. A small amount of powder was put onto a slide, and a drop of the cyclohexane/Span mixture was added, before placing a coverslip. Amazingly, the particles appeared well dispersed, even though there was no vortexing or sonication. This prompted two ideas: 1) to try sample dispersion without sonication 2) to fill the measurement cell with Span 1% v/v in cyclohexane. Previously, although the sample had been made up in the cyclohexane/Span mixture, the cell was filled with just cyclohexane (from which the background was taken), before adding the sample drop-wise. This dramatic dilution of the Span may have been causing the particles to aggregate. Indeed, implementing these two ideas solved the sizing problem, and meaningful geometric diameter data were achieved.

Surprisingly, the initially inconsistent effects observed in water were used to an advantage. Samples were prepared in water + 0.02% v/v Tween 20 [added to enhance wetting, and hence promote release (Watts *et al.*, 1990)], and allowed to incubate (37°C) for 2 h in order to completely dissolve the lactose. Measurement of the diameter could then be used as an estimation of the diameter of the particles *in vivo*, after deposition in pulmonary fluid. For these measurements, following the initial work as part of the factorial experiments, a small-volume dispersion unit was used with the Malvern Mastersizer, rather than the magnetic-stirrer cell. This apparatus allowed for better dispersion of the sample, and could operate with a more powerful lens, allowing particles less <500 nm diameter to be detected.

For the nasal formulations (Chapter 8 of this thesis), methanol was found to be an excellent dispersing medium, and was used with the magnetic-stirrer cell, in the Malvern Mastersizer.

2.4.2 Microscopy

Light microscopy was used to check the presence of micron-sized particles, and to qualitatively express their flow in the dry state, or in water.

Scanning electron microscopy (SEM) (Cambridge Stereoscan 90B) was used to observe particle morphology. SEM was conducted by staff members Dave McCarthy and Kate Keen at the School of Pharmacy, University of London.

2.4.3 Other physical characterisation techniques

The following techniques were used in specific Sections, and full methodology can be found in the appropriate chapters of this thesis. Particle diameter assessment of PLGA-based formulations in aqueous media were also measured by **photon correlation spectroscopy**, and imaged by **transmission electron microscopy** (Section 4.6.1). **Laser diffraction of dry powders** was performed using the RODOS/HELOS equipment (Sympatec, UK) as described in Sections 6.3.2 and 6.3.3.

Particle surface charge (Zeta potential) was measured by **laser doppler electrophoresis,** whilst glass transition temperature was measured by **differential scanning calorimetry** (Section 4.6.1). For the nasal formulations, **X-ray powder diffraction** (Section 8.3.3) and **thermo-gravimetric analysis** (Section 8.3.4) were performed to measure powder crystal content and water content, respectively.

2.5 Techniques to assess antibody properties

2.5.1 Gel electrophoresis

Poly(acrylamide) gel electrophoresis (PAGE) measured the migration according to molecular weight of protein molecules along a poly(acrylamide) gel, when a voltage was applied. Sodium dodecyl sulphate (SDS)-PAGE was employed for protein analysis, using the anionic surfactant SDS, which denatured proteins by surface contact with the polypeptide backbone. It conferred a fixed negative charge *per* unit mass to the protein molecules, thereby allowing their separation by molecular weight. Heavier molecules migrated more slowly, and thus over a fixed time period travelled less distance along the gel. Therefore, PAGE was used to identify changes in the antibody molecular weight, and thus could detect aggregation or fragmentation, resulting from structural damage during the formulation process. Two methods were used in the present work, one with reducing conditions, and one without.

2.5.1.a) Reducing SDS-PAGE

A standard protocol was followed for making the solutions required for a 10% poly(acrylamide) separating gel and stacking gel. The gels contained an acrylamide/bis-acrylamide mixture, TEMED, Tris and hydrochloric acid, as well as 10% SDS.

Samples and standards were prepared in PBS. For samples of the modified-release (MR) (PLGA) formulation, typically 5 mg of powder formulation was dispersed in 0.5 mL PBS for 2 h, before centrifuging at 10,000 RPM for 5 min, and collecting the supernatant. The nasal formulations (Chapter 8 of this thesis) were simply dissolved in PBS, and followed by appropriate dilution. Samples and standards were then mixed in a 1:1 ratio with a sample buffer containing SDS and mercapto-ethanol, after which these mixtures were heated in boiling water for 2 min.

Ammonium persulphate (10% m/v aqueous solution) was added to the gel mixtures to cause polymerisation, just prior to adding to the cast. First, the separating gel was put into the cast, with overlay added on top. The gel was allowed to set for 45 min, before pouring off the overlay and adding the stacking gel, which was also given 45 min to set around a 10-tooth plastic comb. The gel was then put into the gel container, and a Tris/glycine/SDS (TGS) buffer was added. The comb was removed, and after rinsing each well with buffer, 20 μL of a sample or standard was added to each well. Electrophoresis was performed at 200 V for 45 min. The gel was then collected, and stained using a silver staining kit, before being digitally photographed.

2.5.1.b) Non-reducing gel

In most of the work described in this thesis, a non-reducing method was used. The same protocol was followed, except a Tris/glycerol sample buffer was used, instead of heating with mercaptoethanol. The sample and buffer were mixed at a 1:1 ratio with no heating. Mercapto-ethanol reduced the disulphide bridges of proteins. Therefore, by avoiding its use it was possible to analyse the antibody molecule whole, rather than fragment it into light and heavy chains. Because the whole antibody molecule had a relatively high molecular weight, a 7.5% poly(acylamide) separating gel was used, so that the antibody would migrate further through the gel. In order to prevent this gel melting, it was run at 100 V for 2 h. The gel was then stained with Coomassie blue (SimplyBlue, Invitrogen, Carlsbad, USA) and photographed digitally.

2.5.2 Enzyme-Linked Immunosorbent Assay (ELISA)

ELISA has been widely used as another method for measuring protein integrity. Like the Bradford assay, ELISA can be used to quantitatively detect the concentration of a sample. However, unlike the Bradford assay, which detects the presence of certain amino acids, ELISA will only measure a specific protein in its active, undamaged, conformation. In this case, the protein of interest was human IgG, and thus ELISA has been used to determine if the formulated antibody remained immunologically active.

Here, a capture/sandwich ELISA method was used. The assay was performed on an ELISA 96-microwell plate (Fisher Scientific International) that had a special adsorbent surface. The plate was coated with a capturing, anti-human IgG, goat antibody. The remaining surface of the plate was blocked with fraction V bovine serum albumin (BSA). Samples containing the human antibody of interest were added to the plate, and, if still active, were captured by a specific interaction. The bound antibody was then detected by using a second anti-human IgG, goat antibody that was conjugated to a peroxidase enzyme. Again, the binding of this antibody relied on a specific immunological interaction that required the human IgG to be in its active conformation. This enzyme catalysed a colour-producing reaction, allowing quantification of the antibody concentration. A schematic diagram of the assay is given in Figure 2.1.

Figure 2.1 Schematic diagram of the enzyme-linked immunosorbent assay (ELISA) capture method (OPD = o-phenylenediamine substrate)

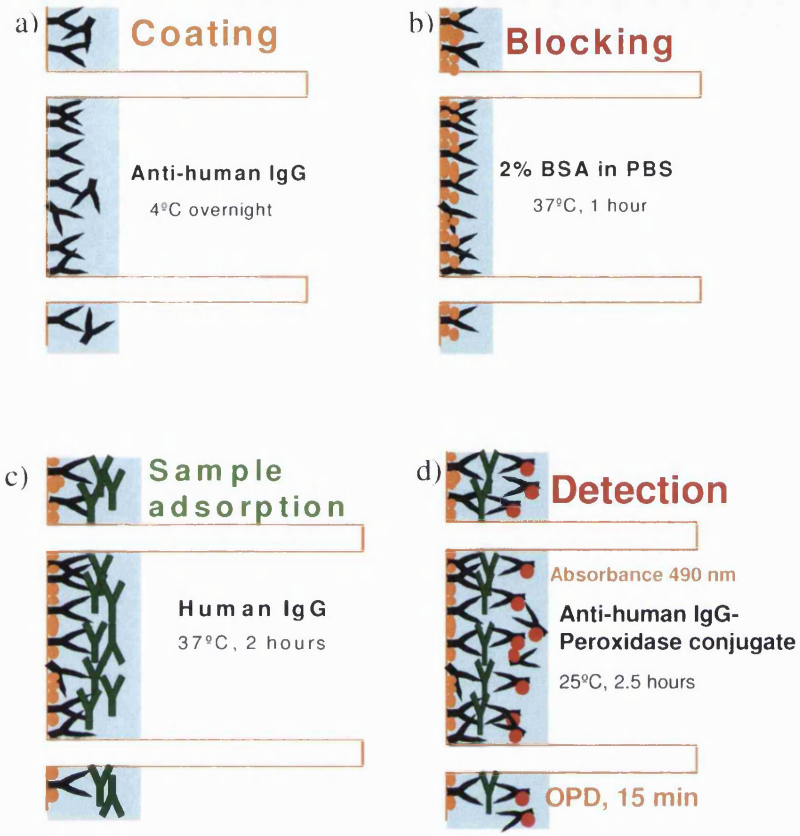

2.5.2.a) Development of an ELISA method

Three plates were run to determine the optimum concentrations of reagents to use. Standards concentrations of 10, 5, 2.5, 1.25, 0.625 down to 0 ng/mL were used. Plates were run using the capturing antibody at a concentration of 2.5, 5 and 10 µg/mL, blocking with 1, 2 or 4% m/v BSA, and using 1 in 2500, 1 in 5000 or 1 in 10,000 dilution of the anti-human IgG peroxidase conjugate antibody. Parameters were then chosen based on the quality of the calibration graphs produced (in terms of correlation coefficient and largest absorbance range). It was found that the middle values for each variable produced the best results, although for some parameters there was little difference.

2.5.2.b) Protocol for ELISA assay

- A 96-microwell plate was coated with a 5 µg/mL solution of anti-human IgG, prepared in a carbonate-bicarbonate buffer. Fifty microlitres were added to each well, and the plate was kept refrigerated (~+4°C) overnight.

- The plate was washed three times with a PBS + 0.05% v/v Tween, washing buffer.

- Each well was blocked with 100 μL of 2% m/v BSA in PBS, and incubated at 37°C for 1 h.

- The plate was washed three times with the washing buffer.

- Samples were prepared by releasing 10 mg of microparticles in 0.5 mL PBS for 2 h. The samples were centrifuged for 3 min at 13,000 RPM, and the supernatants collected. The protein concentration of the supernatants was measured by the Bradford assay as described above. For the nasal formulations (Chapter 8 of this thesis), powder was dissolved in PBS at an appropriate concentration to be measured by the Bradford assay. Depending on this result, the supernatants were then diluted 5,000 or 10,000 times in PBS, by a four-step, serial dilution. The 100 μg/mL IgG standard used for the Bradford assay, was also diluted in this way so as to give a 10 ng/mL solution, from which the other ELISA standards (5, 2.5 and 1.25 ng/mL) were made.

- The diluted samples and standards, as well as blank PBS (50 μL of each), were added to each well, with six wells for each sample. The plate was then incubated for 2 h at 37°C.

- The plate was washed 5 times with the washing buffer.

- Fifty microlitres of a 1/5000 dilution of anti-IgG peroxidase conjugate, in PBS, was added to each well, and the plate was kept at room temperature for 2.5 h.

- The plate was washed five times to remove any unbound conjugate-antibody.

- Urea substrate (50 μL) for the peroxidase enzyme was added to each well. Colour development over 15 min took place, after which the reaction was stopped with 50 μL 2N sulphuric acid (H_2SO_4).

- The absorbance of each well was measured at 490 nm (Opsys MR, Dynex Technologies, USA).

- The equation of the calibration line was used to calculate the concentrations of the samples. Taking into account the dilution factor, this was expressed as a percentage of the Bradford assay concentration, i.e. the percentage of protein that was active human IgG.

2.5.3 Field-Flow Fractionation

The SDS-PAGE results were confirmed by asymmetrical field-flow fractionation (FFF) (Wyatt Technology, Santa Barbara, USA). Samples were dissolved in PBS, and the protein concentration was determined using the Bradford assay. The macromolecular components of the samples were then separated by FFF using 1.0 mL/min channel flow and cross-flow of 3.0 mL/min (in Chapter 8 a variable cross-flow raging from 0.5-3.0 mL/min was used), with a cycle length of 35 min. Briefly, the mobile-phase cross-flow (perpendicular to the mobile-phase channel flow) altered the position of protein particles, within the laminar channel flow, according to their size. Larger particles (e.g. antibody aggregates) were pushed towards the base of the channel, where the velocity of the channel flow was lower, thus resulting in a later elution (see Figure 2.2). Eluted protein was detected by ultraviolet (UV) (280 nm), refractive index (RI) and multi-angle light scattering (690 nm) detectors. Peaks were analysed to determine concentration, and molecular weight based on the concentration data from the UV/RI detectors, whilst the hydrodynamic diameter was measured by light scattering (Astra software v. 4.90.04, Wyatt Technology, Santa Barbara, USA). The UV and RI calibration constants for IgG were 2.2052×10^{-5} and 1.34×10^{-5}, respectively. Samples were measured in triplicate using an HPLC auto-sampler (Hewlett Packard, USA). [For a review of the application of this technique to the analysis of macromolecules see Giddings (1993), for a review with particular reference to biopharmaceuticals see and Fraunhofer and Winter (2004), and for its application in measuring antibody aggregation, see Litzén *et al.*, (1993)].

Figure 2.2 Asymmetrical field-flow fractionation. Protein particles flowing along the channel were pushed by the perpendicular cross-flow, with larger particles being forced towards the slower, base of the channel. Therefore, smaller particles were eluted first, where they were detected by UV, RI and light scattering detectors.

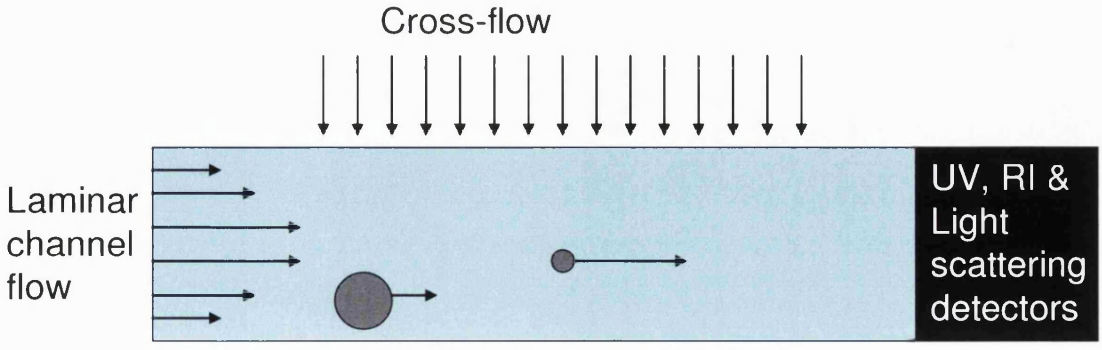

2.6 Formulation toxicity

2.6.1 *In vitro* epithelial cell line viability assay using a tetrazolium dye

The cytotoxicity of the formulations was determined by measuring the cell viability of an *in vitro* cell culture, exposed to them, as a percentage of the viability of untreated cells. Chinese hamster ovary (CHO-K1) cells were cultured in F-12(Ham) + L-glutamine nutrient media, containing 5% fetal calf serum and 1% antibiotics. A 96-well plate was seeded with approximately 20,000 cells *per* well, as 100 µL aliquots, in the same nutrient media. The plate was incubated at 37°C until there was approximately 75% confluence. Suspension/solutions of the formulations were prepared in nutrient media, ranging in concentration from 10-5000 µg/mL. The same concentrations of solutions was also prepared for IgG and sorbitol, lactose and sodium chloride (in Chapter 8 only) for negative controls, and the cytotoxic 25 kDa, branched, poly(ether imide) (PEI), for a positive control. For each concentration of sample, 100 µL was added to a cell-containing well, in triplicate, thus resulting in exposure to concentrations ranging from 5-2500 µg/mL. After 4 h of incubation, 20 µL of a 5 mg/mL solution of 3-(4,5-dimethyl-thiazol-2-yl)-2,5-diphenyl-tetrazolium bromide (MTT) solution was added to each well. After a further 2 h, the media was removed from each well, leaving purple MTT formazan crystals where viable cells (with metabolically active mitochondria) had existed. Dimethyl sulphoxide (100 µL) was added to each well to dissolve the crystals, and the absorbance of each well at 540 nm was determined using a Wallac Victor2 1420 multilabel counter (PerkinElmer, Wellesley, USA).

2.7 Techniques to measure the formulation aerosolisation properties

The following techniques were used to assess the aerodynamic properties of the formulations, and are fully explained in the appropriate chapters of this thesis. The RODOS/HELOS laser diffraction system was used to estimate both dispersibility by **pressure titration** (Section 6.3.2), and particle diameter distribution (Section 6.3.3). Aerodynamic diameter and fine particle fraction were determined by the **'Andersen' cascade impactor** (Section 6.3.4).

The nasal formulations were analysed in terms of **aerosolised particle diameter distribution** (Section 8.3.7), **high-speed video** (Section 8.3.8) and deposition in a **nasal cast model** (Section 8.3.9).

2.8 *In vivo* activity study

An *in vivo* protection study, in a mouse model, was used as a means of testing the activity of a formulated therapeutic antibody (Section 7.3.4).

3 DEVELOPMENT OF A MODIFIED-RELEASE, PULMONARY FORMULATION: REPLACING POLY(VINYL ALCOHOL) WITH DIPALMITOYLPHOSPHATIDYLCHOLINE

3.1 Abstract

Poly(lactide-co-glycolide) (PLGA) microparticles have been used to encapsulate protein drugs to afford stability, modified-release, and the aerodynamic properties required for inhalation delivery. Formulations were manufactured from W/O/W double-emulsions, whereby a model antibody, protected in its own aqueous phase, was dispersed in a dichloromethane phase containing the PLGA, which in turn was dispersed in an external aqueous phase. Microparticles were then produced from the double-emulsions by either solvent evaporation and freeze-drying, or by spray-drying. Typically poly(vinyl alcohol) has been used as an emulsion stabiliser in this method (Ogawa *et al*, 1988). However, when spray-drying, the PVA was retained in the final product, and thus dipalmitoylphosphatidylcholine (DPPC), a component of human lung surfactant, was investigated as an alternative emulsifier. Antibody formulations were produced with various quantities of PVA (0-200 mg), with and without 24 mg DPPC. The double-emulsion external aqueous phase contained 500 mg of lactose (an FDA-approved excipient for pulmonary delivery) to maintain viscosity, and to prevent polymer melting during spray-drying, in the absence of large quantities of PVA.

Without DPPC, 100 mg PVA was the optimum amount for antibody encapsulation efficiency (EE). Below this, the EE decreased, probably due to a destabilisation of the double-emulsion. Addition of DPPC at all PVA concentrations, improved the EE, and >80% EE was achieved, even in the absence of PVA. Reduction of PVA, and the addition of DPPC, both reduced the immediate burst-release. This was possibly due to PVA disrupting the polymer matrix, and DPPC forming a hydrophobic coating on the particles. Although DPPC reduced the aqueous dispersibility of the powder, all spray-dried formulations consisted of microparticles with a large proportion within the 1-5 μm size range desired for pulmonary delivery. Electron microscopy images indicated that the non-PVA, DPPC-containing particles may have had different surface properties compared to PVA-containing particles. The DPPC-containing particles appeared relatively non-aggregated. Formulations produced by solvent-evaporation/freeze-drying had very little residual PVA, but consisted of large, non-dispersible aggregates of nano-sized particles. A further experiment demonstrated the importance of locating the antibody in the internal aqueous phase of the double-emulsion. With the antibody located in the external aqueous phase, a much higher immediate burst-release was observed, presumably since less antibody was entrapped within the PLGA matrix.

3.2 Introduction

Poly-lactide-co-glycolide (PLGA) microparticles are being widely investigated as a biocompatible means of producing systemic and mucosal formulations of protein- and nucleotide-based drugs. Such formulations can afford stability to these otherwise labile compounds, as well as providing an opportunity for modified-release (Freiberg and Zhu, 2004; Bilati *et al.*, 2005). PLGA microparticles are commonly manufactured from emulsions; in the case of biopharmaceuticals, these are often water-in-oil-in-water (W/O/W) double-emulsions. In this procedure, the PLGA is dissolved in an organic solvent, such as dichloromethane (DCM), and an aqueous solution of the drug is added to form the primary emulsion. The primary emulsion is then added to a second aqueous phase, of larger volume, and emulsified to form the secondary emulsion. An emulsifier/stabiliser is added to the aqueous phases to stabilise the emulsions. In the Centre for Drug Delivery Research, at the London School of Pharmacy, as in many literature examples (including the original double emulsion method by Ogawa *et al.*, 1988), the stabiliser typically used was poly(vinyl alcohol) (PVA). PVA is not biodegradable in the same way as is PLGA. In rat studies, subcutaneous injection of a 5% m/m aqueous solution of PVA resulted in anaemia and accumulation in various organs, and thus the FDA has not approved it as an excipient in formulations intended for internal human administration (Owen and Weller, 2003). This would suggest that pulmonary formulations containing substantial amounts of PVA are unlikely to be accepted by Worldwide Regulatory Authorities.

Once a stable double-emulsion has been created, microparticles can be produced by a technique involving solvent-evaporation. The double-emulsion, solvent-evaporation method was first described by Ogawa *et al.* (1988), and a modified version has been used in the present work. Briefly, the double emulsions, described above, were stirred continuously for at least 4 h to allow the DCM to evaporate (typically 1 h *per* 1 mL of DCM). This led to precipitation of the PLGA, and encapsulation of the drug within. The resultant microparticles then underwent at least two washing steps, where, after centrifugation, the pellet of microparticles was re-dispersed in water, and re-centrifuged. Finally, the product was lyophilised in a 24 h cycle. It was often assumed that the PVA content of the final product is negligible, since any water-soluble components in the external phase would largely have been removed during the washing steps.

More recently, the Centre for Drug Delivery Research has investigated spray-drying as an alternative method of microparticle production. Spray-drying is becoming increasingly popular for this application, due to its robustness and relative simplicity (Schwach *et al.*, 2003; Blanco-Prieto *et al.*, 2004). In this work, the double-emulsion

formulations described above have been immediately fed into the spray drier, resulting in rapid evaporation of the DCM and the water, generating a dry-powder product. PLGA microparticles have been produced by simple spray-drying an organic solution of the polymer (e.g. Blanco *et al.*, 2006). However, here an emulsion system was used to avoid denaturation of the antibody. Also, this method reduced the required volume of organic solvent. Unfortunately, though, unlike the solvent-evaporation method, PVA could potentially be retained in the final product, as all components were dried without any prior washing. The only possibility of removing some PVA would be to dry it less efficiently than the other components, causing it to deposit on the walls of the drying chamber, and so not be contained within the final product.

Therefore, because spray-dried formulations may have contained substantial amounts of potentially toxic PVA, in the present work dipalmitoylphosphatidyl choline (DPPC) was investigated as an alternative emulsifier. DPPC, a surface-active molecule, is one of the components of human lung surfactant, and is approved for use in pulmonary delivery by the FDA. Naturally occurring at the lung surface, DPPC has been shown to make PLGA microparticles undetectable to macrophages, and thus prolong their residence on the mucosa (Evora *et al.*, 1998). Other potential advantages were improved particle dispersibility (Weers *et al.*, 2007) and increased protein stability (Sandor *et al.*, 2002). Although emulsions containing DPPC, have been spray-dried successfully (Dellamary *et al.*, 2000), and its incorporation in a PLGA-PVA double-emulsion/solvent-evaporation (not spray-dried) formulation has been published (Evora *et al.*, 1998), the literature contains no published examples of where DPPC has replaced the use of PVA.

PVA may also provide protein and polymer protection during spray-drying. Therefore, to reduce the need for PVA, lactose has been added to the external phase for this purpose. Disaccharides, such as lactose, have been shown to protect macromolecules in spray-drying processes. In this work, the lowest molecular weight PLGA 50:50 (1A, 7 kDa) commercially available has been used, since it has the shortest aqueous degradation time, of 2-3 weeks. This was thought to be most appropriate for pulmonary delivery, since clearance mechanisms and safety concerns would probably prohibit longer durations of residence. However, melting temperature is low at this molecular weight, and thus lactose has been used to improve thermal stability in the spray drier. Lactose, being a GRAS (Generally Regarded As Safe) excipient for pulmonary delivery, and also having shown to enhance the aerosolisation properties of microparticles, would appear to be favourable to utilise for this application (Bosquillon *et al.*, 2004b).

3.3 Aim

The aim of this work was to produce a biocompatible, PLGA-based micro-particulate formulation for the encapsulation of a therapeutic antibody, suitable for pulmonary delivery. Double-emulsion formulations were produced using human normal immunoglobulin G (IgG), as a model therapeutic antibody. Firstly, solvent-evaporation and spray-drying methods were compared in terms of the product yield, encapsulation efficiency (EE) of the IgG, and the residual PVA content. Secondly, an attempt was made to find the minimum amount of PVA that was required to produce microparticles with high yield, high EE and low IgG immediate burst-release, with or without DPPC in place.

3.4 Methods

Microparticles were produced from the double-emulsions by either solvent-evaporation and freeze-drying, or by spray-drying as described in Sections 2.2.1 and 2.2.2, respectively. Initially, the following spray-drying parameters were used: inlet temperature 110°C, aspirator 55%, atomization flow rate 800 L/h, and pump speed 14%. This resulted in an outlet temperature of 50-60°C. Powders were collected and stored in a dessicator at room temperature until they were analysed 1-2 days later.

Sixteen batches were produced to test five different amounts of PVA with and without DPPC (detailed in Table 3.1). When used, DPPC was dissolved in the DCM phase with the PLGA, as described by Evora *et al.* (1998). Some batches were produced without protein to provide negative controls.

Table 3.1 Quantities of ingredients used in experiment batches. The stated masses of poly(vinyl alcohol) (PVA) were split equally between the internal and external aqueous phases.

Batch	*IgG (mg)*	*PVA (mg)*	*DPPC (mg)*
1	10	200	0
2	10	200	24
3	0	100	0
4	0	100	24
5	10	100	0
6	10	100	24
7	10	50	0
8	10	50	24
9	0	20	0
10	0	20	24
11	10	20	0
12	10	20	24
13	0	0	0
14	0	0	24
15	10	0	0
16	10	0	24

The amounts of PVA specified in Table 3.1 were split evenly, by mass, into the two aqueous phases. Batches 1 and 2 were also produced by the solvent-evaporation method to serve as a comparison.

Batches were characterised, in triplicate, in terms of EE, burst-release within 2 h (methods described in Sections 2.3.1-2.3.3) and PVA content. PVA content was determined by a PVA assay based on the method by Takeuchi *et al.* (1998). Briefly, 5 mg of each batch of particles and 10 mg of PVA (as a standard) were each incubated in 1 mL 0.5 M sodium hydroxide (NaOH) at 60°C, overnight, until the standard had visibly dissolved. Samples were centrifuged to exclude any undigested PLGA, or denatured protein. Several dilutions of the PVA standard were made using further NaOH, in order to produce a calibration graph. For each sample, 50 μL was added to 3 mL of 4% boric acid, 0.6 mL of iodine solution and 6.35 mL water. The iodine solution consisted of 2.5 g potassium iodide and 1.27 g iodine in 100 mL water. These mixtures were vortexed thoroughly, and 200 μL of each were added in quintuplet to a 96-well plate. The absorbance of each well was measured at 630 nm using a microplate reader (Opsys MR, Dynex Technologies, USA), and an average of the five readings was calculated. The standard concentrations used are given in Table II, Appendix I.

For EE and 2 h burst-release, the blank batch with the closest DPPC content to the sample being analysed, was used. Geometric diameter was measured immediately after dispersion in water, as described in Section 2.2.6. Morphology was analysed by SEM and light microscopy. For some of the spray-dried batches, reducing-SDS-PAGE was conducted to determine whether the spray-drying conditions had adversely affected the antibody structure (Section 2.5.1). Ten milligrams of formulation was incubated in 1 mL PBS at 37°C for 2 h, and loaded into the gel either as a suspension of particles, or as supernatant having centrifuged the samples (as described in Section 2.5.1a).

3.5 Results

The spray-dried batches were produced with yields ranging between 23-38%, except for batch 13, where no powder was produced. The lack of an emulsifier or protein in this batch prevented a stable emulsion being formed, such that all material sank to the bottom of the beaker as solid clumps, before spray-drying could occur. Particularly where lower masses of PVA were used, the presence of DPPC appeared to increase the yield. For the batches produced by solvent-evaporation, the yields were 45% without DPPC, and 55% with DPPC.

3.5.1.a) Encapsulation efficiency

The calibration curve for the Bradford assay (in NaOH) had the equation: $y = 243.53x^2 - 168.34x + 23.705$, with an R^2 value of 0.9987. This was used to calculate the unknown protein concentrations.

The EEs of the spray-dried batches are given in Figure 3.1 for various PVA contents, with and without DPPC. It can be seen that DPPC appears to have increased EE at all PVA contents, and prevented the reduction in EE observed when PVA content was decreased. Both solvent-evaporation batches had an average EE of 78%.

Figure 3.1 Encapsulation efficiency (EE) of IgG in spray-dried microparticulate formulations prepared with varying amounts of poly (vinyl alcohol) (PVA) and dipalmitoylphosphatidylcholine (DPPC). EE was determined by the Bradford assay (n=3 + SD).

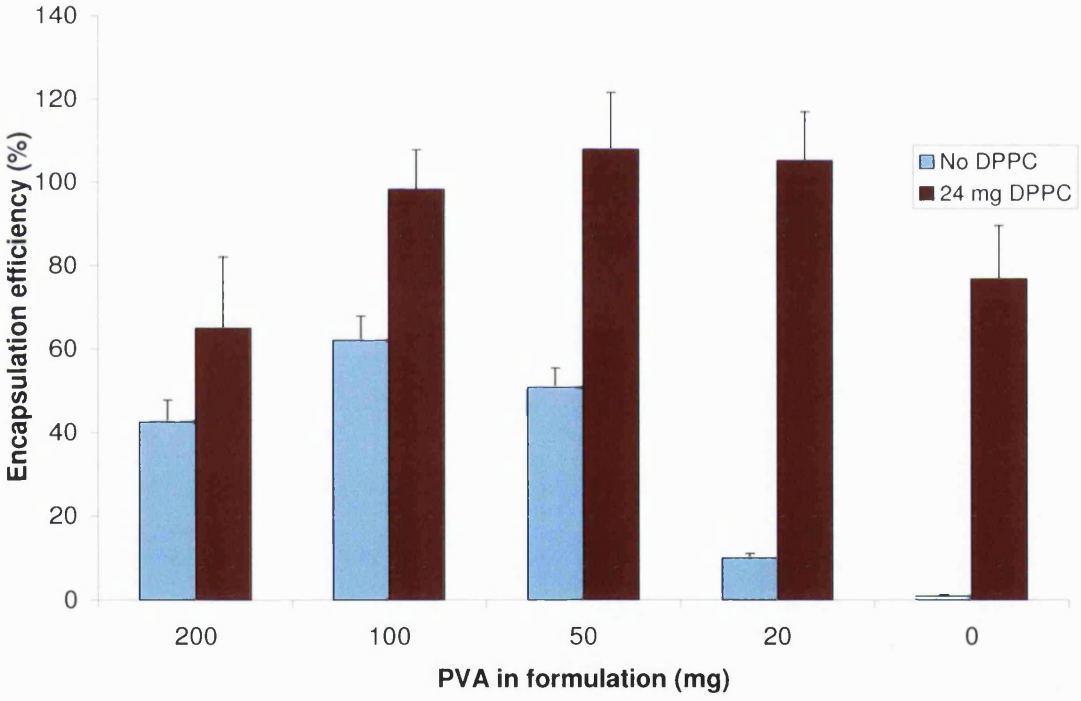

3.5.1.b) PVA content

The standard graph for the PVA assay was a straight line with equation $y = 0.1046x + 0.06$, $R^2 = 0.9898$. The results (Figure 3.2) indicated that the proportion of PVA in the spray-dried formulation was almost the same as in the original formula. However, for batches produced by solvent-evaporation the PVA content was approximately 2% m/m.

Figure 3.2 Poly(vinyl alcohol) (PVA) content of spray-dried microparticulate formulations of IgG. Formulations were analysed by the iodine-based PVA assay described by Takeuchi *et al.* (1998), and the results were compared with the mass of PVA in the double-emulsion, prior to spray-drying (n=3 + SD).

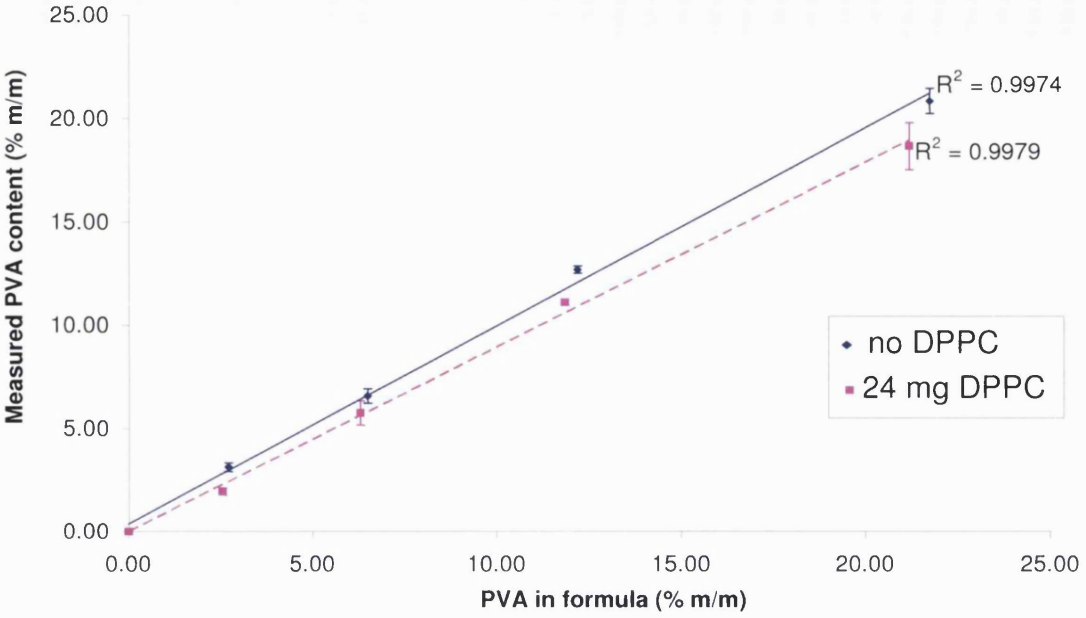

3.5.1.c) Immediate IgG burst-release

The percentage of loaded IgG that was released by 2 h (to indicate the initial burst-release) is given in Figure 3.3. The Bradford assay calibration curve (in PBS) had the equation $y = 183.48x^2 + 113.44x - 85.249$, $R^2 = 0.9981$. DPPC generally decreased 2 h burst-release, as did a reduction in PVA content. The burst-release of the non-DPPC containing formulation, produced by solvent-evaporation was 21% ± 1% (n=3).

Figure 3.3 Initial burst-release of IgG from spray-dried microparticulate formulations. Burst-release was determined by measuring the protein release within 2 h incubation in PBS at 37°C, and expressed as a percentage of the total IgG loading (n=3 + SD).

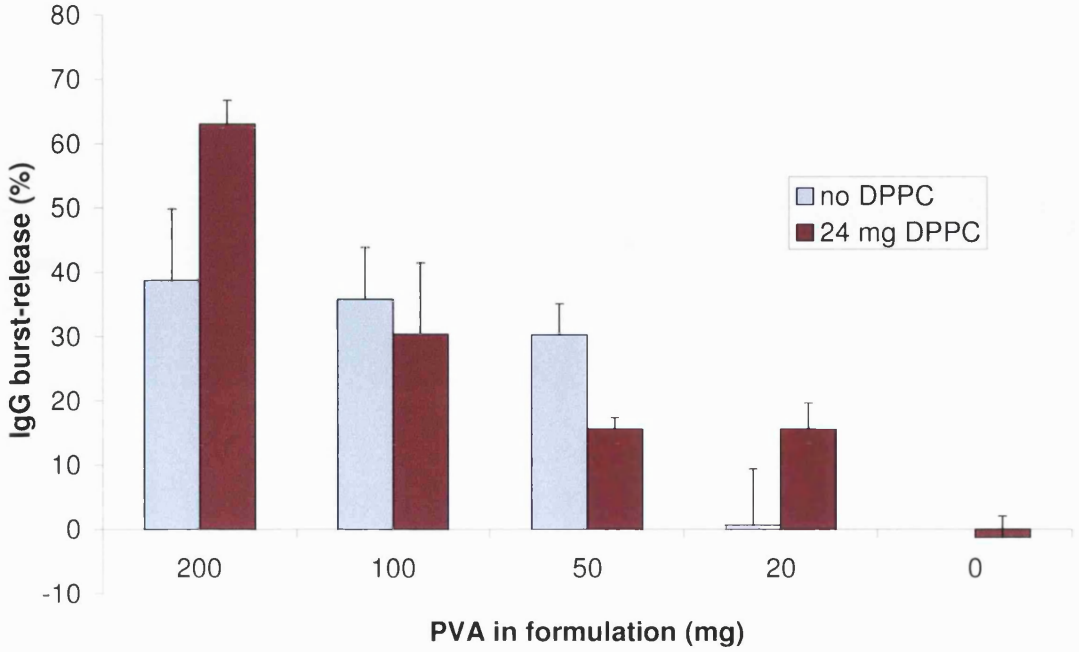

3.5.1.d) Geometric diameter

All spray-dried formulations had similar diameter distributions: a range of approximately 1-10 µm and a mean volume diameter of 3-4 µm. For the DPPC-containing particles, there was an aggregate peak when dispersed in pure water. However, this was removed by adding 0.02% v/v Tween 20 as a dispersing agent. Figure 3.4 illustrates the particle diameter distribution for such a formulation. The formulations manufactured by solvent-evaporation and freeze-drying, did not appear to consist of individual microparticles. Despite the use of Tween 20 and sonication, only large aggregates of particles of several hundred microns could be detected.

Figure 3.4 Geometric diameter distribution of a spray-dried, DPPC-containing, poly(lactide-co-glycolide) (PLGA) microparticulate formulation of IgG, using 0.02% v/v Tween 20 as a dispersing agent. It can be seen that >95% of the volume of particles were smaller than 10 µm, with no apparent aggregate peaks.

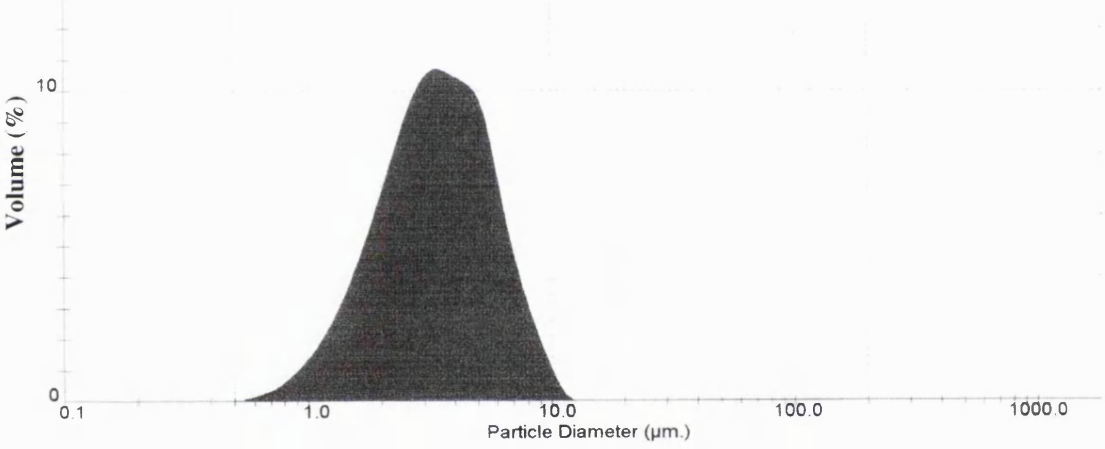

3.5.1.e) Scanning electron microscopy (SEM)

SEM images are shown in Figures 3.5-3.7.

Figure 3.5 Scanning electron micrograph of PVA-containing microparticles. The two images shown are of the same sample viewed at different levels of magnification. Spherical microparticles (mostly <5 µm), with a smooth surface were observed, although there was some evidence of particle aggregation.

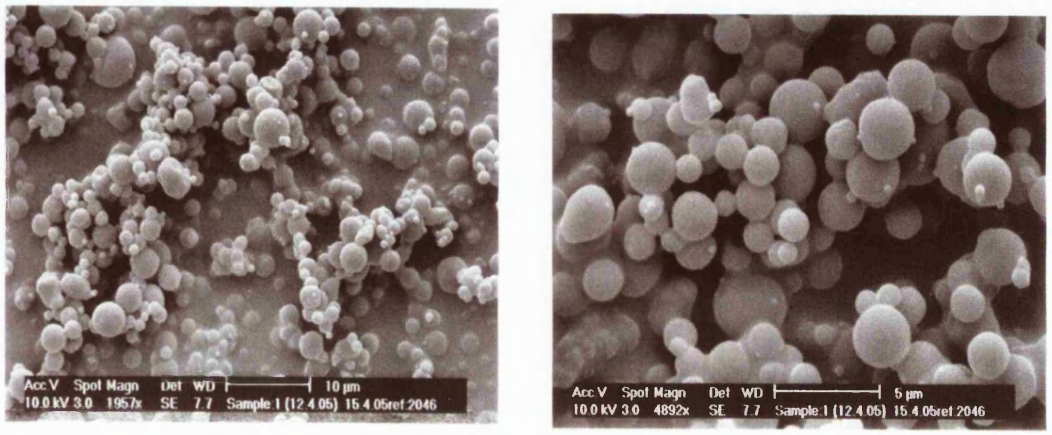

Figure 3.6 Scanning electron micrograph of non-PVA, DPPC-containing microparticles. The two images shown are of the same sample viewed at different levels of magnification. Spherical microparticles (mostly <5 µm) were observed. However, many particles appeared to have a rough surface, although they appeared well dispersed.

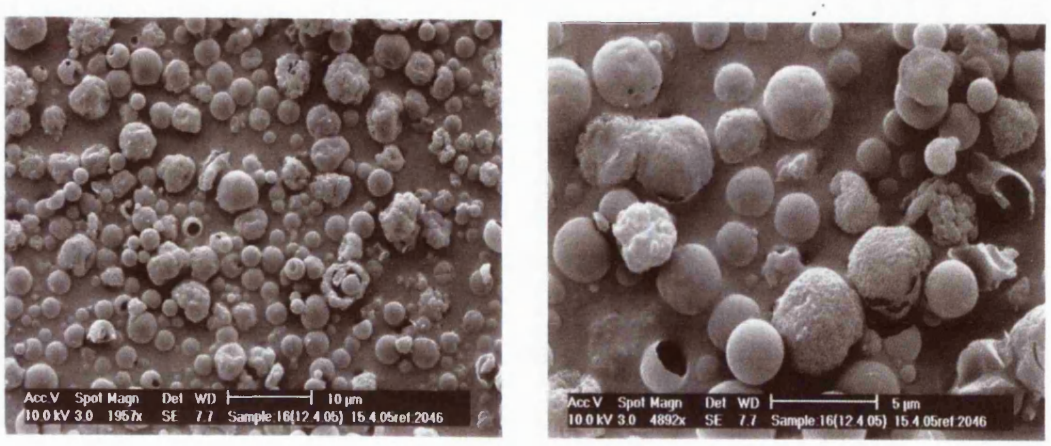

Figure 3.7 Scanning electron micrograph of solvent evaporated, freeze-dried non-PVA, DPPC double-emulsion. It appeared that this formulation was composed of large, irregular particles. However, it could be seen that these particles were aggregates of nano-sized spheres, which may have been formed from the emulsion droplets.

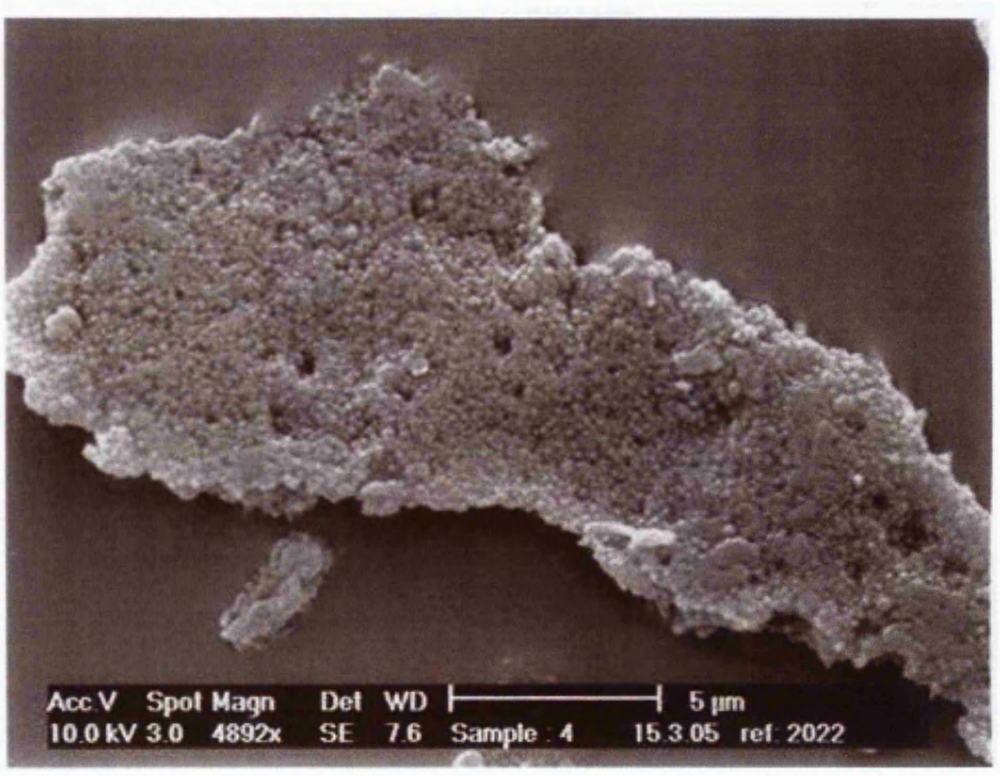

3.5.1.f) SDS-Gel electrophoresis

Figure 3.8 depicts a photograph of the gel produced by reducing SDS-PAGE. There appeared to be two major bands for all samples containing IgG, whether formulated or unformulated, suspensions or supernatants, and regardless of the excipients. These two major bands were absent for the blank formulations. Intensity quantification could not be performed because of the non-continuous intensity of the bands. However, approximate concentrations can be estimated by the qualitative observation of the IgG standards (lane 1, Figure 3.8), since the band intensities visibly decreased with decreasing IgG concentration (100 down to 20 µg/mL).

Figure 3.8 Gel electrophoresis of IgG-containing microparticles. IgG formulations (lanes 4-7) were incubated in PBS, 37°C, for 2 h, before loading the suspension onto the gel, or centrifuging and using the supernatants. Reducing conditions were used, and protein migration was detected using a silver-based staining system. Formulations were compared with unformulated IgG at different concentrations (lane 1: 100, 80, 60, 40 and 20 µg/mL), and blank formulations that contained both PVA and DPPC.

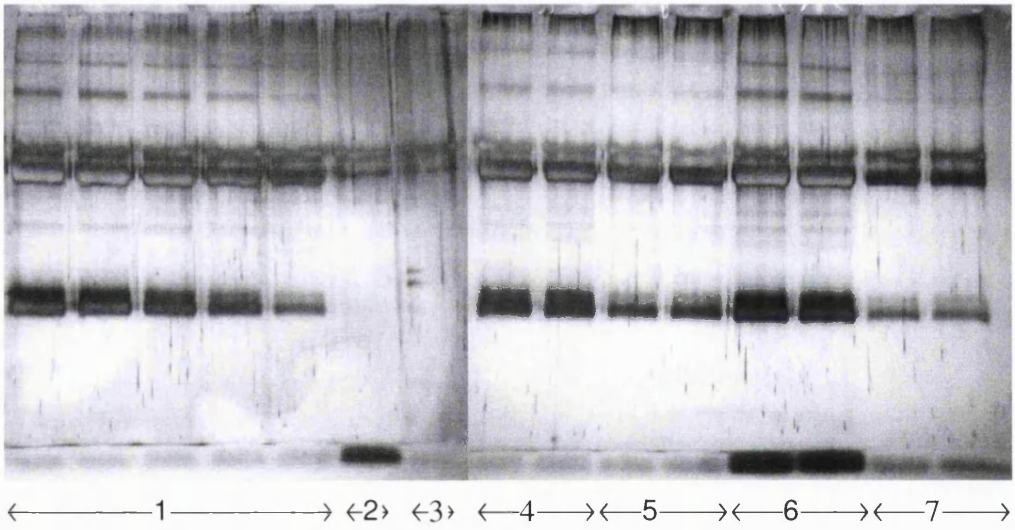

1. IgG standards (100 - 20 µg/ml)
2. Blank particle suspension
3. Blank particle supernatant
4. PVA-containing particle suspension
5. PVA-containing particle supernatant
6. DPPC-containing particle suspension
7. DPPC-containing particle supernatant

3.6 Discussion

3.6.1 Comparison of solvent-evaporation and spray-drying methods

From these data it was obvious that the PVA content of microparticles produced by spray-drying was appreciably higher than microparticles produced by the solvent-evaporation method. For the latter method it would appear that the assumption of negligible PVA content was reasonable, and with only approximately 2% m/m PVA [a value consistent with other studies (Panyam *et al.*, 2003)], the particles formed were largely composed of PLGA. Therefore, despite the large mass proportion of PVA in the starting material, the washing steps appeared to efficiently remove PVA from the final product. However, for spray-drying, as expected, PVA was retained in the final product in the same proportion as it was in the starting materials.

The protein loading of microparticles produced by solvent-evaporation was approximately twice that of the spray-dried formulations. This would be expected, since *per* gram of powder, the spray-dried particles contained less IgG due to the PVA and lactose content. Unlike the solvent-evaporation procedure, where the water-soluble antibody only remained in the final formulation if it was encapsulated by PLGA, in the spray-drying approach the antibody (and all other water-soluble excipients) was retained in the final product, since there were no washing. Therefore, as expected, higher EEs were achieved with the spray-drying method (Lane *et al.*, 2006). However, whereas PLGA has the matrix properties required to efficiently encapsulate and control the release of IgG, the IgG in the spray-dried formulation, not encapsulated by PLGA was likely to release rapidly, and may have been damaged due to heat exposure. It was demonstrated from the initial burst-release properties, that the spray-dried particles, containing large amounts of PVA, did not have the low initial burst-release characteristics of the microparticles produced by solvent-evaporation. It was likely that the spray-dried particles quickly dissolved in PBS when their major components were lactose and PVA, since they are water soluble. The PVA in the internal aqueous phase probably disrupted the formation of a complete PLGA matrix. Any antibody juxtapositioned to PVA, rather than PLGA, would have been released upon PVA dissolution. The remaining PLGA matrix fragments may also have had a larger surface area, again causing the rapid release of protein from these surfaces.

Whereas the laser diffraction and SEM data suggested that the spray-dried formulations were composed of microparticles, this was not true for the solvent-evaporation/freeze-dried formulations. When the freeze-dried powder was re-dispersed in water, fragments

of several hundred microns were detected by laser diffraction. However, SEM images revealed that these fragments were actually composed of aggregated, spherical, nanoparticles. The 200 mg of PVA in these formulations was relatively little compared the amount typically used for the double-emulsion, solvent-evaporation method (e.g. Ogawa *et al.*, 1988). This small amount was chosen with the aim of minimising the PVA content in the spray-dried batches, while forming a stable emulsion. It would seem that with this formulation and emulsification parameters, nano-sized droplets were formed. Perhaps, due to the low PVA content, or simply because of the small size, the freeze drying process caused these potential nanoparticles to aggregate, and lose their individuality. Trehalose (5, 10 and 20% m/m) was added to the suspensions prior to freeze-drying as a means of preventing this aggregation (see Wang, 2000), but it had no effect. However, even if they could be dispersed as nanoparticles, particles of this size would be inappropriate for pulmonary deposition, since particles <200 nm are predominantly exhaled (Gonda, 1992). Spray-drying, on the other hand does not rely on the size of the emulsion droplets to determine particle diameter. Rather, it is dependent on the droplet size generated by the spray drier nozzle. Thus, dispersible microparticles were produced.

3.6.2 Protein loading

Without DPPC, 100 mg PVA was the optimum amount for protein encapsulation. Below this, the encapsulation efficiency (EE) decreased to ~0%. This may have been due to a lower stability of the double-emulsion, due to less PVA acting as a stabiliser. Without any emulsifier, a stable emulsion could not be formed, particularly due to the relatively low inherent viscosity of PLGA 1A (0.08-1.12 dL/g). In the situation of an unstable emulsion, protein encapsulated by PLGA was not spray-dried, since the oil-phase droplets coalesced, and settled to the bottom of the beaker. The addition of DPPC, at all PVA concentrations, improved EE to a maximum of ~100% (Kaye *et al.*, 2006a). This finding agreed with the work of Mu and Feng (2001), who found adding lipid emulsifiers, increased the entrapment of paclitaxel in PLGA microparticles. DPPC probably coated the surface of the oil phases, preventing their coalescence. As PVA content was reduced, DPPC acted as an alternative emulsifier, thus preventing a loss of encapsulation capability.

Although the formulations with DPPC all contained 24 mg DPPC, as a percentage, this increased as the amount of PVA decreased. This may explain why EE increased in the DPPC formulations as PVA decreased, until PVA content was below 50 mg per batch, when possibly the absence of PVA was an overriding factor.

3.6.3 PVA content

The PVA assay data demonstrated that the PVA content of the final product was proportional to, and almost equal to, the amount of PVA in the starting materials. DPPC slightly reduced the amount PVA retained in the final product. Perhaps if there were atomised droplets containing only PVA, these would be less efficiently dried and collected if coated with DPPC.

3.6.4 Burst-release of IgG within 2 h

A reduction of PVA content reduced the initial burst-release. A possible explanation was that in the microparticle structure, large amounts of PVA disrupted the continuity of the polymer matrix. Thus, on contact with water, the PVA dissolved leaving channels in the PLGA matrix, or even caused mass fragmentation of the PLGA matrix. This would have left the matrix with a larger surface area, and any protein on the surface would quickly be released, and go into solution, in the media.

It is difficult to make judgements about those batches that contained little or no PVA, and no DPPC. These formulations had a very low total protein loading, and therefore measuring what fraction of this was released, was obviously difficult due to the limited sensitivity of the Bradford assay. In those formulations with DPPC, when no PVA was present, particles had a very low immediate burst-release (Kaye *et al.*, 2006a). As well as this being caused by a lack of PLGA matrix disruption by PVA, another explanation could have been that DPPC led to a more hydrophobic particle surface, delaying wetting and dispersion, and thereby further delaying release. This hypothesis was supported by geometric volume diameter data, and also by microscopy observations of these formulations, in which the particles appeared to be more dispersed.

3.6.5 Geometric diameter

It should be noted that the measurements in this experiment were conducted in water, rather than the optimised dispersion system discussed in Section 2.4.1. Without Tween 20, there was a bimodal volume distribution, with a main 1-10 μm peak, presumably representative of the individual microparticles, followed by a smaller peak of larger diameter. This second peak probably consisted of aggregates of microparticles (tens of microns), and was an artefact of incomplete dispersion. Aggregate peaks were particularly evident for DPPC-containing formulations. As suggested for the 2 h burst-release data above, DPPC may be packed at the liquid/air interface during spray-drying, thus coating the microparticle surfaces and giving them a higher hydrophobicity. In

aqueous media this would reduce the tendency for the microparticles to disperse spontaneously. Addition of 0.02% v/v Tween 20, a water soluble surfactant, to the dispersion media, removed the second peak of aggregates. For all formulations, a large fraction of the particles were within the desired 1-5 μm diameter required for successful airway delivery. However, according to Figure 3.4, some of the particles were smaller than the approximate 2 μm separation limit of the standard cyclone in the Büchi 191 spray drier. This may have been due to the water-soluble components of the formulation (particularly lactose), beginning to dissolve in the aqueous dispersion media, or possibly if the particles were very dense, allowing them to sediment in the cyclone. When measuring particle diameter in water, it was therefore important that the reading was taken as quickly as possible, and also that the vortexing time for each sample was kept constant.

3.6.6 Electron microscopy observations

SEM images indicated that the non-PVA, DPPC-containing particles may have had some surface roughness. This may have been due to a lack of PVA at the surface or indeed the presence of DPPC at the surface. If DPPC had formed a non-porous coating around the droplets being spray-dried, the vapour pressure within the droplet may have increased. This pressure may have pulled in on the drying-particle crust, resulting in dimpled particle surface (Masters 1991; Maury 2005). Also, these particles appeared less aggregated, and thus could have been potentially more free-flowing and less-cohesive, relative to the PVA-containing particles. This was consistent with other findings discussed above, and may have been due to a more hydrophobic surface resulting from employing the DPPC. Although in wet conditions such microparticles may have dispersed less easily, in a dry-powder state (and perhaps in hydro-fluorocarbon propellants) they may have been less agglomerated than PVA-containing particles, since hydrophobic interparticulate interactions, would have been smaller than hydrophilic interactions (Hickey *et al.*, 1994). (This was further explored as described in Chapter 6 of this thesis).

The SEM findings were further supported from observations using a light microscope. When dispersed in water on a microscope slide, the PVA-containing particles appeared separated and free-flowing. However, the non-PVA, DPPC-containing particles appeared as aggregates in small clusters. This would suggest that the particles had a hydrophobic surface. However, this property could be the reverse for dispersion in a non-aqueous propellant, or as a dry-powder formulation, and may have helped reduce hydration related formulation damage.

3.6.7 Gel electrophoresis

On the SDS-PAGE gels (Figure 3.8) two major bands were present. Unfortunately, the bands were non-continuous preventing intensity quantification. However, the effect of concentration could be seen, and the samples were present with an expected qualitative intensity. Given that the antibody was the only protein in the formulation, the fact there were two major bands suggested that the antibody had become fragmented. However, this could not have been due to a problem with the formulation process, since the unformulated IgG controls also showed exactly the same pattern of bands. Indeed, the literature (Beck *et al.*, 2005) confirmed that analysis by reducing SDS-PAGE often produces two bands which represent the light and heavy chains of an antibody. The antibody had split into its composite chains, possibly due to the reduction of disulphide bridges during heating with mercapto-ethanol.

3.7 Conclusion

Unlike the double-emulsion, solvent-evaporation method, spray-drying of a double-emulsion preparation led to almost all of the PVA used as an emulsion stabiliser being retained in the final product. It was possible to produce microparticles that efficiently encapsulate IgG (>80% EE) without any PVA in the formulation. This has been achieved by the inclusion of DPPC, an endogenous component of lung surfactant, as an alternative emulsion stabiliser, together with lactose. DPPC, as well as potentially being a more acceptable excipient than PVA for a formulation for pulmonary delivery, may in fact elicit a range of other formulation advantages, such as enhancing encapsulation efficiency, controlling protein release and improving powder flow properties. However, the use of this formulation for the solvent-evaporation method appeared to be limited, since this emulsion system formed nanoparticles which aggregated on freeze-drying.

The spray-dried formulation containing DPPC and no PVA was selected as a lead formulation for further optimisation. The advantages of having no PVA in the formulation outweighed the 20% maximum reduction in EE. Moreover, this formulation produced microparticles of the diameter desired for pulmonary delivery, with a low IgG immediate burst-release, and interesting surface properties.

3.8 Further understanding the spray-dried, double-emulsion system

3.8.1 Aim

In the formulation described thus far, the antibody was contained within an internal aqueous phase. Certainly, in the case of the solvent-evaporation method, this approach was taken to ensure that antibodies were encapsulated by the polymer, or dispersed within the polymer matrix, rather than being washed away in the external aqueous phase of the emulsion, during the washing steps prior to freeze-drying. However, in the case of spray-drying, it could be questioned whether this approach was in fact necessary, since virtually all material became part of the final product, regardless of which phase it was in. Therefore, it seemed possible to simply make a single O/W emulsion, with the antibody in the external aqueous phase.

It was hypothesised that a double-emulsion was, however, beneficial. There may be no loss of EE as a consequence of the antibody being added to the external phase. However, it was thought that the antibody would be released instantly, since it would not be encapsulated by the polymer, but rather be adsorbed on the PLGA surface. In fact, if this were to be the case, there would be no need to include PLGA in the formulation at all. Also, the antibody might be more susceptible to damage by shear or heat during emulsification and spray-drying. This hypothesis was tested by comparing such formulations.

3.8.2 Method

Three double-emulsion, spray-dried, formulations were produced containing PLGA, lactose and DPPC as described in the previous Section (containing no PVA). However, 20 mg of IgG was used in either the internal aqueous phase, the external aqueous phase, or split evenly between the two aqueous phases. All other aspects of emulsion production and spray-drying were as described in Section 2.2.1-2.2.2. Formulations were assessed in terms of EE, IgG burst-release by 2 h and released antibody stability by non-reducing SDS-PAGE (Sections 2.3.2, 2.3.3 and 2.5.1, respectively).

3.8.3 Results

The EE and 2 h burst-release results are summarised in Table 3.2:

3.2 Summary of encapsulation efficiency (EE) and 2 h (burst-) release data for spray-dried, double-emulsion, formulations of IgG, with the IgG located in various phases of the emulsion.

	EE (%, n=3)	Burst-release (%, n=3)
20 mg IgG internal phase	90 ± 3.2	37 ± 2.4
10 mg IgG internal 10 mg IgG external	91 ± 4.5	32 ± 2.0
20 mg IgG external phase	88 ± 0.4	58 ± 2.8

Figure 3.9 is a photograph of the SDS-PAGE results.

Figure 3.9 Gel electrophoresis of 2 h burst-release samples from spray-dried IgG formulations. Formulations were prepared by the spray-drying of double emulsions, with the IgG located in various phases of the emulsions. The formulations were incubated in PBS for 2 h at 37°C, prior to analysis of the released IgG (collected by centrifugation) by sodium dodecyl sulphate, poly acrylamide gel electrophoresis using non-reducing conditions. (Lanes: 1: molecular weight marker, 2: unformulated standard IgG, 3: blank formulation, 4+5: 20 mg IgG internal phase, 6+7: 10 mg IgG in each phase, 8+9: 20 mg external IgG).

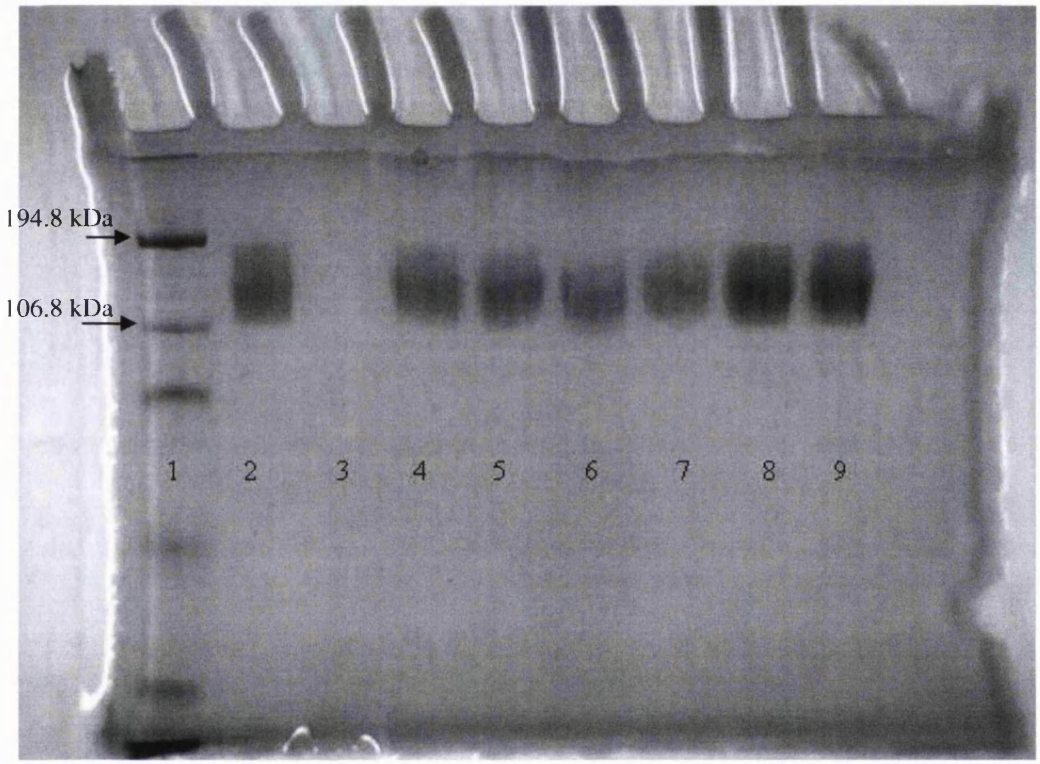

3.8.4 Discussion

The PLGA formulation was prepared by the spray-drying of a W/O/W emulsion. Previously, the antibody was added only to the inner aqueous phase that was dispersed within the PLGA-containing oil phase, both of which were then dispersed in an external aqueous phase. The hypothesis was that this would entrap the antibody within the polymer while the liquid feed was being spray-dried, resulting in a low initial burst-release. Immediate burst-release was presumed to occur due to antibodies on the surfaces of the PLGA particles. This hypothesis was certainly true for the solvent-evaporation method, where the oil phase, only, was evaporated over a few hours. However, when spray-drying, both the oil and aqueous phases were evaporated extremely rapidly, while the liquid feed was atomized. Therefore, the ordering in each emulsion droplet may not have been at all stable, but rather a random mixture of antibody, polymer and other exipients were probably dried into each single particle. Thus, when a low initial burst-release was observed, this could have been just because of an electrostatic, or hydrophobic, interaction between the polymer and the antibody, when dispersed in aqueous media, rather than the antibody being physically entrapped

within the polymer matrix.

However, changing the location of the antibody in the emulsion did affect the initial burst-release. As expected, when the entire quantity of antibody was within the external phase, a higher burst-release was observed by 2 h. However, in this case, there was not 100% immediate burst-release as would be expected, if the hypothesis was completely true. Also, where there was a 50/50 distribution of antibody, the 2 h burst-release was the same (or slightly lower) as if it had been all located internally.

These data may suggest that some of release retardation could have been due to a hydrophobic, or electrostatic, interaction between the antibody and the polymer surface. The hydrophobic polymer chain may adsorb to antibody hydrophobic amino acid side chains. Alternatively, carboxylic acid polymer end-groups may interact *via* an electrostatic interaction with amine groups on the antibody. However, there must have been some reliance on a physical encapsulation, as some increase in immediate burst-release was seen when the antibody was added entirely to the external aqueous phase. It would seem that the surface interaction may have had a limited capacity, such that 10 mg of external antibody was able to be retained to the same extent as if it were all encapsulated internally, whereas 20 mg was not fully retained. Of course, in the case of 20 mg antibody in the internal phase, some of this must have escaped to the surface, as 30% burst-release was observed within 2 h, and it is likely that some further antibody was retained by a surface interaction.

The SDS-PAGE data suggested that having the antibody in the internal phase was not important for antibody stability. The final two 'lanes' of the gel depicted on Figure 3.9, were from the batch with 20 mg external antibody. The bands in these lanes were denser because of the higher 2 h burst-release concentration, but there appeared to be no aggregates, or fragments. It should also be noted that non-reducing conditions were used, allowing the IgG molecule to remain intact, and thus appearing as a single band of approximately 150 kDa (c.f. Figure 3.8).

3.8.5 Conclusion

This experiment demonstrated the importance of using the double-emulsion system for the spray-dried formulation. Formulating the antibody in an internal aqueous phase appeared to improve encapsulation within the polymer, such that a reduced initial burst-release was observed. However, the data would suggest that surface interactions were also important. On the other hand, this work suggested that the antibody can be added to the external phase without compromising its stability.

4 FACTORIAL EXPERIMENTS TO OPTIMISE THE PULMONARY ANTIBODY FORMULATION

4.1 Abstract

The previous chapter described the development of a spray-dried double-emulsion IgG antibody formulation, containing polylactide-co-glycolide (PLGA), dipalmitoyl-phosphatidylcholine (DPPC) and lactose. The manufacturing process and excipient content of this formulation was optimised by means of three separate factorial experiments. For each experiment, response data were analysed by a factorial ANOVA to find main effects and interactions, significant at 95% confidence intervals. For the first-two experiments, optimal parameters were calculated based on the data collected, and the outcomes desired.

The first experiment (2^4 + 3 centre points, factorial) investigated the spray-drying parameters. Parameters that resulted in a spray-drying outlet-temperature of 50-60°C produced non-aggregated microparticles containing active IgG. A high rate of atomizing air flow resulted in the greatest increase in product yield. The second (2^3 + centre points) factorial experiment investigated the effect of varying the primary and secondary homogenisation durations and the external phase volume of the double-emulsion. Longer homogenisation time and a larger external phase volume reduced IgG immediate burst-release, and particle diameter polydispersity. The third (2^4 + 3 centre points) factorial experiment measured the effects of varying the amounts of IgG (formulated 1:1 with sorbitol) (10-50 mg), PLGA (50-350 mg), DPPC (10-40 mg) and lactose (100-500 mg). Yield increased with PLGA and lactose content, whereas increasing DPPC to 40 mg reduced the yield by ~10%. Increasing the amount of antibody statistically significantly increased the immediate burst-release from <15% to ~50%. Electron microscopy identified that only optimal excipient combinations produced spherical, non-aggregated microspheres. Assessment of the data led to the centre-point value being chosen for the three excipients, incorporated with 20 mg IgG.

The optimised formulation was found to have a median geometric volume diameter of 3-5 μm in cyclohexane, and of ~400 nm in water, presumably owing to PLGA nanoparticles that freely disperse as the lactose component of the microparticles dissolved. The presence of these nanoparticles was confirmed by transmission electron microscopy and photon correlation spectroscopy. It was anticipated that this mechanism would allow microparticles of inhalable diameters to part-dissolve in pulmonary fluid, into nanoparticles small enough to avoid phagocytosis.

4.2 Introduction and aims

Having decided to use DPPC as a replacement for PVA in the spray-dried microparticle formulation, the aim of this experiment was to optimise the formulation by a series of three factorial experiments, in terms of yield, EE, release properties and microparticulate physical characteristics. Factorial experimental design offered a way of investigating several parameters simultaneously, and measured both the individual and the combined effects.

Firstly, the spray-drying parameters of the Department's spray drier were optimised for the formulation [factorial experiments have previously been used to optimise spray-dring parameters – e.g. Sebti and Amighi (2006)]. The main aims of this experiment were not only to ensure that the yield was being maximised, but also to determine whether adjusting the parameters could be an effective method of engineering particles with different physical properties. Secondly, the homogenisation times and external phase volume were considered important variables to investigate. Previous work suggested that emulsion droplet size had little impact on the diameter of spray-dried particles. Therefore, if homogenisation time could be reduced, less shear stress would be incurred on the antibody. Similarly, external phase volume was investigated in this experiment, because if reduction was possible, the duration of the spray-drying run would be shortened. Also, the external phase volume has the largest impact on feed viscosity, which is thought to impact spray-dried droplet, and thus particle size. Finally, the third experiment aimed to optimise the amount of antibody and amounts of each of the excipients used in the formulation. The aim of this third experiment was to maximise the antibody loading, and reduce unnecessary use of excipients.

4.3 Factorial experiment to optimise the spray-drying parameters

4.3.1 Methods

Statistical software (Minitab v.14, Minitab Inc.) was used to design, and analyse, a 2^4 factorial experiment. At 2 different levels (corner points), 4 parameters were tested, namely, inlet temperature, aspiration, atomizing air flow and pump speed. The levels were chosen based on the parameters that were currently being used, experience of parameters that were unlikely to succeed, and then following the principle of using a range wide enough to make a measurable difference, but within the operational

extremes (Armstrong and James, 1996). Given that only one batch was made for each combination of parameters, three identical centre-point batches were manufactured to give an indication of the magnitude of pure error, relative to the effects of the parameters. These centre-points were also to give an insight into the curvature of any observed effects. All batches were made using the chosen formulation described in the previous Section. Table 4.1 lists the combination of parameters used in each of the 19 batches.

Table 4.1 Design of factorial experiment to investigate the spray-drying parameters used for the formulation of IgG. Batches 17, 18 and 19 represented the centre-points.

Batch	*Pump Speed (%)*	*Spray Flow Rate (L/h)*	*Aspirator %*	*Inlet Temperature (°C)*
1	7	400	55	80
2	21	400	55	80
3	7	800	55	80
4	21	800	55	80
5	7	400	75	80
6	21	400	75	80
7	7	800	75	80
8	21	800	75	80
9	7	400	55	140
10	21	400	55	140
11	7	800	55	140
12	21	800	55	140
13	7	400	75	140
14	21	400	75	140
15	7	800	75	140
16	21	800	75	140
17	14	600	65	110
18	14	600	65	110
19	14	600	65	110

Each batch contained 500 mg lactose, 200 mg PLGA 1A, 24 mg DPPC, 10 mg IgG and 10 mg sorbitol, formulated as a W/O/W double emulsion, as described in Section 2.2.1. A non-protein batch was made for comparative loading measures.

The resulting outlet temperature and yield were recorded for each batch. Powders were stored in a dessicator at room temperature, assessed for EE, in triplicate, by the Bradford assay (Section 2.3.2), and geometric volume diameter, by laser diffraction, after simple dispersion in water containing 0.02% v/v Tween 20 (Section 2.4.1). ELISA was used to assess the effect of outlet temperature on antibody activity (Section 2.5.2). SEM images were also produced for each formulation (Section 2.4.2).

4.3.1.a) Statistical analysis

Statistical significance was assessed by employing 95% confidence levels. The data was analysed using a factorial analysis of variance (ANOVA) to identify statistically significant terms (main effects and interactions). The data were then re-analysed using fewer terms, in order to obtain a normal distribution model with an improved fit. The fit was assessed by looking at the residual plots, the p-value for "lack of fit" and from the R^2 values. The best model was achieved by removing the least significant terms, as identified by the Pareto plot, generally leaving in only those terms that appeared significant in the original analysis. Factorial plots were then produced of the significant terms based on the fitted means from the new model. This process is exemplified with the outlet temperature data described below, and in Appendix V. The data were then used to statistically select optimal parameters for achieving the desired outcomes (chosen as described in Section 4.3.2g). This optimal batch was made and checked for reproducibility.

4.3.2 Results

A summary of all the collected data for each batch is given in Table III, Appendix IV.

4.3.2.a) Outlet temperature

In order to provide an example of the statistical analysis method, the process of generating the outlet temperature results is given in Appendix V.

Having decided on the most appropriate model for the data, factorial plots for the statistically significant effects were produced (Figure 4.1). All of the main effects (individual parameters) had a significant influence on outlet temperature. However, it can be seen that increasing inlet temperature caused a large increase in outlet temperature (40°C), whereas increasing spray flow resulted in just a small decrease in outlet temperature (<5°C). It can be seen from the centre point values that there was little curvature in the data, suggesting that over that range, the relationships were approximately proportional. This was substantiated by the clear absence of statistical significance in the curvature, as indicated by the large p-value for curvature in the ANOVA summary Table (see Table VIII, Appendix V).

Figure 4.1 The effect of spray-drying parameters on the outlet temperature of the spray-drying process. The variables shown had statistically significant ($p<0.05$, factorial ANOVA) main effects on the outlet temperature, when spray-drying a double-emulsion formulations of IgG. The values shown are the fitted means generated by the statistical model that had the closet fit to the raw data. It can be seen that outlet temperature increased most with increasing inlet temperature, increased less so with increasing aspiration, and decreased with increasing pump speed, and decreased slightly with increasing spray flow. The centre-point values indicated that these relationships were linear (•=corner point, ■=centre point).

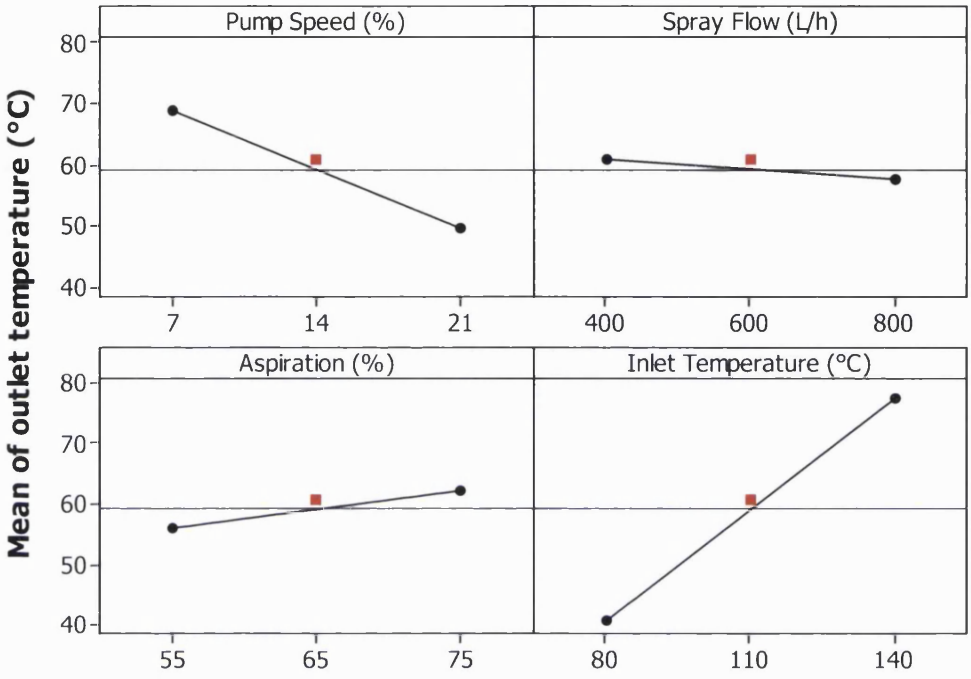

4.3.2.b) Yield

The process described above, and in Appendix V, was used to analyse the yield data. The chosen model had an R^2 value of 98.66%. The statistically significant effects are summarised in the normal probability plot in Figure IX, of Appendix VI. There were significant main effects and second-level interactions.

Figure 4.2 indicates that percentage yield increased linearly as spray flow, inlet temperature and aspiration were increased, with spray flow rate having the largest effect. Increasing pump speed decreased the yield. However, the interaction of spray flow rate with aspiration, pump speed and inlet temperature, means that the change in yield resulting from an increase in these parameters, was dependent on the level of the other parameter in the interacting pair. The effect of this is represented by the two-way interaction plot in Figure 4.3.

Figure 4.2 The effect of spray-drying parameters on the yield of a double-emulsion formulation of IgG. The variables shown had statistically significant ($p<0.05$, factorial ANOVA) main effects on the product yield, when spray-drying a double-emulsion formulation of IgG. The values shown are the fitted means generated by the statistical model that had the closet fit to the raw data. It can be seen that yield increased most with increasing spray flow, and to a lesser extent with increasing inlet temperature and aspiration. Increasing pump speed slightly decreased the yield. The centre-point values indicated that these relationships were linear (•=corner point, ■=centre point).

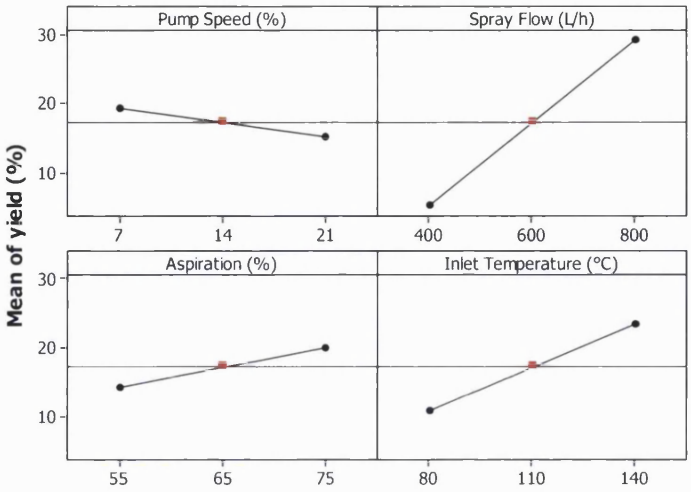

Figure 4.3 Interaction plot of spray-drying parameters affecting yield of a double-emulsion IgG formulation. The plots shown indicate statistically significant ($p<0.05$, factorial ANOVA) second-level interactions. The six boxes represent all of the possible two-way interactions. Absence of a plot within a box was indicative of no statistically significant interaction. The values shown are the fitted means generated by the statistical model that had the closet fit to the raw data. For example, it can be seen that aspiration and spray flow interacted, such that at 400 L/h spray-flow, a 20% increase in aspiration caused a slight decrease in yield, whereas at 800 L/h spray flow, the same increase in aspiration increased yield (•=corner point, ■=centre point).

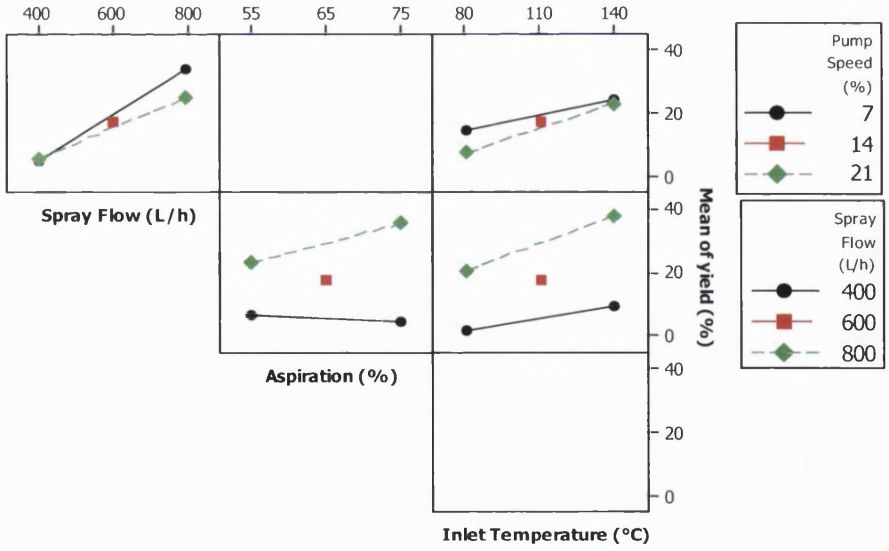

From the interaction plot it can be seen that the increase in yield caused by increasing spray flow rate, was reduced when a high pump speed was used. Similarly, the level of spray flow rate reduced the increase in yield that could be achieved by increasing inlet temperature. In the case of aspiration, when a spray flow of 400 L/h was used, increasing aspiration resulted in a decrease, rather than an increase, in yield.

4.3.2.c) Encapsulation efficiency

There were several main effects and interactions that statistically significantly affected the EE (Normal probability plot given in Figure X, Appendix VI).

The main effects, second-level interactions and third-level interactions are represented by Figures 4.4, 4.5 and 4.6, respectively. The number of interactions and the centre-point values made it difficult to meaningfully interpret the data.

Figure 4.4 The effect of spray-drying parameters on the IgG encapsulation efficiency (EE).
The variables shown had statistically significant ($p<0.05$, factorial ANOVA) main effects on the EE. The values shown are fitted means. The higher settings of both aspiration and inlet temperature resulted in increased EE. However, EE at the centre point settings was far lower than the EE at lower aspiration and inlet temperature settings. This suggested curvature in the data, and possibly interactions of variables.

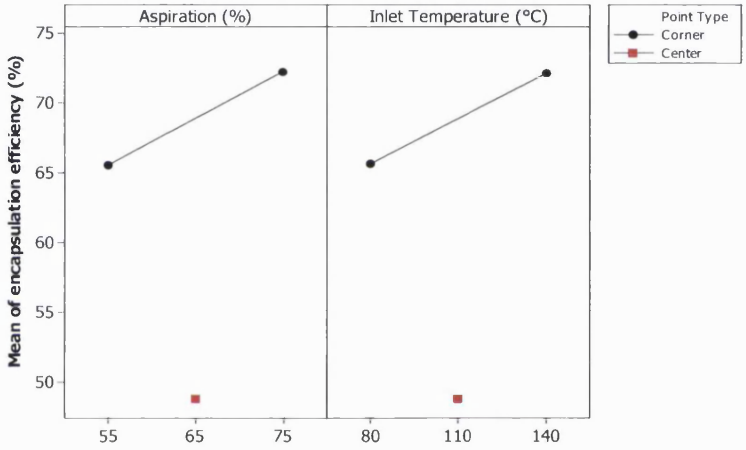

Figure 4.5 Interaction plot of spray-drying parameters affecting IgG encapsulation efficiency.
The plots shown indicate statistically significant ($p<0.05$, factorial ANOVA) second-level interactions. The six boxes represent all of the possible two-way interactions. Absence of a plot within a box was indicative of no statistically significant interaction. The values shown are the fitted means. For every interaction the EE at the centre point parameters was found to be lower than the mean EE of each corner point (•=corner point, ■=centre point).

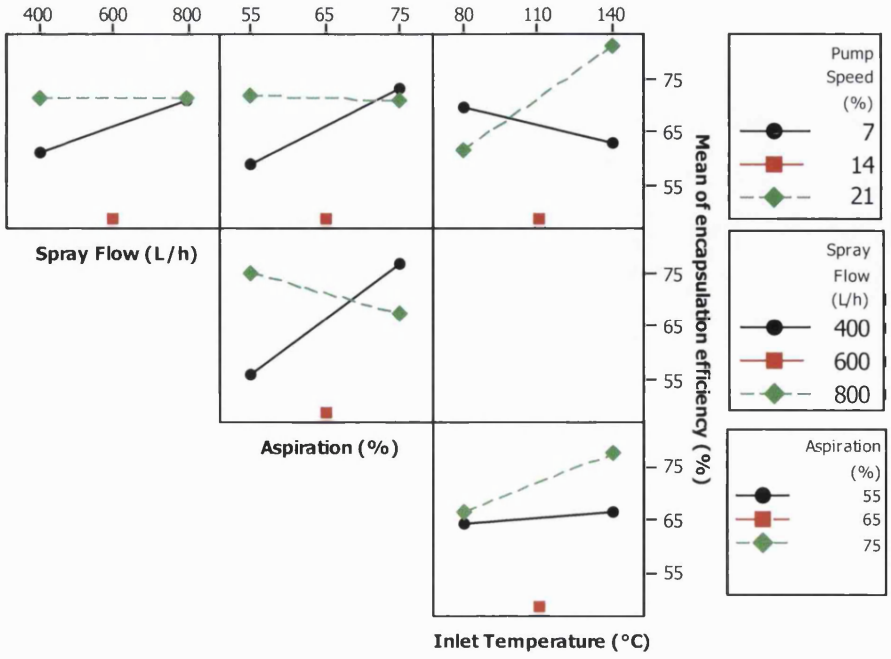

Figure 4.6 Cube plot of spray-drying parameters affecting IgG encapsulation efficiency (EE).
This diagram maps the EEs of individual batches, based on the spray-drying parameters used. This 3-dimensional representation is required to fully appreciate the affect of the four spray-drying parameters on EE, due to the statistically significant ($p<0.05$, factorial ANOVA) third-level interactions (•=corner point, ⊕=centre point).

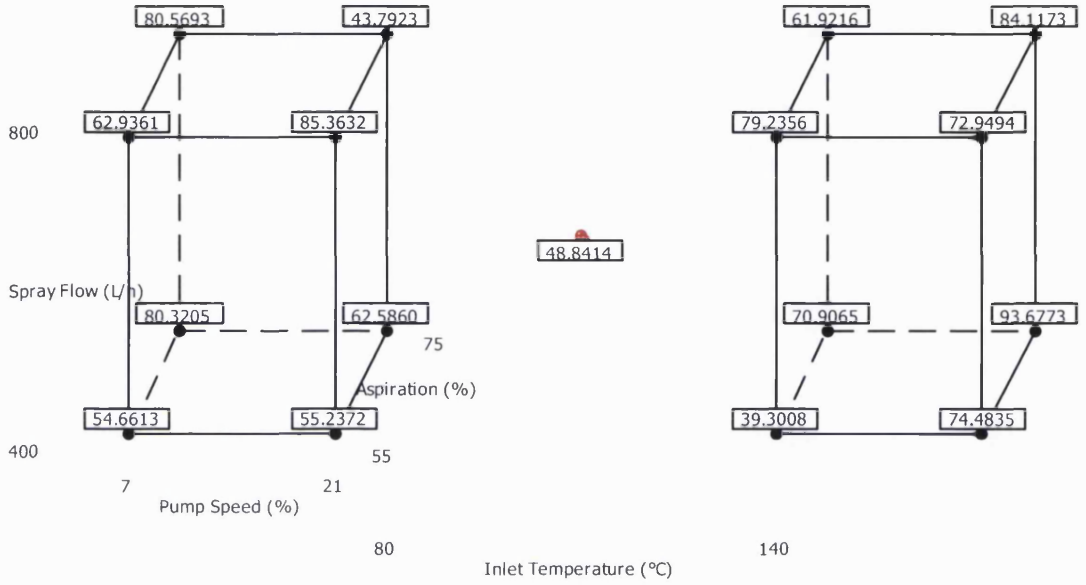

It can be seen in Figure 4.4 and 4.5 that there was substantial curvature in the data, due to the low apparent EE of the centre-point batches. This prevented a simple interpretation of the interactions. However, the data model was retained, since it was likely to be of some use when predicting spray-drying parameters that would produce microparticles with an optimal EE.

4.3.2.d) Scanning electron microscopy

Scanning electron microscopy (SEM) images were very revealing in identifying the importance of choosing appropriate spray-drying parameters. There were a wide variety of morphologies, with many batches appearing not to be composed of the micron-sized particles required for this application. The quality of the product seemed to correlate well with the outlet temperature used for batch production. Batches produced using spray-drying parameters resulting in an outlet temperature of less than 50°C, resulted in SEM images of particles of poor quality, as illustrated in Figure 4.7a. It can be seen that the microparticles did not exist individually, and there appeared to be a degree of crystallisation. Above 60°C the material appeared melted, with a lack of individual microparticles (Figure 4.7b). It was only those batches produced between 50-60°C that appeared to be comprised of individual microparticles of between 1 and 10 µm in diameter. An example of such a batch is given in Figure 4.8. There was also some evidence from the SEMs that batches produced at the lower atomizing spray flow, consisted of larger particles, as illustrated in Figure 4.9.

Figure 4.7 Scanning electron micrographs of IgG formulations spray-dried at an outlet temperature of a) < 50°C, b) > 60°C. Neither image indicated the presence of individual microparticles. At outlet temperatures <50°C bridging of particles appeared to occur due to residual moisture (evident by the visible presence of crystallisation). Above >60°C particles appear to be melted together.

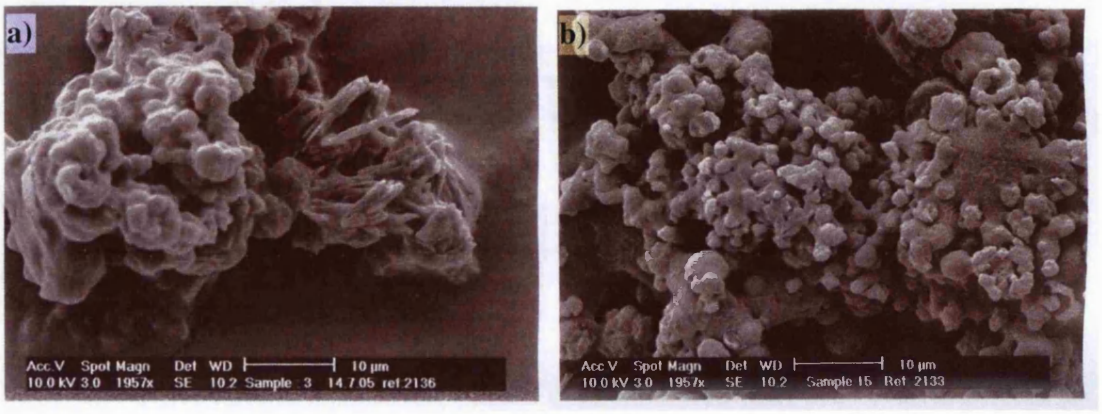

Figure 4.8 Scanning electron micrographs of an IgG formulation produced at an outlet temperature between 50-60°C. Individual microparticles, mostly <5 µm, were observed. This suggested that particles were dried effectively, whilst avoiding melting.

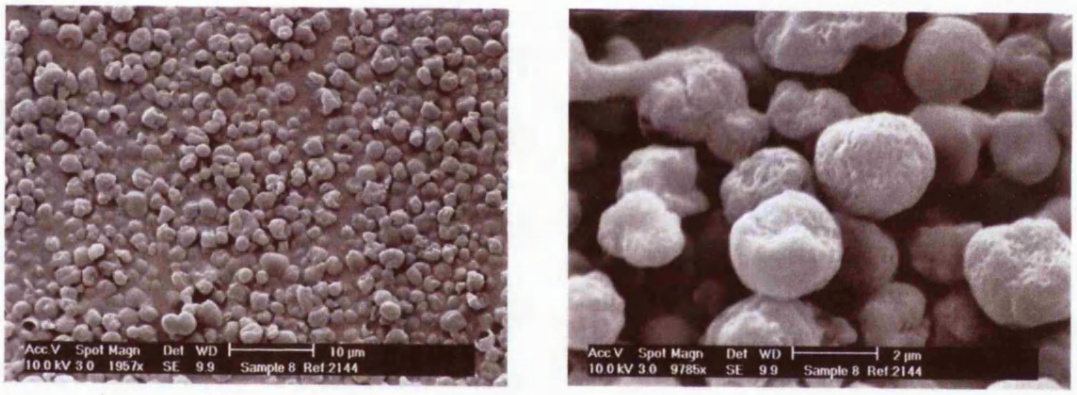

Figure 4.9 Scanning electron micrograph of an IgG formulation spray-dried at a low spray flow rate. The formulation was spray-dried with an atomising air flow of 400 L/h. At this flow larger droplets were generated, resulting in larger particles (some >10 µm). However, these particles were not dried efficiently, resulting in low yields.

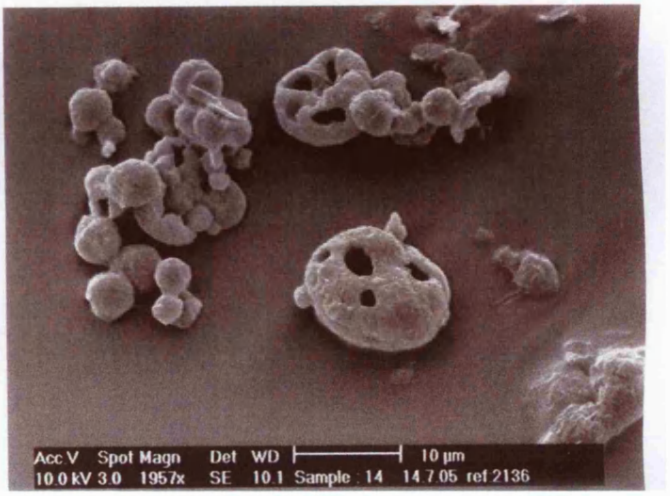

4.3.2.e) Geometric diameter

The SEMs indicated that for many batches, the product did not consist of individual microparticles. Therefore, it was unreasonable to anticipate that reliable laser diffractometry data could be produced, since in many cases there were no *micro*particles to disperse. The laser diffractometry data produced probably reflected that of the particles remaining after the lactose had dissolved. These data did not correlate well with the diameters observed in the SEMs. Therefore, it was decided that no useful purpose would be served by statistically analysing any of the geometric diameter data.

4.3.2.f) ELISA

The antibody activity was compared between three batches that had been produced at a wide range of outlet temperatures. Figure 4.10 illustrates the ELISA results, with active antibody expressed as a percentage of the total protein content.

Figure 4.10 Enzyme-linked immunosorbent assay (ELISA) of IgG released from microparticulate formulations spray-dried at various outlet temperatures. The concentration of IgG determined by ELISA was expressed as a percentage of the total protein concentration measured by the Bradford assay. (n=3, mean ± SD).

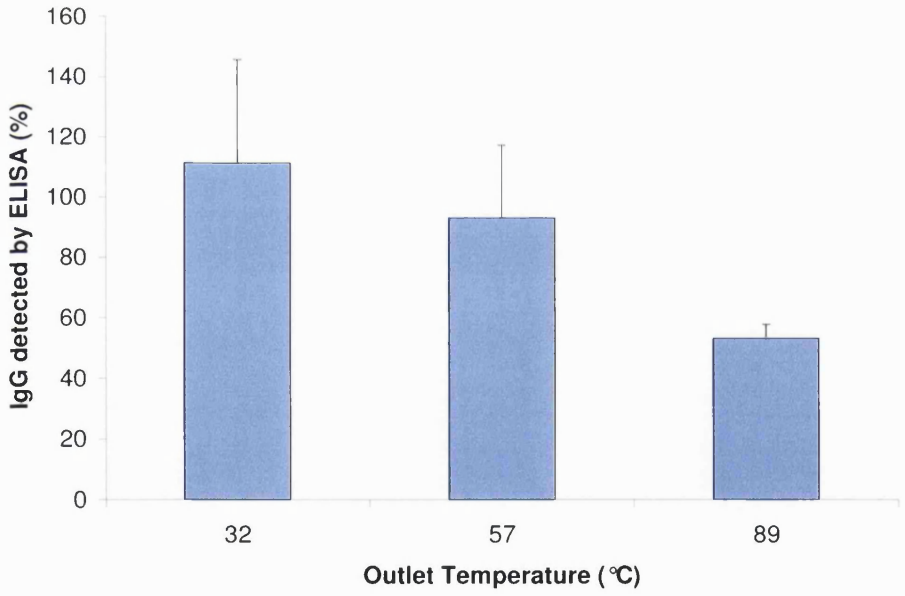

4.3.2.g) Response optimisation

The statistical models for outlet temperature, yield and encapsulation efficiency were used to derive optimal parameters for spray-drying. Based on the SEM results a target outlet temperature of 50-60°C was chosen, in order to ensure the production of individual microparticles. The model was contrained to maximise yield and EE, thereby ensuring minimum values of at least 20% and 50%, respectively. The optimisation scheme and results are given below in Table 4.2.

Table 4.2. Response optimisation for spray-drying parameters. The response data generated by the factorial experiment were used to predict spray-drying parameters that would produce an IgG formulation with the desired characteristics. Parameters were selected that would achieve a spray-drying outlet temperature of 50-60°C (optimal for particle morphology), and maximise yield and encapsulation efficiency (EE). These characteristics were weighted and prioritised equally.

	Goal	*Lower*	*Target*	*Upper*
Outlet Temp (°C)	Target	50	55	60
Yield (%)	Maximum	20	100	100
EE (%)	Maximum	50	100	100
Global Solution				
Pump Speed (%) = 7		Aspiration (%) = 75		
Spray Flow (L/h) = 800		Inlet Temperature (°C) = 80		

A batch was produced using the above recommended parameters, and compared for reproducibility with batch 7 of the original experiment. A batch using the pre-optimisation settings (7%, 800 L/h, 65%, 110°C) was also made along with another set of parameters that also appeared promising from a logical observation of the data (21%, 800 L/h, 55%, 140°C). It was important to include these other options, since the computer optimisation could not include centre-point data. The parameter selection optimised by the computer model reproduced well, and was superior in terms of yield and EE compared to the other batches (data not shown).

4.3.3 Discussion

4.3.3.a) Factorial experimental design

For this work, it was decided to investigate, using a factorial experiment, chosen spray-drying parameters. Usually, experiments were conducted by investigating one variable at a time, keeping all others constant. However, with so many potential variables, and little prior insight as to which ones would be most important, the factorial approach was felt to be an efficient way of screening several variables simultaneously.

Efficiency was certainly a major advantage of this approach, since with four variables, as in this experiment, only a quarter of the number of batches needed to be made to obtain data with the same precision (i.e. n=8) (Fisher, 1951). This was because for each variable, eight batches were made for each of the two corner values. For example, (referring to Table 4.1) eight of the batches were produced with an inlet temperature of 80°C (batches 1-8) and eight batches were produced with an inlet temperature of 140°C (batches 9-16). Of course, these eight batches were different with regard to the other three variables (i.e. spray flow, aspiration and pump speed) but any differences between the two sets of eight (batches 1-8 versus batches 9-16), not due to random variability, could be ascribed as an effect of inlet temperature. Therefore, each batch in the

experiment provided information regarding all four variables. In order to investigate these variables with the same precision (n=8), the classical way, would have required four groups of sixteen experiments.

However, efficiency of data analysis was not the only major advantage of the factorial experimental design. If each variable was to be investigated in a separate set of experiments, there would have been no insight into how other factors might have influenced the effect of the variable being examined. For example, if increasing the spray flow was only advantageous in the presence of a higher inlet temperature, or indeed that this interaction was only dependent on a low aspiration, this would not have been identified by separate experiments. With factorial design, the total system of possible interactions was explored in its entirety (Fisher, 1951). In this experiment, there were four batches where inlet temperature was high, while aspiration was low, which could be compared to the opposite four batches. In addition, the four batches where both variables were high could be compared with the four batches where both were low, thus allowing statistically significant interactions to have been detected.

It is mentioned above, that when comparisons were made in factorial experiments, there could have been two sets of eight batches to compare for each factor, but within these eight batches nothing else was the same (i.e. the other variables were at different levels). Although this may appear to be a compromise, it was in fact another advantage of factorial design. This is because any conclusions made about the effect of a given factor, applied not only to a specific set of other experimental conditions, but were robust for a wide range of other settings (Fisher, 1951).

However, there were some disadvantages of factorial design. Firstly, each variable was only tested at two levels. Therefore, trends could not be detected, and thus it was hard to extrapolate to values that had not been included. The use of centre-points helped to determine if there were straight line relationships, but was not so useful in the case of interactions. It was possible to design factorial experiments with more than two values for each variable, but this would have rapidly increased the number of individual experiments required. Of course, for the reasons given above, this would still be fewer experiments than having tried to achieve the same precision of information for each variable individually. Secondly, the interpretation relied heavily on statistical analysis, and therefore, was only as good as the statistical model chosen to fit the data. Altering the model just slightly could move effects either side of being statistically significant. Finally, because all interactions were explored, the findings could have been very complicated, and difficult to comprehend or interpret. It was very difficult to rationalise

the effect of any factor if there was a statistically significant three-way or four-way interaction with other factors. However, as described for the EE data, provided a suitable statistical model could be fitted to the data, the computer model could then be used to select an optimal combination of factors, based on all the main effects and interactions.

Ideally, factorial experiments should just be used as a screening tool, to rapidly assess which of the possible variables were worthy of further investigation (Armstrong and James, 1996). Factorial experiments have also provided a valuable method for optimising a process, when approximate values for each variable were already known, as was usually the case for the work described in this thesis.

4.3.3.b) Outlet temperature

The effect of spray-drying parameters on the resultant outlet temperature represented a good example of how factorial experimental design could accurately detect the direction, and relative magnitude, of several variables, with the findings being exactly as would be expected from logical predictions. However, the outlet temperature can have important consequences on the final product. The outlet temperature is the temperature of the air carrying the solid particles before entering the cyclone. This temperature results from the heat and mass balance in the drying cylinder, and thus could not be directly regulated. The outlet temperature was, however, important to maintain, because due to the intense heat and mass transfer, and loss of humidity, the particles within the spray drier could be regarded as having the same temperature as the air. Thus, the outlet temperature described the upper thermal load on the particles. Hence, the outlet temperature was set by controlling the other spray-drying parameters.

Obviously, increasing the inlet temperature would cause a substantial increase in the outlet temperature, and this was detected by the experiment. However, one aim was to maintain the least difference between the inlet and outlet temperatures, so as to avoid exposing the feed to a very high inlet temperature. Therefore, other parameters that could regulate outlet temperature needed to be considered. It was evident from the results of the factorial experiment that increasing pump speed, and to a lesser extent spray flow rate, linearly decreased outlet temperature. This was expected, since pumping in more solvent would cool the system, as would increasing the rate of cool atomization air to entering the nozzle. Increasing the aspiration, increased the outlet temperature, since hot air from the inlet was sucked into the drying chamber at a faster rate (Büchi, 2002). Thus, a high aspiration, with a low pump speed (and a low

atomisation air flow), allowed a high outlet temperature, without the need for a very high inlet temperature.

4.3.3.c) Yield

All four parameters had a linear effect on yield. The atomisation spray flow caused the largest increase in yield. Increasing the spray flow resulted in finer droplets from the nozzle, since there was more atomization pressure. Finer droplets are known to dry faster, and the increased pressure would spread them out over a larger area of the drying chamber. The result was less wet material becoming adhered to the walls of the drying chamber, and therefore, more dry product flowing through into the cyclone and collector. For this reason, although it was found that reducing atomization to 400 L/h could produce some larger particles, the yield was very low since the spray drier did not have the drying capacity to efficiently dry these larger droplets (this is discussed further in Chapter 8) (Maury *et al.*, 2005b). Also, adding in more cool, dry, atomizing air may have decreased the overall humidity, thereby enhancing drying of the particles.

The increases in yield, resulting from an increased inlet temperature and aspiration, were probably related to the increase in outlet temperature that they caused. Thus, the material was more efficiently dried, and so less became adsorbed to the drying chamber. The opposite is true for pump speed, since a faster rate of liquid entered the system, which resulted in cooling, less efficient drying, and so a decreased yield.

However, these factors statistically significantly interacted, particularly in the case of spray flow rate. It would appear from the results obtained that using the effects of pump speed, aspiration and inlet temperature to enhance yield, was only likely to be effective if a high spray flow was employed.

4.3.3.d) Encapsulation efficiency

EE is an example of where the results of factorial experiments can become too complicated to interpret. Spray-drying parameters did appear to affect the amount of protein present in the final product, since batches ranged from 46-98% EE. Note that EE was not related to the product yield. Statistically, many factors, including third and fourth-level interactions, were responsible for this variation. In terms of spray-drying, a high EE resulted from either protein being retained in the final product, or at least being retained in preference to other excipients. Therefore, some instances of high EE may be due, for example, to lactose not being dried efficiently. The data were particularly difficult to interpret, because the centre-point values were so low. There is no obvious explanation as to why the centre-point settings were found to be much lower than either of the extremes. This could be put down to an anomaly, but in fact, the centre point was

the only batch to be repeated three times. However, in terms of process optimisation, there was value in generating these data, since the statistical model could then be used to select parameters that would give a good EE.

4.3.3.e) Scanning electron microscopy (SEM)

The SEM results revealed that the parameters which gave the highest yield, did not necessarily produce a useable product. The particle morphology correlated quite well with the outlet temperature used to produce the material. Crystallisation could be seen on images from low temperature batches. This was probably the result of residual water, due to incomplete drying. The residual solvent allowed crystal growth as dissolved material slowly came out of solution. This also resulted in the agglomeration of individual particles, and potentially to instability of the protein due to phase separation (Bosquillon *et al.*, 2004b). It has also been reported that residual water can plasticize PLGA due to a reduction in glass transition temperature (Blasi *et al.*, 2005). At very high temperatures, the thermal load on the droplets became too great, resulting in melting of the particles as they were formed, again causing them to stick together and lose their individuality. It was probably the PLGA in particular that melted. For either scenario, material was produced that could not be realistically assessed in terms of particle diameter. Only when the outlet temperature was maintained between 50-60°C, were individual microparticles produced, presumably since this achieved an appropriate balance between the material being dry, but yet not melting (Kaye *et al.*, 2006b).

It did appear from the SEMs that it might be possible to engineer larger particles by reducing the spray flow. In general, if there was less atomising pressure, droplets were broken up more coarsely, resulting in larger particles. Indeed, this has also been found by other studies, including and Millqvist-Fureby (2005). Larger microparticles of 10-15 μm would potentially be desirable for nasal delivery (Illum and Fisher, 1997). However, with the current formulation and available spray drier, this method of increasing particle size did not appear viable. Lower temperatures were required than in the aforementioned study, and therefore, at low spray flow rates, drying was inefficient, giving very poor yields, as found in the present experiment. Elversson and Millqvist-Fureby (2005) also found that increasing feed concentration could increase particle size, and this approach was investigated as described in the next Section of this Chapter.

4.3.3.f) ELISA

Just as the resultant outlet temperature appeared to affect the stability of the polymer, it was thought that high temperatures may denature the antibody molecule. ELISA only detects IgG when in its active structure and conformation. It appeared from the data, that using parameters which resulted in a very high outlet temperature may cause a loss

of activity. However, ELISA is a very sensitive technique, working in nano-scale concentrations. Therefore, given that this experiment relied on the accuracy of the Bradford assay at relatively low release concentrations, just to have achieved a positive result in the correct order of magnitude was considered promising, despite the large error bars for each batch. Thus, it was sensible to conclude that at the outlet temperatures of interest, the antibody appeared to remain mostly active, which was essential for this formulation.

4.3.3.g) Response optimisation

The statistical models were used to determine optimal spray-drying parameters, in terms of outlet temperature, yield and EE. The range of options was mainly limited by the requirement of the outlet temperature to lie between 50 and 60°C. In broad terms, there were three ways of achieving this. The first would be to use the centre-point settings, but given their low apparent EE, and lower yield due to the lower spray flow, they were probably not optimal. In any case, the centre-point data could not be computed as part of the results optimisation procedure. The other two options were to use both a high inlet temperature, and use a low aspiration and high pump speed to compensate, or to use a low inlet temperature with high aspiration and low pump speed. In both cases, the spray flow was set high to maximise yield. The computed data suggested the latter combination to be superior, presumably because that combination more closely met the temperature, yield and EE targets. However, this recommended batch was compared with the former option, and the original settings (similar to the centre-points, but with high spray flow and low aspiration). The former option was preferred, since a higher pump speed would mean more batches could be produced *per* day. However, it was indeed the settings indicated to be optimal by the computed data that performed best, and it was these parameters that were used for further investigations. It must be remembered that these were the optimal parameters for this particular formulation only, using this particular Büchi-191 spray drier.

4.3.4 Conclusion

Factorial experimental design was successfully used to investigate the effects of four spray-drying parameters on the production of microparticles for airway delivery. The approach had been useful in finding optimal settings for spray-drying the formulation, with the findings of this investigation being an improvement over the previously used settings. This work also improved the understanding of the system, highlighting those parameters most likely to influence a given characteristic of the microparticles. Thus, it was now possible to predict the likely consequence of altering various parameters.

4.4 Factorial experiment to investigate the effect of homogenisation and external phase volume

4.4.1 Method

A 2^3 factorial design was employed to measure the effects of the duration of the primary homogenisation, the duration of the secondary homogenisation and the volume of the external aqueous phase of the double-emulsion, as variables in the manufacturing process. Given that the previously used homogenisation times (3 and 8 min) and external phase volume (100 mL), were considered to be at the high end of those commonly used, they were chosen as the upper (corner-point) values in the current factorial experiment. The parameters used for each batch are outlined in Table 4.3.

Batches were produced in a random order, using the same formulation as the previous experiment, produced by the same method as described in Section 3.3. The double-emulsions were spray-dried, with the optimised settings of inlet temperature 80°C, aspiration 75%, spray flow 800 L/h, pump speed 7% (Section 2.2.2). A non-protein batch was also produced to act as a control in the Bradford assay.

The batches were characterised in terms of yield, encapsulation efficiency, 2 h burst-release, scanning electron microscopy and geometric diameter. The latter was performed using the optimised method of measuring the dry size in cyclohexane + 1% v/v Span 80, and the partially-dissolved diameter, after incubating in water + 0.02 % v/v Tween 20 for 2 h. All methodology used is described in Section 2.3-2.4.

Table 4.3 Design of factorial experiment to investigate the manufacturing parameters used for the formulation of IgG. Batches 9, 10 and 11 represented the centre-points.

Batch	*1st Homogenisation (min)*	*2nd Homogenisation (min)*	*External Phase Vol. (mL)*
1	1	2	20
2	3	2	20
3	1	8	20
4	3	8	20
5	1	2	100
6	3	2	100
7	1	8	100
8	3	8	100
9	2	5	60
10	2	5	60
11	2	5	60

4.4.2 Results

All batches were produced successfully, with an operating outlet temperature of 54-55°C. A summary of the data collected is given in Table IV, Appendix IV.

4.4.2.a) Yield

The yields were all relatively comparable, and were satisfactory for a spray-drying process (ranged 37-48%). Statistically, it was only the third-level interaction, between all three variables, that had a significant effect on the yield. It can be seen from the data (Table IV, Appendix IV) that the yield of the centre points were lower than of the other batches.

4.4.2.b) Encapsulation efficiency

With the original data it was difficult to fit a statistical model. However, the best available model identified batch ten as an anomaly, and thus the statistics were re-run without batch ten. This vastly improved the fit, with the best model giving an R^2 of 95%, and residuals normally distributed between ±4. Secondary homogenisation time and external phase volume were found to have significant effects on the encapsulation efficiency (EE), as illustrated in Figure 4.11. Increasing both factors resulted in an increase in EE, although there was some curvature in the data. For secondary homogenisation time, the data suggested that EE was most improved when the homogenisation time was increased to 5 min, with further time increases having a less appreciable effect.

Figure 4.11 The effect of manufacturing parameters on the IgG encapsulation efficiency (EE). The variables shown had statistically significant ($p<0.05$, factorial ANOVA) main effects on the EE. The values shown are fitted means from the statistical model. The longer duration of secondary homogenisation, and the larger external phase volume resulted in an increased EE. However, EE at the centre point settings was closer to the EE at the higher values compared to the EE at the lower values. This suggested curvature in the data, and possibly interactions of variables.

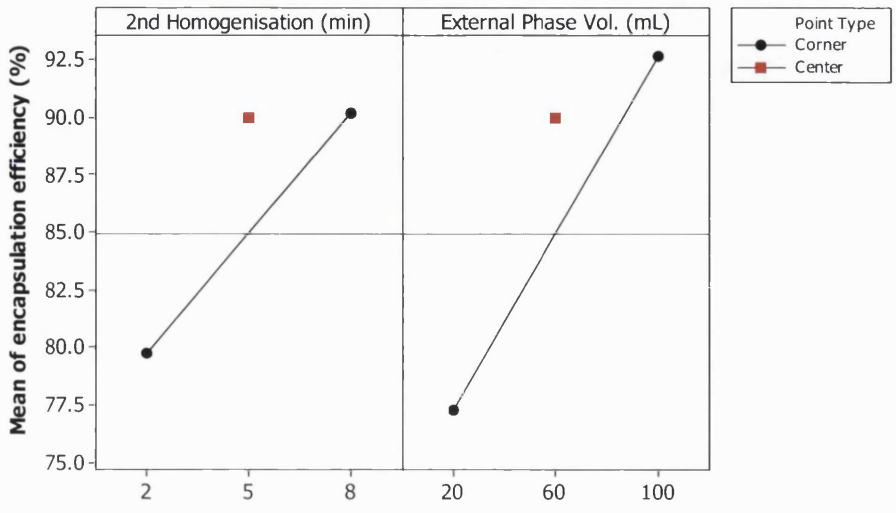

4.4.2.c) Burst-release within 2 h

Secondary homogenisation time and external phase volume were both found to significantly affect the initial burst-release from the microparticles. The confidence in these findings was improved by discarding one of the centre point readings which did not fit the data. However, there was an interaction between the two statistically significant factors. The main effects and interaction are illustrated in Figures 4.12-4.13.

Figure 4.12 The effect of manufacturing parameters on the IgG burst-release.
The variables shown had statistically significant ($p<0.05$, factorial ANOVA) main effects on the IgG burst-release (the percentage of the IgG load released from the formulation in PBS after 2 h incubation at 37°C). The values shown are fitted means from the statistical model. The longer duration of secondary homogenisation, and the larger external phase volume resulted in a lower burst-release. However, burst-release at the centre point parameters was greater than either extreme (•=corner point, ■=centre point).

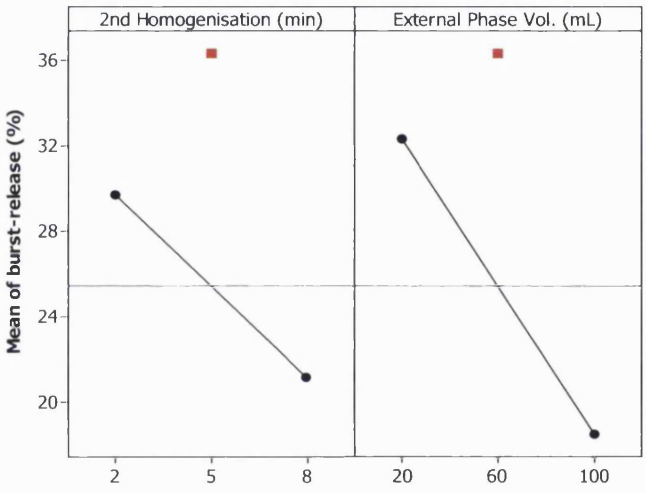

Figure 4.13 Interaction plot of manufacturing parameters affecting IgG burst-release.
The plot indicates the statistically significant ($p<0.05$, factorial ANOVA) interaction of external phase volume with secondary homogenisation duration in determining the proportion of IgG release after 2 h. The values shown are the fitted means. With an external phase volume of 20 mL, initial burst-release was increased when secondary homogenisation lasted just 2 min rather than 8 min. Conversely, with 100 mL external phase volume, the duration of secondary homogenisation did not affect IgG burst-release by 2 h.

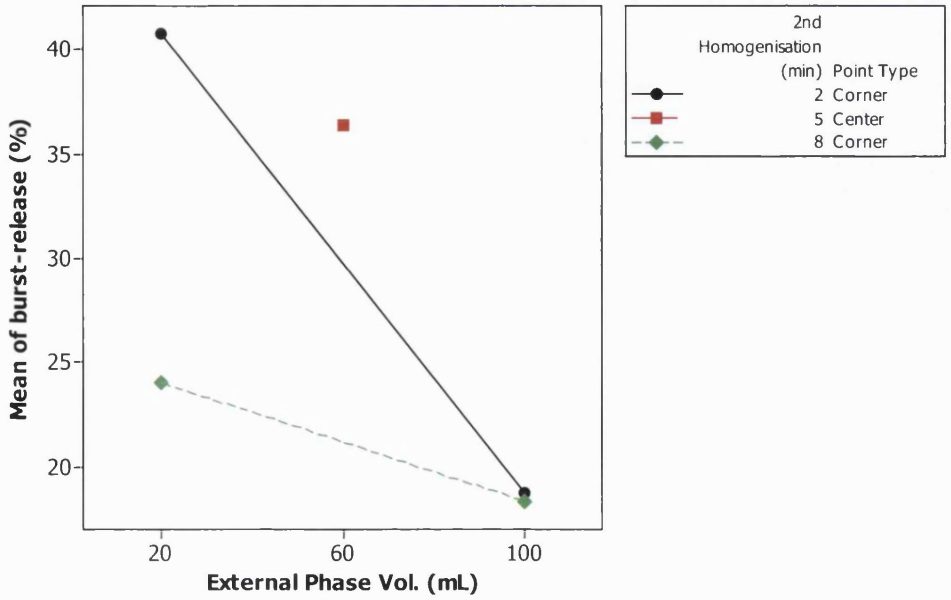

Increasing both external phase volume and secondary homogenisation time reduced the initial burst-release, although the centre-points had the highest initial burst-release. However, the interaction plot shows that external phase volume had less effect on immediate burst-release when a longer secondary homogenisation time was employed. When a secondary homogenisation time of only 2 min was used, the burst-release by 2 h was greater than the centre-point parameters.

4.4.2.d) Geometric diameter

The D50% (the diameter that 50% of the particles were less than) was only statistically significantly affected by the secondary homogenisation time. This effect is illustrated in Figure 4.14.

However, a change from 2 min to 8 min homogenisation time only resulted in a D50% increase of less than 1 µm. Also, given the centre-point D50%, it would appear that homogenisation time only had an effect if it was increased to more than 5 min.

Figure 4.14 The effect of secondary homogenisation duration on the particle diameter of the IgG formulation. Secondary homogenisation duration was the only variable to statistically significantly ($p<0.05$, factorial ANOVA) affect the formulation's particle median geometric volume diameter (D50%). Particles were dispersed in cyclohexane, and measured by laser-diffraction. The values shown are fitted means from the statistical model. The centre-point value would appear to indicate that the relationship was not linear.

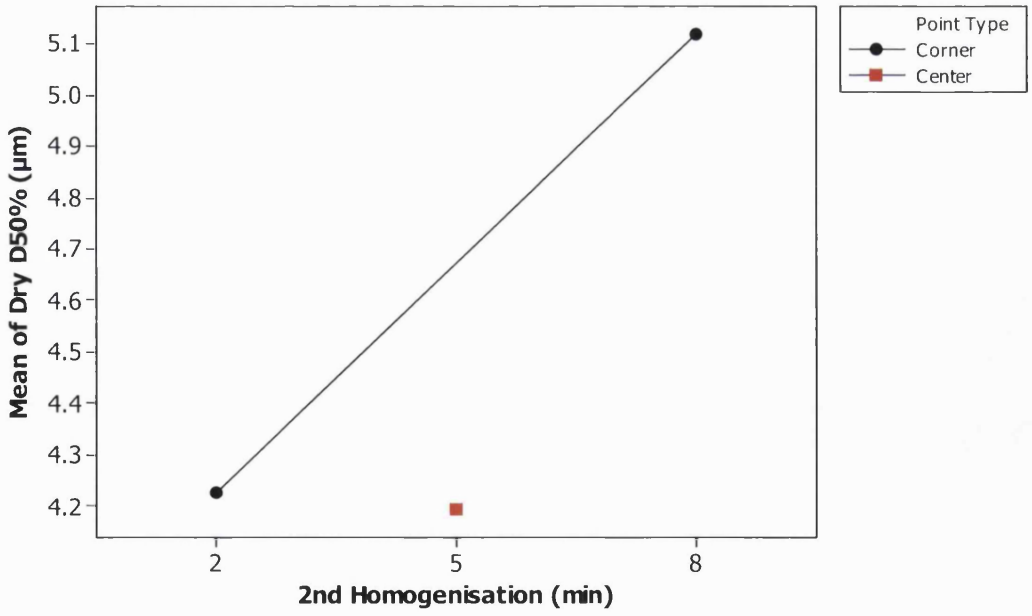

The ratio of D50%:D90% was used to assess monodispersity. Higher values for this ratio indicated particles were more polydispersed as there was a greater difference between D50% and D90% (monodisperse particles=1). The significant main effects and interaction are illustrated in Figures 4.15 and 4.16, respectively.

Figure 4.15 The effect of homogenisation duration on particle diameter polydispersity.
The ratio of D50%:D90% was used as a measure of particle diameter polydispersity. Increasing primary and secondary homogenisation duration was found to statistically significantly ($p<0.05$, factorial ANOVA) reduce the particle polydispersity of the IgG formulation. However, the centre-point settings gave the greatest D50%:D90%, suggesting a very non-linear relationship. Particles were dispersed in cyclohexane, and measured by laser-diffraction. D50% (the volume median diameter) and D90% (the diameter that 90% of the volume of particles was smaller than) were derived from the same diameter distribution.

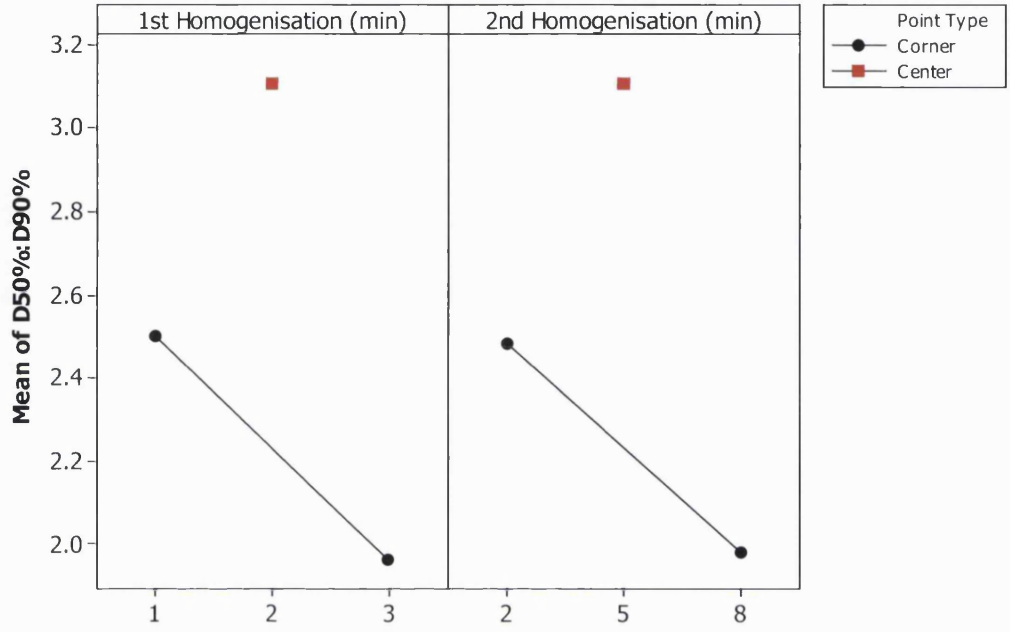

Figure 4.16 Interaction plot of manufacturing parameters affecting particle polydispersity.
The plot indicates the statistically significant ($p<0.05$, factorial ANOVA) interaction of external phase volume with secondary homogenisation duration in determining the particle diameter polydispersity [defined by the ratio of D50% (volume median diameter) to D90% (diameter which 90% of the volume of particles are smaller than)]. The values shown are the fitted means. Varying secondary homogenisation duration only affected D50%:D90% when the external phase volume was 100 mL, increasing the ratio from ~1.7 to ~2.6.

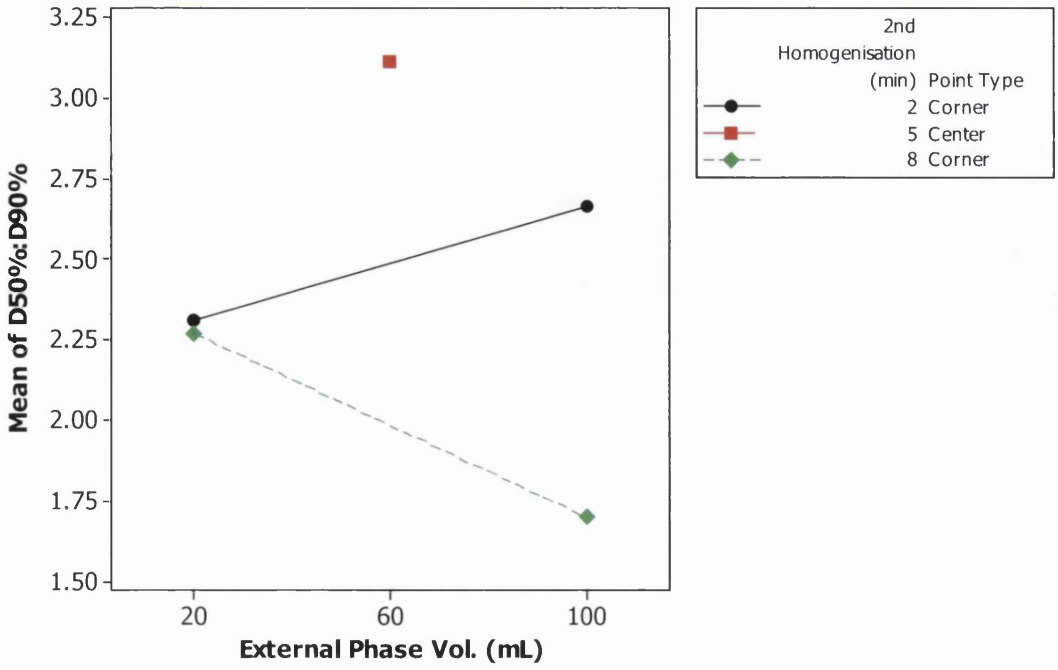

Increasing both primary and secondary homogenisation duration reduced polydispersity. However, the centre-points were the most polydispersed batches. Although external phase volume was not a significant main effect, if the secondary homogenisation time was controlled, increasing external phase volume could have either increased or reduced polydispersity (and thus, external phase volume influenced the effect of secondary homogenisation). Figure 4.17 and 4.18 are examples of the measured geometric diameter range for two batches with external phase volumes of 20 mL and 100 mL, respectively. The latter is clearly a more monodispersed distribution.

Figure 4.17 Geometric diameter distribution of an IgG formulation produced with a double-emulsion external phase volume of 20 mL. The sample was dispersed in cyclohexane, and measured by laser diffraction.

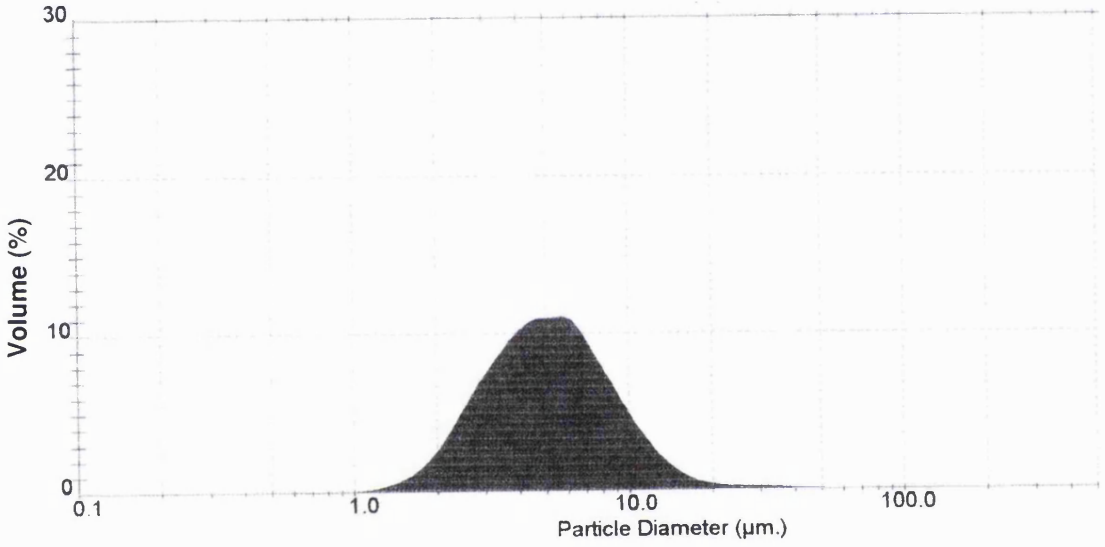

Figure 4.18 Geometric diameter distribution of an IgG formulation produced with a double-emulsion external phase volume of 100 mL. The sample was dispersed in cyclohexane, and measured by laser diffraction.

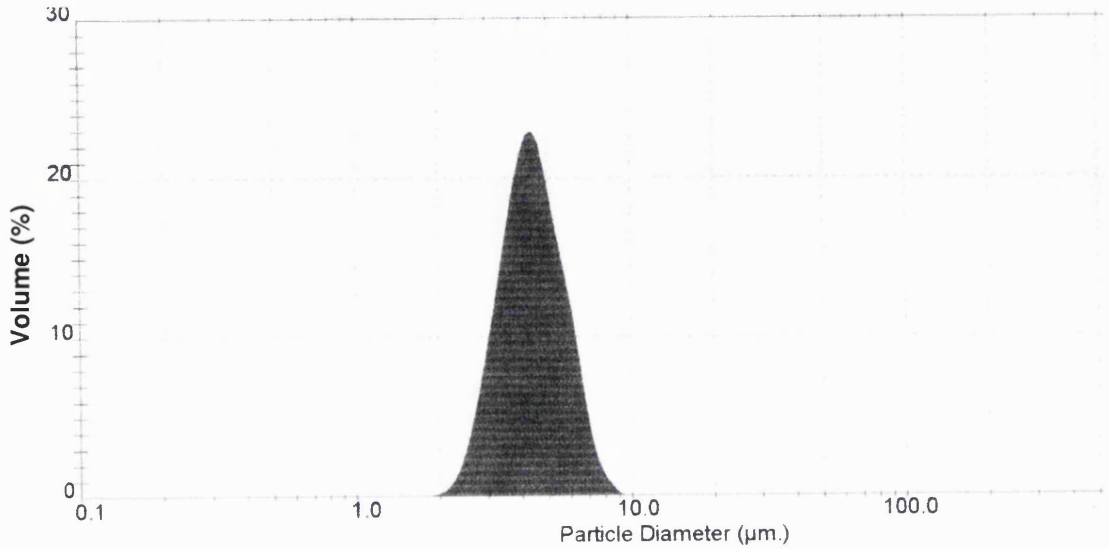

The particle diameter, after allowing soluble components to dissolve in water, was only significantly affected by external phase volume. This effect, although clearly present from the raw data, could only be detected if the centre-points were removed from the model (due to their high variability). A factorial plot of the effect is given in Figure 4.19. There was also some evidence of an effect of primary homogenisation time, but this was not statistically significant from the data available. An example distribution of these smaller particles, in water, is given in Figure 4.20.

Figure 4.19 The effect of emulsion external phase volume on particle diameter in water.
External phase volume was the only parameter found to statistically significantly ($p<0.05$, factorial ANOVA) decrease the particle modal diameter of the IgG formulation, when dispersed in water + 0.02% v/v Tween 20 (incubated for 2 h at 37°C). The centre-point values were removed from the analysis due to their high variability.

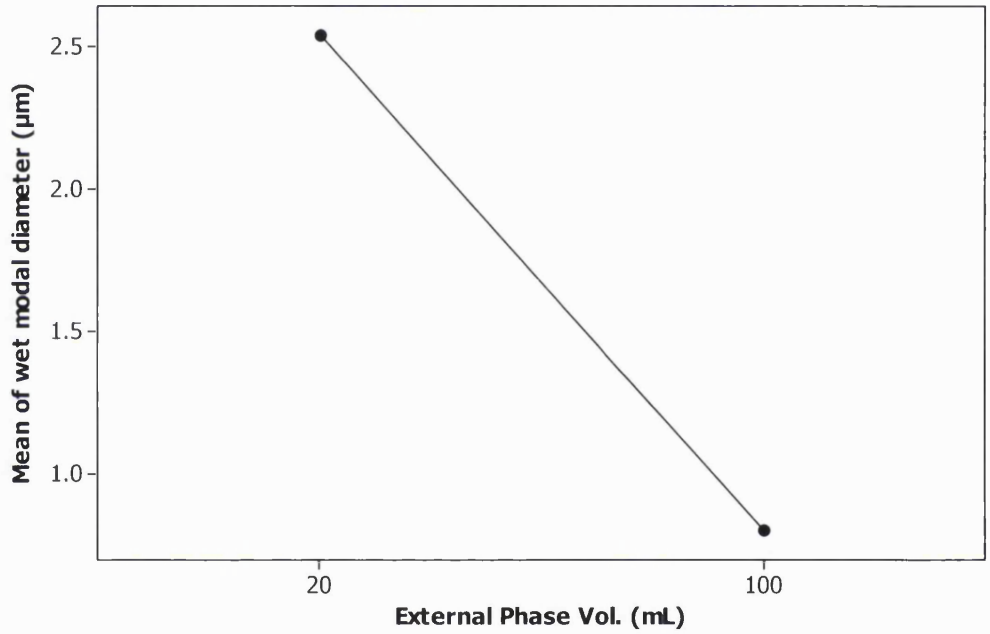

Figure 4.20 Geometric diameter distribution of an IgG formulation dispersed in water.
The formulation was produced with a double-emulsion external phase volume of 100 mL. The sample was dispersed in water + 0.02% v/v Tween 20, and incubated for 2 h at 37°C, prior to measurement by laser diffraction. Mean particle diameter was ~1 µm, i.e. smaller than in Figures 4.17 and 4.18.

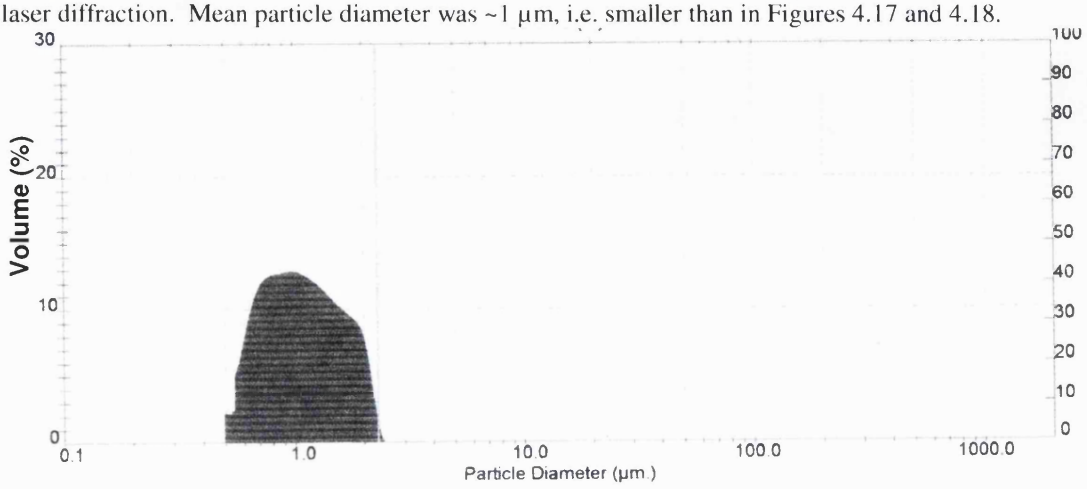

4.4.2.e) Scanning electron microscopy

Unlike the previous experiment, all of the batches produced spherical, individual microparticles in the 1-10 μm diameter range. There was also some visual correlation with the geometric diameter and polydispersity findings.

4.4.2.f) Response optimisation

Based on the statistical models for each response, optimal parameters were selected with the aid of the Minitab software. Table 4.4 outlines the response targets, the result, and the predicted responses when these chosen parameters were adopted.

Table 4.4 Response optimisation for external phase volume and homogenisation time. The response data generated by the factorial experiment were used to predict parameters that would produce an IgG formulation with the desired characteristics. Parameters were selected (top-half of Table) that would maximise yield and encapsulation efficiency (EE), target particle diameter to theoretically respirable ranges, and minimise the initial burst-release, diameter polydispersity and diameter in water. All factors were given equal weighting and priority.

	Goal	*Lower*	*Target*	*Upper*
Yield (%)	Maximum	25	100	100
EE (%)	Maximum	50	100	100
2 h Burst-Release (%)	Minimum	0	0	30
Dry Mode Dia. (%)	Target	1	3	5
Dry D50% (μm)	Target	1	3	5
D50%:D90%	Minimum	1	1	3
Wet mode Dia. (%)	Minimum	0	0	2

Optimal Parameters:

1st Homogenisation (min) = **3**

2nd Homogenisation (min) = **8**

External phase volume (mL) = **100**

Predicted Responses of the Optimal Parameters:

Yield (%) = 39.8, desirability = 0.19700

EE (%) = 93.0, desirability = 0.85975

2 h Burst (%) = 14.1, desirability = 0.53000

Dry Mode (μm) = 4.2, desirability = 0.38669

Dry D50% (μm) = 4.2, desirability = 0.41338

D50%:D90% = 1.4, desirability = 0.78466

Wet mode (μm) = 1.1, desirability = 0.46750

Composite Desirability = 0.47

4.4.3 Discussion

This experiment provided a good test for the reproducibility of the optimised spray-drying parameters determined in the previous study. All batches produced good yields, and the outlet temperature remained almost constant throughout. This experiment also aimed to investigate other parameters in the manufacturing process. It was known that when producing microparticles by solvent-evaporation, the method of homogenisation could dramatically affect the product characteristics. Increasing the duration of homogenisation, resulted in a finer dispersion, within the continuous phase, thus resulting in smaller particles (Sturesson *et al.*, 1999). Such engineering can produce microparticles ranging from hundreds of nanometres to tens of micrometers. However, the composition and size of microparticles, when produced by spray-drying, was dependent on the droplet formation as the liquid feed was atomised from the nozzle. Therefore, it would be expected that provided the emulsion feed was stable (i.e. the disperse phase was evenly distributed throughout the continuous phase), properties such as droplet size of the disperse phases would have no bearing on the characteristics of spray-dried particles. This allowed shorter durations of homogenisation to be used, saving time and also reducing shear forces on the protein, which may have lead to structural damage. This experiment set out to determine if this indeed was true, or if in fact, reducing homogenisation durations would impact on the properties of spray-dried microparticles.

The other parameter investigated was the volume of the emulsion external aqueous phase. This was the largest phase in the double-emulsion system, and thus a change in volume of this phase would have the most appreciable impact on liquid feed concentration. Other studies had found that liquid feed concentration can affect particle size (Elversson *et al.*, 2003; Elversson and Millqvist-Fureby, 2005), and given that spray flow adjustment cannot be effectively used with the available equipment, this was investigated as a means of controlling particle size. There was also an interest in reducing external phase volume as a method of decreasing the time to spray dry one batch. The optimised spray-drying setting used a pump speed of 7%, which meant that spray-drying an emulsion of approximately 100 mL, required almost 1 h. If the volume could have been reduced to 20 mL without any detrimental effects, the time *per* batch would obviously have been reduced by 80%.

The results discussed below demonstrated that these parameters did affect the characteristics of the final product. However, many of the effects were not revealed as clearly as anticipated, because of the design of the experiment. Due to the fact that only

three parameters were investigated, there were only four batches of a given parameter, at a particular level. This made it more difficult to detect statistically significant effects and interactions, against the inevitable background variability. Also, in retrospect, it was probably inappropriate to investigate external phase volume and secondary homogenisation in the same experiment, as the two variables are intrinsically related: increasing homogenisation time increased the energy input to break up the disperse phase, whereas decreasing the continuous phase volume increased the viscosity of the emulsion, and thus increased the energy required to achieve the same dispersion.

4.4.3.a) Yield

Although there was some variation in the yield, all of the batches were satisfactory. Statistically, it was an interaction of all three variables that produced the variation observed. However, the lower centre-point yields may be attributed to the increased splashing that occurred when homogenising a smaller volume (the 20 mL batches were made using smaller beakers).

4.4.3.b) Encapsulation efficiency

All of the batches had relatively high EEs. However, it was found that longer secondary homogenisation times resulted in higher EEs. The reason for this was not clear. Secondary homogenisation resulted in the dispersion of primary emulsion droplets within the external aqueous phase. These primary emulsion droplets contained an aqueous solution of protein within an organic solution of PLGA. Longer secondary homogenisation could have resulted in smaller, more defined droplets that were less likely to coalesce, releasing the inner protein aqueous phase into the external aqueous phase. Protein that had been well retained within the PLGA phase would be quickly encapsulated within the polymer, as it rapidly dried. The slower drying lactose, in water, may have then formed a shell around the newly formed PLGA particles. Of course, the situation was really more complicated than this, with other surface active ingredients navigating to the interfaces of the drying particle droplets. However, provided the PLGA did not melt, any loss of material, in the form of sticky residue adhered to the wall of the drying chamber, was likely to be lactose from the external aqueous phase. Therefore, in the case of only a 2 min secondary homogenisation, the protein probably leaked out into this external phase, and was more likely to be included amongst the lost material, thus resulting in a lower EE. On the other hand, Sturesson *et al.* (1999) suggested that prolonged mixing time could provoke exchange of material

between the internal and external aqueous phases, although there was no evidence of such an effect in this system.

The same reasoning may be applied to the external phase volume, in that it was easier to form a more stable secondary emulsion when there was a larger continuous-to-disperse phase ratio, and lower phase viscosity. It has also been reported that using higher feed concentrations resulted in greater losses of yield (Elversson and Millqvist-Fureby, 2005). However, here there was no decline in yield *per* se, when smaller external phase volumes were used, and there was no detected secondary interaction between homogenisation time and external phase volume.

In this experiment, the best batches had EE much higher than the previous experiment, despite the parameters being the same. This may have been due to optimisation of the Bradford assay, since the difference between an EE of 80 and 90% is very small in terms of the concentration difference in the Bradford assay (as mentioned in Appendix III).

4.4.3.c) Burst-release by 2 h

The same trends were observed for immediate burst-release as for EE. The same explanation could be applied, in that protein which escaped into the external phase was located on the particle surface, where it was released quickly, rather than being entrapped within the slowly degrading PLGA. However, here there was a statistically significant interaction between secondary homogenisation and external phase volume. If the explanation given above applied, such an interaction would be expected, because both factors were affecting the quality of the emulsion. The interaction suggested that if external phase volume was high, homogenisation time had little effect, but if external phase volume was low, then a reduction in homogenisation time resulted in a large initial burst-release. Therefore, the effect of reducing external phase volume was greater if a shorter homogenisation time was employed. Thus, with 100 mL external phase volume, 2 min homogenisation time appeared to be sufficient to produce a stable emulsion. However, with a 20 mL external phase volume, longer homogenisation duration was required. The high immediate burst-release of the centre-points may have been related to uneven homogenisation, caused by using a small volume in larger glassware (the 20 mL batches were produced in smaller glassware).

4.4.3.d) Geometric diameter

Although some factors were found to significantly affect the particle geometric volume diameter, the D50% or modal diameter did not change by much more than 1 μm, which was not that important, given that the particle diameters ranged from ~1-10 μm. The effect observed with D50% and secondary homogenisation time was in fact opposite to what was be expected. Longer homogenisation durations in the solvent-evaporation method gave smaller particles, due to the generation of smaller polymer droplets (Yang *et al.*, 2001). However, with spray-drying, particle diameter was more dependent on factors that would have altered the droplet generation in the spray-drying nozzle, such as feed viscosity, rather than the emulsion properties. Therefore, why homogenisation time should have had any effect cannot be explained.

There was clearly a difference in the width of the particle diameter range between batches. This was assessed statistically by comparing the ratio of the diameter 50% of the particles were less than (D50%), to the diameter that 90% of the particles, in terms of volume, were less than (D90%). Unfortunately, this analysis did not produce any conclusive answers. However, it appeared that longer homogenisation reduced polydispersity, probably since longer homogenisation resulted in a more even liquid feed viscosity. The emulsification was more thorough, such that the whole system was emulsified uniformly. However, the centre-points had the largest polydispersity. In the case of secondary homogenisation, this might have been because the process was visibly less even as a result of the reduced external phase volume, as described above. There was also an interaction of secondary homogenisation with external phase volume, which indicated that the effect caused by secondary homogenisation was only evident when the external phase volume was 100 mL.

Scientifically, monodisperse particles may seem desirable, as this would suggest a precise, robust process that should be predictable and well characterised. However, in practical terms, polydispersity may not be such an undesirable characteristic. The diameter of the microparticles will determine where in the pulmonary tract they are likely to deposit. Monodisperse particles will mostly deposit within a very close proximity to each other, in terms of depth in the respiratory tract. Whilst this may be useful for targeting to a particular region, for many applications this was not appropriate. Rather, the efficacy of many inhaled commercial products relies on some polydispersity to accommodate the inter-patient variation in anatomy and inhaler technique. Also, for the treatment of lung diseases, a larger area of coverage may be required, such as for the protection to inhaled toxins, asthma or cystic fibrosis. In this

thesis, a formulation was being developed for the pulmonary delivery of a therapeutic antibody to intercept an inhaled airborne pathogen or toxin. Therefore, coverage of large areas of the respiratory tract would be desirable.

The geometric diameter in cyclohexane was used as an estimation of the diameter of the dry particles when expelled from a dry-powder or propellant-driven device. However, a large proportion of this formulation was water soluble, and thus once the microparticle had reached its destination it would partially dissolve in lung fluid. It is after this, that the controlled-release would hopefully take place, as the PLGA slowly degraded, releasing the protein encapsulated within.

In order to determine the diameter of these microparticles, after the water soluble components have been removed, the microparticles were incubated for 2 h in water, prior to laser diffraction. For some batches, there were sub-micron sized particles present, a proportion of which were smaller than 500 nm, which was the limit of using the magnetically stirred cell with the standard lens on the Mastersizer. In some cases, these nanoparticles were a separate peak and a larger, presumably aggregate, peak was also present. There was evidence from the formulations produced by solvent-evaporation that with these homogenisation conditions, using this polymer, nano-sized PLGA particles were produced. Thus, these data suggested that the integrity of these PLGA droplets was maintained during spray-drying, such that when the lactose dissolved, the composite nanoparticles were revealed. As for the variables in this experiment, the only statistically significant factor was external phase volume. Presumably, a large volume allowed for a finer homogenisation of the disperse phase, resulting in smaller internal droplets. This micro-to-nano-particle effect is described further in Section 4.6.

4.4.3.e) Response optimisation

Based on the results of this experiment, data were computed in order to select parameters that would produce optimal microparticles. In this case, 'optimal' was considered to be microparticles with a high yield, high EE, low 2 h burst-release, a dry diameter less than 5 μm, minimised polydispersity and a minimal wet diameter. The parameters selected were the original ones being used before this study, i.e. a maximised primary and secondary homogenisation, and the largest external phase volume. These parameters, in combination with the optimised spray-drying settings, were predicted to produce microparticles of the required characteristics. However, as

discussed above, for different applications, alternative properties may be required. Therefore, rather than this solely being an experiment to optimise the formulation, it was an investigation into parameters that can be adjusted to engineer the final product in order to meet clinical requirements, such as release profile. With further characterisation of the effects, it may be possible to produce customised microparticles that will be of the required polydispersity to cover the area of the lung, wished to be targeted, or to provide a specific amount of instant drug release. Indeed, from the data already collected, the impact on such characteristics of changes in homogenisation and external phase volume could be predicted. However, more focused experimentation would still be required, since this 2^3 factorial design does have its limitations, especially given the complications with many of the centre-point readings.

4.4.4 Conclusion

The duration of emulsion homogenisation has been investigated in the production of spray-dried microparticles. It has been found that changing the duration of homogenisation, thereby affecting the micro-composition of the emulsion, can have profound effects on the atomised droplet composition, and thus alter microparticulate characteristics. A reduction of external phase volume also resulted in statistically significant changes to microparticle properties. This was presumably due not only to concentration effects when spray-drying, but also appeared to be related to the properties of the secondary emulsion, given the number of interactions detected. Although the starting values for these variables were predicted to give microparticles with properties most suited for the intended application, and thus continued to be used, this investigation had highlighted how it might be possible to produce other potentially useful characteristics, without altering the excipient composition.

The geometric diameter studies suggested it was possible to produce microparticles that would transform into controlled-release nanoparticles, on contact with water. This concept is further explored in Section 4.6.

4.5 Factorial experiment to investigate the formulation composition

4.5.1 Method

A 2^4 factorial experiment was used to investigate the optimal amounts of lactose, PLGA, DPPC and IgG in the formulation, in terms of yield, EE, 2 h burst-release, particle diameter and morphology, and to reduce the unnecessary use of excipients. It should be noted that the human IgG used, was in a formulation with a 1:1 mass ratio of sorbitol. These ingredients were not separated, and therefore, where the amount of IgG had been varied, the amount of sorbitol varied with it (in a 1:1 m/m ratio). In the results, when an effect of IgG is mentioned, this includes the contribution of sorbitol. The experimental design is detailed in Table 4.5.

Table 4.5 Factorial experimental design to investigate the effect of formulation composition on the characteristics of a microparticulate formulation of IgG. Batches 17, 18 and 19 represented the centre-points.

Batch	*PLGA (mg)*	*Lactose (mg)*	*DPPC (mg)*	*IgG/sorbitol (mg)*
1	50	100	10	10
2	350	100	10	10
3	50	500	10	10
4	350	500	10	10
5	50	100	40	10
6	350	100	40	10
7	50	500	40	10
8	350	500	40	10
9	50	100	10	50
10	350	100	10	50
11	50	500	10	50
12	350	500	10	50
13	50	100	40	50
14	350	100	40	50
15	50	500	40	50
16	350	500	40	50
17	200	300	25	30
18	200	300	25	30
19	200	300	25	30

The formulations were made as previously described, with all ingredients being added to the same phases as previously. Batches were produced in a random order. The primary emulsion was homogenised for 3 min at 24,000 RPM, and the secondary emulsion for 8 min at 10,000 RPM, using the apparatus and method described in Section 2.2.1. The double-emulsions were spray-dried using the optimised settings of inlet temperature 80°C, aspiration 75%, spray flow 800 L/h, pump speed 7% (see Section 2.2.2). A non-protein batch was also produced for blank readings, and a non-lactose-containing batch was also produced for comparison. Dried formulations were stored in a dessicator, at room temperature, until analysis.

Batches were characterised in terms of yield, encapsulation efficiency, 2 h burst-release and dry and wet geometric diameter as previously described. Due to the high protein content of some batches, where required, dilutions of samples were made before performing the Bradford assay, such that the theoretical protein concentration would be in the 20-200 µg/mL range. Scanning electron microscope images were produced for each batch, and the morphology defined quantitatively as follows:

0 = Individual particles are not clearly defined

1 = Defined particles, but aggregated

2 = Non-aggregated, but irregular shape

3 = Non-aggregated, spherical particles

4.5.2 Results

A summary of the data collected is given in Table V, Appendix IV.

4.5.2.a) Yield

All of the factors that statistically significantly affected yield are highlighted in the normal probability plot, Figure XI, Appendix VI. Lactose, and to a lesser extent PLGA, increased yield, DPPC reduced yield, but the effects were dependent upon the amount of IgG present. These effects and interactions are represented by the factorial plots in Figures 4.21 and 4.22.

Figure 4.21 The effect of excipients on the yield of a double-emulsion formulation of IgG. The variables shown had statistically significant ($p<0.05$, factorial ANOVA) main effects on the spray-drying yield. The values shown are the fitted means generated by the statistical model that had the closet fit to the raw data. Yield increased with poly(lactide-co-glycolide) (PLGA) and lactose, but decreased with dipalmitoylphophatidylcholine (DPPC). The yields at the centre-points were higher than the average of the two corner yields (•=corner point, ■=centre point).

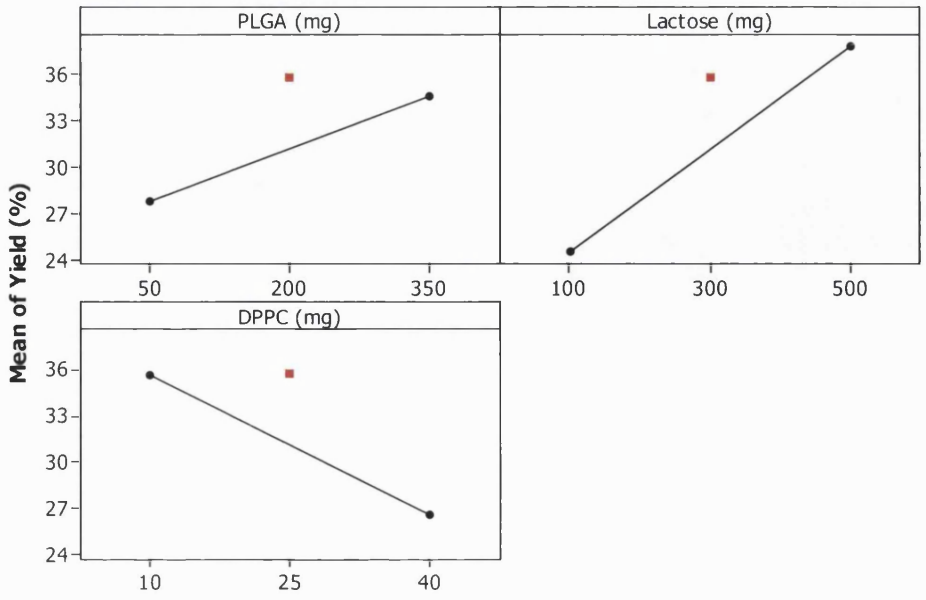

Figure 4.22 Interaction plot of formulation components affecting the IgG formulation yield.
The plots shown indicate the three statistically significant ($p<0.05$, factorial ANOVA) second-level interactions. The values shown are the fitted means generated by the statistical model that had the closet fit to the raw data. For example, it can be seen (left-hand box) that the decrease in spray-drying yield resulting from a low lactose content, was more profound with a low poly(lactide-co-glycolide) (PLGA) content. Using only 10 mg of IgG/sorbitol resulted in a reduced yield if either the amount of PLGA or the amount of lactose was low (right-hand boxes) (•=corner point, ■=centre point).

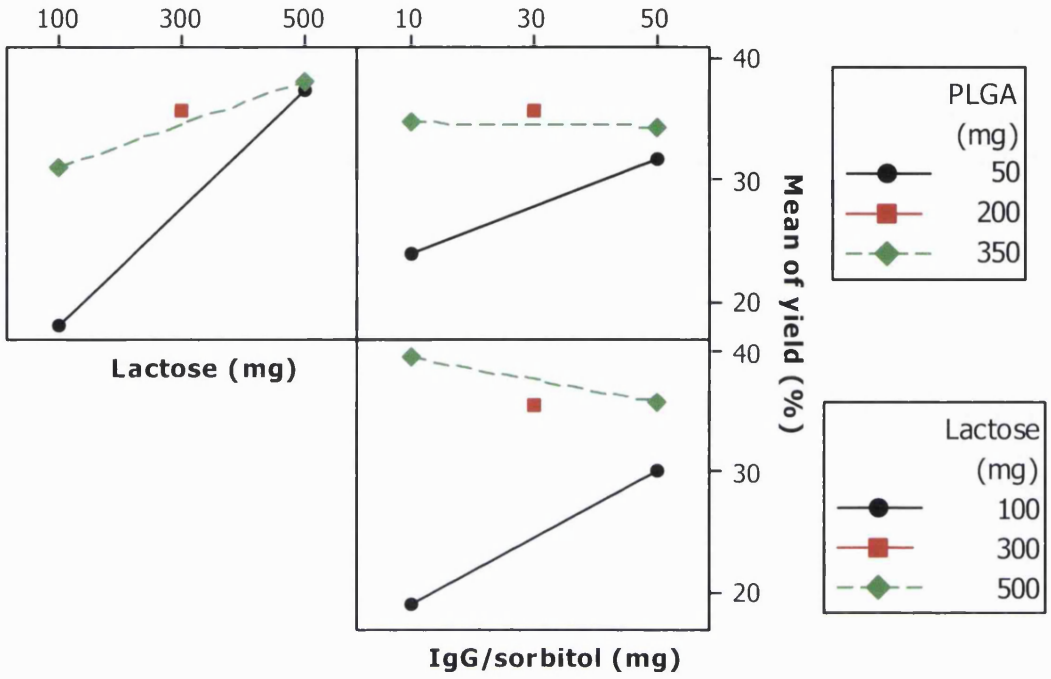

Importantly, there was curvature in the main effects, with only the lowest values in lactose and PLGA, and the highest value of DPPC, causing a major decrease in yield (Figure 4.21). The interactions indicated that increasing PLGA boosted the yield, even in the presence of low lactose, and that the amount of IgG/sorbitol could increase the yield when the amounts of lactose and PLGA were low (Figure 4.22).

4.5.2.b) Encapsulation efficiency

There were numerous factors affecting encapsulation efficiency (EE), although there was a good model to fit the data, with an R^2 value of 98.7%. (All of the significant main effects and interactions are illustrated in Figure XII, Appendix VI).

Of these interactions, the most important appeared to be the decrease in EE caused by lactose, the increase in EE caused by IgG/sorbitol, and the interaction of the two. These effects are given in the factorial plots, Figures 4.23 and 4.24.

Figure 4.23 The effect of formulation composition on the IgG encapsulation efficiency.
The variables shown had statistically significant ($p<0.05$, factorial ANOVA) main effects on the IgG encapsulation efficiency (EE). The values shown are fitted means from the statistical model. Increasing lactose content from 300-500 mg resulted in an 8% reduction in EE. Formulations with the centre-point level of IgG/sorbitol (30 mg) had higher EEs (~84%) than the average of formulations containing either 10 mg or 50 mg. Formulations with 50 mg IgG/sorbitol had a slightly higher EE than formulations with 10 mg IgG/sorbitol.

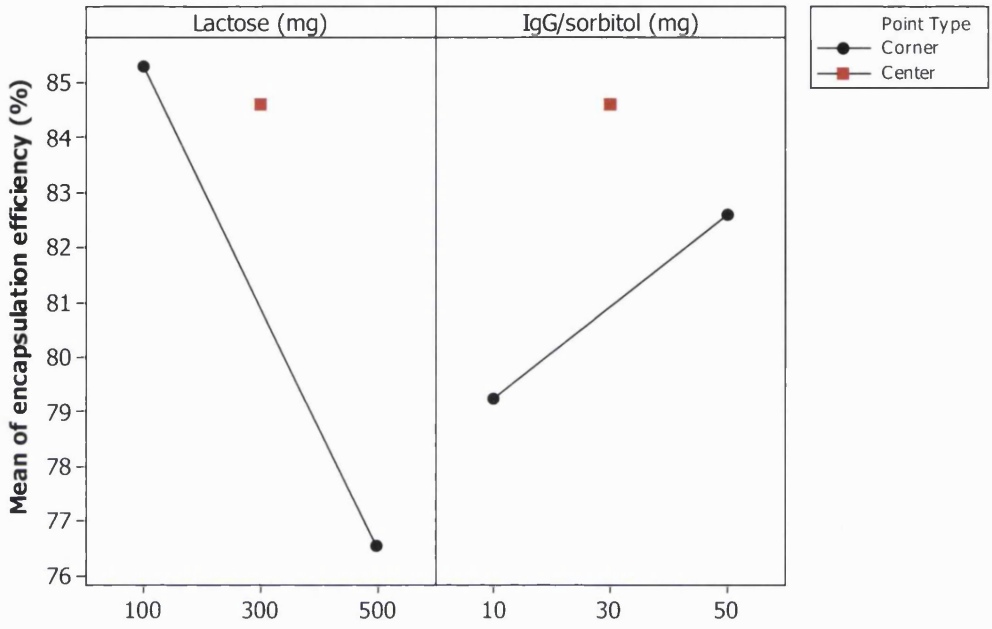

Figure 4.24 Interaction plot of formulation components affecting IgG encapsulation efficiency.
The plot illustrates the statistically significant ($p<0.05$, factorial ANOVA) interaction of IgG/sorbitol content with lactose content in determining the IgG encapsulation efficiency (EE). The values shown are the fitted means. Only at low IgG/sorbitol levels was EE affected by the amount of lactose, there being no notable effect of lactose with 50 mg IgG/sorbitol.

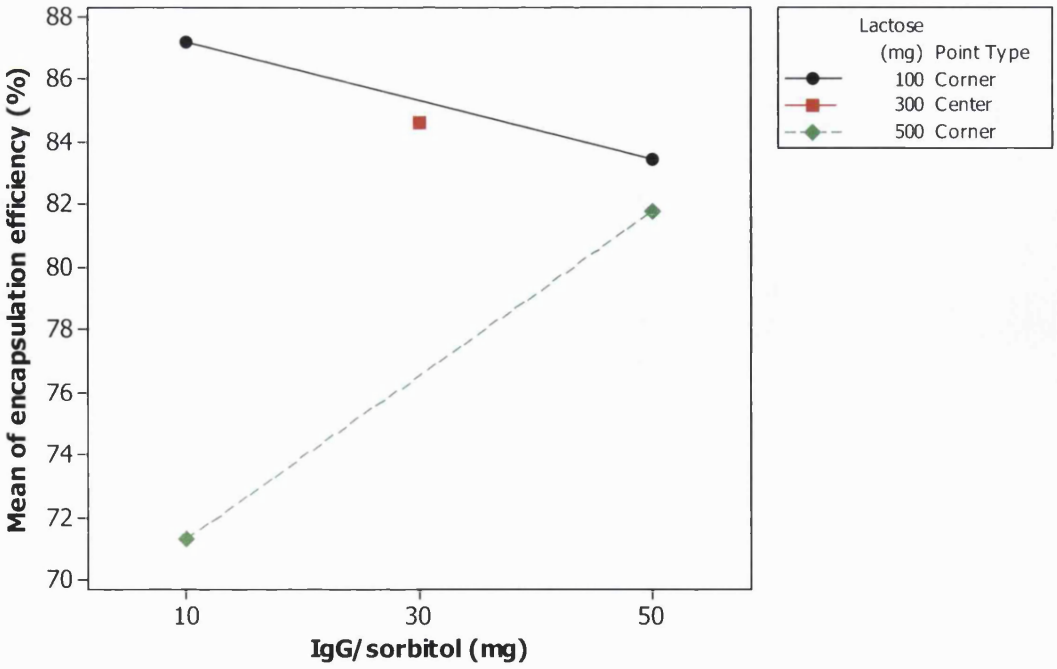

From the centre-point plots it was observed that only 500 mg of lactose resulted in a substantial decrease in EE. For IgG, there appeared to be an optimum level. However, when a low amount of lactose was used, increasing IgG reduced the EE, whereas with a high amount of lactose, increasing IgG led to increased EE.

4.5.2.c) Burst-release by 2 h

Higher levels of IgG and sorbitol statistically significantly increased the initial burst-release, and there was an interaction of this effect with the amount of PLGA. These effects are illustrated in the factorial plots (Figure 4.25 and 4.26). There was also a statistically significant three-way interaction involving PLGA, IgG and lactose.

There was almost a linear relationship of amount of IgG/sorbitol with immediate burst-release, with the centre point plot giving slightly more release than strict proportionality would suggest (Figure 4.25). The interaction indicated that at low amounts of IgG/sorbitol, increasing PLGA reduced the antibody immediate burst-release (Figure 4.26).

Figure 4.25 The effect of the formulation IgG load on the IgG immediate burst-release. The IgG (+ sorbitol) load of the formulation had a statistically significant ($p<0.05$, factorial ANOVA) main effect on the formulation's burst-release (the percentage of the IgG load released from the formulation in PBS after 2 h incubation at 37°C). The values shown are fitted means from the statistical model.

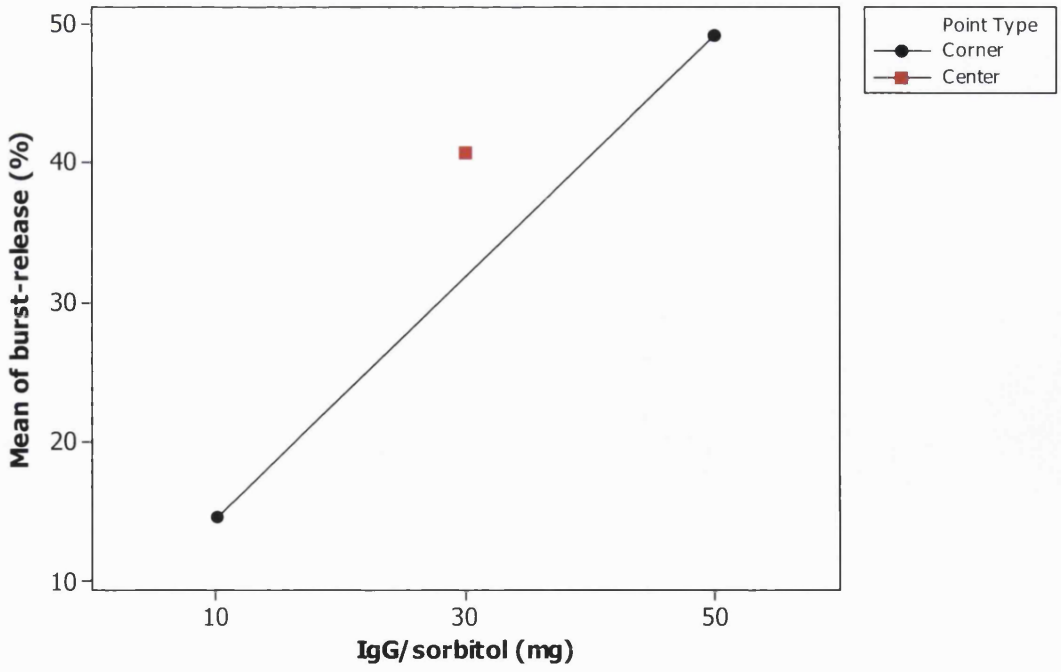

Figure 4.26 Interaction plot of formulation components affecting the IgG immediate burst-release. The plot illustrates the statistically significant ($p<0.05$, factorial ANOVA) interaction of IgG/sorbitol content with poly(lactide-co-glycolide) (PLGA) content in determining the IgG released after 2 h incubation in PBS at 37°C (burst-release). The values shown are the fitted means. With 10 mg IgG/sorbitol loading, burst-release was reduced from ~20% to <10% with a higher PLGA content.

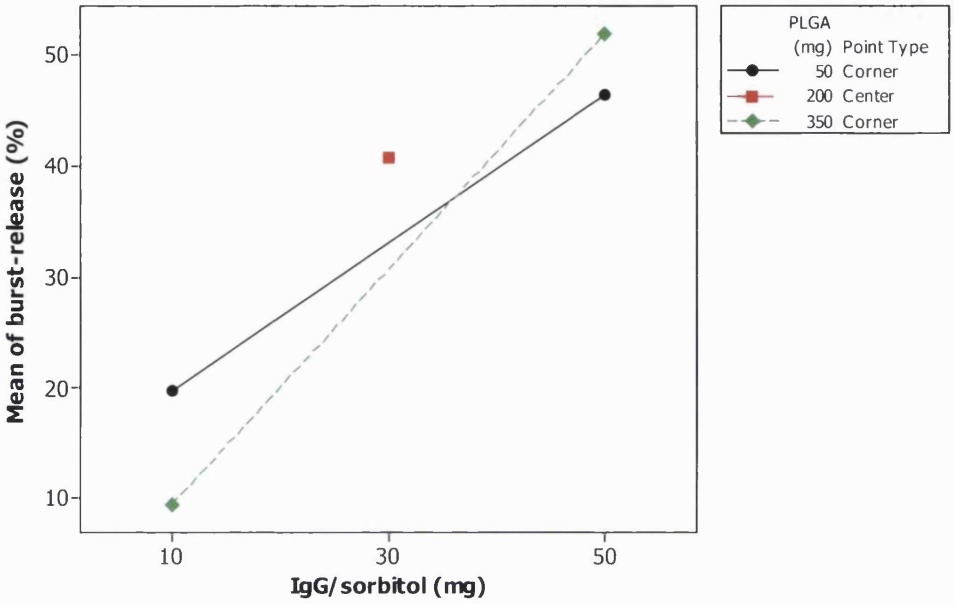

4.5.2.d) Geometric diameter

The D50%, as measured in cyclohexane, was influenced by lactose, PLGA and DPPC, directly. However, there were numerous statistically significant interactions, as detailed by the normal probability plot (Figure XIII, Appendix VI). Of these, the main effects and two-way interactions are given in Figures 4.27 and 4.28.

Figure 4.27 The effect of excipients on the volume median particle diameter (D50%) of the IgG formulation. The three variables shown had statistically significant ($p<0.05$, factorial ANOVA) main effects on the particle D50% in cyclohexane, measured by laser diffractometry. The values shown are the fitted means generated by the statistical model that had the closet fit to the raw data. A 1-1.5 µm increase in D50% was observed where lactose and dipalmitoylphosphatidylcholine (DPPC) content was lower, and where poly(lactide-co-glycolide) (PLGA) content was higher, than the centre-point values (•=corner point, ■=centre point).

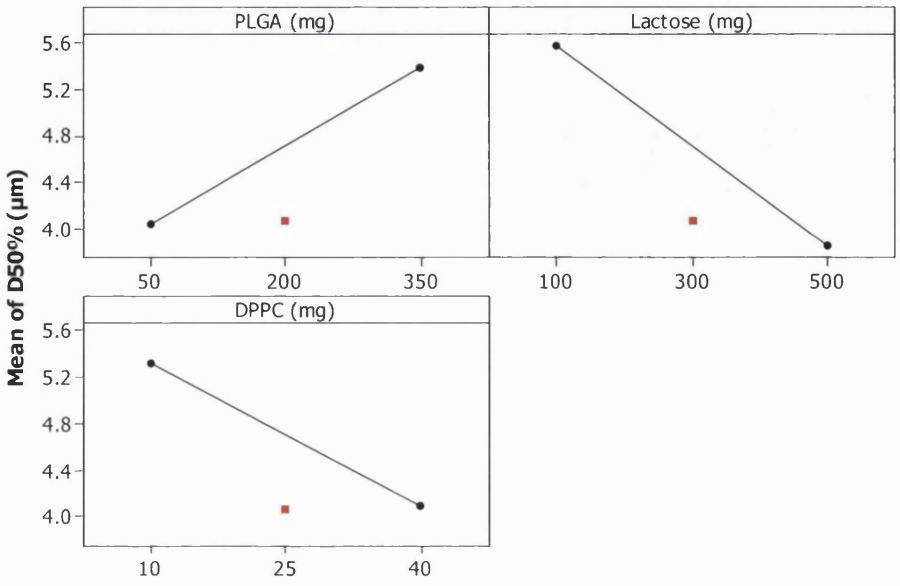

Figure 4.28 Interaction plot of formulation components affecting the volume median particle diameter (D50%). The plots shown indicate statistically significant ($p<0.05$, factorial ANOVA) second-level interactions affecting the D50% measured in cyclohexane, measured by laser diffractometry. The six boxes represent all of the possible two-way interactions. Absence of a plot within a box was indicative of no statistically significant interaction. The values shown are the fitted means (•=corner point, ■=centre point).

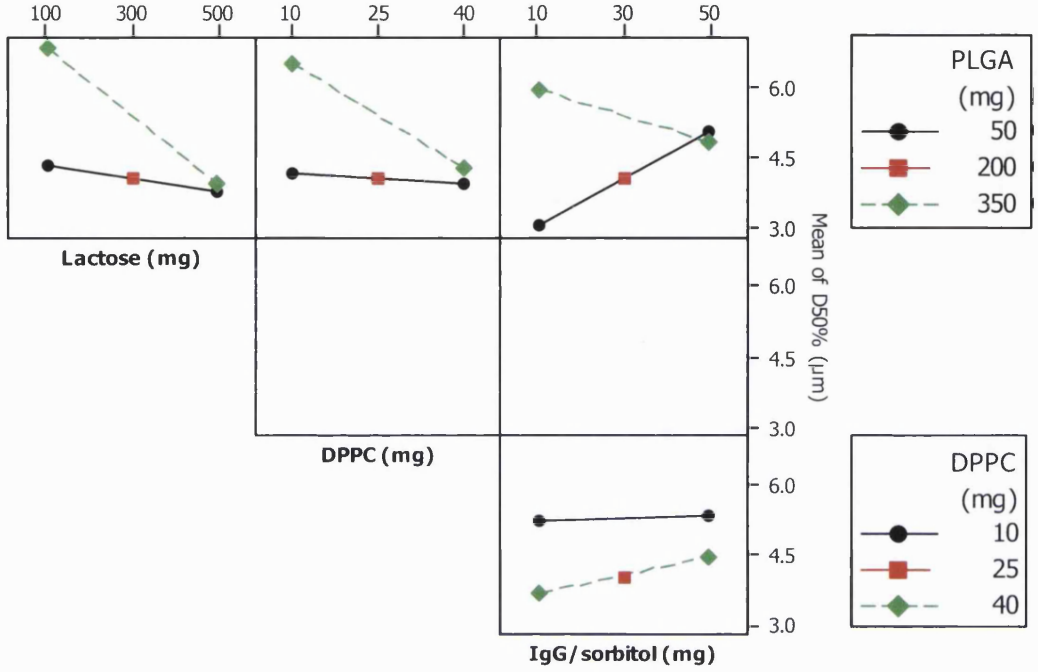

An increase in microparticle diameter was only observed with the highest value of PLGA, and the lowest values of lactose and DPPC (Figure 4.27). One important observation from the interactions is that the diameter increases caused by using low amounts of lactose and DPPC, were only present when 350 mg of PLGA was used (two left-hand boxes, Figure 4.28). Also, the effect of high PLGA appears to be reduced by a high IgG/sorbitol content (Top, right-hand box, Figure 4.28).

The diameter in water + 0.02% v/v Tween 20 measurements were difficult to obtain is some cases. Batches 13 and 15 were clearly the result of aggregation, but were included in the data analysis. There were several statistically significant factors, as illustrated in full in Figure XIV, Appendix VI.

The main effects and secondary interactions are given in Figures 4.29 and 4.30. On average, the centre-points produced the smallest water-insoluble particles, with low amounts of PLGA and high amounts of IgG producing the largest particles. The interactions indicated that IgG and DPPC, actually reduced the particle size, when higher amounts of PLGA were used.

Figure 4.29 The effect of IgG and poly(lactide-co-glycolide) (PLGA) on the volume median particle diameter (D50%) of the IgG formulation in water. The variables shown had statistically significant ($p<0.05$, factorial ANOVA) main effects on the particle D50% (after 2 h, 37°C incubation in water + 0.02% v/v Tween) measured by laser diffractometry. The values shown are the fitted means. Formulations of low PLGA content or high IgG/sorbitol content consisted of aggregated particles (giving a high D50% in water, where as the centre-point formulations consisted of particles smaller than those measured by dispersion in cyclohexane (•=corner point, ■=centre point).

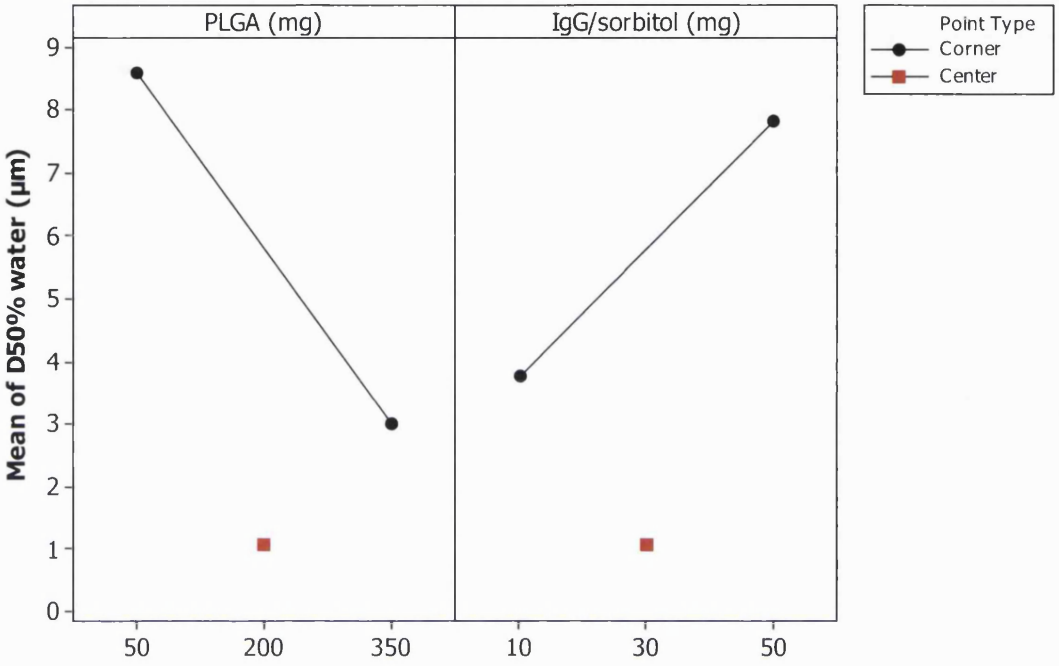

Figure 4.30 Interaction plot of formulation components affecting the volume median particle diameter (D50%) in water. The plots shown indicate the three statistically significant ($p<0.05$, factorial ANOVA) second-level interactions affecting the D50% (after 2 h, 37°C incubation in water + 0.02% v/v Tween), measured by laser diffractometry. The values shown are the fitted means. It can be seen (left-hand box) that the small particles achieved with the centre-point formulations can also be achieved using 40 mg dipalmitoylphosphatidylcholine (DPPC) with 350 mg poly(lactide-co-glycolide) (PLGA) (•=corner point, ■=centre point).

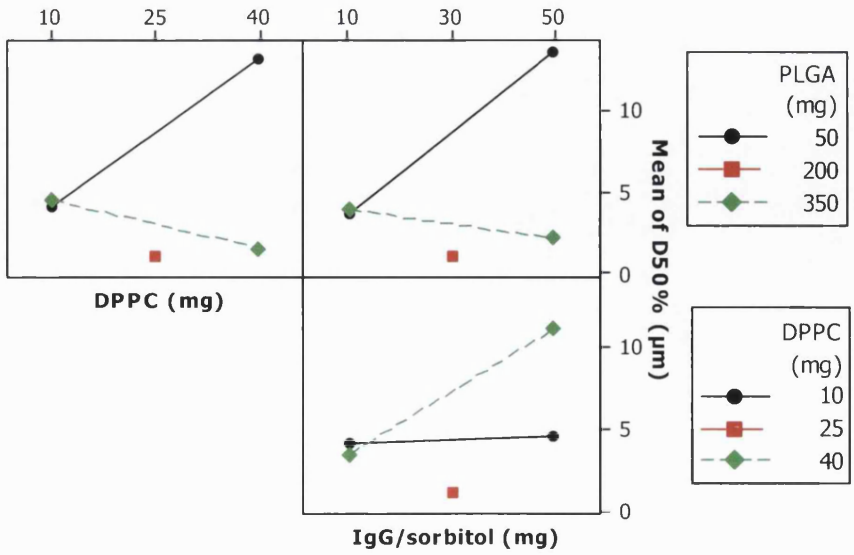

4.5.2.e) Scanning electron microscopy

Unlike the previous experiment, there were obvious differences in microparticle morphology between batches of different excipient composition. However, deviation from micron-sized, spherical particles was not as extreme as the spray-drying parameters experiment. The scanning electron micrograph (SEM) images were ranked as described above, and statistically analysed. High amounts of PLGA significantly reduced particle quality, whilst increasing DPPC increased particle quality, and these factors interacted, as did DPPC with lactose. The significant effects are fully illustrated in the normal probability plot, Figure XV, Appendix VI.

Figures 4.31 and 4.32 are the factorial plots of these effects. They clearly indicate that the centre-point amounts of PLGA and DPPC produced the best particles. One important observation from the interactions was that low amounts of PLGA did not produce particles of good morphology when high amounts of lactose and DPPC were not present (Figure 4.32).

Figure 4.31 The effect of poly(lactide-co-glycolide) (PLGA) and dipalmitoylphosphatidylcholine (DPPC) content on the particle morphology of the IgG formulation. The two variables shown had statistically significant ($p<0.05$, factorial ANOVA) main effects on the morphology of the microparticulate formulation. Morphology was measured on a quality rating based on scanning electron micrograph images, where 0 = Individual particles are not clearly defined, 1 = Defined particles, but aggregated, 2 = Non-aggregated, but irregular shape and 3 = Non-aggregated, spherical particles. The values shown are the fitted means. Formulations with the centre-point values of PLGA and DPPC, produced formulations that consisted of the more spherical and individual microparticles (•=corner point, ■=centre point).

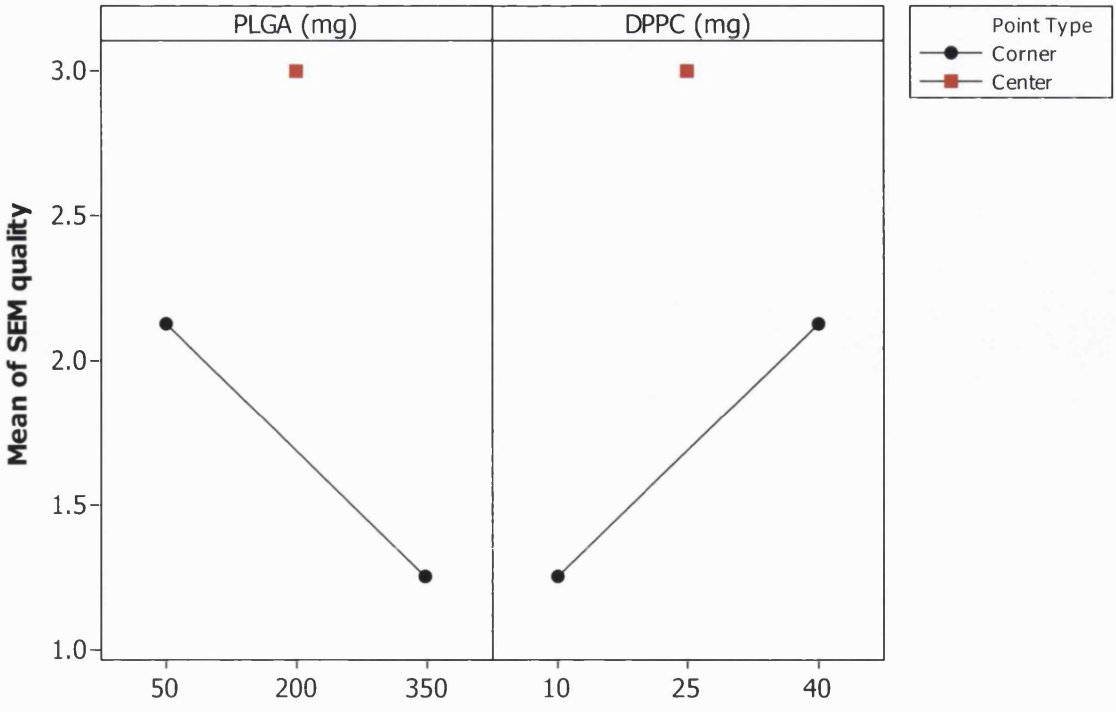

Figure 4.32 Interaction plot of formulation components affecting the particle morphology. The plots shown indicate the three statistically significant ($p<0.05$, factorial ANOVA) second-level interactions affecting the microparticulate morphology of the IgG formulation. Morphology was measured on a quality rating based on scanning electron micrograph images, where 0 = Individual particles are not clearly defined, 1 = Defined particles, but aggregated, 2 = Non-aggregated, but irregular shape and 3 = Non-aggregated, spherical particles. The values shown are the fitted means. Formulations with low amounts of both lactose and dipalmitoylphosphatidylcholine (DPPC), and high amounts of poly(lactide-co-glycolide) (PLGA), produced the least spherical and most aggregated microparticles. The centre-point formulations had a more desirable microparticulate morphology than any other excipient combination (•=corner point, ■=centre point).

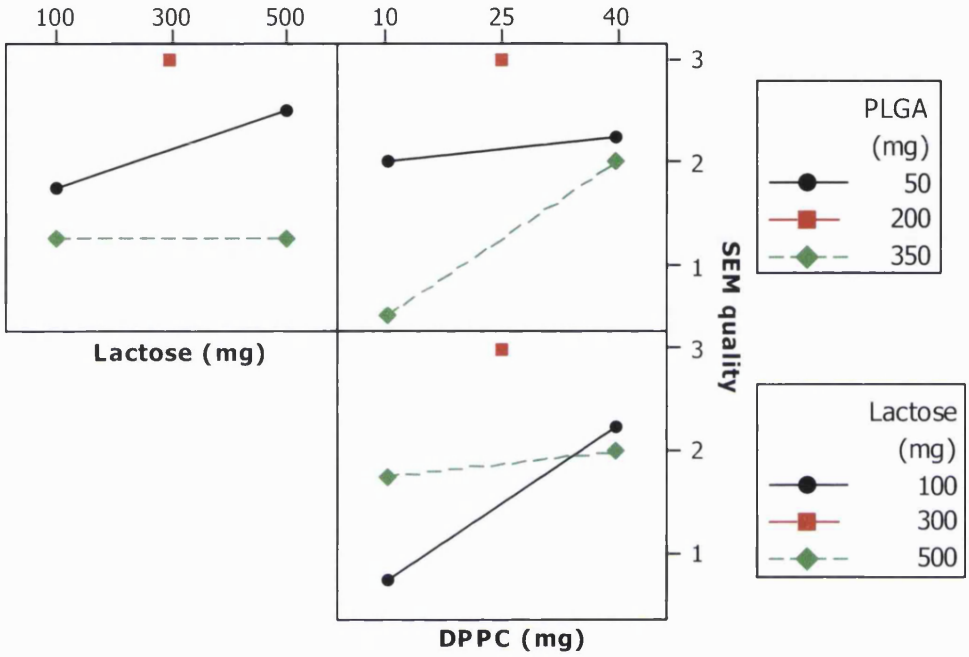

4.5.2.f) Process optimisation

An optimal formulation of excipients was selected, using the statistical models highlighted above. The same preferred characteristics were chosen as detailed previously, and are detailed in Table 4.6.

Table 4.6 Response optimisation for formulation components. The response data generated by the factorial experiment were used to predict excipient amounts that would produce an IgG formulation with the desired characteristics. These were high yield and encapsulation efficiency (EE), low IgG instant burst-release, a targeted diameter range (D50% in cyclohexane) suitable for inhalation, small particles in water (D50% wet), and maximum particle morphology quality. Because of the advantageous characteristics of the centre-point formulations, the response optimisation process was not successful. However, the Table lists the formulation characteristics that were desired. All factors were given equal weighting and priority.

	Goal	Lower	Target	Upper
Yield (%)	Maximum	25	100	100
EE (%)	Maximum	60	100	100
2 h Burst (%)	Minimum	0	0	30
D50% (μm)	Target	1	3	5
D50% wet (μm)	Minimum	0	0	2
Morphology	Maximum	2	3	3

Unfortunately, no optimal combination could be found to meet all of these requirements. Only by appreciably compromising some factors could optimal parameters be selected. One reason for this was that the response optimiser could only use a parameter at its centre-point value, if all other parameters were also used at their centre-point value, i.e. the result of response optimisation could only be a combination that has been physically tested in the experiment. Therefore, Table 4.7 has been produced manually, based on the above findings, to summarise the optimum choice for each ingredient, for each characteristic.

Table 4.7 Optimal amounts of each excipient for various characteristics of the IgG formulation. The data from the factorial experiment was analysed, each characteristics in turn, to determine the optimal amount of each formulation component. An overall optimal composition was determined by considering all of the characteristics. (EE: IgG encapsulation efficiency, 2 h burst-release: IgG release after 2 h incubation in PBS at 37°C, dry D50%: median particle diameter dispersed in cyclohexane, wet D50%: median particle diameter after 2 h, 37°C incubation in water + 0.02 % v/v Tween 20).

	PLGA (mg)	***Lactose (mg)***	***DPPC (mg)***	***IgG/sorbitol (mg)***
Yield (maximise)	200 or 350	300 or 500	10 or 25	-
EE (maximise)	-	100 or 300	-	10 or 30 or 50
2 h burst-release (minimise)	350	-	-	10
Dry D50% (2-5 μm)	50 or 200	300 or 500	25 or 40	-
Wet D50% (minimise)	200 or 350	-	25 or 40	30
Morphology quality (maximise)	50 or 200	300 or 500	25 or 40	-
Optimal	**200**	**300**	**25**	**10 or 30**

4.5.3 Discussion

This experiment investigated the contribution of each excipient to the formulation. While all have been included on a rational basis, (i.e. PLGA for controlled-release, lactose for powder flow and thermal protection, and DPPC for emulsification and macrophage evasion), the quantities had been chosen from empirical experience. Another aim of this investigation was to consider the amount of antibody present. The current formulation, when EE results were considered, had an antibody content of ~1%. Ideally, the antibody to excipient ratio should be maximised, such that the minimum amount of excipients are used to generate a desirable dosage form. The results of this factorial experiment indicated that varying ingredient amounts (within the ranges of this investigation), caused statistically significant changes to the characteristics of microparticles produced. The results obtained are discussed below.

4.5.3.a) Product Yield

At the spray drier settings used, lactose dried very efficiently. Therefore, the larger the proportion of lactose in the formulation, the higher the resultant yield. Because PLGA was dissolved in a volatile solvent, it also dried well, provided it did not melt during the drying process. The interactions were interesting, although it must be remembered that as a percentage of the formulation, reducing the amount of one excipient, would necessarily increase the proportion of the others. This is particularly important when the lower amount of lactose was used. When only 100 mg of lactose, and only 50 mg of PLGA, were used, the proportion of DPPC in the formulation became quite large, and the yield fell to approximately 20%. Indeed, as an individual factor, DPPC was identified to reduce yield. Batches containing high amounts of DPPC felt more "greasy", and could not be easily removed from the collecting glassware. Another interesting observation was that DPPC was not directly soluble in DCM, but rather required the presence of a certain amount of PLGA (see Chapter 5). When preparing the batches with high DPPC, and low PLGA, the DPPC did not dissolve, for the same reason. If after homogenisation, the DPPC was not in solution, or at least present as a very fine suspension, this may well have reduced the spray-drying yield.

4.5.3.b) Encapsulation efficiency

High levels of lactose appeared to reduce the encapsulation efficiency (EE), although there was little difference between the low (corner) level and the centre-point. When the proportion of lactose was high, the yield increased, because it was dried effectively, and was retained in the final product. Therefore, when lactose was low, EE was higher, since the antibody was probably better retained in the final product than some of the other remaining components. It was also possible that this finding was related to the sensitivity Bradford assay, used to measure the concentration of protein present. Appendix III describes how lactose, or at least a compound formed from a reaction with lactose, appeared to interfere with the Bradford assay, reducing the measured concentration. Therefore, it was possible that changing the concentration of lactose present in a sample, would have affected the result. However, an experiment was performed that showed the effect of lactose on the Bradford assay was only present to a notable degree after 3 h of incubation. Thus all of subsequent experiments of this type were performed with 2 h incubation.

The apparent optimum amount of IgG, in terms of EE, may be related to the interaction with lactose. On average, the centre-point value of IgG gave the highest EE, because of

the degree of change caused by lactose, at low IgG levels. If the effect of lactose was due to interference in the Bradford assay, this would explain why the effect was only present at low IgG levels; the high loading samples were diluted prior to performing the Bradford assay, and thus would contain less of the potentially interfering chemicals. Assuming there was little difference between 100 mg and 300 mg of lactose in this respect, then increasing the amount of IgG, reduced EE (Figure 4.24). This could be related to the reasoning described in Section 4.4.3b, where antibody that migrated into the external phase, was slightly less likely to be included in the final product. Certainly, overloading the primary emulsion with protein would result in a larger gradient for this diffusion. Although the work in Chapter 3 showed that the presence of DPPC increased EE, it would appear from these data that changing the quantity had no further effect.

4.5.3.c) Burst-release by 2 h

The explanation of the burst-release by 2 h results follows on from the previous discussion. Protein escaping into the external aqueous phase was likely to have been on the microparticle surface, and thus be released instantaneously on contact with water. Having an increased concentration of antibody within the internal aqueous phase would drive this process. The interaction with PLGA content, suggested that the polymer matrix had a limited capacity. At a low level of IgG loading, increasing the amount of PLGA, reduced the initial 2 h burst-release. This was presumably because there was more polymer to encapsulate the protein. At higher protein loading, this difference in PLGA was probably not enough to impact the immediate 2 h burst-release.

4.5.3.d) Geometric diameter

Numerous factors were found to influence the D50%. However, given their relative lack of importance, the significant three-way interactions were not considered further and so will not be discussed. The centre-point values indicated that only 350 mg PLGA, or 10 mg DPPC, or 100 mg lactose, resulted in larger particles. This increase in the D50%, of 1-1.5 μm, was probably the result of aggregation, as clearly evident in some of the SEM images. Too much PLGA, relative to lactose, or indeed too little lactose, relative to the PLGA, may have resulted in PLGA particles starting to melt during the drying process, due to a lack of thermal protection, thereby resulting in the formation of larger particles. In greater amounts, DPPC probably reduced this process by surface protection of each PLGA particle. This hypothesis is supported by the interactions present, which indicated that the effect of high PLGA only persisted when lactose and DPPC were low, and the effects of low lactose were only present with the

highest amount of PLGA. The reduction in the effect of high PLGA by increasing the amount of IgG, may actually have been due to the increased amount of sorbitol (included 1:1 with IgG), which has similar thermal protection properties to lactose.

When performing the laser diffraction measurements on samples dispersed and incubated in water, there was a clear difference between three types of sample. Some produced the sub-micron peak, found in the previous experiment, there were others that gave 2-5 μm peaks, not dissimilar from the original microparticle distribution, and others that gave peaks larger than the original microparticle size, presumably due to aggregation of the insoluble components. From the statistical analysis, the latter case appeared to apply to those batches either containing low amounts of PLGA or high amounts of IgG, but with the centre-points forming smaller particles than either extreme. However, the interactions suggested that for low PLGA, aggregation only occurred with high DPPC or high IgG, with a combination of these two also giving aggregation. The intermediate types of particles were produced with low DPPC or low IgG, regardless of the amount of PLGA. The smallest types of particles were only achieved with the centre point values or a combination of high PLGA and high DPPC. These results were surprising, given the findings for dry particle diameter (dispersed in cyclohexane). There, it was found that high PLGA, with low DPPC, increased particle diameter, presumably because of melting. However, with high DPPC, higher amounts of PLGA were protected from aggregation, and it would appear that indeed these particles had surface properties to allow good dispersion in water. High DPPC with low PLGA may have presented a problem, because the proportion of emulsifier was too great. Rather than being active on the surface of PLGA particles, lumps of DPPC formed in water, as relatively large aggregates. For this purpose, it seemed that the centre-point combination was the ideal proportion. The effects of IgG may also have been due to its surface activity. As expected, lactose did not have any statistically significant effects. Although it may have contributed to particle formation in the spray drier, it dissolved in water, and therefore was not likely to have affected particle dispersion.

4.5.3.e) Scanning electron microscopy

A range of morphologies were present, varying from, individual spherical microparticles, to more aggregated, irregular shaped particles. In order to identify whether the morphologies were related to the effect of excipient amounts, the scanning electron microscopy (SEM) images were ranked from 0-3 according to quality. Of course, it is appreciated that this response value is not statistically valid (ordinal values

for responses are not acceptable (Armstrong and James, 1996)), and may be subjective, compared to non-subjective data. However, it was used merely as a simple way of drawing qualitative overall conclusions from the SEM images. It was found that high PLGA and low DPPC reduced microparticulate quality. This correlated with the diameter measurements by laser diffraction. However, based on averages, the centre-point formulations were superior in terms of quality. Referring back to the raw data, there were some non-centre-point batches that achieved a fully acceptable SEM rating of 3. These batches either contained a high lactose to PLGA ratio, or had high PLGA with high DPPC, plus high sorbitol and IgG.

4.5.3.f) Response optimisation

The response optimiser was limited to using combinations that had been tested as part of the factorial experiment. Therefore, it could not, for example, use 200 mg PLGA with 500 mg lactose, or any other centre-point value with other parameters at their corner-points. As a result, it could not generate an optimum formulation to meet all the requirements. However, Table 4.7 attempts to reveal optimum values by summarising the findings. The values in the Table are simplistic, as only the main-effects have been fully considered. This was because, in most cases, considering all of the interactions would have meant that where an option of two values is given, this choice was likely to have somewhat depended upon the choice of value for another parameter. It would appear from the Table 4.7, and all of the previous discussion, that the centre point values for PLGA, lactose and DPPC, produced the best combination of characteristics. The only characteristic limiting IgG loading was the initial burst-release, and thus on the evidence available, 10 mg IgG was the optimum. Indeed, increasing the maximum allowable burst-release within 2 h to 45%, allowed response optimisation to be performed, with the centre-point values being selected, and meeting all other criteria.

Therefore, expressed in other terms, the outcome of this experiment was to demonstrate that reducing lactose from 500 mg to 300 mg, was beneficial in terms of improving microparticle characteristics. As well as potentially increasing EE, using less lactose delivered a higher amount of antibody, *per* unit mass of formulation. Another possibility would be to increase the IgG loading to 15 or 20 mg. The only potential disadvantage, based on these data, would be in terms of immediate burst-release, which was assessed in Section 4.6.

Of course, there are other responses (not measured in this experiment) that could be affected by the relative quantities of these excipients. For example, the full release

profile had not been measured. This was likely to be affected by PLGA, the amount of IgG loading, and possibly also by DPPC. DPPC had also been included for its ability to protect microparticles from phagocytosis. However, it would seem that the quantity used should have been adequate for this effect (Evora *et al.*, 1998; Jones *et al.*, 2002). The antibody activity was not considered here (see Chapter 5). Excipients such as lactose and PLGA may offer protection against the conditions of manufacturing (Andya *et al.*, 1999). Thus the ratio of these excipients to IgG may have an impact on antibody stability. Also, aerosolisation properties were probably affected by lactose and DPPC, in a dry-powder or propellant-based system (Bosquillon *et al.*, 2001; 2004b).

In terms of particle morphology and particle diameter in water, the superiority of the centre-point formulation would suggest that the excipient levels chosen for this experiment were too broad. Further experiments would be needed to "fine-tune" these results. It was clear that using 25 mg DPPC was an optimal amount to include, and attempting to "fine-tune" this further was unlikely to have had much of an impact on the overall formulation. It might have been possible to reduce the lactose to 200 mg, without producing too much impact on yield and microparticle size or morphology. However, there was little to be gained in terms of protein content (this would have increased by approximately 0.5%, depending on IgG content), and it may have hindered aerosolisation. Certainly, it was worth investigating if higher IgG contents can be used. Increasing PLGA to 250 mg may have been a useful strategy in order to incorporate 20 mg IgG, while maintaining a low initial burst-release, without necessarily adversely affecting particle morphology. This could be tested as a 2^2 factorial experiment. If, for the present application, a two-phase release profile would be required, (with some initial release, followed by a phase of slow release), one way of achieving this was to incorporate a high protein load.

4.5.4 Conclusion

This investigation identified various possibilities for improving the current formulation, in terms of the amount of ingredients used. It appeared that the amounts of PLGA and DPPC being used prior to this experiment were optimal compared to the other amounts tested. Lactose, although important for yield, provided no other advantages, when more than 300 mg was incorporated. The intention of any formulation should be to use the minimum amount of excipients required to deliver the maximum amount of drug. The only factor prohibiting the amount of antibody to be increased above 10 mg, was the initial burst-release within 2 h. However, it was thought possible to double this amount, and still produce an acceptable formulation (Kaye *et al.*, 2006c).

4.6 Characterisation of the optimised formulation

4.6.1 Method

The findings of the three factorial experiments were combined, and three batches of the optimised formulation were produced. It was decided that 20 mg of IgG would be used, since this could double the drug loading without too much compromise on immediate burst-release. Because 300 mg of lactose was to be used, it was thought that the external phase volume could therefore be reduced to 70 mL, as the feed concentration would be less. This reduction in volume could be fully compensated by increasing secondary homogenisation to 10 min. Reviewing the data, there appeared to be no advantage of 3 min primary homogenisation over 2 min, and so 2 min was employed thereafter to reduce the shear stress that the antibody would be subjected to.

A high-performance cyclone and collector was obtained for the spray drier. This cyclone had a higher separation efficiency, and was able to collect particles < 2 μm that would have otherwise passed through to the filter. However, because transit time through the drying chamber was slower with the high-performance cyclone, an inlet temperature of 90-100°C was required to maintain an outlet temperature of 55°C. Also, the pump speed was rounded to 8%, since this represented a feed rate of ~2 mL/min.

4.6.1.a) Optimised formulation for the pulmonary delivery of IgG in controlled-release microparticles

The optimised formulation consisted of 20 mg IgG and 20 mg sorbitol in 2 mL water, 200 mg PLGA plus 25 mg DPPC in 4 mL DCM, and 300 mg lactose (as 316 mg lactose monohydrate) in 70 mL water. Homogenisation was for 2 min at 24,000 RPM followed by 10 min at 10,000 RPM. The resulting double emulsion was spray-dried at 2 mL/min (8%), with 75% aspiration, 800 L/h atomisation airflow, and adjusting the inlet temperature to between 90-100°C to achieve an outlet temperature of 55°C.

The optimised batches were characterised in terms of yield, EE (Section 2.3.2), glass transition temperature, zeta potential (see below) and particle morphology and diameter (Section 2.4.1-2.4.2). Dry particle diameter was determined in cyclohexane (see Section 2.4.1a). In order to improve the characterisation of the particles in aqueous media, a small-volume dispersion unit with a high-power lens was used in the Mastersizer. These samples were further analysed by photon correlation spectroscopy, and imaged using transmission electron microscopy (see below).

4.6.1.b) Differential scanning calorimetry

Differential scanning calorimetry (DSC) was used to estimate the glass transition temperature (T_g) of the formulation. Amorphous materials, such as those produced by spray-drying, exist in the more stable 'glassy-state' at temperatures below their T_g. DSC compared the energy (current) required to steadily raise the temperature of a sample compared to a reference. Peaks in energy flow related to thermal transitions in the material, such as T_g. DSC measurements of the formulation and the unformulated pure PLGA were made using a Pyris I DSC (PerkinElmer Instruments, UK), and analysed using Pyris v.3.80 software (PerkinElmer LSA Ltd., UK). After calibrating with indium, powder samples (5-10 mg) were accurately weighed into aluminium pans, which were sealed and measured from -10°C to +200°C at 10°C/min. Each sample was allowed to cool before re-running the heating cycle. The T_g value of the second cycle was used, since any residual moisture would have been removed during the first cycle.

4.6.1.c) Zeta-potential

Laser Doppler electrophoresis (ZetaMaster, Malvern Instruments, UK) was used to measure the zeta potential of the formulation particles, as an estimation of surface charge. The technique measured changes in the Doppler Effect resulting from the movement of particles between oppositely charged electrodes. Powder formulation (~5 mg) was suspended in 5 mL, 10 mM potassium chloride solution by brief vortexing (Cyclone, Clifton UK), and sonication in an ultrasonic bath (Clifton, UK). The suspension was diluted ~10 times, to give a count reading between 2000-4000 kcps. For each of the 3 samples measured, 5 reading were recorded. Zeta potential was calculated, using the Smoluchouski or Huckle approximation, with the appropriate software (PCS v.1.52, Malvern Instruments, UK).

4.6.1.d) Photon correlation spectroscopy

Photon correlation spectroscopy (PCS) was used as an alternative method to laser diffraction for measuring particle diameter in aqueous media. This technique used dynamic light scattering (light source: 2 mW helium-neon laser, 633 nm) to detect the Brownian motion of particles, from which particle diameters were calculated by an algorithm consisting of several methods. Therefore, this technique could only be used to measure particles <~3 μm (depending on density), since particles larger than this would have sedimented, rendering Brownian motion undetectable. Powder formulation (~5 mg) was suspended in 1 mL water + 0.02 % v/v Tween 20, and incubated for 2 h at

37°C, in order to dissolve the aqueous soluble components. Samples were diluted ~5 times to give a count reading of 20,000-40,000. Two samples of the formulation were measured, and for each sample the mean Z-average diameter (a unique expression of average particle diameter, particular to PCS) and polydispersity were recorded from 10 readings. The average particle diameter distribution of each sample was also recorded.

4.6.1.e) Transmission electron microscopy

Transmission electron microscopy was used to image the particles suspended in aqueous media. Powder formulation (~5 mg) was suspended in 1 mL water + 0.02 % v/v Tween 20, and incubated for 2 h at 37°C, in order to dissolve the aqueous soluble components. Several samples were prepared by placing a drop of the suspension on a Formvar/carbon coated copper grid (200 mesh, TAAB, Aldermarston, UK) which was then blotted and air dried. The transmission electron microscopy (TEM) pictures were captured (by Dave McCarthy of the School of Pharmacy, Univeristy of London) using an FEI-Philips (Eindhoven, Netherlands) BioTwin CM120 with a Lab 6 emitter and 120 kV accelerating potential.

4.6.2 Results

Higher yields of 63 ± 1% were obtained using the high-performance cyclone. EE was 87 ± 6%, and burst-release by 2 h was 15 ± 0.9%. From the DSC data it appeared that the formulation had a T_g peak at 30.3°C (half-CP extrapolated). This was ~3°C higher than the pure PLGA polymer. Zeta potential measurements indicated that the particles carried very little charge (1.6 ± 2.5 mV, n=3).

4.6.2.a) Particle morphology and diameter

Figure 4.33 is an SEM image of the formulation. It can be seen that the formulation consisted of non-agglomerated, mostly spherical, microparticles. The microparticles appear to have a range of diameters <5 μm, including a small proportion of sub-micron particles (<1 μm).

Figure 4.33 Scanning electron micrograph of the optimised, spray-dried, IgG formulation. The formulation appeared to consist of microparticles of 1-5 µm diameter.

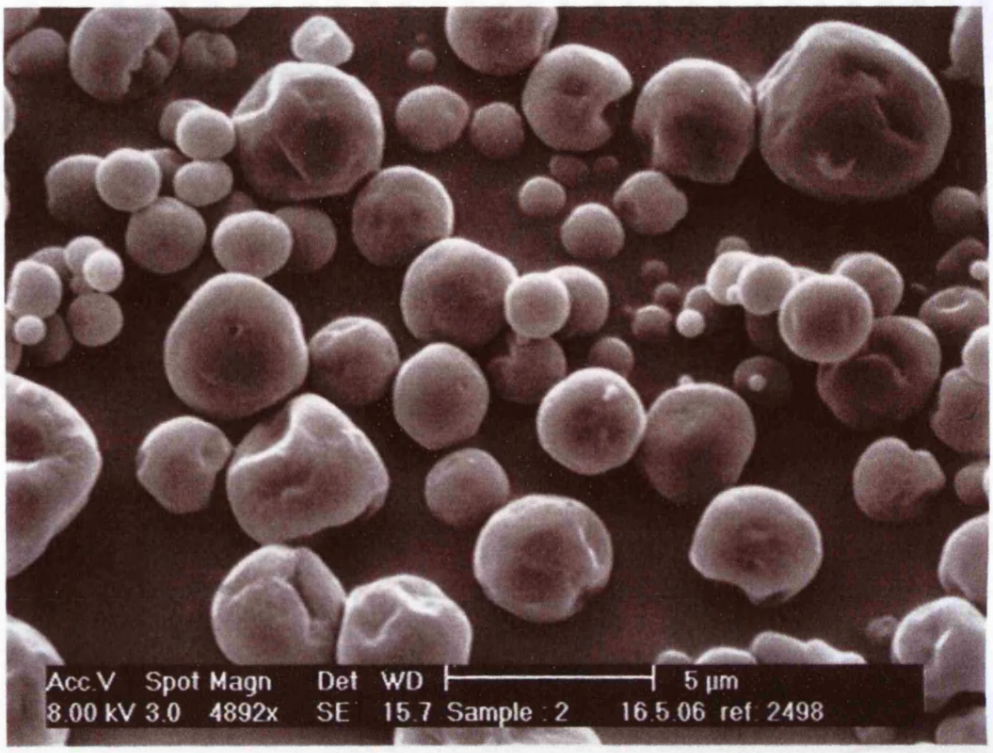

The laser diffraction results are summarised in Table 4.8.

Table 4.8 Geometric particle diameters of the optimised formulation in different dispersion media, measured by laser diffractometry. The following derived diameter values are given: D50%: volume median particle diameter, D90%: diameter that 90% of the volume of particles was smaller than (values are mean ± SD, n=3).

Dispersion conditions	D50% (µm)	D90% (µm)
Cyclohexane + 1% v/v Span 80	4.2 ± 0.2	7.1 ± 1.0
Water + 0.02% v/v Tween 20	0.41 ± 0.05	1.1 ± 0.2

Figure 4.34 compares example volume diameter distributions obtained in the different dispersion mediums using laser diffraction. The particle diameter distributions of the samples dispersed in aqueous media were also measured by PCS. The Z-average diameter was 456 nm ± 40 nm, and the polydispersity index was 0.11 ± 0.60 (n=2). An example volume distribution is given in Figure 4.35.

Figure 4.34 Geometric volume diameter distribution of optimised microparticles, a) dispersed in cyclohexane, and b) after 2 h of incubation at 37°C in water + 0.02% v/v Tween 20. Both samples were measured by laser diffractometry.

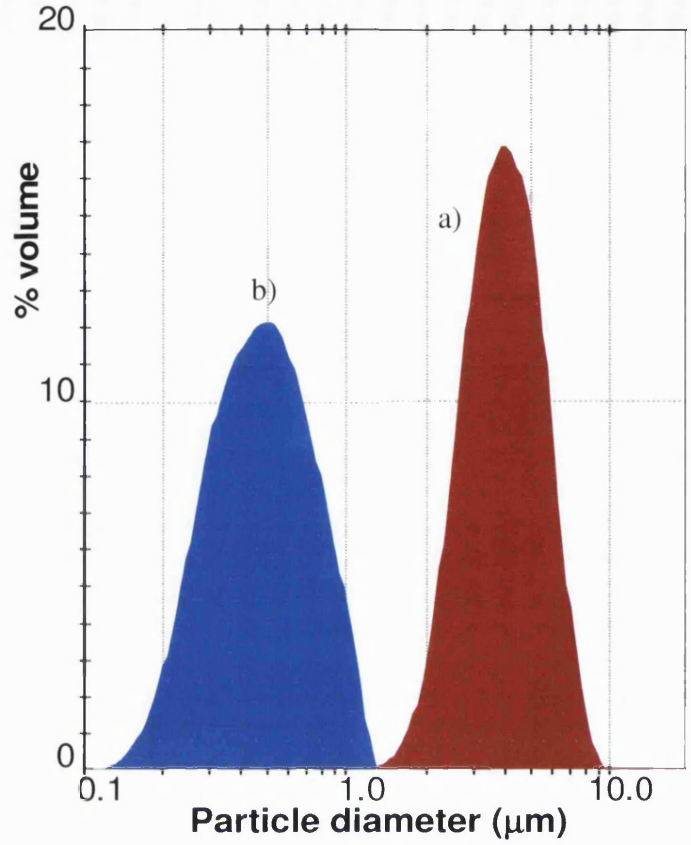

Figure 4.35 Volume distribution of particles incubated (2 h, 37°C) in water + 0.02 % v/v Tween 20, as determined by photon correlation spectroscopy.

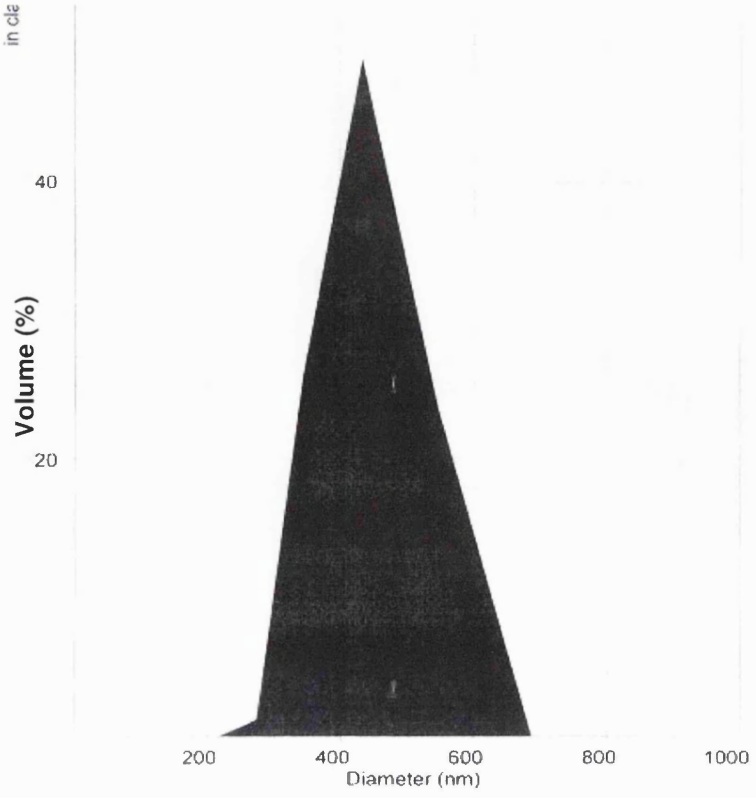

Images of these nanoparticles were captured using TEM. An example is given in Figure 4.36. This further confirmed the presence of nano-particles, which had morphological characteristics consistent with them being solely composed of PLGA. It would appear that some of the particle population had diameters even less than the 300 µm detected by the other techniques.

Figure 4.36 Example transmission electron microscopy (TEM) image of poly(lactide-co-glycolide) nanoparticles produced upon incubation of microparticulate formulation in aqueous media. The IgG formulation was incubated in water + 0.02% v/v Tween 20 for 2 h at 37°C, before TEM analysis. Nanoparticles were observed, confirming the results of laser diffractometry and photon correlation spectroscopy sizing methods.

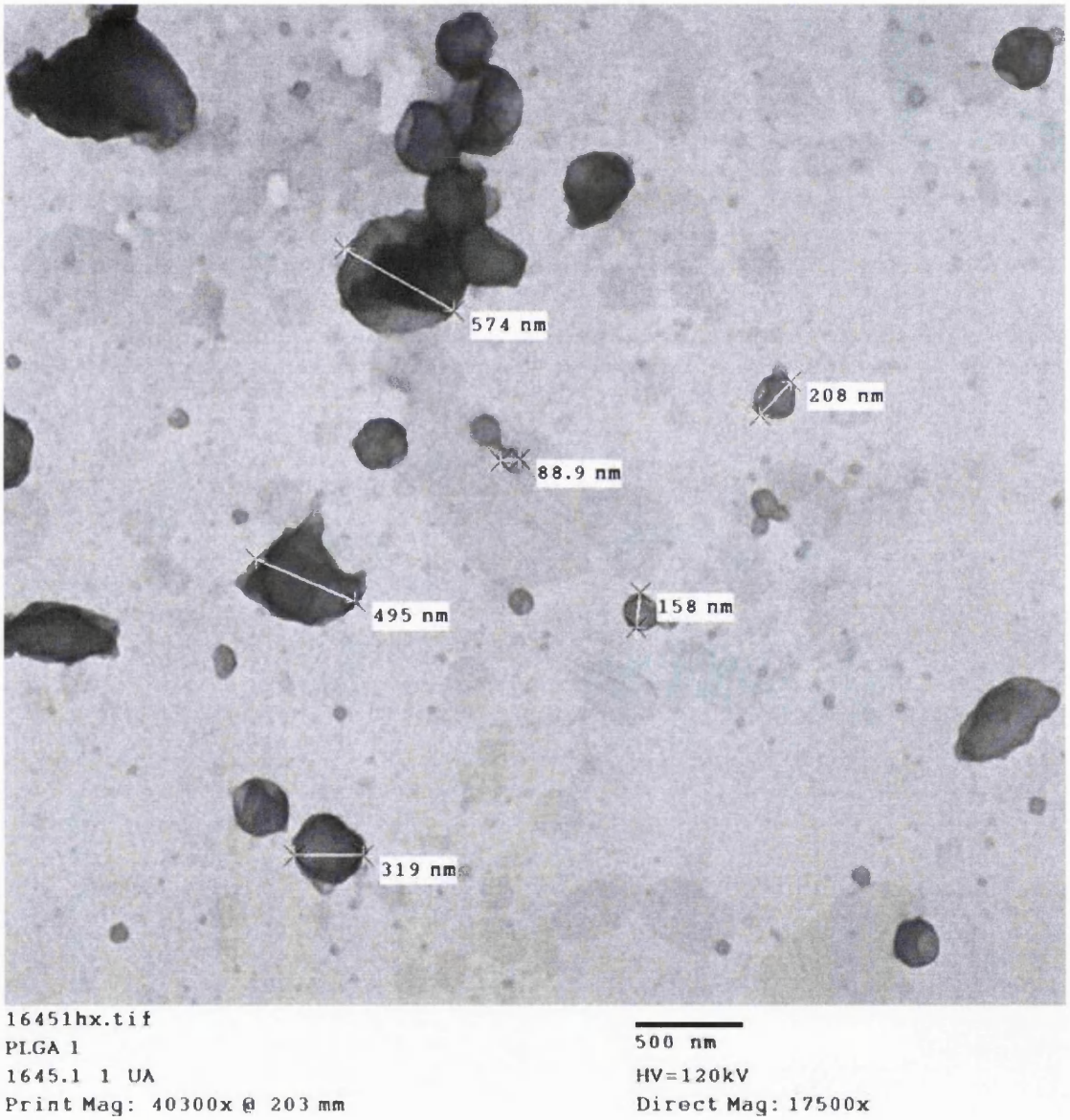

4.6.3 Discussion

As expected, use of the high-performance cyclone improved the product yield. This cyclone was able to separate particles from the air stream more efficiently, trapping those particles < 2 µm that would normally have passed through to the filter. Indeed the SEM images identified that there were some very small, sub micron particles.

However, also contributing to the yield increase was the fact that this cyclone used a smaller-volume collecting vessel, which made powder recovery easier. Despite the requirement for a higher inlet temperature, the optimised formulation and manufacturing parameters produced powder composed of individual microparticles with a high EE. Increasing the IgG loading to 20 mg did not appear to increase the immediate burst-release to an unacceptable proportion.

The particles appeared to have approximately zero net charge. This was expected, since the major component of the particles, PLGA, is not ionised in pH neutral water. The presence of the other excipients caused the formulation to have a T_g of just over 30°C, which was 3°C greater than the pure polymer. This could be crucial to the commercial potential of the formulation. A formulation is likely to have better long-term stability if stored below its T_g, since the component molecules would be less flexible, and thus less able to participate in chemical reactions. If a formulation has a T_g >30°C, this may enable it to be stored at room temperature ("in a cool, dry, place"), rather than require refrigeration, which would potentially be a big disadvantage for such a product.

4.6.3.a) Particle diameter

Other than serving as a check for the optimised parameters, the main purpose of this work was to fully characterise the micro-to-nano-particle effect previously revealed. When dispersed in cyclohexane, the distribution was as seen previously, i.e. microparticles of 1-10 μm, with an average of approximately 4 μm. The sub-micron particles that appeared on the SEM image, seemed not to be sufficiently numerous enough to contribute to the volume distribution.

The use of the small-volume dispersion unit, with high powered lens, considerably improved detection of nanoparticles after dispersion in aqueous media. After 2 h incubation at 37°C, there appeared to be no particles greater than 1 μm, with the majority between 400-600 nm (Kaye *et al.*, 2006c). In most cases, there were no aggregate peaks, suggesting that these nanoparticles dispersed very well. These data were confirmed by PCS, which produced a very similar volume distribution, and TEM. The diameters of these nanoparticles also appeared to correlate well with the SEM produced by evaporating and freeze-drying this double-emulsion formulation (see Figure 3.7). It was therefore believed that the size of the final microparticles was controlled by the droplet size of the spray drier atomisation, and also that the size of the nanoparticles contained within was controlled by the droplet size of the DCM, disperse phase, in the emulsion. When spray-drying, these DCM droplets, containing the dissolved (yet water-insoluble) PLGA, would have evaporated to create PLGA

nanoparticles at the size of these droplets. These were immediately trapped within larger particles of lactose, created by the drying of larger droplets of liquid feed produced by the spray drier. These larger droplets consisted of lactose solution (the external phase of the double-emulsion) containing the smaller droplets of the PLGA dissolved in DCM. The presence of these nanoparticles in aqueous media was further confirmed by TEM. There appeared to be some very small nanoparticles that perhaps did not appear on the PCS distribution, due to their low volume contribution.

This micro-nano-particle phenomenon could well be the key to the success of the formulation. Essentially, the formulation was comprised of microparticles that are used to deliver a package of nanoparticles. One to five micrometers, is an ideal size for pulmonary delivery, being known to potentially deliver the antibody to the target region of the lungs, due to aerodynamic principles. Thus, unfortunately, this has evolved to be the ideal geometric diameter for macrophage detection, and subsequent phagocytosis. Unless a vaccine is being formulated, or a drug targeted to macrophages, this fate of the microparticles is an unwanted effect, especially in the case of a controlled-release formulation, where the particles are needed to remain in the lungs for several days. One method for potentially avoiding phagocytosis is to use large porous particles. These are geometrically too large to be phagocytosed, but due to their low density, have the required aerodynamic diameter for pulmonary delivery. However, achieving controlled-release with a porous particle would be difficult, as the pores give the particle a large surface area, from which drug can diffuse. With this formulation another potential method is possible. Upon delivery, the microparticles partially dissolve to form nanoparticles, from which drug will be released. Nanoparticles of this diameter are too small for macrophage detection (Grenha *et al.*, 2005), and thus can reside at the lung surface for the duration of release, without removal by phagocytosis.

This system could have potential applications for other types of drug delivery. For example, nanonisation is one method of formulating water-insoluble drugs. However, nanoparticles cannot be handled very easily in solid form, since they are very cohesive due to their high surface area. This approach would be a simple method of nanonising such drugs, provided they can be dissolved in an organic solvent. It also then produces a micron-sized powder that is easier to handle for tablet compression or reconstitution for injection.

Tsapis *et al.*, (2002) and Grenha *et al.*, (2005) both described a similar concept of microparticles containing nanoparticles by spray-drying. However, both authors presumed the prior availability of nanoparticles. In the former case, they were pre-

manufactured polystyrene nanoparticles, whilst in the latter case they were pre-prepared chitosan nanoparticles. These examples were easy to produce and handle, and it would be difficult to apply these elsewhere. In the system described in this thesis, the nanoparticles were created whilst the emulsion droplets were dried (during the spray-drying process), and so no handling of nanoparticles was required at any stage. Also, given that the nanoparticles in the present work are composed of biodegradable PLGA, the potential for the undesirable effects thought to be associated with nanoparticle exposure should be relatively small (Medina *et al.*, 2007).

4.6.4 Conclusion

An optimal formulation of IgG has been produced and characterised. The results of the three factorial experiments have been combined effectively. The concept and utility of modified-release nanoparticles within the microparticles has also been explored.

4.7 General conclusion

The work with DPPC and PVA, and the three factorial experiments, has led to the development of a formulation that should fulfil many of the requirements for the delivery of antibody to the airways. The excipients used are all bio-compatible, and with the exception of PLGA, are GRAS for pulmonary delivery. PLGA entraps the antibody within a slowly degrading matrix, thus affording controlled-release to the system, as evidenced by the reduced initial burst-release. DPPC was required to form the double-emulsion system, but also contributed to the morphology of the microparticles, and their dispersion in water, as well as potentially prolonging their residence in the lung, by avoiding macrophage detection and removal (Evora *et al.*, 1998). Lactose enhanced the spray dying properties, increasing yield and protecting other excipients from damage (Andya *et al.*, 1999). Also, it must be remembered that the model antibody used in these experiments was formulated in a 1:1 mass ratio with sorbitol. It has previously been identified that the addition of a dissacharide to the internal aqueous phase of a double-emulsion, protected proteins within the same phase, from homogenisation-induced conformational changes (Fu *et al.*, 1999). Additionally, sorbitol has been demonstrated to protect IgG from spray-drying-induced aggregation (Maury *et al.*, 2005a). The spray-drying method used, produced microparticles of an acceptable diameter, with a relatively good efficiency, and appeared not to damage the structure of the antibody. These experiments have also identified how characteristics such as initial burst-release, particle diameter, and polydispersity of diameter, can potentially be engineered by manipulating the amount of excipients or other manufacturing parameters.

5 MODIFYING THE ANTIBODY RELEASE PROFILE FROM THE POLY(LACTIDE-CO-GLYCOLIDE) FORMULATION BY USE OF BASIC SALTS AND ALTERNATIVE POLY(ESTERS)

5.1 Abstract

The IgG formulation, optimised in the work in the previous chapter of this thesis, was developed further by investigating the use of basic salts, and alternative polymers as a means of modifying the IgG release profile. These experiments provided an opportunity to additionally characterise the formulations in terms of release profile and released antibody stability.

Basic salts, when added to the internal aqueous phase of the emulsion, were found to affect the amount of immediate IgG burst-release. Sodium bicarbonate had the largest effect, almost doubling the 2 h burst-release to nearly 30%. However, for all formulations the cumulative IgG release in pH 7.4 phosphate-buffered saline (PBS) did not increase following the initial burst.

Substituting half of the 7 kDa poly(lactide-co-glycolide) (PLGA) in the formulation for 2 kDa poly(lactic acid) (PLA) had little effect on the IgG release profile in pH 7.4 PBS. However, in a pH 2.5 glycine release media, continuous IgG release was observed, which was more rapid for the formulation containing only 7 kDa PLGA. This was thought to be due to the increased crystallinity of PLA more than compensating for its lower molecular weight. The release media of lower pH was thought to reduce IgG adsorption onto the particle surface, due to the antibody carrying a greater net charge.

Methyl and lauryl end-capped PLGA polymers were compared to the uncapped PLGA used in the previous chapters of this thesis. Reduced IgG release was observed with the end-capped polymers, suggesting that a hydrophobic interaction between the antibody and the polymer was responsible for preventing IgG release. Hence, this interaction was increased with the more hydrophobic (capped) polymers.

The IgG released from all formulations, during 2 h incubation in release media, was demonstrated to be non-aggregated, and biologically active, when analysed by gel electrophoresis, field-flow fractionation and enzyme-linked immunosorbent assay. There was evidence that IgG released by 7 days was also stable. Formulations were also shown to be non-toxic to *in vitro* Chinese hamster ovary, epithelial cell lines, when they were exposed to very high formulation concentrations of up to 2500 μg/mL.

5.2 Introduction and aims

The previous two chapters of this thesis have described the development and optimisation of a PLGA-based, controlled-release formulation of IgG. Although the modified-release properties had been optimised in terms of burst-release by 2 h, the full release profile of the formulation had not been characterised. The polymer manufacturer estimated that the PLGA 1A used in this work had an aqueous degradation time of 1-3 weeks. However, this could have been affected by other excipients in the formulation, and may not have correlated with the antibody release profile. Drug release from PLGA was thought to occur by three processes: rapid dissolution of drug on the polymer surface, diffusion through the polymer matrix and release due to polymer degradation. In the case of a large protein drug, such as an antibody, these processes may contribute in varying degrees to the release profile. For example, diffusion of a hydrophilic protein through a hydrophobic polymer matrix was likely to be much slower than the diffusion of a small drug molecule. In addition, there may well be interactions between the antibody and the polymer that alter release.

The literature describes the measurement of *in vitro* protein release from polymer microparticulate systems as proving to be very difficult to measure, often with poor *in vitro-in vivo* correlation (IVIVC). Generally, an initial burst-release was observed, followed by many days of little or no release (Witschi and Doelker, 1998b, Jiang *et al.*, 2002; Schwendeman, 2002; Tamber *et al.*, 2005). The above authors have suggested numerous reasons for this, including high particle concentration relative to an *in vivo* distribution, lack of suitable dispersion, sink conditions not being achieved, the generation or prevention of an acidic microclimate, readsorption of protein onto microparticles, and/or that *in vivo* enzymes may contribute to polymer degradation. One method of improving IVIVC, suggested by Jiang *et al.* (2002), was to use a pH 2.5 glycine release buffer, rather than pH 7.4 PBS. Although this may not appear to resemble physiological conditions, the authors gave two main reasons in support of this approach. Firstly, using a pH 7.4 buffer prevented the development of the acid microclimate within the system that was generated as lactic acid, and glycolic acid was hydrolysed from the polymer chain. This microclimate would further have catalysed the polymer degradation, and thus increased the release. *In vivo*, the local area would develop a lower pH, allowing the continuation of polymer degradation. Secondly, at pH 7.4 the protein was prone to aggregation, unfolding and readsorption on to the particle surface. Although aggregation may not be too much of a problem in a standard solution, in a suspension of microparticles there was a huge (hydrophobic) surface area

[A 5 mg sample of inhalable microparticles contains ~750 million particles with a surface area more than 1000 times greater than that of a tablet of the same mass (Patton and Byron, 2007)] . Released antibody could unfold to reveal its hydrophobic surfaces, allowing re-adsorption onto the particle surface. One study suggested that a peptide had particular affinity for readsorption onto lower molecular weight PLGAs, such as the type used in the present work (Witschi and Doelker, 1998a). Also, unfolded protein was much more likely to aggregate to shield these hydrophobic surfaces from water, than would protein in its usual quaternary structure. At lower pH, away from the isoelectric point, the protein carried a net charge, potentially stabilising the individual molecules. Alternative pH release media have also been investigated by Yang and Cleland (1997).

In this work, the first experiment investigated a concept widely published in the literature [e.g. Sandor *et al.* (2002), and see the review by Schwenderman (2002)] of using basic salts in PLGA formulations, with the aim of improving release of protein. There was the suggestion that an acidic microclimate generated during degradation of PLGA microparticles could damage protein, and thereby prevent release (Fu *et al.*, 2000). Using basic salts has been shown to improve protein release, by reducing protein aggregation in several PLGA-based delivery systems (Zhu *et al.*, 2000).

The second experiment used 2 kDa poly(lactic acid) (PLA) as an alternative polymer to PLGA. The PLGA 1A used here was 7 kDa, the lowest 'off-the-shelf' manufactured molecular weight. Given that degradation time increased with molecular weight, it was postulated that using 2 kDa PLA may have an increased degradation-rate, and thus release-rate. In a previous study, the release of beclometasone dipropionate (BDP) from microparticles composed of 2 kDa PLA was prolonged and continuous, compared to microparticles composed 15 kDa PLGA, where (BDP) release stopped after an initial burst (Wichert and Rohdewald, 1993). However, PLA, being more crystalline, may have actually degraded more slowly than PLGA for a given molecular weight (Witschi and Doelker, 1998b). Also, protein, unlike BDP, is not soluble in the polymer, and so would not easily diffuse out of the matrix. Therefore, the question was whether the lower molecular weight of the PLA would have more than compensated for its increased crystallinity, and thus have given a faster release of protein.

The final experiment compared end-capped variations of PLGA to the uncapped PLGA that has been used in this work, in terms of their antibody release. One possible explanation for incomplete release, could be a charge interaction between free carboxyl groups at the ends of the polymer chains, and amine groups on the antibody. By using

PLGAs that have these carboxyl groups capped by an alkyl group, such an interaction, if it existed, would be reduced, allowing antibody to be released.

As well as measuring the quantity of released antibody, the experiments in this Chapter further characterised the stability of the released antibody by a range of techniques. In the third experiment, the *in vitro* cell-line toxicity of the formulation was investigated.

5.3 Effect of basic salts on protein release profile

5.3.1 Method

Formulations were composed as specified in Section 4.6.1a) and manufactured as described in Section 2.2.1-2.2.2. However, 5 mg of either sodium bicarbonate ($NaHCO_3$), sodium carbonate (Na_2CO_3), magnesium carbonate ($MgCO_3$) and zinc hydroxide/carbonate compound ($Zn(OH)_2/ZnCO_3$) were added to the internal aqueous phase. A further batch was made with no addition of any salt. Each batch was measured in triplicate for EE and release. At this time, the release profile method described in Section 5.4.1 had yet to be developed. Twenty milligrams of the powder formulation were weighed into an Eppendorf tube, and 1 mL of PBS was added. The tubes were shaken in a 37°C incubator (Weiss Gallenkamp, UK). At given time-points the tubes were centrifuged (10 min, 5000 RPM), and the supernatant was removed and analysed by the Bradford assay. Fresh PBS (1 mL) was added to each of the tubes before incubating them until the next time point. The 2 h burst-release samples were also analysed for antibody stability by ELISA (Section 2.5.2). The entire experiment was repeated three times. However, because some of the spray-drying conditions were varied, the results have not been combined quantitatively. Nevertheless, the overall qualitative findings were considered.

5.3.2 Results

Figures 5.1, 5.2 and 5.3 are the EE, release and ELISA of the formulations, respectively. The antibody released was measured for a further 6 days. However, little further release was detected after day 2. In the repeat experiments, the same rank order of salts was observed for a 2 h burst-release: $MgCO_3>NaHCO_3>Na_2CO_3>Zn(OH)_2/ZnCO_3$. However, the position of the no-salt formulation did vary from having the lowest initial burst-release (as presented in Figure 5.2) to having an initial burst-release greater than Na_2CO_3. In all experiments $Zn(OH)_2/ZnCO_3$ had a faster release rate between 2 h and 8 h, such that the cumulative release overtook that of Na_2CO_3. In all experiments, the ELISA detection was lower for the $Zn(OH)_2/ZnCO_3$ formulation than for the other formulations.

Figure 5.1 Encapsulation efficiency of IgG in spray-dried, microparticulate, poly(lactide-co-glycolide) formulations containing various basic salts, added to modify the release properties (mean + SD, n=3)

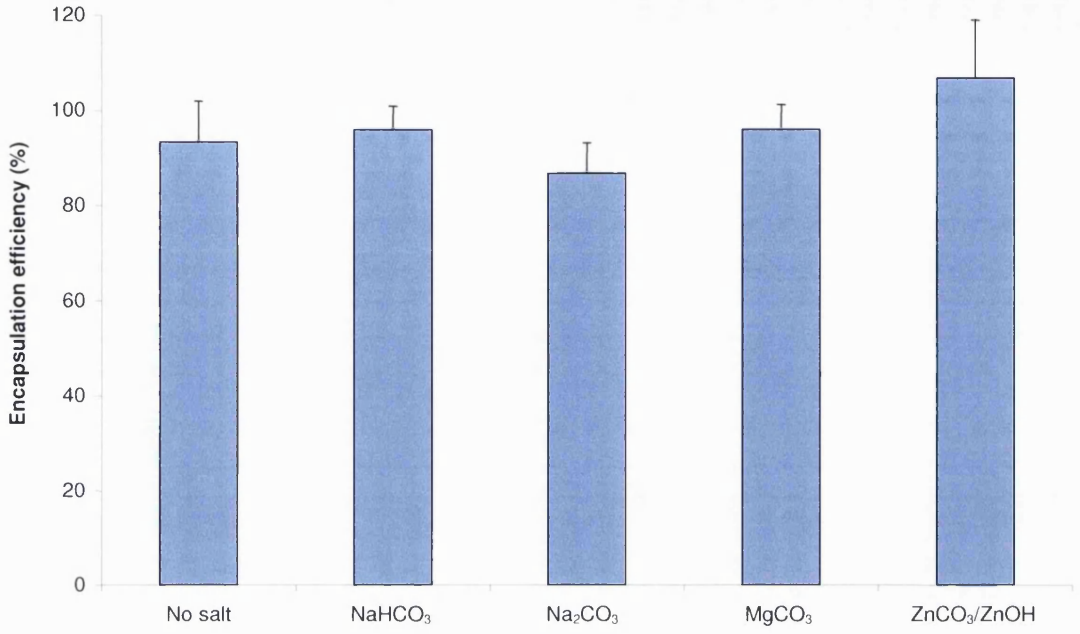

Figure 5.2 Cumulative release of IgG from spray-dried, microparticulate poly(lactide-co-glycolide) formulations containing various basic salts, using pH 7.4 PBS release media (mean + SD, n=3)

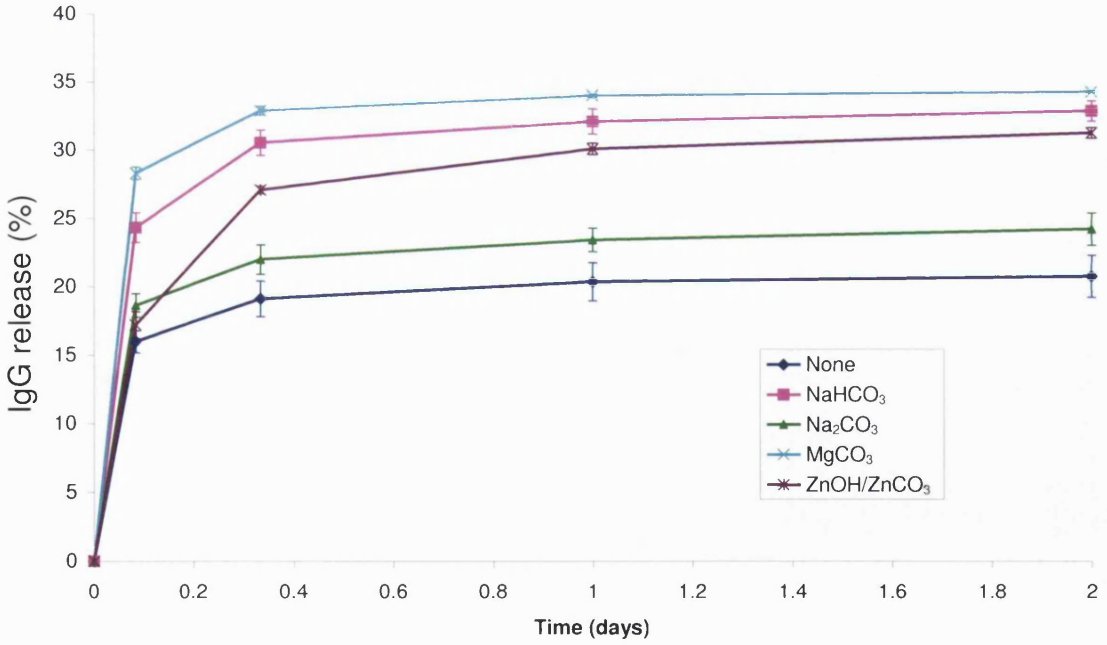

Figure 5.3 Enzyme-linked immunosorbent assay (ELISA) to measure the biological activity of IgG released from spray-dried, microparticulate poly(lactide-co-glycolide) formulations containing various basic salts. The concentration of IgG determined by ELISA was expressed as a percentage of the total protein concentration measured by the Bradford assay (mean + SD, n=3).

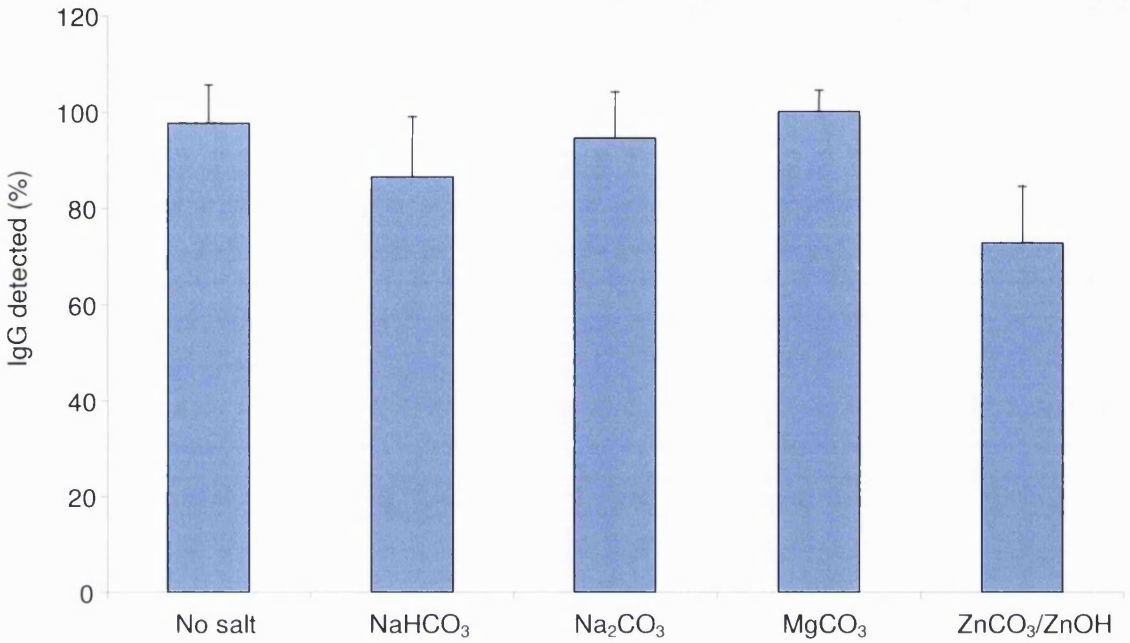

5.3.3 Discussion

The IgG release profile observed was typical of protein-loaded, PLGA microparticulate systems published in the literature (Schwendeman, 2002). After an initial burst-release, there was little further release, with or without the presence of basic salts. This was similar to the finding of Shao and Bailey (1999). The lack of release was thought to be a problem of the *in vitro* method (Jiang *et al.*, 2002), rather than a reflection of the likely *in vivo* performance of this formulation. It had been postulated that the acidic microclimate generated by PLGA degradation may have damaged protein, preventing its release after the initial burst (Fu *et al.*, 1999). However, the addition of basic salts did not appear to affect this stage of the release profile, suggesting the acidic microclimate causing antibody damage was not responsible for this problem. Nevertheless, some interesting observations on the initial burst-release properties could be made. The presence of just 5 mg of a basic salt clearly affected the 2 h burst-release. In the literature, basic salts have been added at 3-10% of the polymer weight. However, in these examples the solvent-evaporation method was typically used, and thus some of the salt may have been washed out of the final product. This can also result in more porous particles. In the case of the spray-drying method used here, although it was found that higher amounts of salt resulted in the particles appearing more spherical, 5

mg was the maximum that could be added without reducing yield and powder quality. However, at this level, there was no difference in the particle morphology previously observed (see Figure 4.33). Despite the increase in initial burst-release, none of the tested salts enabled continued IgG release after 1-2 days.

There are a number of possible reasons why the presence of these salts affected the initial burst-release. It is possible that the presence of the salt, or possibly the carbon dioxide it produced in solution, disrupted the polymer matrix, creating pores. The increased surface area of a porous particle would be expected to give a higher initial burst-release. Another possibility was that the salt affected the primary emulsion, causing some of the antibody to escape to the external phase. The reason for the rank order of basic salts was not clear. However, there was a correlation between the amount of initial burst-release, and the aqueous solubility of the salt.

Zinc salts were chosen because of their known protein-stabilising effects (Vanbever *et al.*, 1999a). However, in the present work, it appeared that compared to no salt or other salts, zinc was detrimental to the stability of released IgG, as detected by ELISA.

5.3.4 Conclusion

The presence of basic salts did not enhance the *in vitro* release profile of IgG from the PLGA formulation. However, there was some impact on initial burst-release, which could be further explored, should this characteristic of an IgG formulation need to be modified in the future.

5.4 Substitution of 7 kDa PLGA for 2 kDa PLA

5.4.1 Method

Formulations were produced as described in Section 4.6.1a). Triplicate batches were made containing 200 mg of 7 kDa PLGA as before, and 3 batches were made substituting 100 mg of the PLGA for 100 mg 2 kDa PLA (Lakeshore Biomaterials, USA). Although the plan was to use 200 mg of the PLA, it was found that without the presence of at least 100 mg of the PLGA, the DPPC would not dissolve in the DCM. Therefore, only 100 mg of the PLGA could be substituted for PLA, since a stable primary emulsion could not be made without the DPPC being in solution. A further batch containing only 100 mg PLGA, i.e. with no PLA, was made as a control, in order to determine if any of the observed effects were actually due to the presence of the PLA, rather than the absence of PLGA.

For each batch, the EE (in triplicate) and the release profiles were determined, in both pH 7.4 0.15 M PBS + 0.01% v/v Tween 20, and pH 2.5 0.1 M glycine + 0.01% v/v Tween 20 buffers. This followed a similar procedure to the measurement of 2 h burst-release described in Section 1.3.3. Powder formulation (~60 mg) was accurately weighed into 15 mL tubes. The appropriate volume of release media (~ 3 mL) was added to give a 20 mg/mL suspension. The tubes were shaken and incubated at 37°C (Weiss Gallenkamp UK). At each time point the tubes were centrifuged for 10 min at 5000 RPM (Megafuge 1.0, Heraeus Sepatech, Germany), and the supernatant was collected for analysis of protein content by the Bradford assay (Section 1.3.1). The supernatants were replaced with fresh release media of the same volume, the formulations pellets were resuspended in the media, and the tubes were incubated until the next time point. At the termination of the release experiments, the remaining pellets were dissolved with 0.5 M NaOH, and assayed for protein using the Bradford assay. The stability of the IgG released from the formulations after 2 h in PBS, was determined by SDS-PAGE, FFF and ELISA (see Sections 2.5.1-2.5.3).

5.4.2 Results

Figure 5.4 compares the EE of the formulations. The polymer appeared to have no impact on the EE, which was consistently above 80%

Figure 5.5 and 5.6 are the release profiles in pH 7.4 and pH 2.5, respectively. In the former case, the profile was similar to that previously observed: an initial burst-release, followed by a long period of very little release. However, there was a second burst of

release between days 3 and 6, resulting in approximately 70% of the loaded antibody being released after 35 days. The batch with only 100 mg of polymer had a higher initial burst-release. In pH 2.5 buffer, after an initial burst of release, there was continued release from all formulations, with the 200 mg PLGA formulation releasing the most IgG (almost 90% after 35 days). Analysis of the centrifuged pellets remaining at 35 days, detected most of the unreleased protein (Figures 5.7 and 5.8).

Figure 5.4 Mean encapsulation efficiency of IgG in microparticulate formulations containing poly(lactide-co-glycolide) (PLGA) and poly(lactic acid) (PLA) polymers (n=3, + SD)

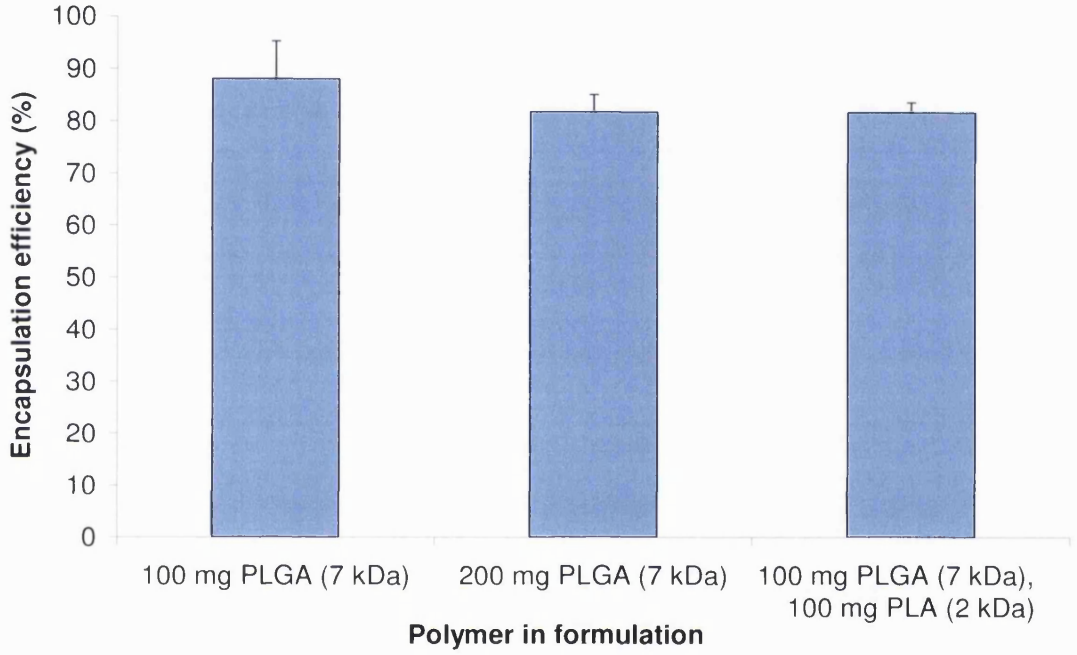

Figure 5.5 Cumulative IgG release from poly(lactide-co-glycolide) (PLGA) and poly(lactic acid) (PLA) microparticulate formulations in pH 7.4 PBS + 0.01% v/v Tween 20 (n=3, mean + SD)

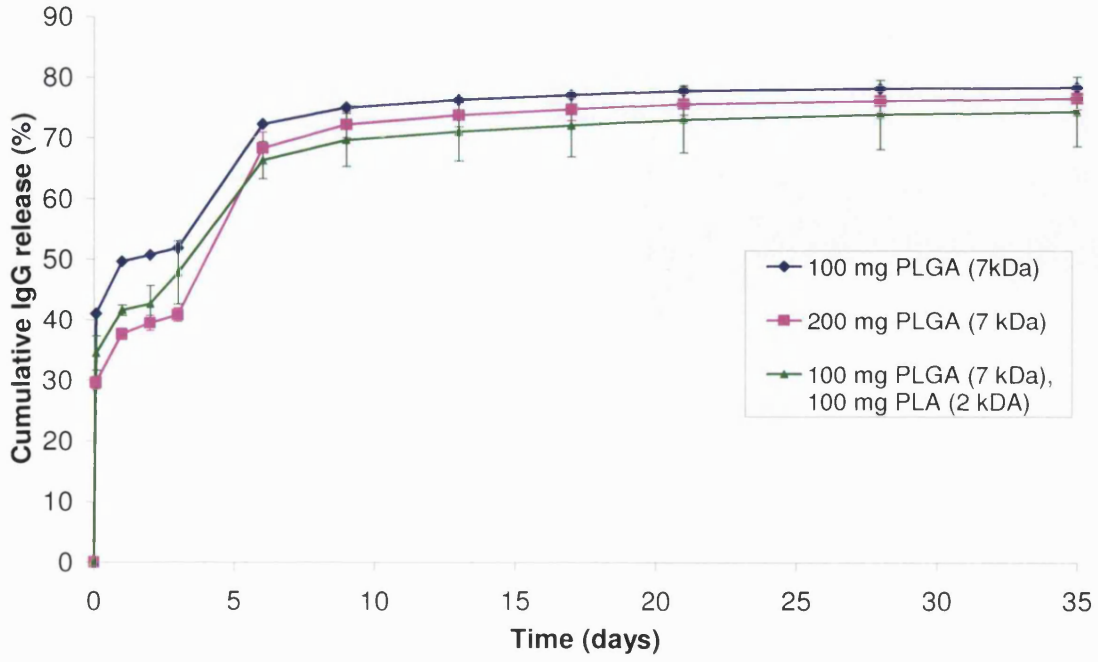

Figure 5.6 Cumulative IgG release from poly(lactide-co-glycolide) (PLGA) and poly(lactic acid) (PLA) microparticulate formulations in pH 2.5 0.1 M glycine + 0.01% v/v Tween 20 (n=3, mean ± SD)

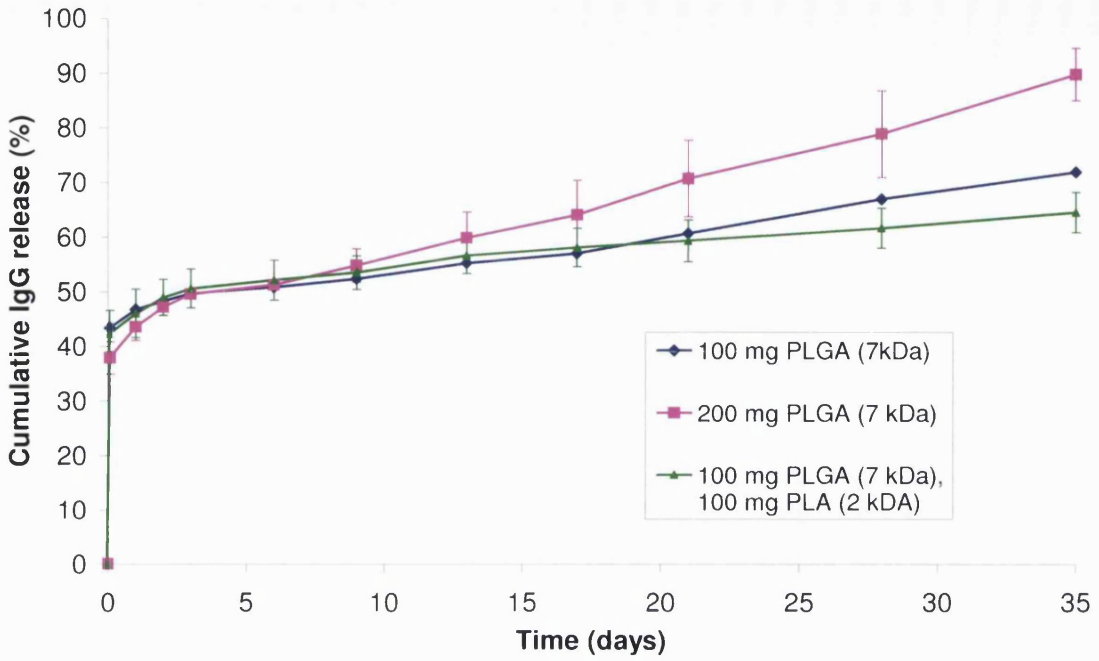

Figure 5.7 Total IgG released in pH 7.4 release media from microparticulate formulations containing poly(lactide-co-glycolide) (PLGA) and poly(lactic acid) (PLA). Cumulative release after 35 days in pH 7.4 PBS + 0.01% v/v Tween 20, and subsequent analysis of the remaining pellet, following dissolution in 0.5 M NaOH (n=3, mean + SD, except 100 mg PLGA, where n=1).

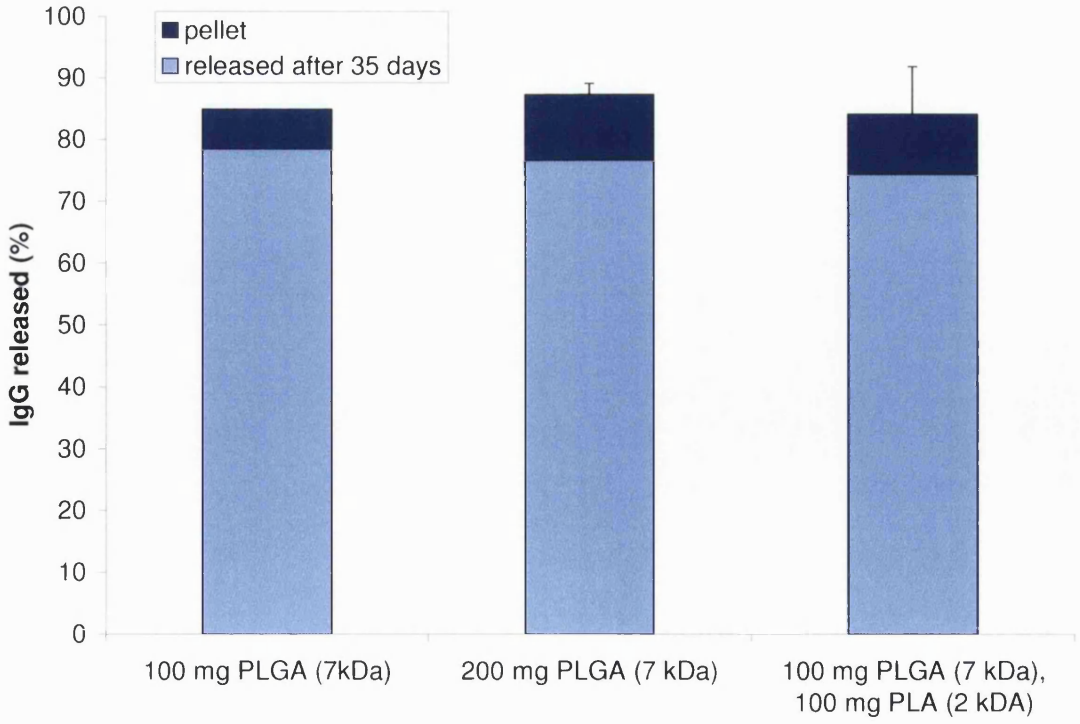

Figure 5.8 Total IgG released in pH 2.5 release media from microparticulate formulations containing poly(lactide-co-glycolide) (PLGA) and poly(lactic acid) (PLA). Cumulative IgG release after 35 days in pH 2.5 0.1 M glycine + 0.01% v/v Tween 20 and subsequent analysis of the remaining pellet, following dissolution in 0.5 M NaOH (n=3, ± SD except 100 mg PLGA, where n=1).

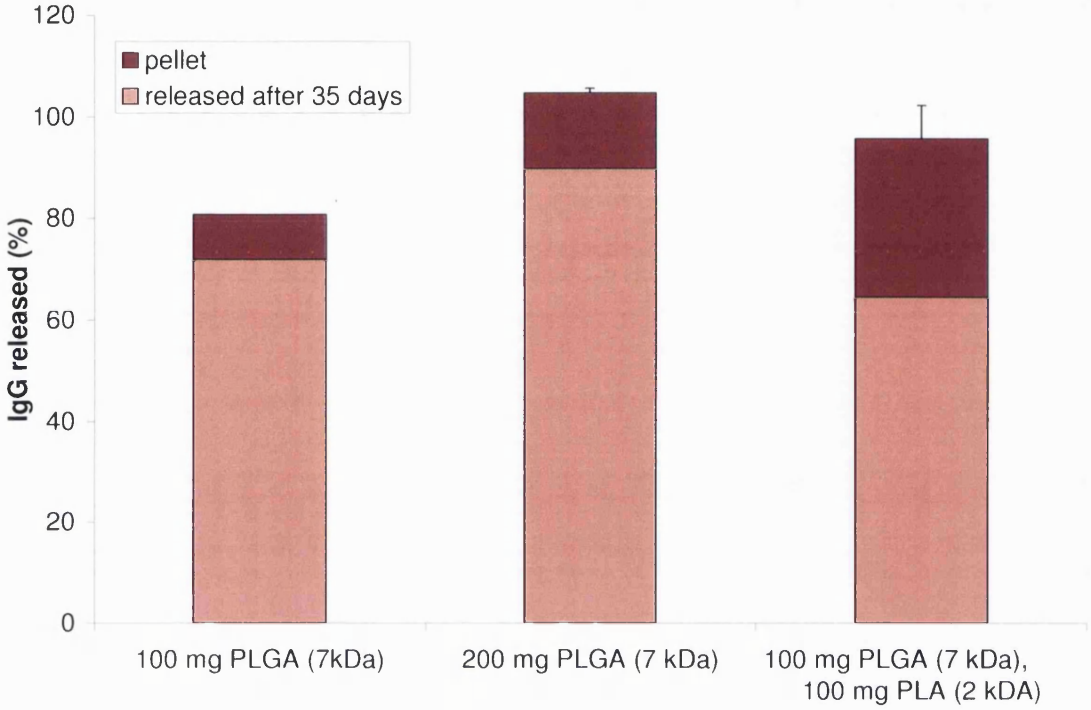

Figure 5.9 is a photograph of a non-reducing SDS-PAGE gel of protein released from the formulations containing the various polymers. For the formulation containing only 100 mg of polymer, there was a faint additional band of higher molecular weight as well as the IgG monomer band.

Figure 5.9 Gel electrophoresis of protein from the 2 h burst-release samples of formulations containing various poly(lactide-co-glycolide) (PLGA) and poly(lactic acid) (PLA) polymers.
1: standard IgG, 2: blank formulation, 3: 100 mg PLGA, 4+5: 200 mg PLGA,
6+7: 100 mg PLGA + 100 mg PLA.

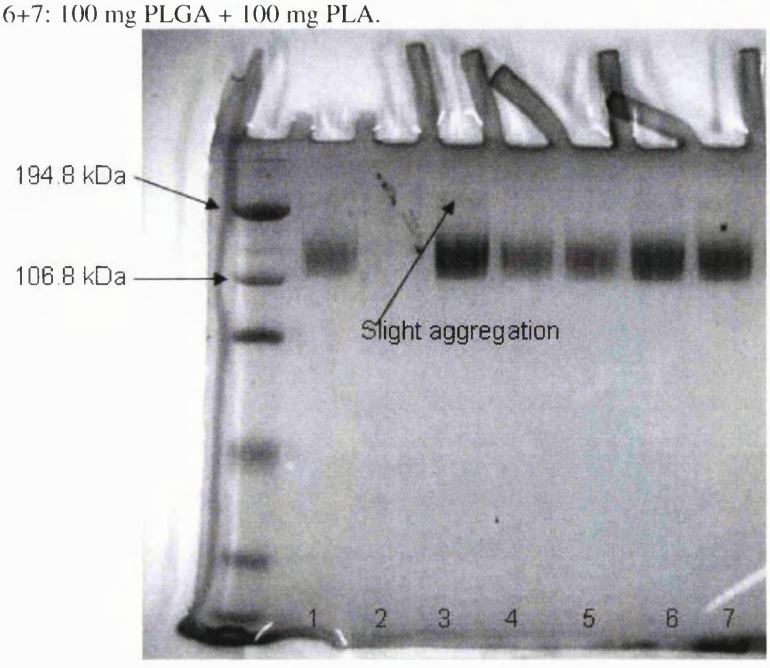

Tables 5.1 a) and b) summarise the FFF data obtained from the RI and UV detectors, respectively. Mass recovery was lower and less consistent for the standards than for the samples. The molecular weight of the detected IgG monomer was consistent between samples. However, the two detection methods led to a difference in calculated molecular weight. The fraction of detected protein that was in its monomeric form was lowest for the formulation containing 100 mg of PLGA only. Interestingly, for the other formulations, the formulated antibody had a higher monomer fraction than the unformulated antibody (standard). Figures 5.10 and 5.11 illustrate the data for the 7 kDa PLGA formulations and for the standard. They both demonstrate the reproducibility of the IgG molecular weight, and the greater presence of a dimer peak for the standard, compared to the formulated IgG.

Table 5.1 Field-flow fractionation analysis of IgG in 2 h burst-release samples from particulate formulations containing poly(lactide-co-glycolide) (PLGA) and poly(lactic acid) (PLA). Data from a) refractive index, and b) UV detectors (n=3, mean ± SD, except 100 mg PLGA, where n=1).

a) RI detector	**% Recovery**	**Monomer MW (kDa)**	**% Monomer**
Standard	66 ± 28	138 ± 3	96 ± 3
100 mg PLGA	87	140	94
200 mg PLGA	83 ± 7	138 ± 3	99 ± 1
PLGA/PLA	84 ± 6	141 ± 4	100 ± 1

b) UV detector	**% Recovery**	**Monomer MW (kDa)**	**% Monomer**
Standard	55 ± 22	164 ± 2	92 ± 2
100 mg PLGA	74	163	94
200 mg PLGA	71 ± 7	162 ± 5	98 ± 1
PLGA/PLA	77 ± 1	162 ± 3	100 ± 1

Figure 5.10 Molecular weight of IgG detected by field-flow fractionation vs. channel retention time. The scatter plots compare the molecular weight of an unformulated IgG standard (n=1) with IgG released from microparticulate, poly(lactide-co-glycolide) (PLGA) formulations (n=3). They share the same monomeric molecular weight (~160 g/mol), although unformulated IgG appeared to have a more defined dimeric (~320 g/mol) population. In the background the corresponding UV absorbance peaks are shown.

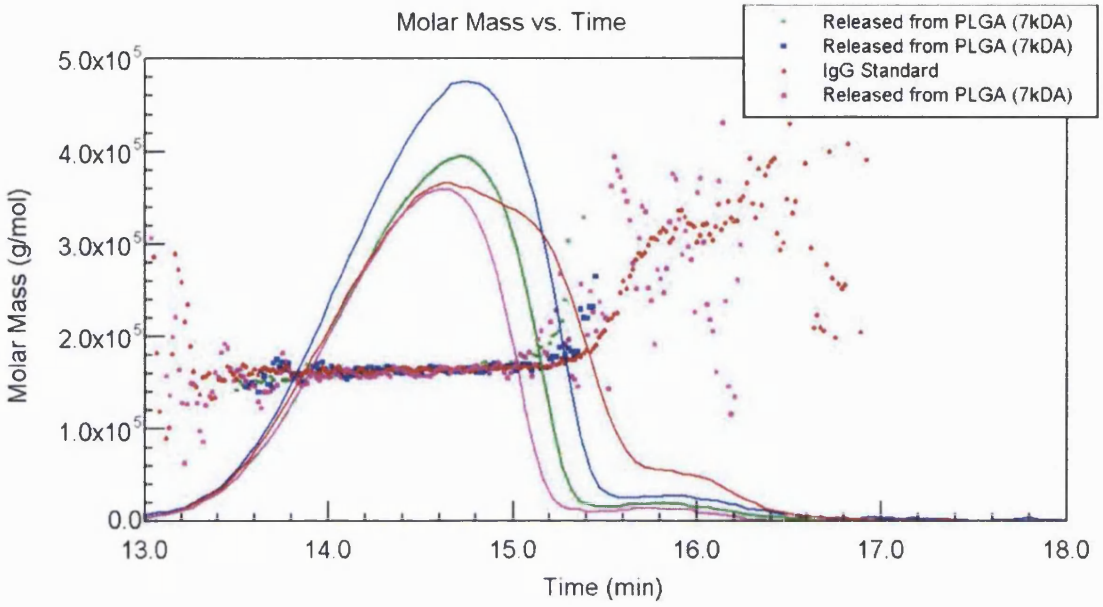

Figure 5.11 Illustration of monomer fraction of IgG detected by UV field-flow fractionation. This is another representation of the data in Figure 5.10, comparing the detected molecular weight of IgG released from microparticulate formulations (n=3) with an unformulated IgG standard. All samples share similar monomeric weight, which accounts for a larger fraction of the formulated IgG detected.

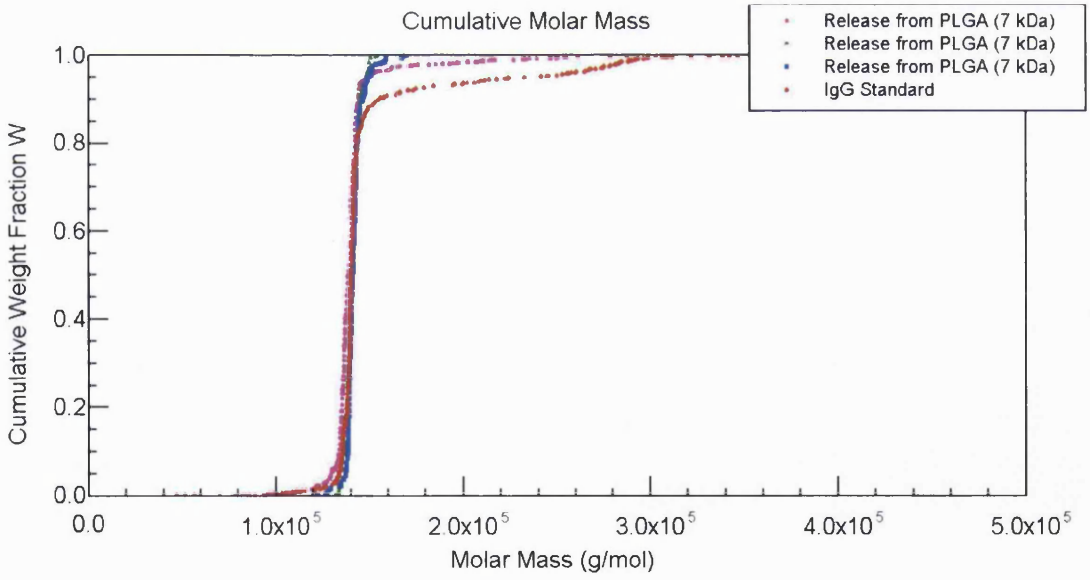

Figure 5.12 represents the results of the ELISA assay. Active IgG was detected within acceptable ranges for all samples.

Figure 5.12 Enzyme-linked immunosorbent assay (ELISA) of IgG released from microparticulate formulations containing various poly(lactide-co-glycolide) (PLGA) and poly(lactic acid) (PLA) polymers. The concentration of IgG determined by ELISA was expressed as a percentage of the total protein concentration measured by the Bradford assay. (n=3, mean + SD, except PLGA 100 mg, where n=1).

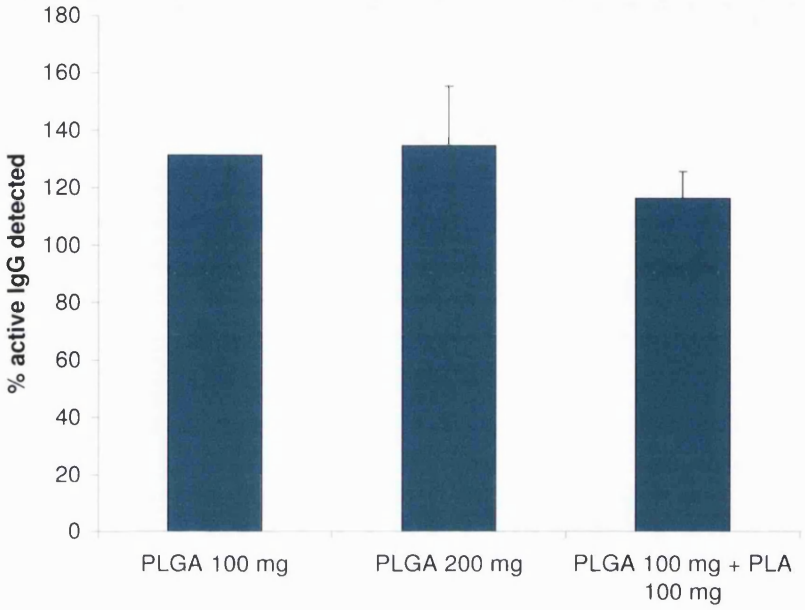

5.4.3 Discussion

As explained above, this experiment aimed to determine whether exchanging a 7 kDa polymer for a 2 kDa polymer would increase the antibody release rate as a result of faster degradation. As well as answering this question, a number of other interesting observations were made.

Firstly, it was surprising to find that DPPC would only dissolve in DCM in the presence of the PLGA, and not with PLA or with no polymer present. Even if an interaction between the dissolved polymer and DPPC was required for the DPPC to dissolve, and given that PLGA and PLA are both polymers (with similar functional groups), this was an unexpected finding. With DPPC not in solution, a stable primary emulsion could not be formed, and thus the experiment proceeded using a minimum of 100 mg PLGA to dissolve the DPPC. Given the results described here, this phenomenon was explored further. It was found that increasing the temperature of the mixture caused the DPPC to dissolve. However, when conducting the homogenisation on ice, the DPPC would 'crash out' unless the required quantity of polymer was present. The manufacturing process of the polymers was then considered, with the hypothesis that perhaps a catalyst or impurity could be contaminating the PLGA, which happened to aid dissolution of the DPPC. The most obvious impurity would be unreacted starting reagents from the polymerisation reaction – i.e. acidic monomers. Therefore, the pH of the primary emulsions were measured, and indeed it was found that for 7 kDa PLGA-containing emulsions, the pH was acidic (approximately pH 3), whereas for all others it was

neutral. This suggested that DPPC required an acid environment to be soluble in DCM. Indeed, the addition of acetic acid to the polymer-DPPC-DCM mixture caused the DPPC to go into solution. This finding was applied to future experiments involving other polymers.

Secondly, this work used an alternative buffer system to characterise the antibody release profile. For all polymer systems, in pH 7.4 media, following a large, two-phase, burst-release, little further release was observed, whereas in pH 2.5 media, antibody release was continuous, and close to zero-order (Kaye *et al.*, 2006c). In pH 7.4, the two phases of burst-release at 2 h and day 6 could have been related to surface antibody release, and release by diffusion, respectively (Tamber *et al.*, 2005). As explained above (Section 5.2), previous authors (Jiang *et al.*, 2002) have suggested that the improvement in release experienced using a lower pH buffer could be due to improved protein stability, enhancement of polymer degradation, and/or reduced protein re-adsorption to the microparticle. In this case, the former of these points may have not been true, as here IgG was used rather than the lysozyme in the aforementioned publication. Antibodies are usually formulated at pH 5 for stability reasons. Indeed deamidation and aggregation of antibodies has been reported to be less at pH 4 than at pH 7 (Zheng and Janis, 2006). Nevertheless, at pH 2.5 the antibody would have carried a greater net positive charge, which may have contributed to its stability, and the prevention of hydrophobic bonding. On the other hand, at this pH the carboxyl groups on polymer molecules were unlikely to have been charged, reducing the possibility for an electrostatic interaction between the polymer and the antibody. The next section addresses which of these two factors was most critical during the use of end-capped polymers. Importantly, Jiang *et al.*, (2002) considered the profile obtained with this buffer to correlate more closely with *in vivo* release. The authors studied release following subcutaneous injection, which could be considered a similar deposition site to the lungs, in terms of having a small liquid volume for dissolution.

Thirdly, FFF was used to detect IgG released from formulations, with the aim of determining molecular weight and the degree of aggregation. As other authors have found (e.g. Pollit, 2006; Gabrielson *et al.*, 2007), mass recovery was incomplete and inconsistent, compared to other separation and analysis techniques. This limited the use of FFF as a quantification tool. The even higher variability of the standards may have been due to one of the three repeats being the first sample to be analysed of the set. It appeared that the first sample to be analysed, after preparing the machine, gave a particularly low recovery, as if it were coating the channel surface, allowing subsequent runs to pass through. Although the RI and UV detection methods gave different

molecular weight readings for the monomer, both values were close to the approximate IgG molecular weight of 150 kDa. The discrepancy may have been due to inaccuracies in the respective calibration constants. As expected from the SDS-PAGE gel, where there appeared to be some aggregation for the formulation containing only 100 mg polymer, the monomer content of this sample was lower than for other formulations. However, the monomer content was still >90%, and dimers were the only detected aggregate. The obvious explanation for this was that the polymer stabilised the antibody during the formulation process, and thus a lack of polymer resulted in antibody instability. However, this result could be due to there having been less polymer for any aggregates to re-adsorb onto, prior to collecting the sample. One interesting observation was that antibody released from formulations containing 200 mg polymer, had a higher monomer content than the unformulated antibody (Kaye *et al.*, 2006c). Again, it could be claimed that the formulation excipients appeared to stabilise the protein from aggregation. However, another explanation was that dimers may have preferentially bound or have been re-adsorbed onto the microparticle surface, and thus were not free to be collected and analysed in the 2 h release sample. Due to the FFF technique not having 100% recovery, it would be difficult to determine which, if any, of these two theories was the correct one.

Finally, as to the effect on release of incorporating PLA, it would appear that the higher crystallinity of PLA (Witschi and Doelker, 1998b; Spiers *et al.*, 2000) more than compensated for its lower molecular weight, since release (in pH 2.5 buffer) from PLA formulations was slower than PLGA. However, this difference may not have been solely due to slower polymer degradation. Perhaps IgG diffused less easily from PLA, or it formed a less porous structure than PLGA. Although, as expected, the pH 7.4 2 h burst-release from the 100 mg polymer formulation was higher, presumably due to a reduced encapsulation capacity, the overall release profile in pH 2.5 was slower than 200 mg PLGA. This was an unexpected result. One possible explanation is that because for the release-study a formulation mass:volume ratio was used, a formulation with only 100 mg polymer would have generated less of an acidic microclimate.

5.4.4 Conclusion

The use of a lower molecular weight PLA did not appear to increase the rate of antibody release from the microparticulate formulation. Although polymer degradation rate was known to increase with reducing molecular weight, the molecular weight difference here appeared to be more than compensated for by the increased crystallinity of PLA over PLGA. However, all formulations released stable IgG after 2 h, and up to 90% IgG release was achieved using pH 2.5 release media.

5.5 Use of PLGAs with capped end-groups

5.5.1 Method

Formulations of IgG were produced using the optimised emulsification-spray-drying method described previously. Triplicate batches were prepared using 200 mg of one of three types of PLGA (all supplied by Lakeshore Biomaterials, USA):

1. The uncapped (carboxyl-end-group), 7 kDa PLGA previously used.
2. A methyl-capped, 7 kDa PLGA.
3. A lauryl-capped, 7 kDa PLGA.

For the capped polymers, 150 μL of acetic acid was added to the DCM in order to dissolve the DPPC. Although smaller volumes of acetic acid were able to get the DPPC into solution, 150 μL was the minimum volume required for the DPPC to remain dissolved during emulsification on ice. Microparticle physical properties were analysed by laser diffraction and SEM (Section 2.4.1-2.4.2). The lauryl-capped formulation did not disperse in cyclohexane, and so methanol was used. Antibody EE was determined, and the stability of the released antibody was analysed using SDS-PAGE, ELISA and FFF (all methods described in Sections 2.5.1, 2.5.2 and 2.5.3, respectively). As well as measuring the stability of IgG released during the first 2 h, attempts were made to analyse the antibody released after this time, up until day 7. In order to achieve this, formulations were incubated in various release media, including PBS + 0.01% v/v Tween 20, pH 2.5 0.01 M glycine + 0.01% v/v Tween 20 and 5% sucrose solution. A full IgG release profile was measured in the former two buffer systems as described in Section 5.4.1. The *in vitro* cellular toxicity of the uncapped and methyl-capped formulations was investigated using the MTT assay (see Section 2.6.1).

5.5.2 Results

5.5.2.a) Antibody encapsulation and release

The use of capped polymers did not alter the product yield, or particle morphology. For these polymers, stable primary emulsions were only formed in the presence of acetic acid. There were subtle differences in the particle diameters (summary of diameters given in Table 5.2). Figure 5.13 indicates that EE was decreased by approximately 10% when the methyl-capped polymer was used.

Table 5.2 Geometric volume derived diameters of microparticulate formulations produced using various uncapped and capped poly(lactide-co-glycolide) polymers. Samples were dispersed in organic solvent (cyclohexane and methanol) and also measured after 2 h incubation in water + 0.02% v/v Tween 20 (n=3, mean ± SD).

	D10% (μm)	D50% (μm)	D90% (μm)	Span
Uncapped (cyclohexane)	2.5 ± 0.1	4.0 ± 0.1	6.3 ± 0.3	0.9 ± 0.0
Methyl-capped (cyclohexane)	2.0 ± 0.1	4.4 ± 0.1	9.2 ± 0.6	1.6 ± 0.1
Lauryl-capped (methanol)	1.8 ± 0.0	3.7 ± 0.2	7.0 ± 0.2	1.4 ± 0.1
Uncapped (water)	0.16 ± 0.02	0.38 ± 0.01	1.2 ± 0.1	2.7 ± 0.2
Methyl-capped (water)	0.15 ± 0.05	0.35 ± 0.08	0.81 ± 0.11	1.9 ± 0.3
Lauryl-capped (water)	0.20 ± 0.02	0.55 ± 0.07	1.3 ± 0.2	2.1 ± 0.1

Figure 5.13 Encapsulation efficiency of IgG in microparticulate formulations produced using uncapped and capped poly(lactide-co-glycolide) (PLGA) (n=3, mean + SD)

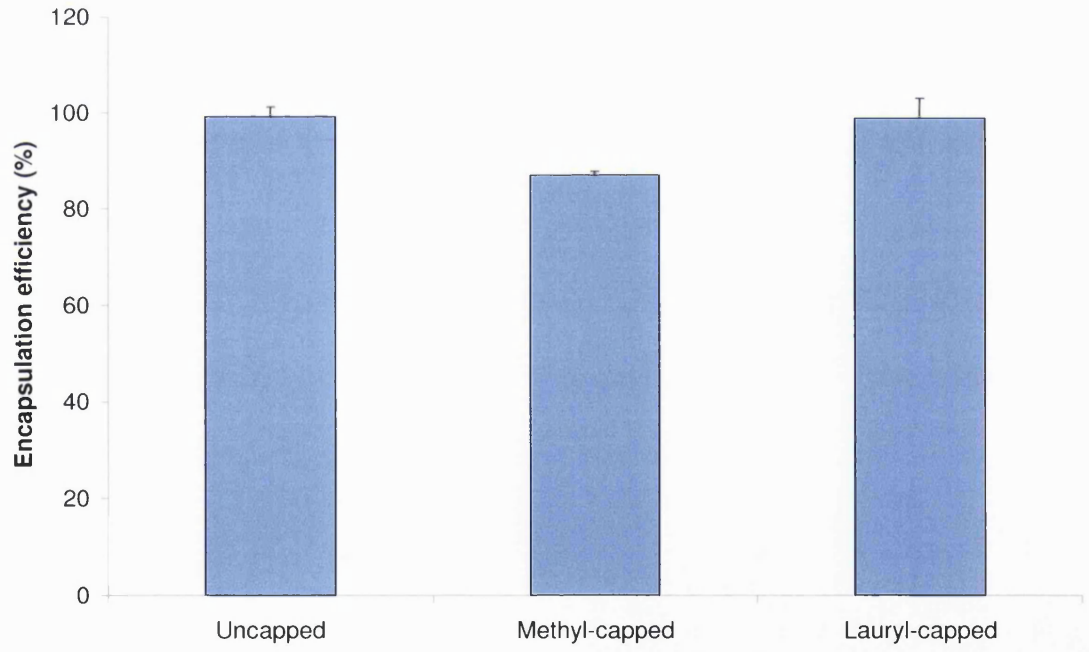

The IgG release profile in the pH 7.4 buffer is given in Figure 5.14. The use of capped polymers did not alter the release profile, other than reducing the initial burst-release by 10-15%, and thus the total cumulative IgG release.

Figure 5.14 Cumulative IgG release from microparticulate formulations composed of various capped and uncapped poly(lactide-co-glycolide) polymers in pH 7.4 PBS + 0.01% v/v Tween 20 (n=3, mean ± SD)

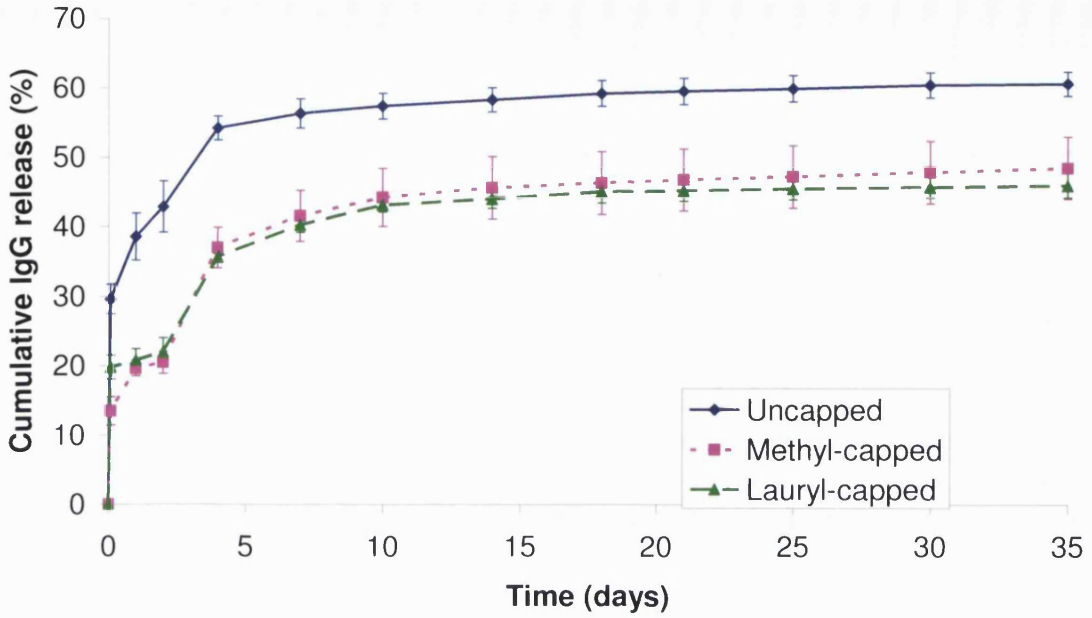

Figure 5.15 illustrates the IgG release profile in the pH 2.5 buffer system. The uncapped PLGA formulation gave a continuous release pattern similar to that observed in the previous experiment. The methyl-capped polymer provided a similar profile, with higher initial burst-release, and then a decreased rate of release. Antibody release from the lauryl-capped PLGA formulation terminated very quickly. The pellets of this formulation hardened and then disintegrated over the first 10 days, such that the protein could not be recovered at the end of the experiment.

Figure 5.15 Cumulative IgG release from microparticulate formulations composed of various poly(lactide-co-glycolide) polymers in pH 2.5 0.01 M glycine + 0.01% v/v Tween 20 (n=3, mean ± SD).

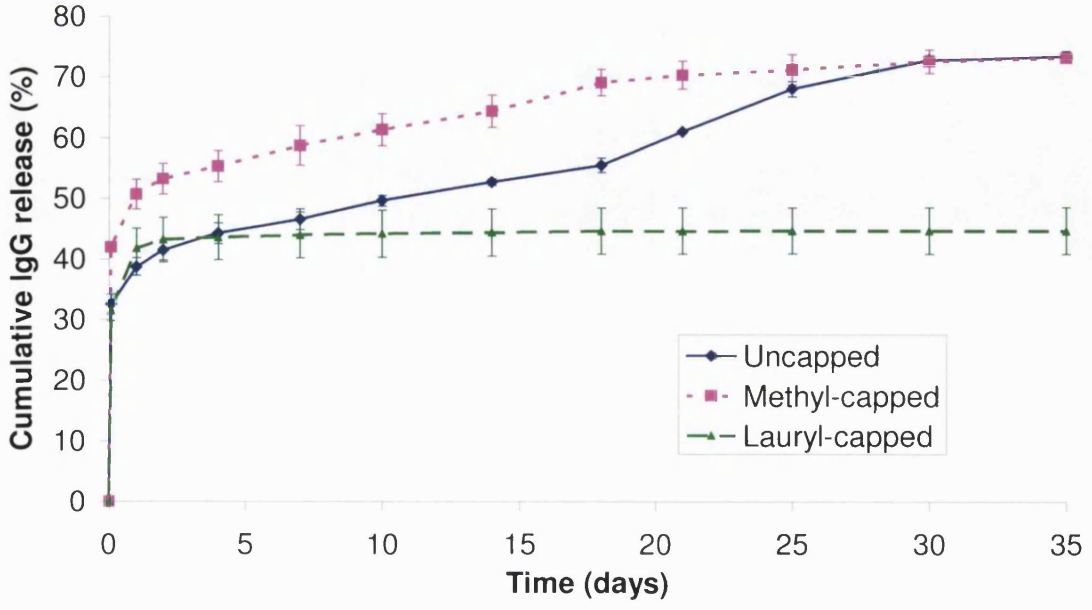

5.5.2.b) Antibody stability

Figure 5.14 is a comparison of SDS-PAGE gels analysing the protein released from the formulations. Released antibody was measured in both pH 7.4 and pH 2.5 release media, after 2 h and after 7 days. The 2 h release samples in pH 7.4 (Figure 5.16a) appeared similar to that previously observed, with a single IgG band of approximately 150 kDa, regardless of the formulation type. However, for the release samples collected after 7 days (Figure 5.16b), the monomeric IgG band was mostly absent, and there were two faint bands that may have represented the composite light and heavy chains of the antibody. Analysing the samples in pH 2.5 glycine buffer (Figure 5.16c and d) altered the appearance of the IgG band, and its molecular weight, relative to the marker. However, the samples collected after 7 days in this media appeared the same as after 2 h. There appeared to be aggregate (most likely dimer) bands on all of the 2 h samples, with the capped PLGA formulations giving band of the greatest intensity.

Figure 5.16 Gel electrophoresis of IgG released from microparticulate formulations of uncapped and capped poly(lactide-co-glycolide) (PLGA). a) released in pH 7.4 PBS after 2 h, b) released in pH 7.4 PBS after 7 days, c) released in pH 2.5 glycine buffer after 2 h and d) released in pH 2.5 glycine buffer after 7 days. Key: 1: molecular weight marker (i=194.8 kDa, ii=106.8 kDa), 2: unformulated IgG standard, 3: blank formulation, 4+5: uncapped PLGA formulation, 6+7: methyl-capped formulation, 8+9: lauryl-capped formulation.

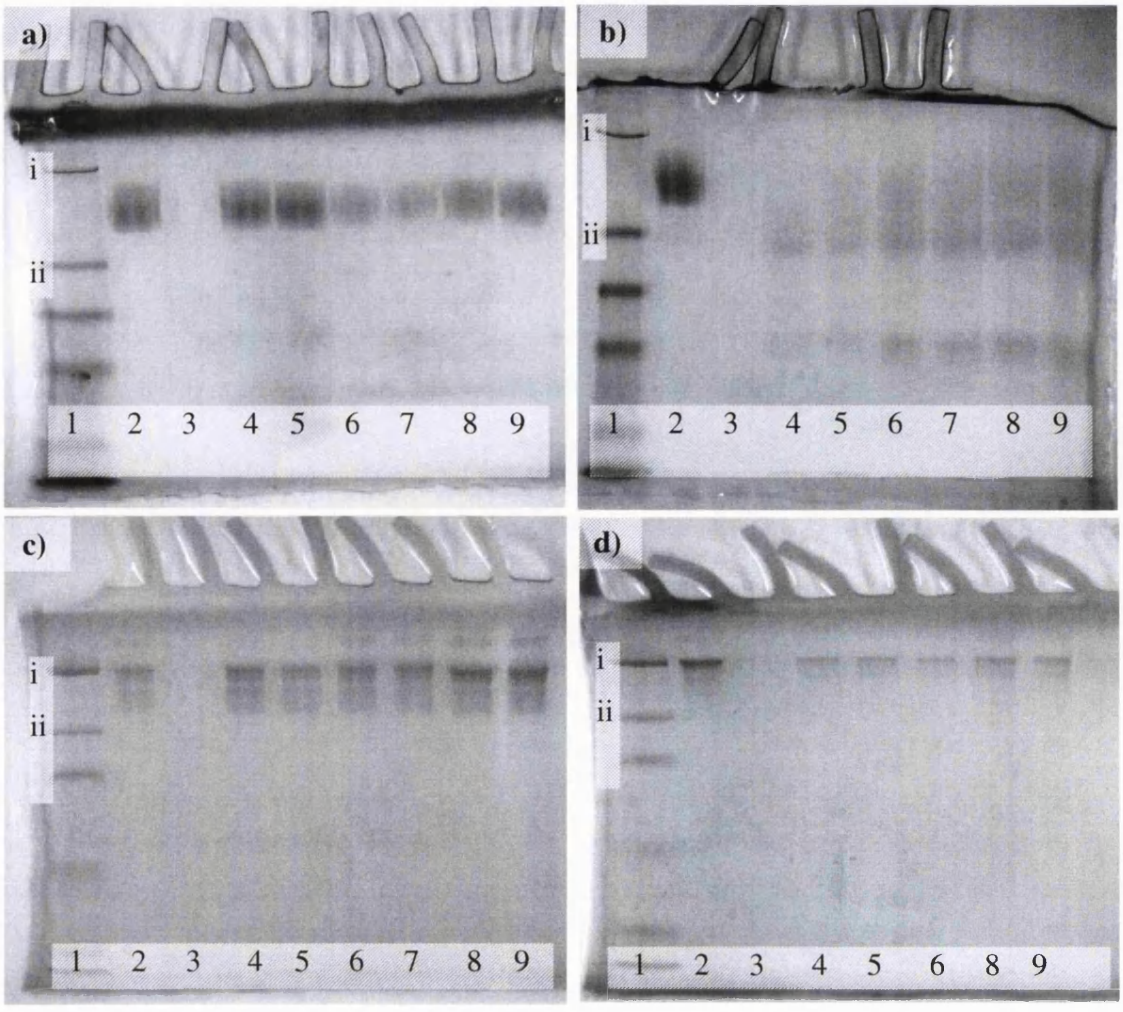

SDS-PAGE was also performed on samples that had been incubated in 5% w/v sucrose solution for 2 h (Figure 5.17). Interestingly, in this release media, the capped formulations gave a much higher initial burst-release (~60%) than the uncapped formulation, whereas in PBS, using capped PLGA had resulted in a lower immediate burst-release. However, it can be seen from the gel electrophoresis that the extra released protein appeared to be aggregated.

Figure 5.17 Gel electrophoresis of IgG released from microparticulate formulations containing uncapped and capped poly(lactide-co-glycolide) (PLGA) in pH 7.4 PBS after 2 h. Key: 1: molecular weight marker (i=194.8 kDa, ii=106.8 kDa), 2: unformulated IgG standard, 3: blank formulation, 4+5: uncapped PLGA formulation, 6+7: methyl-capped formulation, 8+9: lauryl-capped formulation.

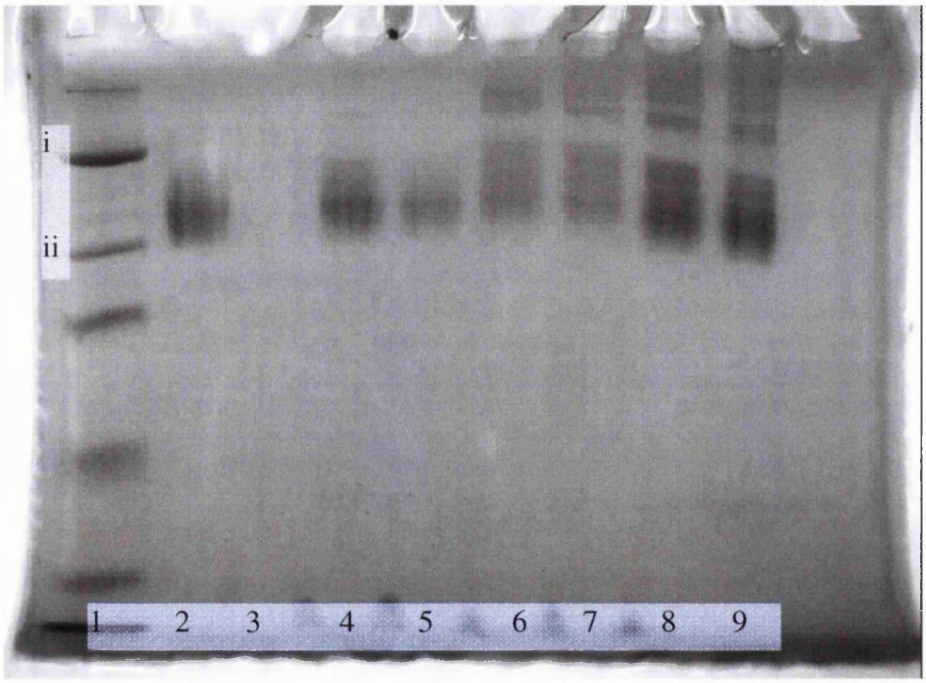

ELISA was conducted on the 2 h and on the 7 day samples released in both pH 7.4 PBS + 0.01% v/v Tween 20 and pH 2.5 0.01 M glycine + 0.01 % v/v Tween 20 media. The results are compared in Figure 5.16. In both buffers there was a decrease in the proportion of the antibody detected after 7 days.

Figure 5.18 Activity of IgG released from microparticulate formulations, composed of various uncapped and capped types of poly(lactide-co-glyolide) (PLGA), in pH 7.4 PBS and pH 2.5 0.01 M glycine release media, as measured by enzyme-linked immunosorbent assay (ELISA). The concentration of IgG determined by ELISA was expressed as a percentage of the total protein concentration measured by the Bradford assay (n=3, mean + SD).

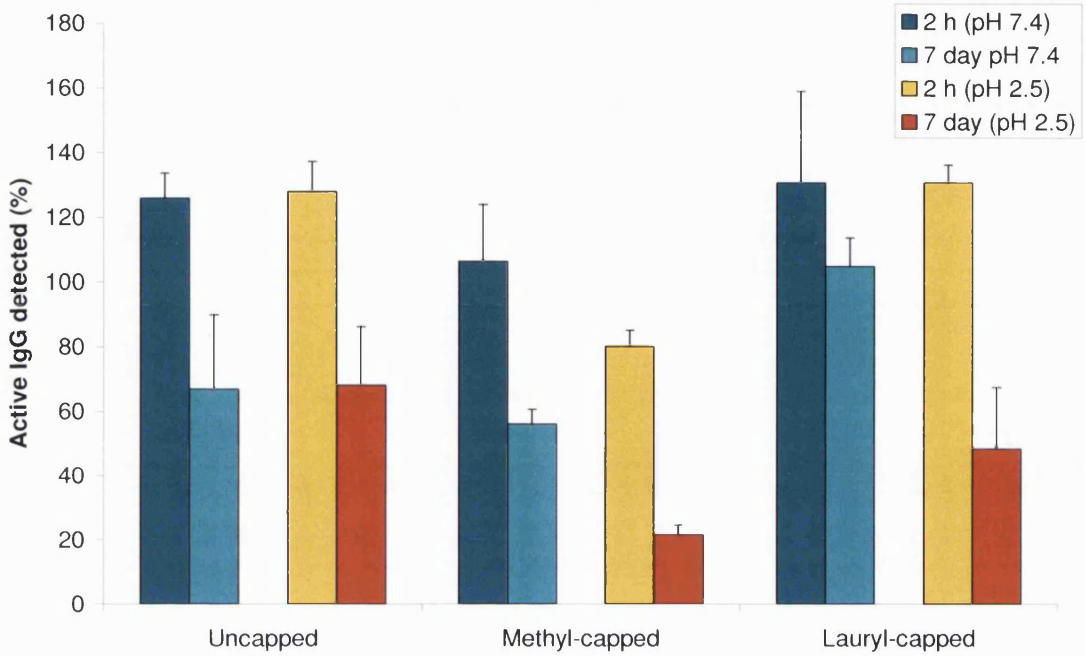

Table 5.3 summarises the data obtained from FFF. The samples analysed were 2 h release samples in pH 7.4 PBS.

Table 5.3 Field-flow fractionation analysis of IgG in 2 h burst-release samples from microparticulate formulations containing capped and uncapped poly(lactide-co-glycolide) polymers. Data from a) refractive index detector, and b) UV detector (n=3, mean ± SD).

a) RI detector	% Recovery	Monomer MW (kDa)	% Monomer
Standard	87 ± 2	144 ± 2	93 ± 1
Uncapped	73 ± 15	140 ± 5	100 ± 0
Methyl-capped	80 ± 11	140 ± 3	100 ± 1
Lauryl-capped	55 ± 18	137 ± 7	99 ± 2

b) UV detector	% Recovery	Monomer MW (kDa)	% Monomer
Standard	77 ± 1	164 ± 3	90 ± 0
Uncapped	63 ± 10	160 ± 3	99 ± 1
Methyl-capped	72 ± 14	160 ± 1	100 ± 1
Lauryl-capped	52 ± 17	157 ± 5	98 ± 3

5.5.2.c) In vitro cell toxicity

Figure 5.19 illustrates the results of the MTT assay, comparing the effect of the formulations on cell viability, and inclusion of positive and negative controls.

Figure 5.19 MTT assay to assess the impact of various concentrations of poly(lactide-co-glycolide) microparticulate formulations on the *in vitro* viability of CHO-K1 epithelial cells, relative to controls (n=3, mean + SD, *=negative control, **=positive control)

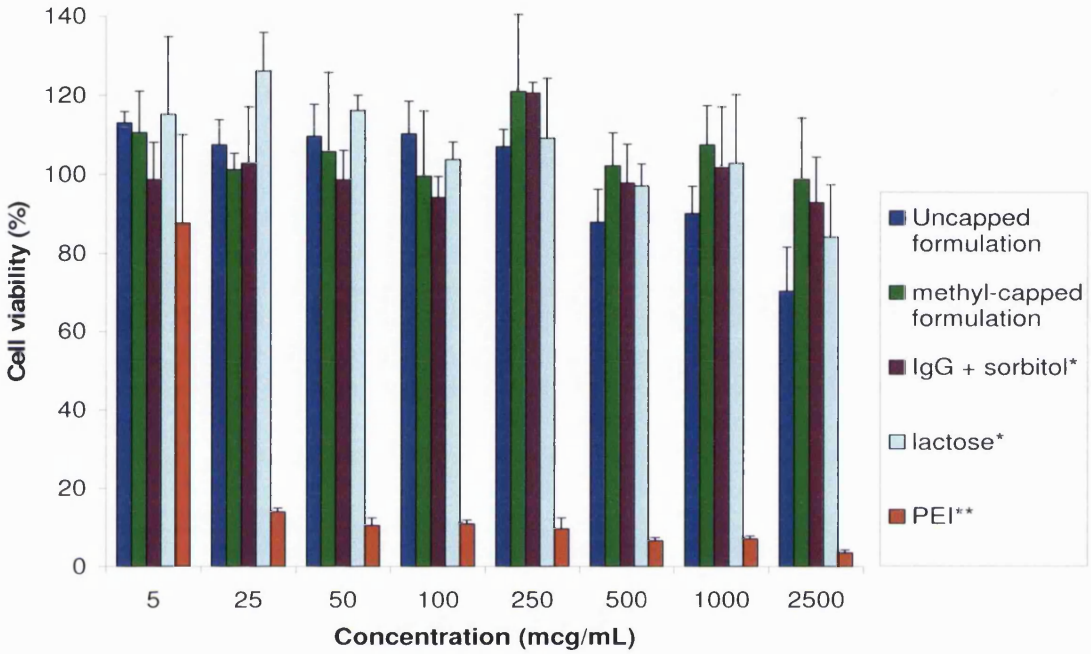

5.5.3 Discussion

5.5.3.a) Antibody encapsulation and release, and particle diameter

The reduced EE of the methyl-capped formulation, relative to the other formulations, was consistently detected in two previous sets of manufactured batches (used to develop the analysis techniques), as well as the in the data set presented here. There was no obvious reason for this. In Chapter 4, low EE was often associated with a high initial burst-release, since both were considered to be due to low emulsion stability and antibody passing into the external aqueous phase. However, here the methyl-capped formulation had a lower initial burst-release than the uncapped formulation. Nevertheless, immediate burst-release in this case may have been reduced due to an enhanced surface interaction with the capped polymer, rather than being related to the amount of antibody located on the particle surface.

The differences in particle diameters that were observed between the various formulations were likely to have been related to the formulation dispersion, as opposed to differences in the geometric diameter distribution of the particles. SEM images did

not reveal any broad changes in particle size distribution with the use of the capped polymers. When sizing with laser diffraction, the various formulations had different dispersion properties in cyclohexane + 1% v/v Span 80, and the lauryl-capped formulation formed large aggregates in this medium. Therefore, for this formulation, methanol was employed as the dispersion medium, since in this solvent the lauryl-capped formulation was found to disperse well, despite not being effective for the uncapped formulation. Interestingly, the methyl-capped formulation dispersed equally well in both dispersion media. Equally, it cannot be assumed that all formulations dispersed with equal efficiency in the water + 0.02 % v/v Tween 20. Small differences in the dispersion efficiency of the system could have resulted in a subtle change in the volume diameter distribution. The particles of least diameter, which because of their high surface area require most energy to disperse, may have remained as agglomerates of multiple particles. If these aggregates were composed of 5 or 10 of the smallest particles, this would not result in a separate aggregate peak, but rather a subtle shift in the particle diameter distribution, or a change in the span. This type of agglomeration was explored further in the dry-state as described in Chapter 6.

The rationale for attempting to incorporate capped PLGAs into the formulation was to improve the rate and completion of antibody release, by reducing the possibility of a charge interaction between amine groups on the antibody protein, and free carboxyl groups on the polymer chains. Unfortunately, the release profile was not improved with the use of capped polymers. In pH 7.4 release media, the same flat profile was observed for all polymers, the only difference being the magnitude of the initial burst-release. It was unknown why the two-phases of burst-release observed in the previous experiment, were less separated, particularly for the uncapped formulation. For the capped polymers the initial burst-release was reduced, suggesting that the antibody was associated to the polymer *via* a hydrophobic interaction, which would of course be increased using capped polymers, as these contain more hydrophobic end-groups than the uncapped PLGA. In pH 2.5 media, the uncapped polymer charge would have been suppressed, and the antibody charge increased. The uncapped polymer formulation gave the most complete release in this media, presumably due to its lower hydrophobicity, given that none of the polymers were likely to be ionised at this pH, thus preventing a charge-based interaction. The IgG released from the uncapped PLGA formulation was not as complete as that observed in the previous Section (Figure 5.6). This may have been due to the 10-fold reduction in the glycine buffer molarity in this experiment. A pH 2.5, 0.01 M glycine buffer was used, since it was hypothesised that reducing the ionic strength of the media would further enhance the charge-induced

stability of the antibody molecules. However, if anything, this change appeared to be detrimental to the antibody stability, perhaps because the consequential reduction in media viscosity caused the antibody to be more liable to shear stress during incubation in apparatus used to shake the sample.

5.5.3.b) Antibody stability

The use of capped polymers did not appear to affect the stability of the antibody released from the formulations, into pH 7.4 release media, after 2 h. In fact, as observed in the previous Section, FFF data indicated that there was a greater proportion of monomeric antibody in the formulated samples, compared to the unformulated control. After a further 7 days of incubation, very little of the released antibody appeared to remain intact, according to SDS-PAGE data. There were no clearly defined bands, but some lower molecular weight staining suggested the presence of fragmented antibody heavy and light chains. However, the ELISA detection was reduced, and the positive result obtained conferred that some of the binding site population remained in its active conformation.

The aim of the 7 day experiment was to determine if antibody encapsulated within the polymer matrix (in addition to antibody located on the particle surface) remained stable during the formulation process. However, the above negative result could have been due to the antibody deteriorating during incubation in the particle-containing release media (Schwendeman, 2002). In order to test this hypothesis, the same experiments were performed in pH 2.5 buffer, where it was believed the antibody was more stable due its greater net charge. Indeed, the results from SDS-PAGE of these samples gave single bands of the same molecular weight as the unformulated control, although the absolute molecular weight, relative to the marker, was not correct, possibly due to the low pH buffer affecting the running of the samples in the gel. However, the ELISA results were less convincing. Detection of standards was also lower when the samples were prepared in this buffer, suggesting that the antibody carried a charge or adopted a conformation in this buffer that reduced binding in the assay. However, such a change would have to be a non-reversible one, given that the standards and samples were diluted at least 10,000-fold in pH 7.4 PBS before analysis.

A further gel was examined by SDS-PAGE to analyse formulations incubated in 5% w/v sucrose solution for 2 h. Sucrose solutions of this concentration have been employed to produce stable liquid formulations of pharmaceutical proteins, such as antibodies (Wang, 1999). Interestingly, this experiment highlighted differences

between the capped and uncapped polymers. The initial burst-release of the capped polymer formulations was much higher, although on the gel, the extra protein appeared to be of higher molecular weight than monomeric IgG. Given the other SDS-PAGE results, there was no obvious explanation for this. It is possible that the presence of sucrose favoured dissolution of these aggregates that would otherwise have remained adsorbed to the particle surface. This would suggest that the capped-polymer formulations did contain aggregated antibody. The sucrose does not seem likely to have caused the aggregation, since this would not explain why the immediate burst-release was increased, with the usual quantity of monomeric antibody still being released, and why only the capped formulations were affected. However, the 7 day release data in pH 2.5 revealed no such evidence of aggregations, for any of the formulations, although there was some evidence of an aggregate band for the capped formulations in pH 2.5 after 2 h. Therefore, the combined data would suggest that while there was no evidence for antibody aggregation within the uncapped PLGA formulation, some aggregation may have occurred when capped PLGA polymers were used.

5.5.3.c) In vitro cell toxicity

The aim of the MTT assay was to identify if the uncapped and methyl-capped formulations inhibited the growth of an epithelial cell line, as a method of predicting if the formulations would be toxic to humans. The growth of the cells in the presence of various concentrations of formulation, relative to untreated cells, was compared with a number of positive and negative controls. The assay method used here was employed to reduce, as much as possible, external sources of variable cell trauma (such as media removal). The data would suggest that the formulation components, and the formulations as a whole, were largely non-toxic to cell growth at all concentrations tested. The small decrease in cell viability that occurred with the uncapped formulation at higher concentrations was probably due to a physical inhibition of cell growth. A light microscope revealed that much of the plate surface of this sample was occupied by microparticles, thus physically restricting the surface area available for cell growth. The small reduction in viability caused by this cannot really be considered as evidence for cytotoxicity of the formulation.

5.5.4 Conclusion

The regular uncapped PLGA was substituted for PLGAs with capped end-groups to prevent potential interactions between the antibody amine groups and carboxyl groups on the polymer. The use of capped PLGA in the formulation of IgG did not increase the

cumulative antibody release, or the release rate, suggesting that if any interactions were occurring between the antibody and the polymer, they were likely to be hydrophobic, rather than electrostatic. The incorporation of capped polymers may also have had an impact on particle dispersibility and antibody stability. Nevertheless, this work demonstrated that given the optimal choice of release media, antibody released from formulations over 7 days, was likely to have been active. There was also evidence to suggest that epithelial cell lines could tolerate the presence of the formulations in relatively large quantities.

5.6 General conclusion

The work described in this Chapter further explored the release properties of the formulation developed in previous chapters. It also examined potential ways of modifying the release properties by use of alternative polymers and excipients. However, the *in vitro* modelling of controlled protein release from a microparticulate system did not prove to be straight forward. Thus, it was difficult to predict how the findings presented here would have translated to *in vivo* pulmonary delivery. From the data obtained, it appeared that the 7 kDa, uncapped PLGA, used in previous chapters would most likely confer the required antibody release properties. The results of the work described in this Chapter further helped to establish that the antibody remained active within the formulation, although again, because of the incubation period required to release all of the antibody, there were complications and unanswered questions regarding this aspect.

6 AEROSOLISATION CHARACTERISATION OF THE PULMONARY ANTIBODY FORMULATION

6.1 Abstract

Various techniques were employed to assess the aerosolisation characteristics of the IgG lead formulation described in the previous chapters. Leucine (0.9% m/m) and/or magnesium stearate (1% m/m) were also added to the formulation, to investigate if these excipients provided any additional improvement to the aerosolisation properties of the formulation.

A 'RODOS' dry-powder feeder was used to disperse the formulations by applying various pressures. Laser diffractometry was used to measure the geometric particle size distribution of the formulation at various dispersion pressures. The degree of particle diameter reduction observed with increasing pressure was used as a measure of powder dispersibility. A larger average particle diameter at low pressures indicated poor dispersibility, since higher pressure was required for full dispersion. It was found that the addition of leucine to the formulation increased dispersibility.

Laser diffractometry was also used to measure the particle diameter distribution of the formulations when dispensed from an Aerolizer® dry-powder inhaler device. There was some evidence that magnesium stearate reduced the variation in diameter distribution from the beginning to the end of the dose.

The aerodynamic diameter and fine particle fraction of the formulations were measured using an 'Andersen' cascade impactor. Formulations were used in an Aerolizer® device. Less than 20% of the IgG dose remained in the capsule and device. The mass median aerodynamic diameter of the delivered formulation was ~4 μm. The fine particle fraction of the delivered formulation was increased by ~20%, to ~58%, with the addition of magnesium stearate and leucine. Leucine, dissolved in the external phase of the double-emulsion, was thought to reside on the surface of the spray-dried particles, reducing inter-particulate forces, and hence increasing powder dispersibility. Magnesium stearate was blended with the spray-dried powder, and may have improved powder flow.

6.2 Introduction

Having developed a formulation for IgG, where it was shown that stable antibody was released, and that the microparticulate characteristics of the formulation would suggest its suitability for pulmonary delivery (see Chapter 5), the next stage was to test its aerosolisation properties in a pulmonary delivery device. Although the experiments thus far have identified that the formulation was composed of microparticles of a geometric diameter appropriate for deposition in the respiratory tract (~1-5 μm), these techniques either involved the imaging of individual particles, or their dispersion in organic liquids. It was therefore necessary to investigate the bulk powder properties of the formulation, in order to determine whether the microparticles would disperse and flow freely in air, since this would ultimately affect how efficiently they would be delivered to the lungs.

The 'RODOS', manufactured by Sympatec, was used to apply a range of dispersion pressures to the powder, and then the diameter distribution of the resultant powder particles was measured by laser diffraction. This technique was used to screen sample vials of the formulation at a range of pressures (pressure titration), and then adapted to measure the diameter distribution of the powder when dosed from a dry-powder inhalation device at a constant airflow.

The 'Andersen' cascade impactor (ACI) was used to determine by inertial impaction the aerodynamic diameter distribution of particles. Unlike laser diffraction, which measured geometric particle diameter, this technique measured the aerodynamic diameter distribution of the particles (de Boer *et al.*, 2002). As described in Chapter 1 (see Equation 1) aerodynamic diameter is related to the density of the particles as well as to their geometric diameter and shape, and was an important characteristic for determination of the deposition site in the lung. However, the true aerodynamic diameter of the microparticles could only be measured if the powder was dispersed efficiently, involving deaggregation individual particles. Therefore, an appropriate airflow was selected to be relevant to the inspiratory forces of the human lung. Airflow was passed through the apparatus to withdraw the powder from the device, and suspend the particles. Particles were removed from the airflow according to their aerodynamic diameter, due to the 90° change in flow direction caused by the collection plates of the ACI. Smaller particles avoided impaction by being able to change direction with the airflow, at each obstacle. Larger particles had too much inertia to change direction, and so hit the collection plate (Hickey and Thompson, 1992). The ACI had a series of six collection plates, with the cut-off diameter becoming progressively smaller further

down the impactor. At the end of the experiment, the quantity of particles on each collection plate was measured. A schematic diagram of the ACI apparatus used is given in Figure 6.1. This method did not provide aerodynamic diameter measurements on a continuous scale, but rather categorised particles into size ranges according to the cut-off diameter of each stage, which was calibrated according to the airflow used (see US Pharmacopoeia 29, 2006 for calculations).

Figure 6.1 Schematic diagram of the 'Andersen' Cascade Impactor (ACI). The apparatus illustrated incorporates the preseparator, the 60 L/min conversion kit and the cut-off diameters when operated with this airflow (diameter ranges from Copley (2007)).

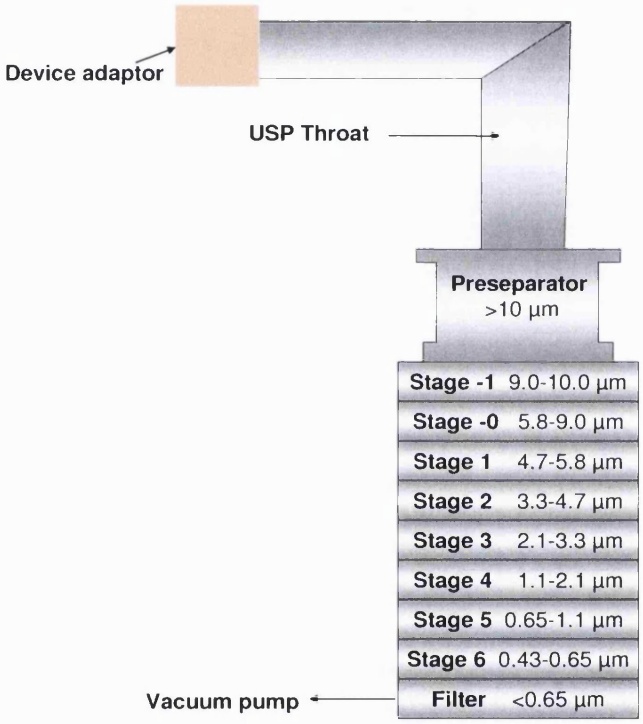

The inhalation device used was Novartis's Aerolizer® (illustrated in Figure 6.2). This device used hard capsules filled with dry powder, allowing the easy preparation of doses. In dry-powder formulations, to aid powder flow and dispersion, typically the micron-sized drug particles have been physically mixed with a lactose carrier of a much larger particle diameter (tens of microns). However, this can result in large quantities of drug being deposited in the oropharynx, due to the microparticles adhering too strongly to the carrier (since the composite particle diameter would be >~5 µm). Also, using a lactose carrier would substantially reduce the quantity of drug *per* unit mass of bulk powder. Given that the microparticulate formulation described here contained the excipients lactose and DPPC, which were both believed to be beneficial for aerosolisation, and the already low antibody content of the formulation, it was decided to use the formulation without a carrier of larger diameter. However, in order to maximise the dispersion properties of the powder, the addition of 1% m/m magnesium stearate and 1% m/m L-leucine were explored.

Figure 6.2 Photograph of the Aerolizer® (Novartis Pharmaceuticals Ltd., UK).

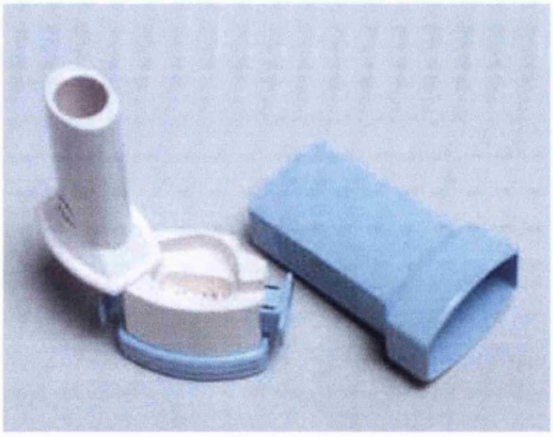

Magnesium stearate has been commonly used in tablet formulations as a glidant or lubricant (Han *et al.*, 1986), and has been used experimentally in inhaled powder formulations (Zeng *et al.*, 1998; Newman, 2006). It was thought that the addition of magnesium stearate to the pulmonary formulation may improve powder flow, by reducing the adherence of powder to the capsule and device, and possibly by improving powder dispersion. Leucine, a hydrophobic amino acid, has been investigated for improving the aerosolisation properties of microparticulate powder formulations, primarily by the reduction of interparticulate forces (Staniforth, 2002; Li *et al.*, 2003; Najafabadi *et al.*, 2004; Rabbani and Seville, 2005).

6.3 Method

6.3.1 Preparation of formulations

The spray-dried, double-emulsion optimised formulation of IgG (Flebogamma®) was produced using the parameters described in Section 4.5.1.a), and by following the methodology detailed in Section 2.2.1-2.2.2. Magnesium stearate (1% m/m) was added by serial blending with the spray-dried powder, followed by mixing in a Turbula blender (WAB, Switzerland) for 15 min. L-Leucine (0.9% m/m) was added to the external aqueous phase prior to emulsification and spray-drying. A formulation was produced that was both spray-dried with leucine (0.9% m/m), and blended with magnesium stearate (1% m/m).

6.3.2 Pressure titration of IgG formulations

This technique was used to compare the dispersion properties of the formulations directly, without the use of an inhalation device. Samples of the spray-dried powders (~5 mg) were dispersed with compressed air, through a 'RODOS' dry-powder feeder (Sympatec, UK). The particle diameters of the resultant aerosols were determined with

an in-line Helium Neon Laser Optical System ('HELOS') laser diffractometer (Sympatec, UK). Particle diameter distributions were calculated using WINDOX 4.0 software (Sympatec, UK), from which the D90% (labelled X_{90} in the software) (i.e. the diameter that 90% of the volume of particles was smaller than) was recorded. Each formulation was measured using a range of compressed air pressures (0.5 – 2.0 bar), with one repeat reading being performed for each of the three lowest pressures. For each formulation, the D90% was plotted against the pressure in order to determine the pressure required to achieve maximum powder dispersion. [This experiment was performed with Andy Smith, of Sympatec, UK.]

6.3.3 Geometric particle diameter distribution of aerosolised formulations

Powder formulation (25 mg) was loaded into Quali-V®-I hypromellose (HPMC) two-piece, hard capsules (Qualicaps Europe, Spain). Capsules were loaded into an Aerolizer® dry-powder inhalation device (supplied by Novartis Pharmaceuticals Ltd., UK), which was used according to the manufacturers instructions (Novartis, 2006). The loaded capsule was pierced, and tipped forward out of the capsule chamber, allowing it to spin freely. The device was fitted to an airtight adaptor, and an airflow of 28.3 L/min was applied. The geometric particle diameter distribution of the resultant aerosol was measured by the 'HELOS' laser diffractometer (Sympatec, UK) at multiple time-points during the actuation. Distributions towards the beginning, middle and end of the actuation were selected for comparison between each formulation. [Again, this experiment was performed with Andy Smith, of Sympatec, UK.]

6.3.4 Determination of aerodynamic particle diameter and fine particle fraction using the 'Andersen' cascade impactor (ACI)

The method used, to determine the aerodynamic particle diameter and fine particle fraction, was similar to that described in the British (2001) and European (2005) Pharmacopoeias. An airflow of 60 L/min, was chosen based on a previous ACI study with the Aerolizer® (Criée *et al.*, 2006). An 8-stage (+ filter and USP throat) ACI Mark II (Copley Scientific Ltd., UK) was set up with a 60 L/min conversion kit according to the manufacturers instructions, incorporating a pre-separator unit, as specified by the aforementioned pharmacopoeias for the analysis of powder inhalers (see Figure 6.1 for the apparatus used). The collection plates were coated with a 75:25 v/v ethanol:glycerol solution. Sodium hydroxide solution (0.5 M) was used as the collection solvent, since this had been used for encapsulation efficiency experiments to hydrolyse and dissolve the PLGA in the formulation. The pre-separator unit was filled with 10 mL 0.5 M

NaOH prior to commencing each experiment.

Powder formulation (25 mg) was accurately weighed into Quali-V®-I capsules, which were loaded into an Aerolizer® dry-powder inhalation device, used as described above. For each experiment, a total of 6 capsules were drawn into the impactor. For each capsule, the 60 L/min airflow was applied for 15 s, with the device positioned in the USP throat by means of an airtight adaptor. After actuation, the device and empty capsule were weighed. Upon completion of the experiment, the ACI was disassembled, with the powder on each plate, the powder deposited in the throat and the filter each being collected into 10 mL 0.5 M NaOH. Where there was substantial powder deposition on the underside of the upper stages, this was collected and added to the powder from the plate below it. The antibody concentration of the NaOH solutions was determined by the Bradford assay (Section 2.3.1). The amount of antibody deposited on each stage was calculated as a proportion of the total dose. 'CITDAS' software V 1.12 (Copley Scientific Ltd., UK) was used to calculate the mass median aerodynamic diameter (MMAD) (by the 50% value of the log-probability plot of cumulative % undersize vs aerodynamic diameter), and the fine particle fraction (FPF), which was defined as the percentage mass of the delivered dose with an aerodynamic diameter < 5 μm (calculated from the interpolated data. The ACI experiment was performed three times for each formulation. The FPF of each formulation was compared with the standard formulation by a one-way analysis of variance (ANOVA) with Dunnett multiple comparison test (as used by Learoyd *et al.*, 2008 and Seville *et al.*, 2007). The FPF of formulations were then compared with each other by means of a one-way ANOVA with the Newman-Keuls multiple comparison test. The statistical significance level was set at ≤ 0.05.

6.4 Results

The addition of 1% m/m leucine to the external aqueous phase did not affect the spray-drying yield or encapsulation efficiency.

6.4.1 Pressure titration

Figure 6.3 illustrates the result of the pressure titration experiment for the four formulations, using the RODOS/HELOS equipment. For all formulations, there was some decrease in the D90% with increasing pressures from 0.5-2.0 bar, with rate of change decreasing towards a minimum D90% value at 2.0 bar. The change in the D90% was greatest for the standard formulation of IgG, suggesting that more pressure was needed to fully disperse the particles, and therefore that this formulation was the

least dispersible. The addition of magnesium stearate appeared to increase dispersibility slightly, as indicated by the reduced D90% at 0.5 bar (relative to the D90% at 2.0 bar). However, the formulations containing leucine were found to be appreciably more dispersible than the standard and magnesium stearate-containing formulations, with < 1 µm reduction in D90% over the pressure range measured. The addition of magnesium stearate to the leucine-containing formulation did not appear to have any further effect on dispersibility, with the pressure-titration curves almost completely superimposed.

Figure 6.3 Particle diameter Vs pressure titration of IgG formulations using Sympatec 'RODOS' dry-powder feeder and 'HELOS' laser diffraction equipment. The geometric diameter that 90% of the volume of particles were smaller than (D90%), was measured at various dispersion pressures. At a pressure of 2 bar it was assumed the formulation was fully dispersed, given the relatively small reduction in diameter between 1 and 2 bar. The gradient in D90% over the pressure range was used as an indication of the dispersibility of the formulation, with a small gradient indicating a good dispersibility. (For the three lowest pressures n=2, mean ± SD; otherwise n=1).

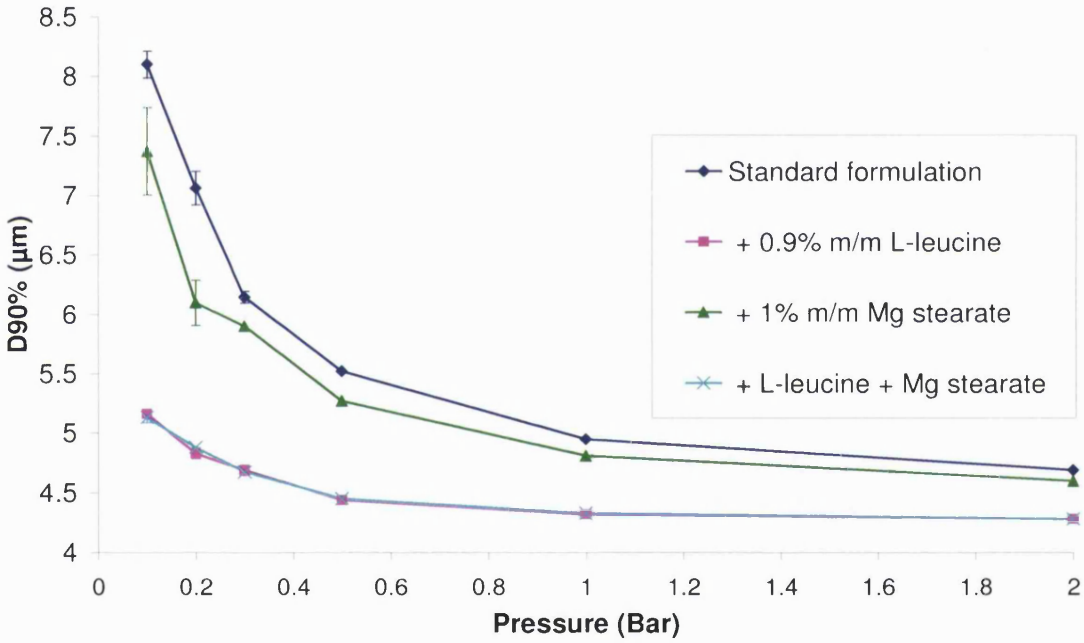

6.4.2 Geometric particle diameter distribution of aerosolised IgG formulations

Figures 6.4-6.6 illustrate the particle diameter distributions for the standard formulation, the standard formulation with leucine and the standard formulation with leucine and magnesium stearate, respectively. These formulations were aerosolised from an Aerolizer® dry-powder device at 28.3 L/min. The three curves on each graph represent different time-points during the aerosolisation. For the first two graphs it appeared that there was a decrease in particle diameter (a reduction in aggregation) as the time increased. However, the addition of magnesium stearate appeared to reduce this variation with time.

Figure 6.4 Geometric particle diameter distribution of a spray-dried, microparticulate formulation of IgG, aerosolised from an Aerolizer® device. The powder was drawn from the device at an airflow of 28.3 L/min. The diameter distribution was measured using HELOS laser diffractometry (Sympatec, UK), at three time points (0.06 s, 0.22 s and 0.41 s).

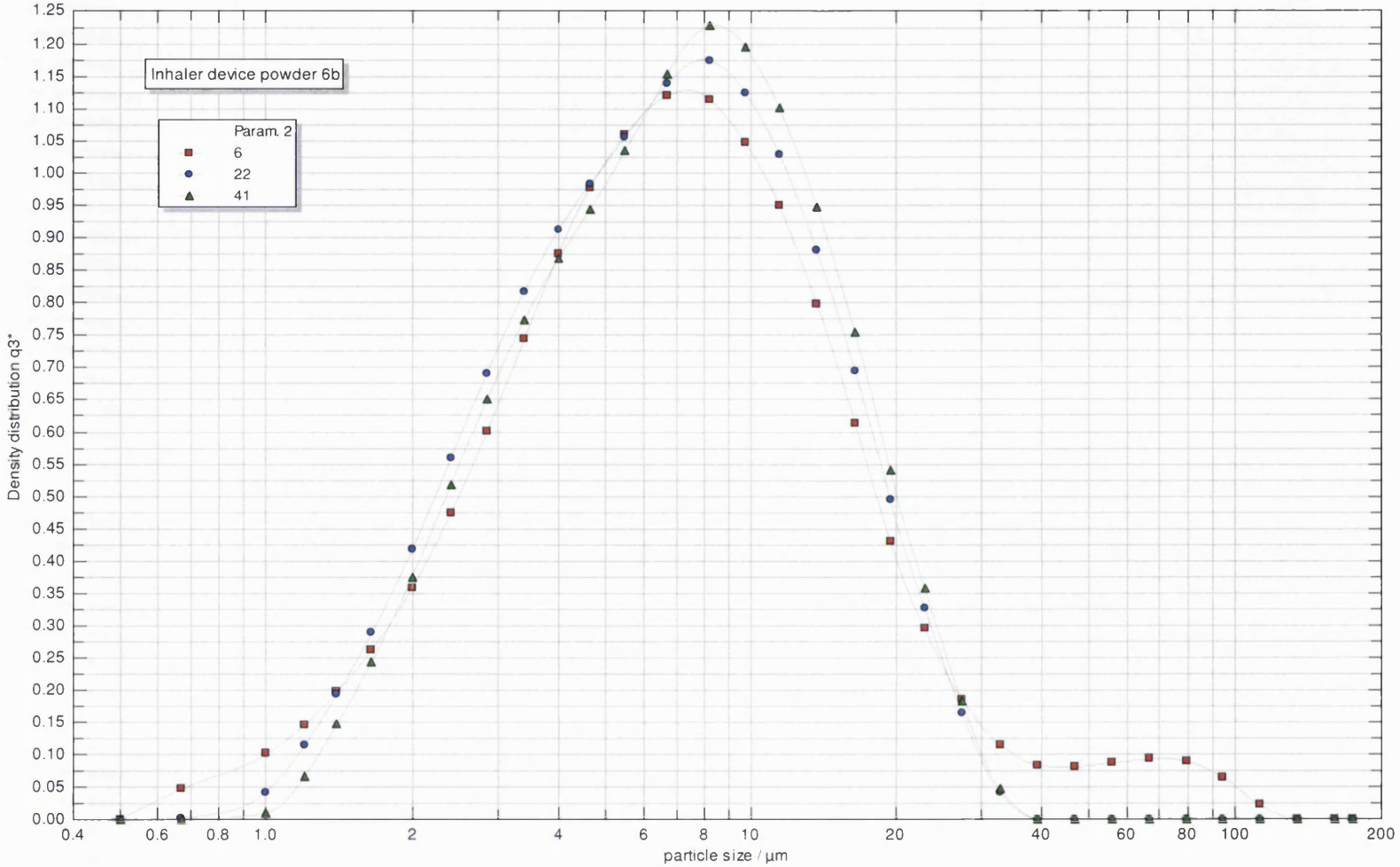

Figure 6.5 Geometric particle diameter distribution of a spray-dried, microparticulate formulation of IgG, with 0.9% m/m leucine, aerosolised from an Aerolizer® device. The powder was drawn from the device at an airflow of 28.3 L/min. The diameter distribution was measured using HELOS laser diffractometry (Sympatec, UK), at three time points (0.07 s, 0.21 s and 0.33 s).

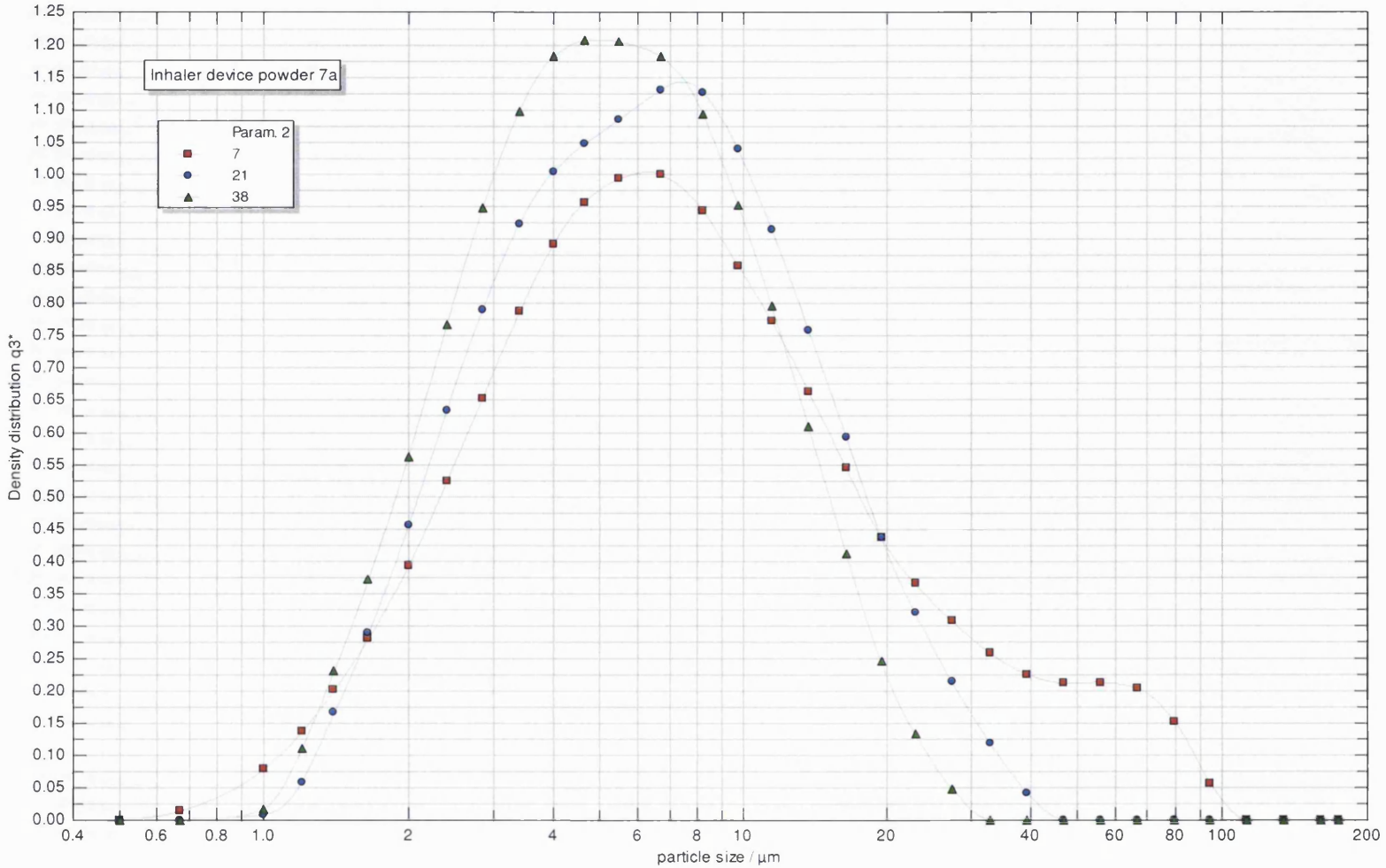

Figure 6.6 Geometric particle diameter distribution of a spray-dried, microparticulate formulation of IgG, with 0.9% m/m leucine and 1% m/m magnesium stearate, aerosolised from an Aerolizer® device. The powder was drawn from the device at an airflow of 28.3 L/min. The diameter distribution was measured using HELOS laser diffractometry (Sympatec, UK), at three time points (0.07 s, 0.21 s and 0.33 s).

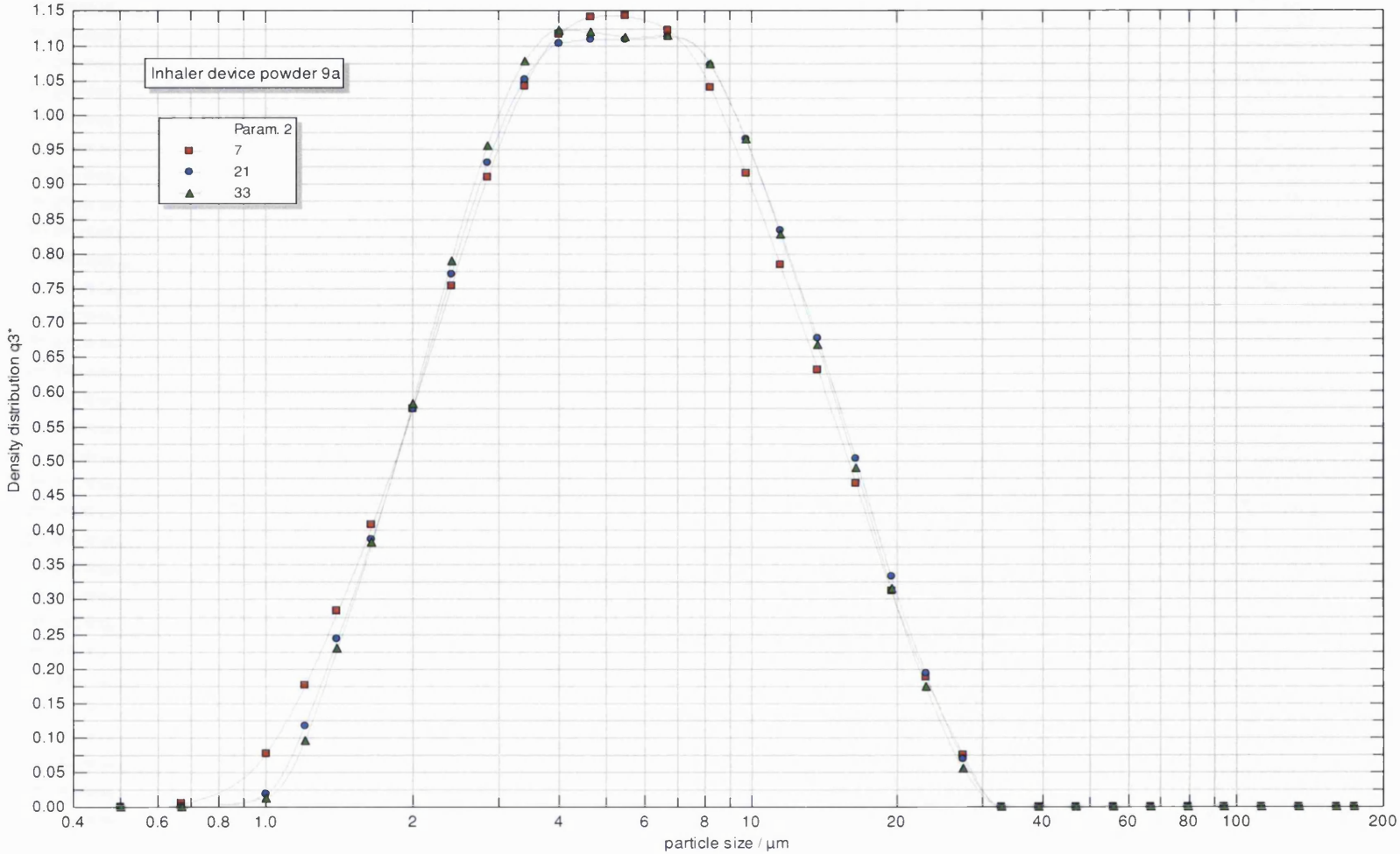

6.4.3 Determination of aerodynamic particle diameter using the 'Andersen' cascade impactor (ACI)

The deposition of each formulation in the different stages of the ACI is illustrated in Figure 6.7. All formulations followed a similar deposition pattern, with 10-20% of the dose remaining in the device, 10-20% deposition in the throat, and then most deposition in the ACI occurring on stages 0-3. For the leucine-containing formulations, there was a reduced throat deposition, and an increase in deposition on stages 1, 2, 3 and 4. For all experiments, there was <25% of the protein dose unaccounted for, thereby meeting the requirements of European (2005) and US (2006) Pharmacopoeias.

Figure 6.7 Deposition of IgG formulations in the 'Andersen' Cascade Impactor (ACI). The spray-dried powder formulations were aerosolised from an Aeroliser® device at 60 L/min. The powder was recovered in 0.5 M NaOH solution, and the protein quantified by the Bradford assay. Powder remaining in the capsule, device and deposited in the USP throat (T) is also shown. The corresponding aerodynamic diameter range for each stage of the ACI was as follows: preseparator (P): >10 µm, -1: 9.0-10.0 µm, - 0: 5.8-9.0 µm, 1: 4.7-5.8 µm, 2: 3.3-4.7 µm, 3: 2.1-3.3 µm, 4: 1.1-2.1 µm, 5: 0.65-1.1 µm, 6: 0.43-0.65 µm, F (filter): <0.65 µm (U=protein unaccounted for). (n=3, mean + SD).

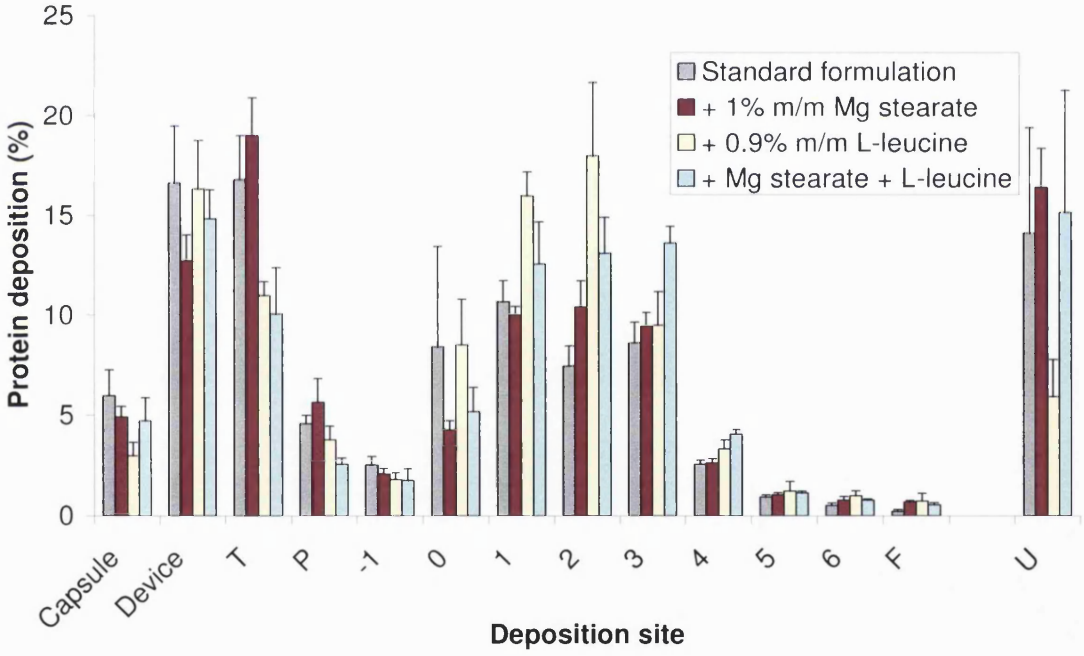

These data were analysed by 'CITDAS' software to determine the FPF and MMAD of each formulation (Table 6.1). The results were calculated by both the US and European Pharmacopoeia methods, which both gave identical values. Addition of leucine, magnesium stearate, or both, statistically significantly increased the FPF compared to the standard formulation ($p<0.05$, ANOVA/Dunnett). The FPF of each formulation was statistically significantly different from each other formulation ($p<0.05$ ANOVA/Newman-Keuls), with the combination of leucine and magnesium stearate having produced the greatest FPF (~58%).

Table 6.1 Fine particle fraction (FPF) and mass median aerodynamic diameter (MMAD) of IgG formulations, calculated from data obtained using the 'Andersen' cascade impactor (ACI).
FPF was defined as the percentage of the delivered protein dose that consisted of particles < 5 μm diameter, where the delivered dose was the protein dose that was deposited from the throat onwards in the cascade impactor. Values were calculated based on the ACI deposition data, generated by aerosolising the powder formulations from an Aerolizer® device with a 60 L/min airflow. *FPFs were found to be statistically significantly different from each other and compared to the standard formulation ($p<0.05$, one-way ANOVA/Dunnett and Newman-Keuls) (n=3, mean ± SD).

	FPF (%)	*MMAD (μm)*
Standard formulation	37.3 ± 3.2	4.74 ± 0.25
+ 1% m/m magnesium stearate	43.1 ± 1.4*	4.06 ± 0.06
+ 0.9 % m/m leucine	52.4 ± 2.5*	4.37 ± 0.08
+ 0.9% m/m leucine + 1 % m/m Mg stearate	57.8 ± 1.4*	3.90 ± 0.23

6.5 Discussion

The aim of the work described in this Chapter was to determine if the PLGA formulation of IgG developed thus far had the aerosolisation properties to make it a good candidate for pulmonary delivery. There were two broad options available to pursue in order to deliver the spray-dried powder appropriately: **1**, suspending the powder in propellant to produce a pressurised, metered-dose inhaler (pMDI), or **2**, aerosolizing the powder directly as a dry-powder inhalation (DPI). A small study was conducted, which attempted to suspend various concentrations of the powder formulation in HFA-134, with or without a small percentage of ethanol. However, it was found that at any concentration which would give a viable antibody dose *per* actuation, the powder was not in a fully dispersed, stable, suspension in the propellant. Although further tweaking with the pMDI formulation may have produced a reasonable suspension, it was decided to pursue only the DPI option, since this required less development work, and could potentially achieve a much higher powder delivery *per* dose: fractions of a milligram versus tens of milligrams (Weers *et al.*, 2007). This was especially important, given that the antibody constituted only ~3% m/m of the microparticulate formulation.

Most of the commercially available DPI products have been formulated by milling the drug into a micronised powder of a respirable diameter range (Hickey *et al.*, 1994). Because of the cohesive nature of these irregular micronised particles, they were always blended with a lactose carrier of larger diameter (~10-150 μm), since this improved the flow properties of the powder for dispensing and dispersion. However, as well as diluting the amount of drug in the formulation, the inefficient separation of the drug from the carrier meant that pulmonary delivery was poor and variable. Whilst such a scenario was acceptable for the cheap, potent, yet high-therapeutic index drugs used in

the treatment of asthma, when delivering biomolecules such as antibodies, a more efficient, reproducible system was required. It was postulated that because the IgG formulation consisted of spray-dried microparticles of a more regular shape and size, and contained excipients such as lactose and DPPC, it would be possible to aerosolise the powder without separate lactose carrier particles. However, small amounts of two additional flow enhancing excipients, magnesium stearate and leucine, were evaluated for further improvement of dispersion and deposition.

6.5.1 Pressure titration

The 'RODOS' dry-powder feeder was used to disperse samples of the dry-powder formulations by applying a range of pressures. Higher pressures provided more energy for the dispersion of the powder into individual microparticles. The D90% was used as the marker for dispersion, since microparticles that were not deagglomerated extended the particle diameter range, and hence caused the D90%, to increase. As expected, at higher pressures, the powder fully dispersed to the point where the D90% was close to its minimum value (4-5 μm), which was comparable to previous data from the laser diffraction of the formulation dispersed in cyclohexane (see Chapter 4). Given the subtle differences between the formulations tested in this experiment, all of the formulations should have had the same D90% minimum. The slightly higher minimum D90% of the non-leucine-containing formulations, and the small change in D90% between 1 bar and 2 bar, suggested that they were not quite fully dispersed at 2 bar. The potential problem with using much higher pressures was that particle attrition may have occurred, which would have caused a dramatic fall in the D90%, and thereby confused the data (Kippax, 2005). However, from the data collected it could be seen that there was a clear difference in dispersibility between the non-leucine and leucine-containing formulations. The relatively flat gradients of the leucine-containing formulation graphs, suggested that even at low pressures (i.e. with little energy input), the formulations were relatively well dispersed. There was a subtle improvement in the initial D90% with the addition of magnesium stearate. However, with leucine present, the addition of magnesium stearate offered no further improvement.

Based on this evidence, it seemed that the leucine-containing formulations would have performed best when used in a DPI device. The limited airflow drawn through the device would only equate to a certain amount of dispersion energy. Therefore, by choosing a formulation that required the least energy to fully disperse, it would have been more likely to be deagglomerated by the airflow through the device, and thus have led to a larger proportion of the dose being inhaled into the lungs.

6.5.2 Geometric particle diameter distribution of aerosolised IgG formulations

For this experiment, the powder formulations were used in an Aerolizer® device. This device was primarily chosen because it could be used with standard hard capsules that were manually filled. However, a previous study has shown that the Aerolizer® performed better than a similar non-proprietary device, in terms of FPF (Criée *et al.*, 2006). In this experiment, an airflow of 28.3 L/min was used to draw powder from the device, and 'HELOS' laser diffractometry measured the geometric particle diameter distribution. The results indicated that at 28.3 L/min, using the Aerolizer®, the powder was not fully deagglomerated, since a substantial proportion of the diameter distribution was greater than the 5 μm D90%, as measured in the previous experiment. However, some of the powder was detected as fully dispersed, individual, microparticles. Although leucine did not appear to appreciably influence the diameter distribution, magnesium stearate in combination with leucine appeared to unify the distribution over the three time points of analysis. Without magnesium stearate, there was a slight reduction in particle diameter as the larger aggregates decreased with time. Magnesium stearate may have acted as a lubricant, reducing friction, and causing the larger aggregates to disperse more rapidly.

6.5.3 Determination of aerodynamic diameter and fine particle fraction using the 'Andersen' cascade impactor (ACI)

The aim of this experiment was primarily to determine the aerodynamic dynamic diameter of the microparticles, and secondly to assess the dispersibility of the powder formulations, in terms of FPF. Therefore, everything was done to maximise the dispersion of the powders, since this would provide the most accurate assessment of particle MMAD. It was decided that an airflow of 60 L/min would be used for the ACI testing, to try and maximise the powder dispersion, given the incomplete dispersion observed in the previous experiment, where an airflow of 28.3 L/min was used. Bosquillon *et al.* (2004a) observed no further increase in FPF when increasing airflow from 60-90 L/min. Although 28.3 L/min was the standard airflow that the ACI was originally calibrated for (see the previously referenced Pharmacopoeias), this ACI was adapted to operate at 60 L/min, and the various cut-off diameters were pre-calculated and provided by the manufacturer. However, in terms of FPF determination, 60 L/min was still considered a clinically relevant airflow, being an achievable, sustainable, peak flow rate for asymptomatic subjects (Clark and Egan, 1994), and when using the Aerolizer® (considered a low resistance device), this was achievable for over 90% of asthmatics (Criée *et al.*, 2006). In fact, this was the flow rate used by Criée *et al.* (2006) when they assessed the Aerolizer® device with the ACI. However, there was a

potential disadvantage in using too high a flow rate, in that inertial deposition would have been increased, causing a greater degree of particle impaction in the throat of the apparatus (Clark and Egan, 1994; Usmani *et al.*, 2005). In this respect, ideally a low airflow rate should be used to maximise the flow of particles into the deeper stages of the cascade impactor (or lungs), based on their aerodynamic diameter. Indeed, this was the principle behind the "soft mist" inhalers, where a puff of aerosolised particles was released at low velocity. However, in the case of a passive DPI, where aerosolisation of the powder was required, choosing the an appropriate airflow was a balance between ensuring it was great enough to fully disperse the particles, while considering the inertial impaction effect of high particle velocity. In practical terms, for a passive DPI, aerosolisation (and hence the use of a higher airflow rate) was the most important factor to maximise deposition efficiency (Hickey *et al.*, 1994).

In addition to the Aerolizer® device itself, the choice of capsule was also important in maximising delivery efficiency. HPMC capsules were chosen in preference to standard gelatine capsules and gelatine-PEG capsules, since they have been shown to acquire less static charge, were less affected by moisture, and were less likely to fragment from puncturing, all of which should have improved powder emptying (Jones, 2006). In the present study (see Figure 6.7) ~5% m/m of the protein dose (measured by powder mass) was consistently found to be remaining in the capsule, appearing as a dusting on the inside capsule surface. A further ~15% of the dose remained in the device. This value was consistent with the emitted dose values from the study by Criée *et al.* (2006), who were measuring the formoterol dose from a standard micronised drug-in lactose carrier formulation, delivered by an Aerolizer® device. They found that the Aerolizer® had a lower emitted dose (i.e. greater quantity remaining in the device) than a standard non-proprietary device. Therefore, at least some of the 10% of protein that in this study remained in the device could have been attributed to the efficiency of the device, rather than the formulation.

In terms of MMAD and FPF calculation, only the emitted (delivered) dose was analysed. Although FPF represented the respirable fraction of the dose, this was understood to invariably overestimate the potential *in vivo* lung deposition, due to lack of consideration for patient variability and clearance mechanisms (Snell, 1997). The largest single deposition site in the apparatus, of the emitted dose, was the throat, which was coated with a dusting of fine powder that accounted for 10-20% of the total dose. This fraction of the powder was likely to have consisted of a combination of agglomerates which had not fully dispersed, and aerosolised particles that impacted due to their inertia at high velocity, as explained previously. It was probably a difference in

the former of these factors that accounted for the almost 10% greater throat deposition of the non-leucine containing formulations. Leucine (in many cases spray-dried) has become widely known as a dispersibility enhancer, with frequent reporting in the literature demonstrating its application in the aerosolisation of powders (Lucas *et al.*, 1999; Staniforth *et al.*, 2002; Najafabadi *et al.*, 2004; Rabbani and Seville, 2005). During spray-drying, the hydrophilic components of the formulation diffused to the centre of the liquid droplets, leaving hydrophobic and surface-active components such as leucine and DPPC at the air/moisture interfaces, and thus on the particle surface (Weers *et al.*, 2007). Hydrophobic interactions would have been smaller than hydrophilic interactions (Hickey *et al.*, 1994), and thus microparticles with hydrophobic surfaces were less attracted to one-another and easier to disperse. Nektar Pharmaceuticals have utilised another amino acid, glycine, in their Exubera® insulin formulations, presumably for the same purpose (Fineberg *et al.*, 2007). It was quite unexpected that DPPC may well have had so many key roles in these formulations. Originally used as a bio-compatible emulsifier for the double-emulsion, it had been shown to aid antibody encapsulation, benefit the drug-release properties (see Chapter 3), and here it may have quite possibly enhanced powder aerosolisation, by increasing the hydrophobicity of the particle surface.

Considering deposition beyond the throat of the apparatus, there was little impaction in the preseparator. This was the site where a lactose carrier would normally be filtered out. In this study, it appeared that if the particles were dispersed and slow enough to pass through the throat, they also largely avoided deposition in the preseparator. The aerosolised powder (approximately 50% of the initial dose) was found to be deposited on a range of stages, with the majority on stages 1-3, but with some deposition detected on every stage, right down to the filter. The leucine-containing formulations had a greater deposition in these stages as a result of the reduced deposition in the throat. The stages of an ACI have been paired with various anatomical deposition sites in the human respiratory tract (see Figure 6.8). However, this is obviously an oversimplification, since aerodynamic particle diameter would not have been the only factor to determine *in vivo* deposition. The patient's breathing pattern, including peak airflow and breath-holding, as well as moisture and pathophysiology, would all cause variation in the lung deposition pattern (Clark and Egan, 1994). The use of idealised throat models and electronic lungs has attempted to improve the IVIVC (Zhang *et al.*, 2007). For all formulations there was an appreciable amount of protein that was unaccounted for. This may have been due to the inaccuracy of the Bradford assay at low concentrations, and powder losses. However, for all experiments, the unaccounted protein was within the ±25% limits specified by the Pharmacopoeias.

Figure 6.8 A correlation between the stages of the 'Andersen' cascade impactor (ACI), and anatomical sites of the human respiratory tract. Lung deposition site is based on particle aerodynamic diameter only. The diameter ranges shown are for an ACI operating with an airflow of 60 L/min (adapted from: www.copleyscientific.co.uk). [The diameters given for each anatomical region are relatively conservative compared to other published values (Gonda, 1992; Lalor and Hickey, 1997; Agu *et al.*, 2001)].

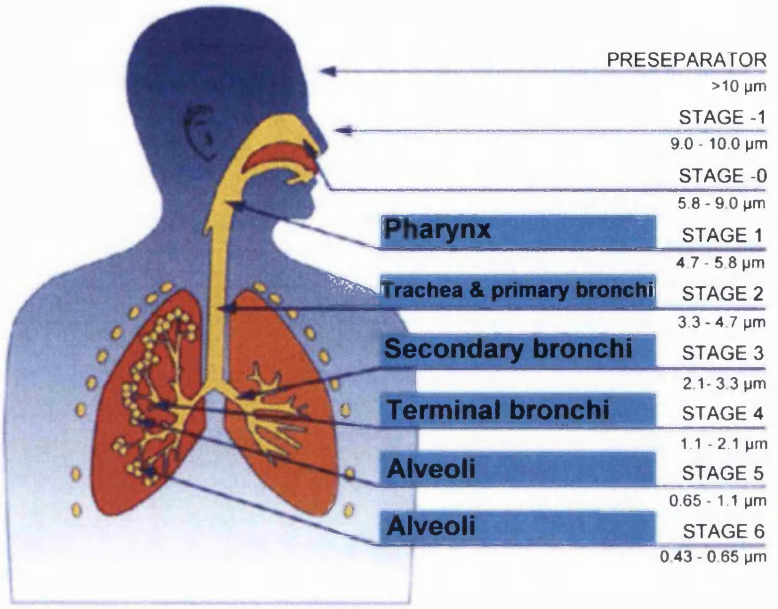

The impaction data were used to calculate the MMAD and FPF. The addition of 1% magnesium stearate appeared to have the most effect on MMAD, causing a decrease of >0.5 µm. This was probably not because the microparticles in this formulation were physically any smaller, or less dense (see Equation 1, Chapter 1) (these were from the same batch of spray-dried microparticles, just with 1% magnesium stearate blended in), but because the formulation was better dispersed. Leucine also caused a smaller reduction in MMAD. This may also be due to improved dispersibility, although the presence of leucine may have reduced the intrinsic particle density (Lucas *et al.*, 1999). Interestingly, FPF did not follow the same rank order, with leucine causing a much larger increase in FPF than did magnesium stearate. The formulation containing both leucine and magnesium stearate had an FPF of 58%, which represented a 20% increase on the standard formulation (this increase was statistically significant, $p<0.05$, ANOVA/Dunnett). This effect was predicted by the pressure titration experiment. All of the formulations were superior to micronised formoterol in a lactose carrier, from an Aerolizer® device, which had an FPF of 26% (Criée *et al.*, 2006). Such a value was typical for passive DPIs of traditional binary lactose-micronised drug blends (Duddu *et al.*, 2002; Weers *et al.*, 2007). Therefore, as anticipated, aerosolisation of these spray-dried powders was better than milled powder, without requiring a lactose carrier. The leucine and magnesium stearate-containing formulation had an FPF comparable with the better performing of the leucine-containing formulations described by Rabbani and

Seville (2005), and was far superior to the leucine/cromoglycate formulations presented by Najafabadi *et al.* (2004). This was despite the fact that the latter author defined FPF as particles which impacted on stage 1 or below (<6.8 μm), rather than the Pharmacopoeial standard of <5 μm, used here. The 58% FPF was also superior to albumin/sugar/DPPC (no leucine) formulations described by Bosquillon *et al.* (2001), and comparable with a dry-powder Pulmosphere® formulation (50 ±10%) (Edwards *et al.*, 1997). As described in Chapter 1 of this thesis, large porous particles, such as Pulmospheres® were at the time hailed as the 'cutting-edge' in pulmonary delivery, and are still a favoured approach for developing the pulmonary formulations of the future. Briefly, these were particles of geometric diameter ~8 μm, but due to their porous nature, and hence low density, they had an MMAD of ~3 μm (Edwards *et al.*, 1997). However, because of their larger physical diameter, surface interactions were reduced, improving dispersion (Weers *et al.*, 2007). Of course, being so porous, such a formulation limited the possibility for slow-release of a protein drug, which was a major desired characteristic of the formulations described here. Therefore, to have achieved FPFs that were on a par with Pulmospheres®, was a good indication that the formulations described in this thesis had at least acceptable aerosolisation properties. However, Pulmospheres® suspended in propellant, in a pMDI, achieved FPFs of up to 70% (Dellamary *et al.*, 2000). Perhaps, if the pMDI route had been pursued with these formulations, similar values may have been achieved. More recently, FPFs of up to 80% have been achieved using leucine in quantities of 20-36% m/m in spray-dried DPI formulations of β2-agonists (Learoyd *et al.*, 2008; Seville *et al.*, 2007). This suggested that increasing the amount of leucine in the formulations of the present work above 0.9% m/m, may have further increased FPF. In addition, the FPF of human growth hormone, PROMAXX® dry-powder particles (a technology described in Chapter 1 of this thesis) was reported to be 67.4%. However, only 62.8% of the dose was emitted from the inhaler (c.f. ~80% for the formulations in this thesis) (Rashba-Step, 2007).

6.6 Conclusion

The work described in this Chapter investigated the aerosolisation properties of the spray-dried modified-release IgG formulation. Small amounts of magnesium stearate, and particularly leucine, were demonstrated to improve the powder dispersibility, initially measured by laser diffraction, pressure-titration. This technique has been shown to be a good predictor of *in vitro* deposition performance in an ACI, using a proprietary passive DPI device. These formulations achieved MMADs and FPFs comparable with other 'novel' pulmonary formulations, and were far superior to the traditional DPI formulations composed of micronised drug with a lactose carrier.

7 FORMULATION AND *IN VITRO* AND *IN VIVO* TESTING OF THERAPEUTIC F1 AND V ANTIBODIES FOR THE TREATMENT OF *YERSINIA PESTIS*

7.1 Abstract

In this work, the formulation described in the previous three chapters, was utilised as a carrier for therapeutic antibodies targeted against the F1 and V subunits of Yersinia pestis, the bacteria responsible for pneumonic and bubonic plague. F1 + V IgG were purified from the sera of macaque monkeys that had been previously immunised with the subunit proteins. The purified F1 + V IgG were used to produce three batches of the double-emulsion, spray-dried, microparticulate, modified-release formulation, containing PLGA, lactose and DPPC.

The stability of F1 +V IgG released from the formulation, after 2 h (37°C) incubation in pH 7.4 PBS, was compared with the unformulated F1 +V IgG, and the model human IgG previously used. Gel electrophoresis, FFF and ELISA all demonstrated that the formulated F1 +V antibody remained biologically active, and at the correct molecular weight (~150 kDa).

Two proof-of-principle studies were conducted to test the *in vivo* activity of the formulated F1 + V IgG. Groups of 5 BALB/c mice were treated either intramuscularly (i.m.) or interperitoneally (i.p.) with the formulated or unformulated F1 + V IgG, prior to subcutaneous (s.c.) *Y. pestis* infection. In the first study, unformulated and formulated antibody were administered 48 h prior to *Y. pestis* infection, with the aim of demonstrating the effectiveness of the modified-release formulation. However, all mice (including those administered unformulated antibody) died within 9 days post infection. This was surprising given that the half-life of the antibodies in mice was previously found to be 6-8 days. Therefore, in the second study, in order to increase the likelihood of achieving a therapeutic benefit with the antibody, 10-fold higher doses of formulated and unformulated antibody were administered 2.5 h before infection. In this study all of the animals that were administered the formulated antibody died within 9 days. However, 2 of the 5 mice that were administered the unformulated antibody survived the 14 days of the study. Therefore, since the *in vitro* release experiments (Chapter 5 of this thesis) suggested that only ~30% of the formulation's antibody load would have been released by the time of infection, the formulated antibody may not have been administered at a dose high enough to generate the plasma levels of free IgG required to confer protection.

7.2 Introduction

Data obtained from the studies described in the previous three Chapters, clearly demonstrated that an antibody formulation had been successfully developed, which possessed antibody modified-release (MR), stability and the aerosolisation properties necessary to enable its feasible use in pulmonary delivery. Throughout this development work, polyclonal human IgG (Flebogamma®) was used as a model antibody. Therefore, the next logical step was to substitute this model antibody for a therapeutic antibody. This was undertaken to firstly test if it could be incorporated stably into the formulation described in this work, and secondly to investigate if the formulated antibody maintained its therapeutic activity, by means of a proof-of-principle *in vivo* study.

Yersinia pestis, the gram-negative bacterium that causes bubonic and pneumonic plague, has been responsible for the deaths of tens of millions of people over the course of history (Hill *et al.*, 2003). Although, at present, outbreaks in humans tend to be relatively small, the ability of *Y. pestis* to rapidly spread *via* airborne droplets to cause the more deadly pneumonic plague, has highlighted the infection as a potential bioterrorist weapon (Hill *et al.*, 2006). The currently available vaccine is a killed whole cell vaccine, which was thought to have limited effectiveness in the protection of pneumonic plague (Williamson *et al.*, 2007), and has been reported to commonly cause a range of non-specific side-effects (Williamson *et al.*, 2005). Vaccines comprising recombinant bacterial subunits, rF1 and rV have been in development, and were found to be potentially effective in studies involving humans and macaque monkeys (Williamson *et al.*, 2005; Williamson *et al.*, 2007). However, vaccination can only be effective when used well in advance of exposure to the bacterium. For the short-term protection, or the acute treatment of plague, which are the more likely paradigms in a biological warfare scenario, vaccination would be less appropriate. Although modern antibiotics have been successfully used to treat cases of plague, resistant strains are emerging, and such strains may be exploited in a deliberate attack (Hill *et al.*, 2003). IgG antibodies represent an alternative short-term treatment option. In the recombinant vaccine studies, serum from immunised subjects, containing antibodies against rF1 and rV, conferred passive protection to mice challenged with *Y. pestis* (Williamson *et al.*, 2005). Monoclonal F1 and V IgG have been developed, which when administered by injection, have been demonstrated to protect mice from an injected *Y. pestis* challenge prophylatically and for up to 48 h post-infection (Hill *et al.*, 2003). Intratracheal aerosol delivery of the same antibodies, protected mice against aerosolised *Y. pestis* challenge

(Hill *et al.*, 2006), suggesting that pulmonary delivery of specific antibodies could be used as a potential treatment for pneumonic plague. However, in order to produce such a medicine for human use, a formulation for the antibodies would be required, that would enable the antibodies to be kept stable in less-well controlled conditions, and which could be easily administered using a portable inhalation device. Thus, two proof-of-principle studies were conducted to test the effectiveness of anti-plague antibodies formulated with the microparticulate formulations that have been described in this thesis.

Rather than using monoclonal antibodies, for these studies, F1 and V IgG were obtained from the sera of cynomolgus macaque monkeys (*Macacca fascicularis*) that had been vaccinated with rF1 and rV recombinant subunits. These sera had previously been shown to compete with a protective monoclonal antibody for binding to the rV antigen in an *in vitro* ELISA study, and to be protective in a mouse model, against challenge with *Y. pestis* by passive transfer (Williamson *et al.*, 2005). The first aim of this work was to demonstrate that purified F1 and V IgG could be incorporated into the formulation, with detectable IgG being released from the formulation. The second aim was to test if the formulated antibody had *in vivo* activity. For these initial studies, a systemic *in vivo* model was used, where the animals were dosed *via* the intraperitoneal (i.p.) or intramuscular (i.m.) route prior to subcutaneous (s.c.) *Y. pestis* challenge. This was more simple to perform than the perhaps more directly relevant, intratracheally dosed, aerosolised challenge model, but was still anticipated to demonstrate whether or not the formulation process affected the protection potentially offered by the antibodies.

7.3 Method

7.3.1 Purification of F1 +V IgG from macaque monkey serum

The macaque monkey serum samples (Defence Science and Technology Laboratory, Porton Down, UK) were pooled, and then centrifuged. The pool of filtered supernatants was diluted 1:1 with 20 mM phosphate buffer, and loaded into a 5 mL protein G column (HighTrap, GE Healthcare, UK), running at 1 mL/min. IgG was then eluted from the column with 100 mM glycine pH 2.5 buffer running at 1 mL/min, with collection continuing for as long as a positive UV reading at 280 nm was present. The collection tubes were neutralised with 1 M Tris pH 9 buffer, and the neutralised eluent was added to a PD-10 buffer exchange column (GE healthcare, UK) in 2.5 mL portions. The columns were washed with 25 mL of phosphate buffered saline (PBS) before adding 2.5

mL of the sample, and then eluting the sample (collected as 3.5 mL in PBS) with a further 3.5 mL of PBS. Samples were pooled together, sterile filtered, and the concentration measured by UV at 280 nm. The purified antibody was collected as 36 mL of a 7.4 mg/mL solution. This procedure was undertaken with Nicky Walker, a staff member at the Defence Science and Technology Laboratory, Porton Down, UK.

Half of the collected antibody solution was concentrated using 15 mL concentration tubes with a 30,000 molecular weight cut-off. Each tube contained 9 mL of the antibody solution, which was then centrifuged at 2500 RPM, at 6°C, for approximately 2 h, after which time just under 1 mL volume was remaining. The concentrated samples were pooled and measured by UV at 280 nm, by preparing a 100x dilution. The concentrated sample, slightly yellow in colour, contained 79 mg/mL protein.

7.3.2 Preparation of formulations containing F1 + V IgG

Three batches of the modified-release PLGA formulation were prepared using the concentrated and purified antibody, with the parameters described in Section 4.5.1.a), following the methodology detailed in Section 2.2.1-2.2.2. The internal aqueous phase was prepared by adding 253 µL (20 mg) of the F1 + V antibody sample to 20 mg sorbitol, diluted up to 2 mL with water. The sorbitol was added to replicate the conditions when using the Flebogamma®, model IgG, which was supplied formulated 1:1 by mass with sorbitol. However, unlike with Flebogamma®, this dilution caused some precipitation to occur (presumably of the antibody, but perhaps of some other impurity, such as urea), which was reversed by the addition of 5 mg sodium chloride. The internal aqueous phase was homogenised for 2 min at 24,000 RPM with 200 mg PLGA 1A and 25 mg DPPC, in 4 mL dichloromethane. The primary emulsion was then homogenised for 10 min at 10,000 RPM with 300 mg lactose dissolved in 70 mL water. The double-emulsion was spray-dried at an outlet temperature of 55°C, 75% aspiration, 800 L/h atomisation and 2 mL/min pump speed.

7.3.3 *In vitro* formulation analysis

The F1 + V antibody encapsulation efficiency (EE) for each batch was measured in triplicate by the Bradford assay (Section 2.3.2). A 10 mg sample from each batch was incubated in 1 mL PBS pH 7.4, at 37°C for 2 h to obtain the immediate burst-release of F1 + V antibody, from the surface of the formulation. For comparison, three similar samples were prepared from formulations loaded with Flebogamma® IgG. The 2 h burst-release samples were analysed by non-reducing SDS-PAGE and ELISA (see

Section 2.5.1-2.5.2 for methods) to confirm that the formulated F1 + V antibody was stable, biologically active and had unchanged molecular weight, compared to the unformulated, purified antibody sample, and Flebogamma®. For the SDS-PAGE experiment, a sample of Flebogamma® was denatured by boiling for 15 min, before being loaded onto the gel, in order to serve as a negative control for protein activity. Field-flow fractionation (FFF) was used to analyse the molecular weight and monomer content of 2 h burst-release (n=3) and unformulated (n=3) F1 + V IgG, as described in Section 2.5.3.

7.3.4 *In vivo* protection studies

This work was performed by staff at the Defence Science and Technology Laboratory, Porton Down, UK. Six- to 8-week old female BALB/c mice (Harlan Ltd., UK) were used for these studies, in accordance with UK legislation relating to animal experimentation (Animals [Scientific Preocedures] Act 1986). For each of the 2 studies, 4 or 5 groups, consisting of 5 mice, were used. The mice received formulated F1 + V IgG, i.p. or i.m., unformulated F1 + V IgG solution i.p., or placebo, microparticulate formulation i.p. (containing no antibodies). In the first study, this treatment (equivalent to 200 μg IgG) was administered 48 h prior to 100 μL s.c. *Y. pestis*, strain GB infection, with an estimated dose of 100 CFU (equal to 100 median lethal doses). For the formulated IgG, 6 mg of microparticulate formulation was administered as either a 100 μL PBS suspension i.m., or a 500 μL PBS suspension i.p. In the second study, a higher dose of formulation (equivalent to 2 mg IgG) and unformulated antibody (2 mg) was administered 2.5 h prior to infection with ~10 CFU. In addition, there was a naïve group that received no form of treatment prior to infection. In this second study, the formulated IgG was administered i.m. only, as 60 mg of formulation in a 350 μL suspension. The dosing schedules are summarised in Tables 8.1. Aliquots of the challenge were cultured to determine the actual CFU of *Y. pestis* delivered *per* mouse. Animals were checked twice-daily, and were culled upon the observation of signs of infection. The time to death (TTD) in days was recorded over a period of 14-days. Statistically significant variation in the TTD was assessed by Student's t-test using Excel® 2003 software (Microsoft Corporation, USA).

Table 7.1 Summary of the dosing schedule for two studies to assess the effectiveness of formulated F1 + V IgG in the protection against *Yersinia pestis* infection, in an *in vivo* mouse model. Each group consisted of 5 BALB/c mice. Formulated IgG suspension, unformulated IgG, or placebo formulation was dosed intraperitoneally (i.p.) or intramuscularly (i.m.). The naïve group received no form of treatment. Mice were infected with *Y. pestis*, GB strain, with a target challenge level of 100 CFU (first study), or 10 CFU (second study) at 0 h. The IgG dose delivered was based on the 3.3% m/m IgG loading of the formulation.

Group	Dose time (h)	Mass of formulation dosed (IgG dose delivered)	Total formulation mass required (mg) for group (n=5)
First study			
1. Formulated IgG, i.m.	-48	6 mg (200 µg)	30
2. Formulated IgG, i.p.	-48	6 mg (200 µg)	30
3. Unformulated IgG, i.p.	-48	(200 µg)	1
4. Placebo formulation, i.p.	-48	6 mg	30
Second study			
1. Formulated IgG, i.m.	-2.5	60 mg (2 mg)	300
2. Unformulated IgG, i.p.	-2.5	(2 mg)	10
3. Placebo formulation, i.p.	-2.5	60 mg	300
4. Naïve	-	-	-

7.4 Results

The average yield of the three batches was 61 ± 1%, and the average EE of all batches was 84 ± 3%.

7.4.1 *In vitro* characterisation of formulated F1 + V IgG

Figure 7.1 is a photograph of the SDS-PAGE gel used to characterise formulated antibody from 2 h burst-release samples. Aside from the denatured Flebogamma® sample, for which there was no visible band, both formulated and unformulated antibody samples appeared as a single band of ~150 kDa, the appropriate molecular weight of monomeric IgG. Interestingly, the bands of the F1 + V antibodies were narrower than the Flebogamma® bands.

Figure 7.2 illustrates the ELISA data. Over 90% of the released antibody concentration measured by the Bradford assay, was detected by ELISA. There was little difference between the Flebogamma® and F1 + V IgG formulations. Table 7.2 summarises the FFF data. The molecular weight detected (~155 kDa) was consistent with the SDS-PAGE data.

Figure 7.1 Gel electrophoresis of F1 + V IgG released from the microparticulate formulation. Key – Lane 1: molecular weight marker (*=194.8 kDa, **=106.8 kDa), 2: unformulated Flebogamma ®, 3: Flebogamma® boiled for 15 min (negative control for protein activity), 4: unformulated F1 + V IgG, 5: placebo formulation (negative control for the presence of protein), 6: formulation containing Flebogamma®, 7,8,9: formulations containing F1 + V IgG.

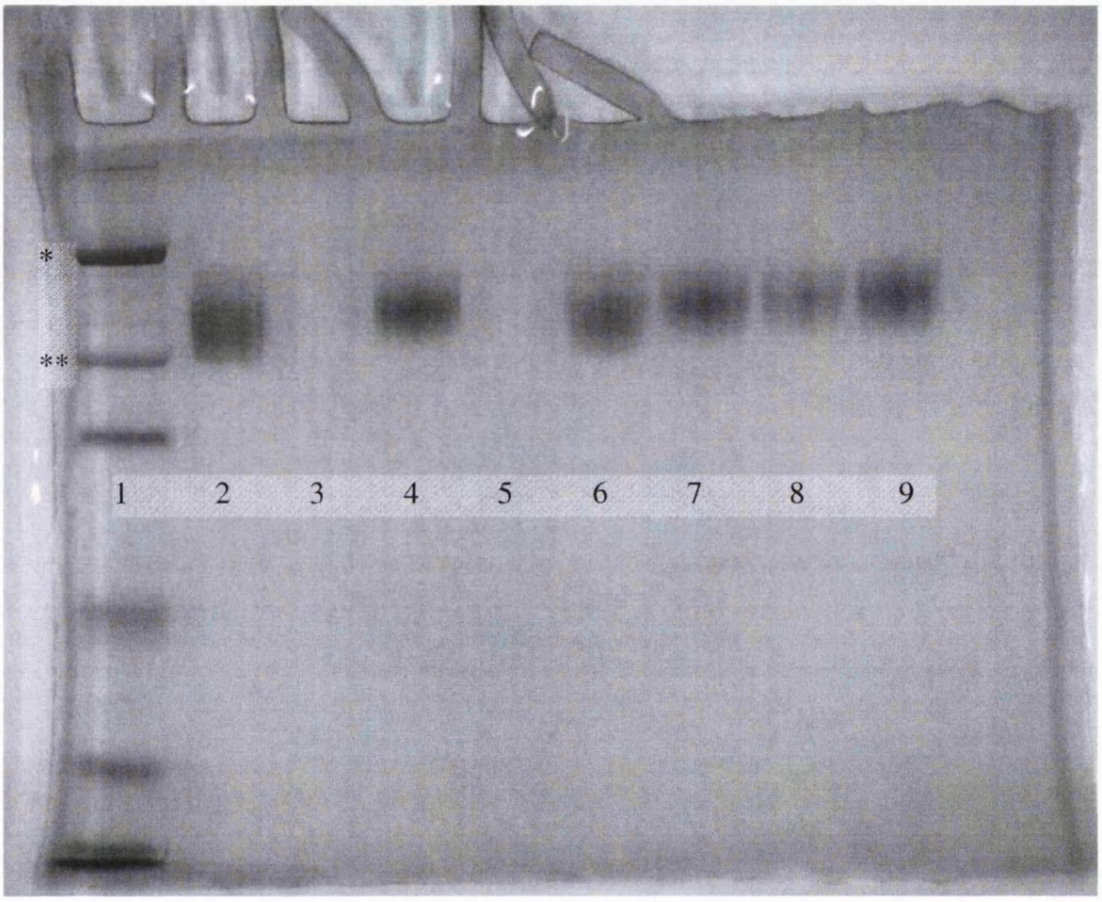

Figure 7.2 Activity of Flebogamma® and F1 + V IgG released from microparticulate formulations, as measured by enzyme-linked immunosorbent assay (ELISA). The concentration of IgG determined by ELISA was expressed as a percentage of the total protein concentration measured by the Bradford assay (n=3, mean + SD).

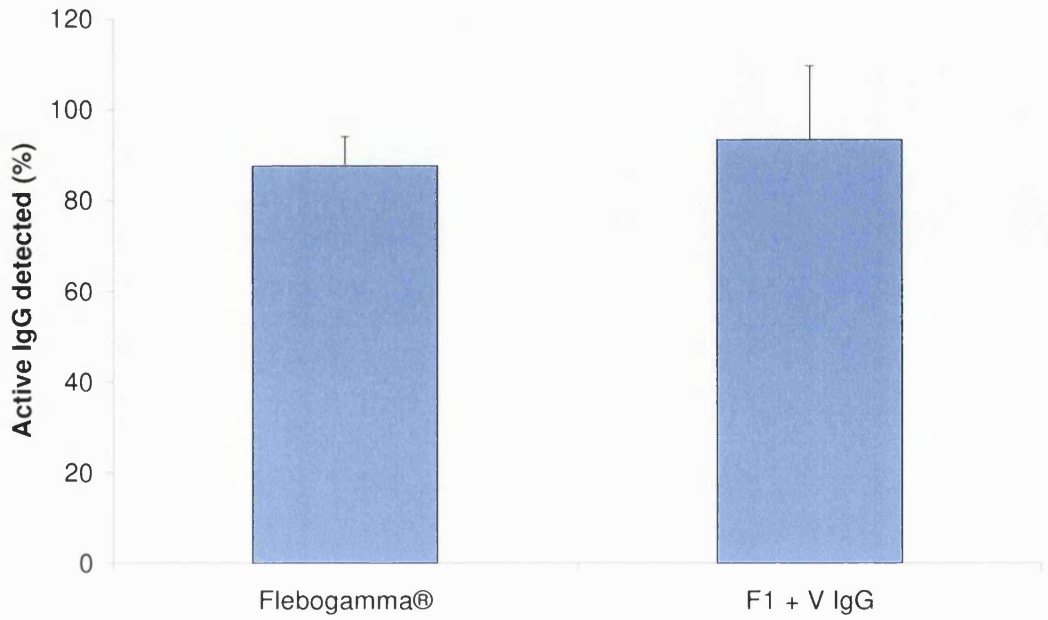

Table 7.2 Field-flow fractionation analysis of F1 +V IgG, either unformulated, or from 2 h burst-release samples from microparticulate formulations. [Data were obtained using the UV detector (n=3, mean ± SD)].

	% Recovery	Monomer MW (kDa)	% Monomer
Unformulated	87 ± 2	158 ± 2	98 ± 2
Formulated	73 ± 15	154 ± 2	100 ± 0

7.4.2 *In vivo* protection studies

The actual delivered dose of *Y. pestis* infection in the first study was 60 CFU. In this study none of the animals survived beyond 9 days after infection (see Figure 7.3). There was a statistically significant increase in the TTD between the small volume i.m. injection of formulated antibody, compared with the i.p. route and the unformulated antibody ($p<0.05$). However, there was no statistically significant increase in TTD with the formulated antibody compared to the placebo formulation.

Figure 7.3 Survival of mice administered with a microparticulate formulation of F1 +V IgG, 48 h prior to challenge with *Yersinia pestis* infection. Three groups of 5 mice were dosed F1 + V IgG (200 µg) as 6 mg microparticulate formulation, administered intramuscularly (i.m.) in a 100 µL suspension, 6 mg microparticulate formulation administered intraperitoneally (i.p.) as a 500 µL suspension, or unformulated administrated as an i.m. solution. A further group was dosed with 6 mg placebo formulation i.p. After 48 h (time=0) animals were challenged with 60 CFU *Y. pestis* administered as a 100 µL subcutaneous injection. Deaths were recorded over a 14-days period. A statistically significant delay in time to death (TTD) was observed in mice treated i.m. with the formulated IgG, compared to both the i.p. route and unformulated IgG ($p<0.01$). However, there was no statistically significant increase in TTD between the formulated IgG and the placebo formulation.

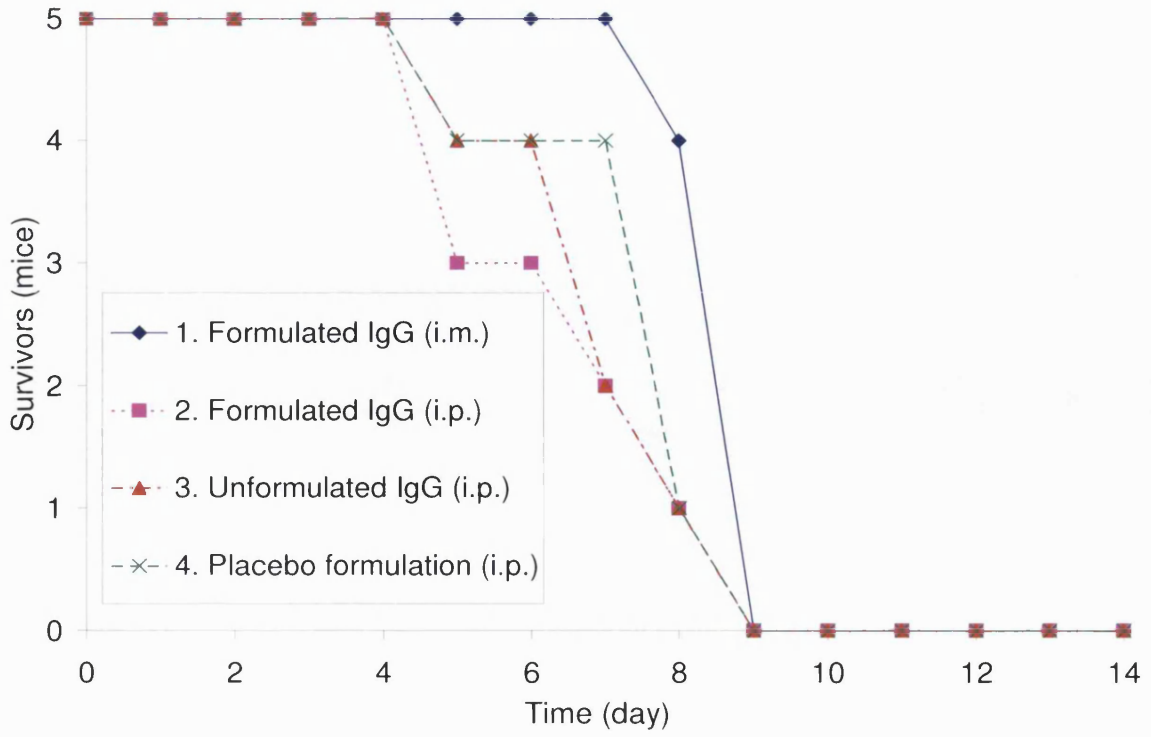

The actual delivered dose of *Y. pestis* infection in the second study was 12 CFU. The mice in all the groups either died, or were culled, within the 14 days of the study, except for the group where the unformulated antibody was administered, where 2 of the 5 mice survived (Figure 7.4). Administration of the either the formulated IgG, or placebo formulation, resulted in no statistically significant increase in TTD compared to untreated animals.

Figure 7.4 Survival of mice administered with a microparticulate formulation of F1 +V IgG, 2.5 h prior to challenge with *Yersinia pestis* infection. Three groups of 5 mice were dosed F1 + V IgG (2 mg) as 60 mg microparticulate formulation, administered intramuscularly (i.m.) in a 350 µL suspension, or unformulated, administrated as an i.m. solution. Two further groups were dosed with either 60 mg placebo formulation i.p., or were left untreated. After 2.5 h (time=0) animals were challenged with 12 CFU *Y. pestis* administered as a 100 µL subcutaneous injection. Deaths were recorded over a 14-days period. There was no statistically significant reduction in TTD between the animals administered formulated IgG and the untreated animals.

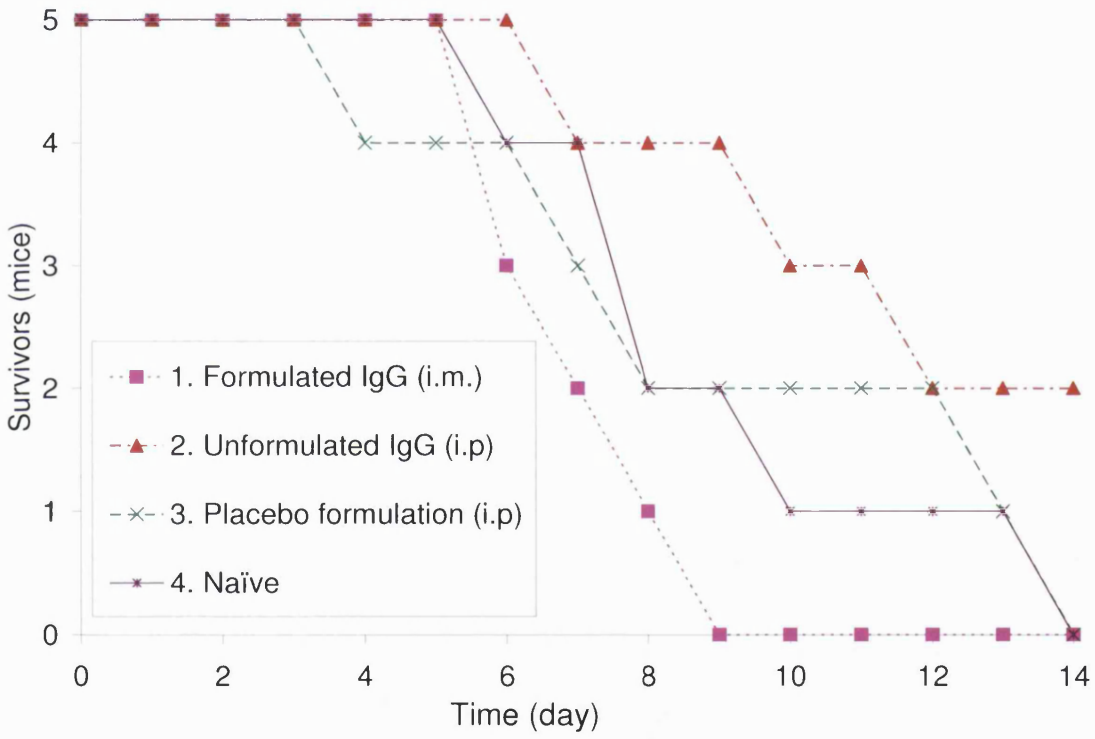

7.5 Discussion

7.5.1 *In vitro* characterisation of formulated F1 + V IgG

As anticipated, substitution of human polyclonal IgG for the F1 + V antibodies did not affect formulation characteristics such as spray-drying yield, EE and particle morphology (observed by SEM – not shown). This was expected, since both antibodies were of the IgG sub-group, and account for only ~3.3% m/m of the total formulation.

The proportion of the antibody load released after 2 h incubation in 37°C PBS (~30%), was consistent with data obtained for this formulation with Flebogamma® (see

Chapters 4 and 5). The SDS-PAGE bands for the released F1 + V IgG appeared unchanged compared to the unformulated sample, both of which were present as single bands of ~150 kDa. Firstly, this suggested that the IgG purification process was successful, since the presence of other serum proteins would have appeared on the gel. Secondly, this confirmed that the formulation process did not alter the antibody molecular weight, or cause aggregation, which was further confirmed by the FFF data. Interestingly, the F1 + V IgG bands on the SDS-PAGE gel were narrower than the Flebogamma® bands. This may have been due to the Flebogamma® being prepared from a wide spectrum of pooled human IgG, whereas the macaque monkey serum would have mainly contained IgG specifically targeted to F1 or V antigens, albeit polyclonal.

Approximately 100% of the protein concentration measured by the Bradford assay was detected as IgG by ELISA, confirming that the formulated antibody remained in an active conformation. However, comparison of the absorbance values of the two standard lines indicated that equivalent concentrations of unformulated Flebogamma®, gave a greater response than the unformulated F1 + V antibodies. This was probably because the ELISA reagents used had a higher binding affinity for human IgG than for IgG from macaque monkeys.

7.5.2 *In vivo* protection studies

The first study was an attempt to demonstrate the MR properties of the formulation, by dosing the antibody 48 h in advance of the infection challenge. Unfortunately, none of the animals survived beyond 9 days. This result was surprising given that the plasma elimination half-life of macaque monkey F1 + V IgG in mice was previously measured to be 6-8 days (although with undetectable levels after 10 days) (Williamson *et al.*, 2005). Thus, the unformulated IgG group should still have had adequate levels of IgG to protect the mice at 48 h post-dose. Since all animals dosed with the unformulated IgG had died by day 9, it could not be claimed that either the formulation process, or being contained within the formulation excipients, had decreased the activity of the antibody. Rather, either the treatment dose was too low, or the unformulated IgG in the mice had been substantially cleared by 48 h. In the latter case, this would have meant that the initial IgG burst-release of the formulation would also have been cleared, and thereby would not have been available to supplement the increasing systemic levels of IgG resulting from the MR portion of the formulation. Therefore, there may have been lower than anticipated plasma levels of IgG at 48 h post-dose due to both clearance and

retarded release. Although there was a statistically significant ($p<0.05$) increase in the mean TTD for the formulated antibody (only when delivered i.m.) compared to the unformulated antibody (8.8 days versus 7.2 days), given that the placebo formulation also gave a statistically significant ($p<0.05$) increase in TTD, and the existence of considerable overlap in individual TTDs between the groups, this statistical finding was considered meaningless in practical terms.

As a result of the findings of the first study, a second study was conducted using a 10-fold higher dose of formulated and unformulated IgG, and a shorter duration between treatment and infection, in order to increase the likelihood of demonstrating some level of protection from the formulated antibody. In this second study the formulated IgG was only administered i.m., since there was some evidence in the first study that this was more effective than the i.p. route. The strength of the *Y. pestis* infection was also reduced by ~10-fold. However, the formulated IgG still failed to protect any of the mice from infection, whereas 2 of the 5 mice administered unformulated IgG survived the duration of the study. Although the IgG doses had been increased from the first study, the surprising fact that only 2 of the 5 mice treated with unformulated antibody survived, suggested that the administered doses were still not high enough. The dose of formulated IgG administered *per* animal (2 mg) was the same as the unformulated IgG dose. However, it was anticipated that after 2.5 h only ~30% of this IgG load would have been released, given the *in vitro* release profiles measured in Chapter 5 of this thesis. With hindsight, if the full 2 mg of unformulated antibody only protected 2 of the 5 mice, ~30% of this dose from the formulation would not have been expected to protect any of the mice in the group receiving formulated antibody. Therefore, an even higher dose of microparticles should probably have been administered in order to achieve plasma IgG levels that would have offered protection. The *in vivo* IgG release profile of this formulation had not been measured. The previous study from which the *in vitro* release profile method used in the work this thesis was partially based, had, in fact, found that *in vivo,* a reduced initial burst-release was observed (Jiang *et al.*, 2002). This reduced initial burst may have been due to the adsorption of endogenous proteins, present in the biological medium, onto the particle surface. Therefore, the concentration of free IgG may have been substantially less than 30% of the unformulated IgG dose.

Despite the inability of these studies to demonstrate that the formulated antibody had provided any *in vivo* protection, they do not provide any evidence to suggest that the antibody was inactivated by the formulation process. Rather, the unformulated antibody had less activity than anticipated from previous serum transfer studies. This loss of

activity may have resulted from the serum purification process, or the storage and transport of the purified antibody. With more information on the concentration of free unformulated IgG required to confer protection, and the IgG release profile from the formulation *in vivo*, a more appropriate dosing schedule could have been devised that would have been more likely to generate positive outcomes.

7.6 Conclusion

Antibodies targeted against F1 and V subunits of *Y. Pestis* were purified from the serum of macaque monkeys. The purified antibodies were incorporated into the MR microparticulate formulation. Antibody released from the formulation appeared to be stable according to three different *in vitro* techniques, relative to both the unformulated antibody and the model antibody formulated in previous chapters of this thesis. Systemic administration of the formulated antibody failed to demonstrate any protection against *Y. pestis* infection in an *in vivo* mouse model. However, given the relative ineffectiveness of the unformulated antibody, and the estimated release profile of the formulation, this was likely to have been due to the administration of an insufficient dose, rather than to the formulation causing inactivation of the therapeutic antibody.

8 DEVELOPMENT AND TESTING OF PARTICULATE FORMULATIONS FOR THE NASAL DELIVERY OF ANTIBODIES

8.1 Abstract

Therapeutic antibodies offer a potential treatment for, or means of protection against, airborne infections. For this application, it may be desirable to deliver the antibody directly into the nasal cavity, one of its potential sites of action, since this would be more efficient and convenient than systemic administration.

Formulations of a model antibody (human IgG) were developed using albumin, sodium chloride and disaccharides. A combination of these excipients allowed the efficient spray-drying (yield >70%) of the antibody into a microparticulate (1-15 μm) dry powder that was rapidly soluble in aqueous media. The water content and crystallinity of the formulations were also measured, with both properties being affected by the substitution of some of the sodium chloride in the formulation, with lactose. The antibody was found to be stable following the formulation process, as determined by gel-electrophoresis, field-flow-fractionation and enzyme-linked immunosorbent assay. Incubation of an *in vitro* epithelial cell line in the presence of solutions of the formulations (at concentrations of up to 2500 μg/mL) was found not affect cell viability.

The aerosolisation properties of the formulations were tested using Bespak's "Unidose-DP™", dry-powder nasal device. The powder aerosol was analysed by laser diffraction, high-speed video and dose deposition in Bespak's nasal cast model. For the latter experiment, a range of additional excipients were either dissolved in the spray-drying liquid feed (leucine), or blended with the spray-dried powder formulation (magnesium stearate, Aerosil® and lactose). The major dose deposition site of the standard spray-dried formulation was the nasal vestibule (~55%). The addition of leucine and Aerosil® resulted in a 10% increase in the deposition beyond the nasal vestibule, with ~45% of the delivered dose being deposited in the turbinates, olfactory region, and nasal-pharynx.

8.2 Introduction

Therapeutic antibodies offer a potential treatment for, or means of protection against, airborne infections. Humanised antibodies can be produced to specifically target antigens on pathogenic bacteria, viruses or toxins. The binding of such an antibody could result in the immobilisation of the pathogen, or the triggering of the host's immune system to phagocytose the pathogen. For this application, it may be desirable to deliver the antibody directly into the nasal cavity, at its site of action, as this would be more efficient than systemic administration, where only a small fraction of the dose would reach the surfaces of respiratory tissues. This is a particular consideration for antibodies, because they are expensive bio-therapeutics, and thus minimisation administered dose would be highly desirable. Furthermore, oral bioavailability of antibodies is invariably very poor. They are broken down by proteases that exist in the gastrointestinal tract. Therefore, delivery by a nasal inhalation device would be a convenient, less invasive method of administration compared to injection, resulting in higher patient compliance.

Potential methods of nasal drug delivery include the use of liquid drops, aqueous sprays, fluoroalkane propellant-based aerosols and dry powders, although for commercially available products only liquid drops and aqueous sprays have been utilised as delivery methods. The dry-powder technique, used in this project, had advantages of drug stability (providing the device is sealed-off from moisture), increased retention in the nasal cavity (Kublik and Vidgren, 1998), and requires less co-ordination from the patient. However, it was important to ensure that the particles constituting the powder possessed the aerodynamic properties required to reach the appropriate areas of the nasal cavity, giving consideration to the fact that the patient's own inspiration pressure will contribute to the dispersion of the powder particles. Spray-drying has become a popular method of producing dry-powder formulations of protein pharmaceuticals, because it is a rapid and easily scalable process. It was a potentially viable option for antibodies, providing the appropriate excipients and conditions could be developed to avoid the common problem of antibody aggregation, due to the thermal and shear stresses of the process (Wang *et al*, 2007).

In this work, a model antibody (human IgG) has been formulated, by spray-drying, as a microparticulate dry powder, which was rapidly soluble in aqueous media. It was anticipated that the composition and diameter of the spray-dried microparticles might negate the need for a separate lactose carrier, as used in the dry-powder formulation of

small drug molecules. The IgG was obtained as an aqueous solution formulated in a 1:1 mass ratio with sorbitol (Flebogamma®), to maintain solution stability. Spray-drying such a solution appeared favourable, since sugars such as sorbitol can form a glassy-matrix around the antibodies, maintaining their stability in the dry state. However, due to the low glass transition temperature (T_g) of sorbitol, modifications to this formulation were required to obtain a stable spray-dried product (Maury *et al.*, 2005a). Therefore, two formulations were developed using other excipients, including bovine serum albumin (BSA), sodium chloride (NaCl) and lactose. NaCl and lactose are FDA-approved excipients for use in dry-powder inhaled formulations, which have also been found to enhance the aerosolisation properties of powders (Chan *et al.*; 1997, Bosquillon *et al*, 2001). After further optimising the formulations in terms of spray-drying yield, they were characterised in terms of antibody content, stability and activity, by a variety of techniques. Particle geometric diameter was measured by laser diffractometry, and water content by thermo-gravimetric analysis (TGA). The formulations were also compared in terms of toxicity on *in vitro* epithelial cell lines, and crystal content by X-ray powder diffraction (XRPD). The aerosolisation properties of the formulations in Bespak's "Unidose DP™", dry-powder nasal devices, were assessed. The powder aerosol from the device actuation was analysed by laser diffraction and high-speed video. The optimised formulations were then used as collected from the spray drier or were blended with various excipients to bring about further improvement to the powder's dispersion properties. The dose deposition in Bespak's nasal cast model was measured for all of the formulations.

8.3 Method

8.3.1 Development of basic formulations

Aqueous solutions containing Flebogamma® (human polyclonal IgG with sorbitol) were prepared iteratively with or without one or more of the following excipients, in various proportions: BSA, NaCl and lactose. These solutions were spray-dried at an inlet temperature of 140°C, 95% aspiration, 800 L/h atomization airflow and 2 mL/min pump speed, to give an outlet temperature of 80-85°C. The spray-drying yields of the chosen formulations were further optimised by adjusting the feed concentration. Solutions were prepared which ranged from 20% m/v to 1% m/v, and product was collected from the collecting vessel, not the cyclone, due to the high temperatures used (see Discussion, Section 8.5).

8.3.2 Characterisation of the optimised formulations

The optimised formulations were characterised in terms of geometric particle diameter by laser diffraction, crystallinity by XRPD (Section 8.3.3), water content by TGA (Section 8.3.4) and toxicity to *in vitro* cell lines by MTT assay (see Section 2.6.1). Protein content and antibody stability were assessed by dissolving the spray-dried powders in PBS, to make protein solutions of 125 μg/mL. These solutions were analysed by the Bradford assay, SDS-PAGE, ELISA and FFF (Sections 2.5.1-2.5.3). The latter was performed using a variable cross-flow (ranging 0.5-3.0 mL/min) in order to screen for higher molecular weight aggregates.

8.3.3 X-ray powder diffraction

X-ray powder diffraction (XRPD) was used to determine the presence of crystalline and amorphous content in the spray-dried formulations. A Philips PW 3710 XRPD was used to analyse the formulations, running at 45 kV, 30 mA, and scanning from 5-45°.

8.3.4 Thermo-gravimetric analysis (TGA)

The water content of the two formulations was determined in triplicate using a Pyris 6 TGA (PerkinElmer, Wellesley, USA), after storage in a vacuum desiccator. A sample of 2.5-4.5 mg of powder was heated from 30-250°C, at 10°C *per* minute. The percentage weight change of the sample was measured, as its water content was evaporated. The water content of formulations was compared using Student's t-test.

8.3.5 Production of powder blends

The spray-dried powder of Formulation F1 (see Results, Section 8.4) was used to produce blends with various excipients, as given in Table 8.1. The excipient was gradually added to the spray-dried powder while mixing. Once addition was complete, the powder was blended (Turbula, WAB, Switzerland) for 15 min. The exception to this was leucine, which was added to the formulation solution prior to spray-drying.

Table 8.1 Details of excipients added to spray-dried nasal formulation F1

Excipient	Quantity added (as a % of F1 mass)	Method of addition
L-Leucine	1	Dissolved in spray drier liquid feed
Magnesium Stearate	1	Blended with spray-dried powder
Aerosil® 200 Pharma	10	Blended with spray-dried powder
Respitose® ML001 (lactose)	100 (i.e. 1:1 mass ratio)	Blended with spray-dried powder

8.3.6 Aerosolisation testing of formulations

Unidose DP™ devices were filled with the basic formulations F1 and F2 and powder blends. The device perforators were filled until completely full, with compression of the powder by gentle tapping. The powder weight that was loaded into each device was recorded. The basic formulations were characterised by aerosol particle diameter (Section 8.3.7) and high-speed video (Section 8.3.8). *In vitro* nasal deposition was determined for the basic formulations, and the blended powders, using nasal cast models, as described in Section 8.3.9).

8.3.7 Laser diffractometry of aerosol

After the filling of nasal delivery devices with the formulations, the particle diameter of the aerosols of six devices for each formulation were analysed by laser diffraction using a Malvern Spraytec (Malvern Instruments, UK). A standard refractive index presentation of 1.5 + 0.5 was used. Data were recorded for 0.5 s at 2500 Hz acquisition frequency, with the laser positioned 3 cm above the device orifice. The data from the six devices were averaged.

8.3.8 High speed video

The aerosol plume from one device of each formulation was recorded at 1000 frames/s under white spot-lights. Several still frames from each video, highlighting the sequence of events, were selected for the purpose of this thesis.

8.3.9 Deposition in Bespak's nasal cast model

Bespak's nasal cast model, a life-size model of the nasal cavity built from MRI images (Kelly *et al.*, 2004), was used to determine the deposition pattern of drug within the nose, when delivered from the device. Three identical nylon nasal casts were used for these experiments. Each cast is made of five anatomical sections: nasal vestibule, front tubinates, olfactory region, rear turbinates and nasal pharyinx, plus a filter and an adaptor to hold the device in a perpendicular position (see Figure 8.1). The casts were assembled with every surface being lined with an artificial mucus composed of a 75:25 ethanol:glycerol mixture. Four Uni-Dose DP™ devices *per* formulation were filled and weighed. For each experiment, two devices were actuated into the cast, one in each nostril, while covering the other nostril and applying a 25 L/min airflow for 12 s. The devices were weighed after actuation, in order to determine the amount of powder remaining in the device. The powder deposited in each of the five compartments of the

cast (nasal vestibule, front turbinate, olfactory region, rear turbinates, naso-pharynx) was collected into 20 mL of PBS, by thorough rinsing to allow powder dissolution. The same procedure was adopted to collect any powder deposited on the adaptor. Powder that had collected on the outside of the actuator was collected on a cotton wool swab and dissolved in 20 mL PBS. The filter was disintegrated in 20 mL PBS. Aliquots of the actuator swab and filter samples were collected using syringe with a 400 μm filter. The protein concentration of all the samples was determined by the Bradford assay. To determine the amount of protein delivered, and remaining in the device, approximately 5 mg was accurately weighed into 1 mL of PBS, and diluted 20-fold, before assaying the protein concentration. The protein deposition in each compartment of the cast was expressed as a percentage of the total protein dose, calculated from the mass of powder in the two devices, and the protein content of the powder. Protein delivery to the "bioavailable" regions of the nasal cavity (an attempted equivalent to the pulmonary fine particle fraction) was determined by summation of the dose in the front turbinates, olfactory region, rear turbinates, naso-pharynx and filter, as a percentage of the delivered dose (i.e. the dose loaded in the devices, minus the dose remaining in the device, on the actuator, on the adaptor, and any unaccounted protein). Each run was performed in duplicate for each formulation. In preparation for the above work, four experiments were conducted (in triplicate, presented in Appendix VII), comparing the two basic formulations, with and without the application of 25 L/min inspiratory airflow (without the use of mucus), and to compare the metal and nylon cast models.

Figure 8.1 Schematic diagram of the nylon nasal cast. The cast is divided into five anatomical sections, with the shape of that part of nasal cavity cut out inside each of them. The filter collects any particles that would theoretically go through to the lungs, and the adaptor holds the device at a fixed angle in the nostril.

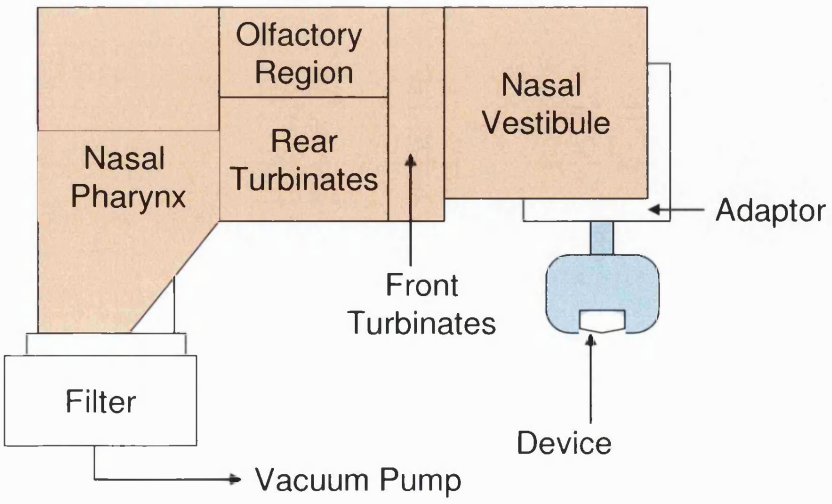

8.4 Results

8.4.1 Development of the IgG formulations

Spray-drying of the received IgG-sorbitol (Flebogamma®) solution alone, with no other excipient, resulted in the product depositing on the walls of the cyclone, rather than in the collecting vessel. A high spray-drying outlet temperature had to be employed in order to dry the powder fully. Therefore, product deposited on the cyclone could not be collected in the final yield, since a very high temperature on the glass surface of the cyclone may have caused protein denaturation. Indeed, this theory was demonstrated by attempting to dissolve a sample from this powder in water. The cyclone-deposited powder did not completely dissolve, leaving visible particles suspended in the solution. This suggested that some physicochemical changes had occurred in the protein structure. Therefore, consideration was given to using a lower outlet temperature, obtaining a wet product, and then completing the drying process by vacuum. However, this was also found not to be a viable option, since this resulted in a powder composed of large agglomerates, as the microparticles generated in the spray drier lost their individuality when collected wet. This observation was found by laser diffraction sizing (data not shown). On the other hand, the product yield in the collecting vessel was improved when the protein-to-sorbitol ratio was increased by the addition of BSA. Incorporation of NaCl was also found to improve product yield. The final formulation (F1) contained the four components (IgG, sorbitol, BSA and NaCl) in a 1:1:1:1 mass ratio. A variation of this formulation (F2) was also prepared by substituting half of the NaCl with lactose.

Reducing the solid concentration of the liquid feed increased the spray-drying yield by ~20% (Table 8.2). There was also a maximum of 2 μm reduction in particle diameter. A 5% m/v feed concentration was chosen for further use, since there was little additional yield advantage of using a 1% m/v concentration. However, the latter had a substantially larger volume, resulting in longer duration of the manufacturing process, thereby increasing the potential for heat-related deterioration of the final product.

Table 8.2 The increase in spray-drying yield, and reduction in particle median volume diameter (D50%) observed with reducing feed concentration of nasal formulation F1 (n=1).

Solid conc. (% m/v)	*Feed volume (mL)*	*Yield (%)*	*D50% (μm)*
20	1.0	63	6.95
15	1.3	72	6.62
10	2.0	76	5.85
5	4.0	81	5.31
1	20.0	81	4.93

8.4.2 Formulation characterisation

8.4.2.a) Laser diffraction and scanning electron microscopy

Both formulations were composed of non-aggregated microparticles, with median volume diameters of approximately 5-7 μm (Figure 8.2 and Table 8.3). Larger droplets could be achieved by lowering the atomisation pressure, or increasing the feed viscosity, but to make an appreciable difference would result in a substantial decrease in yield (see above and Chapter 4). The particle size measured by laser diffraction correlated with the microscopy images (Figure 8.3), with F1 appearing to have small crystals on the particle surfaces. Both formulations appeared to consist of non-spherical microparticles.

Figure 8.2 Typical geometric volume diameter distribution of a spray-dried nasal formulation as measured by laser diffraction in methanol. (Representative diagram from several measurements).

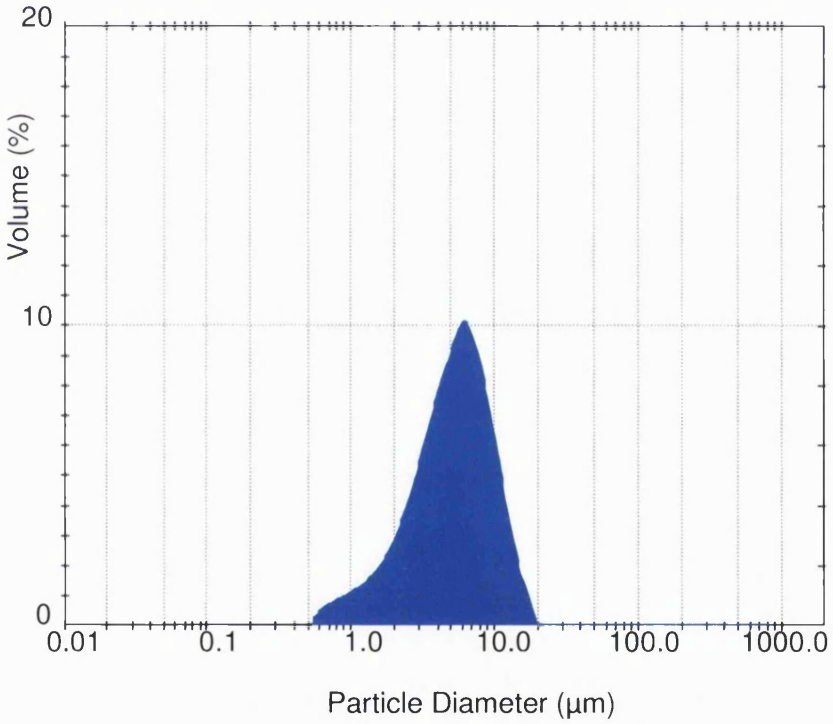

Table 8.3 Geometric derived particle diameters of formulations measured by laser diffractometry. Derived diameters were as follows: D10%: the diameter that 10% of the volume of particles was smaller than, D50%: the diameter that 50% of the volume of particles was smaller than (i.e. median diameter), D90%: the diameter that 90% of the volume of particles was smaller than, (n=3, mean ± SD).

	D10% (μm)	D50% (μm)	D90% (μm)
F1	2.0 ± 0.2	5.4 ± 0.1	10.5 ± 0.2
F2	2.7 ± 0.1	6.6 ± 0.4	12.1 ± 0.8

Figure 8.3 Scanning electron micrograph of a) F1 and b) F2 nasal formulations. Both images depict non-spherical, 'dimpled' microparticles, with the appearance of small crystals on the surfaces of F1.

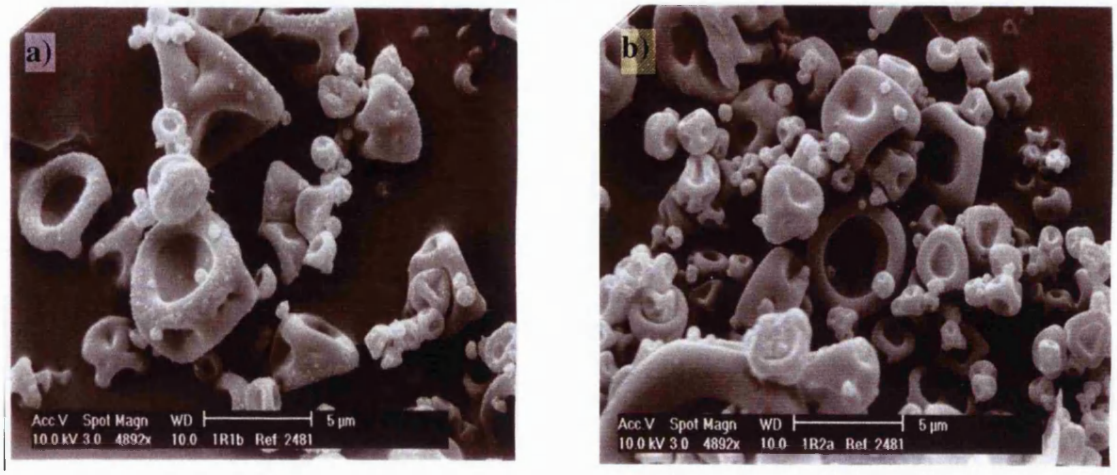

8.4.2.b) X-ray powder diffraction

X-ray-powder diffraction (XRPD) identified that both F1 and F2 powders were largely amorphous in structure, but had some crystalline components too, presumably due to the presence of NaCl in the formulation (Figure 8.4). Formulation F1 had a larger crystalline content possibly due to its higher NaCl content.

Figure 8.4 X-ray powder diffraction to investigate the crystallinity of the basic spray-dried nasal formulations of IgG. Peaks amongst the amorphous background diffraction noise, suggested crystalline regions.

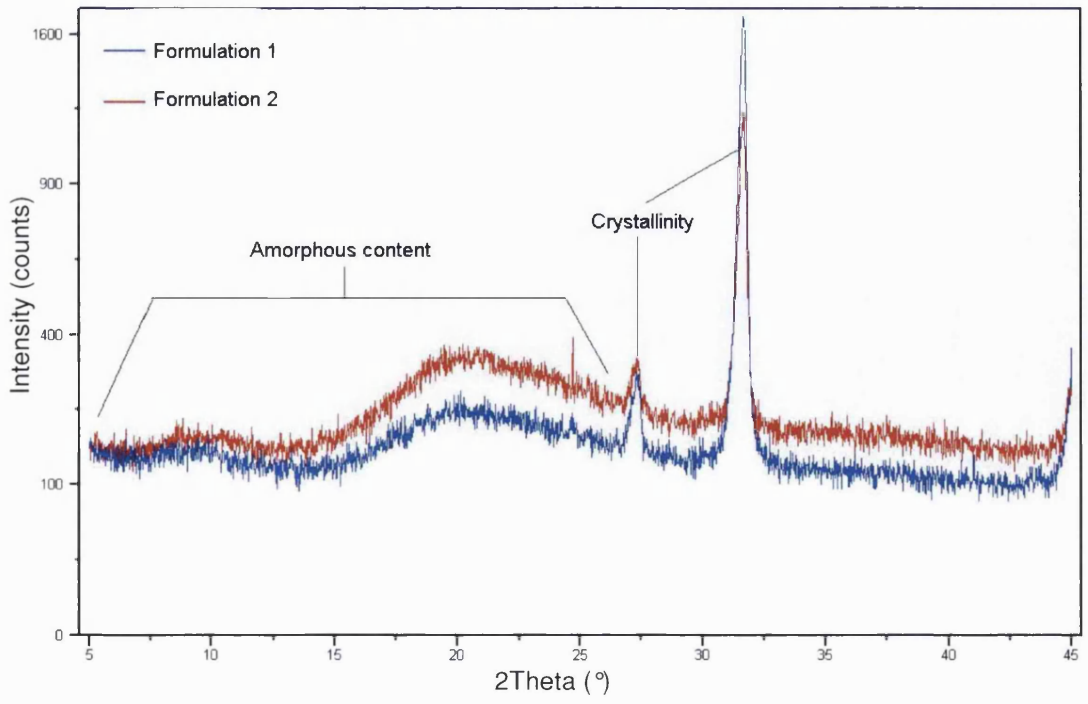

8.4.2.c) Thermo-gravimetric analysis

The water content of the spray-dried formulations was determined by TGA (Table 8.4). Formulation F2 was found to have a ~1% higher water content than F1 (statistically significant, $p<0.05$).

Table 8.4 Thermo-gravimetric analysis of water content in spray-dried, nasal formulations of IgG (n=3, ± SD. Means significantly different $p<0.05$, t-test).

Formulation	*Moisture Content (% m/m)*
F1	1.5 ± 0.3
F2	2.7 ± 0.5

8.4.2.d) Stability of formulated antibody

The Bradford assay determined that the total protein content of both formulations was approximately 50% m/m (as expected given the composition formulations). Gel-electrophoresis analysis (SDS-PAGE) of spray-dried samples identified that the antibody and BSA appeared to remain monomeric, with each having appeared as a single band of the expected molecular weights of approximately 150 kDa and 60 kDa, respectively (Figure 8.5). However, it can be seen that the albumin, even before spray-drying (Lane 2, Figure 8.5), contained impurities of higher-molecular weight. The molecular weights were confirmed by field-flow fractionation (FFF), with the molecular weight of the IgG being approximately 150 kDa (Figure 8.6). There was less than 5% dimerisation, and no higher order aggregates visible on the trace. The ELISA detected approximately 100% of the antibody concentration present in the samples, before and after spray-drying, suggesting that the formulation process did affect the biological activity of the IgG (Figure 8.7).

Figure 8.5 Gel electrophoresis of nasal IgG formulations F1 and F2 before and after spray-drying. Key - Lane 1: Molecular weight marker, 2: Albumin standard before spray-drying, 3: IgG standard before spray-drying, 4: F1 before spray-drying, 5: F1 spray-dried, 6: F1 spray-dried, 7: F2 before spray-drying, 8: F2 spray-dried, 9: F2 spray-dried,*= 150 kDa reference, ** = 50 kDa reference.

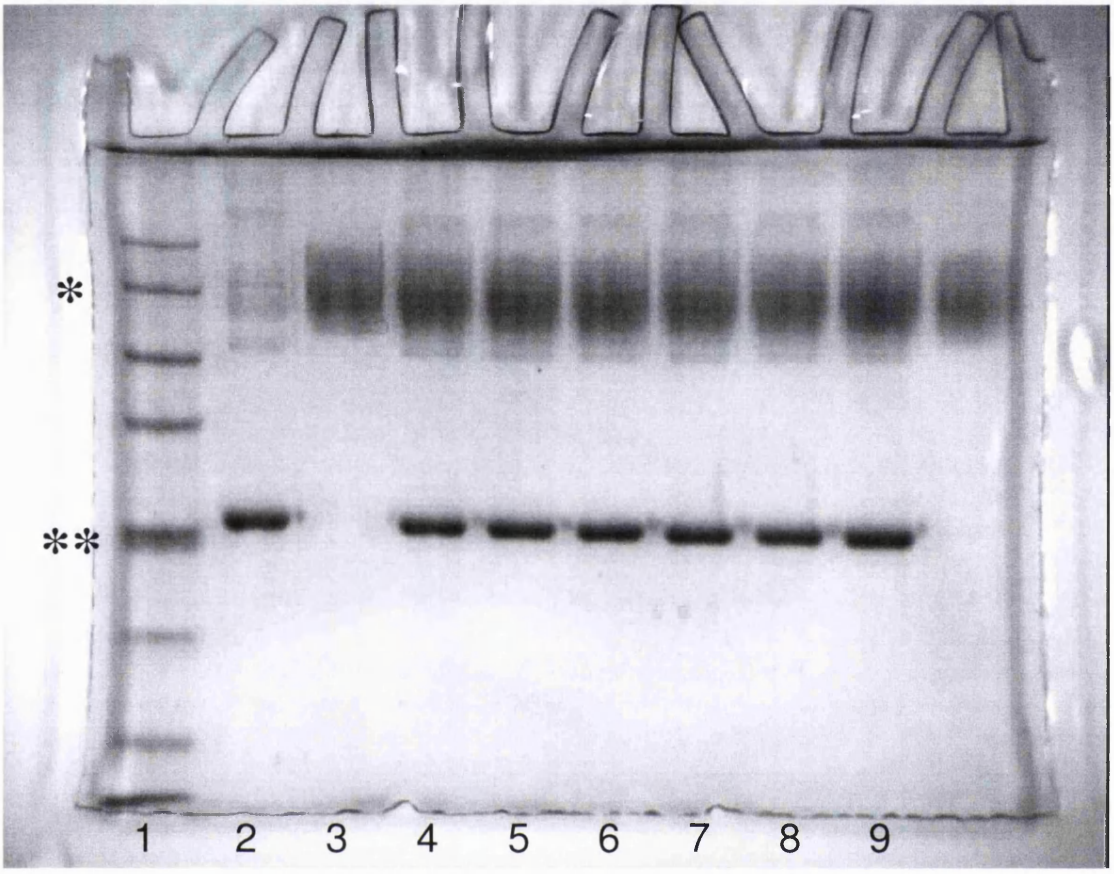

Figure 8.6 An example of molecular mass Vs elution time produced by field-flow fractionation. The two peaks are the BSA (first peak) and IgG (second peak) contained in the formulation. The shoulder on the IgG peak appears to be due to dimers, but impurities in the BSA may also have contributed to it. (The molecular mass axis has been calibrated based on the IgG calibration constant, and thus the BSA molecular mass shown here of ~100 kDa is not accurate).

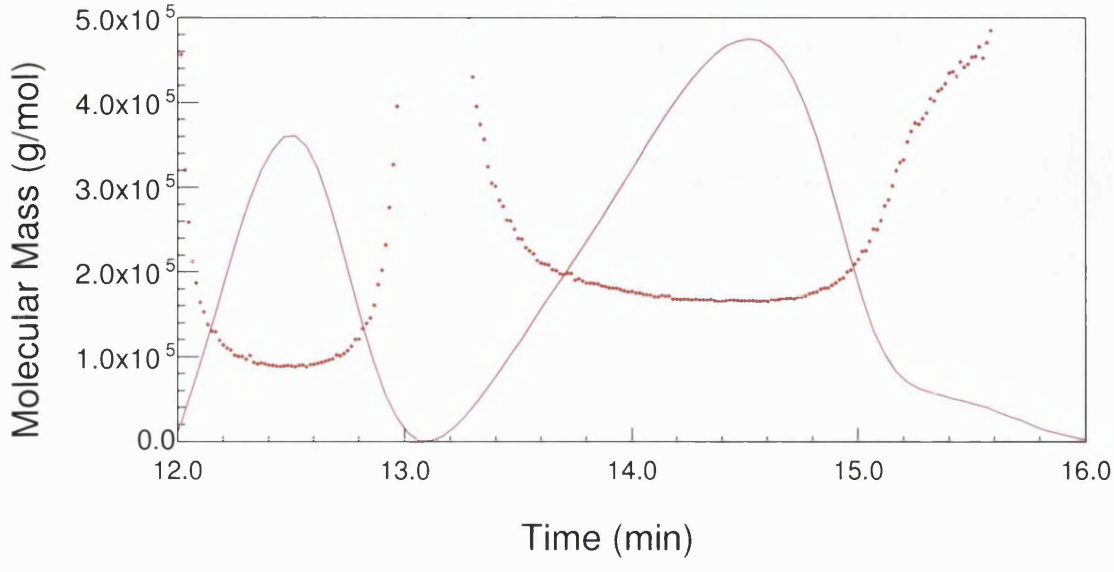

Figure 8.7 Enzyme-linked immunosorbent assay of formulated IgG, to compare the biological activity of the IgG before and after spray-drying (n=3, mean + SD)

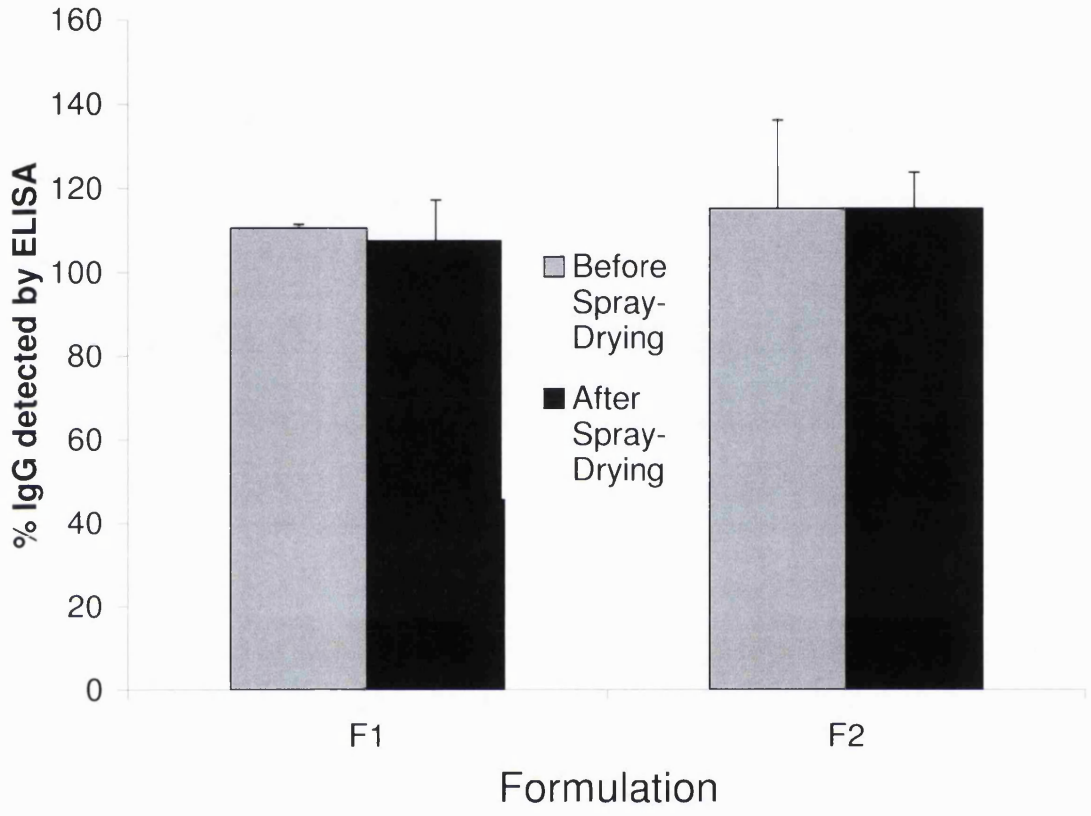

8.4.2.e) In vitro cell toxicity

The results of the MTT assay indicated that neither formulation F1 or F2, or separate samples of lactose or Flebogamma®, were toxic to Chinese hamster ovary-K1, epithelial cell lines when exposed to concentrations of up to 2500 µg/mL (Figure 8.8). However, as expected, the 25 kDa, branched, poly(ether imide) (PEI) positive control was toxic to the cells, causing cell viability to fall below 20% at concentrations of 25 µg/mL or greater.

Figure 8.8 The effect of dose of incubation of IgG formulations on percentage of Chinese hamster ovary cell viability. An MTT assay was used to indicate the *in vitro* viability of CHO-K1 epithelial cells after 4 h exposure to formulations F1 and F2 (n=3 + SD, *=negative control, **=positive control, poly(ether imide) (PEI)).

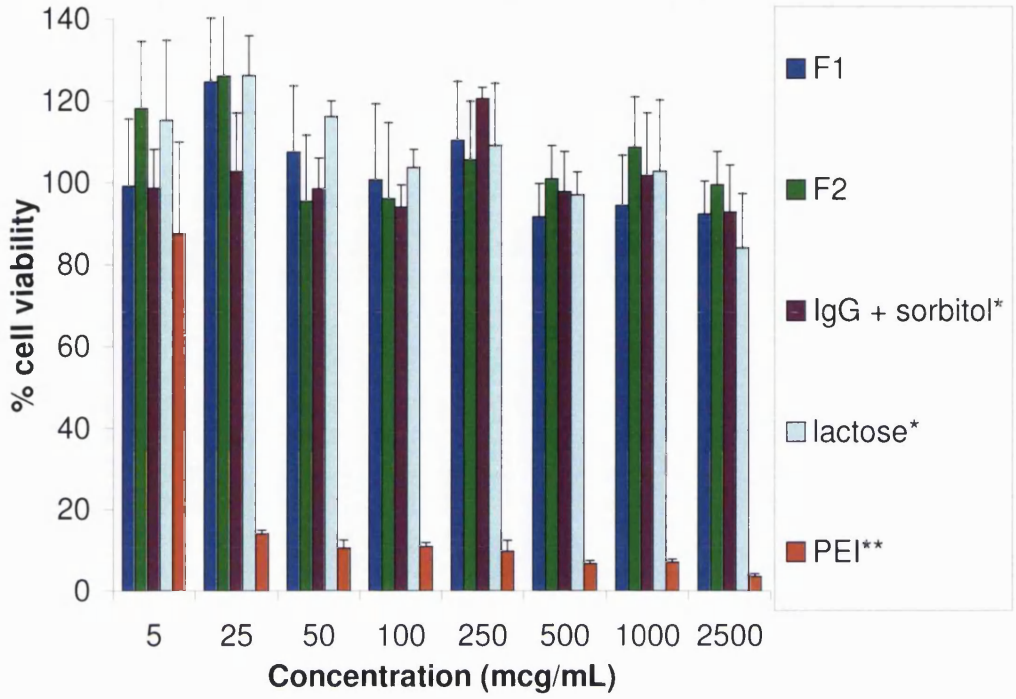

8.4.3 Aerosolisation testing

8.4.3.a) Laser diffraction of aerosol

The Malvern Spraytec was used to measure the diameter of the aerosol particles of formulations F1 and F2, actuated from Uni-Dose DP™ devices. The derived diameters are shown in Table 8.5. Given that laser diffraction of the formulations in ethanol identified that both formulations consisted of microparticles between 1-10 µm in diameter, it would appear that when aerosolised, F1 produced a greater proportion of individual (dispersed) particles, and aggregates < 20 µm, than did F2. Formulation F2 contained more than double the volume of aggregate particles > 60 µm than did F1. The average volume diameter distributions are illustrated in Figure 8.9.

Table 8.5 Derived geometric diameters of aerosol particles of nasal formulations F1 and F2, actuated from Uni-Dose DP™ devices (n=6)

Formulation	*D10% (µm)*	*D50% (µm)*	*D90% (µm)*
F1	8.41	37.1	123
F2	11.1	76.8	151

Figure 8.9 Comparison of particle diameter distributions of formulations F1 and F2 actuated from the Uni-Dose DP™ nasal delivery device, measured by laser diffraction. (Distributions are each an average of six separate measurements)

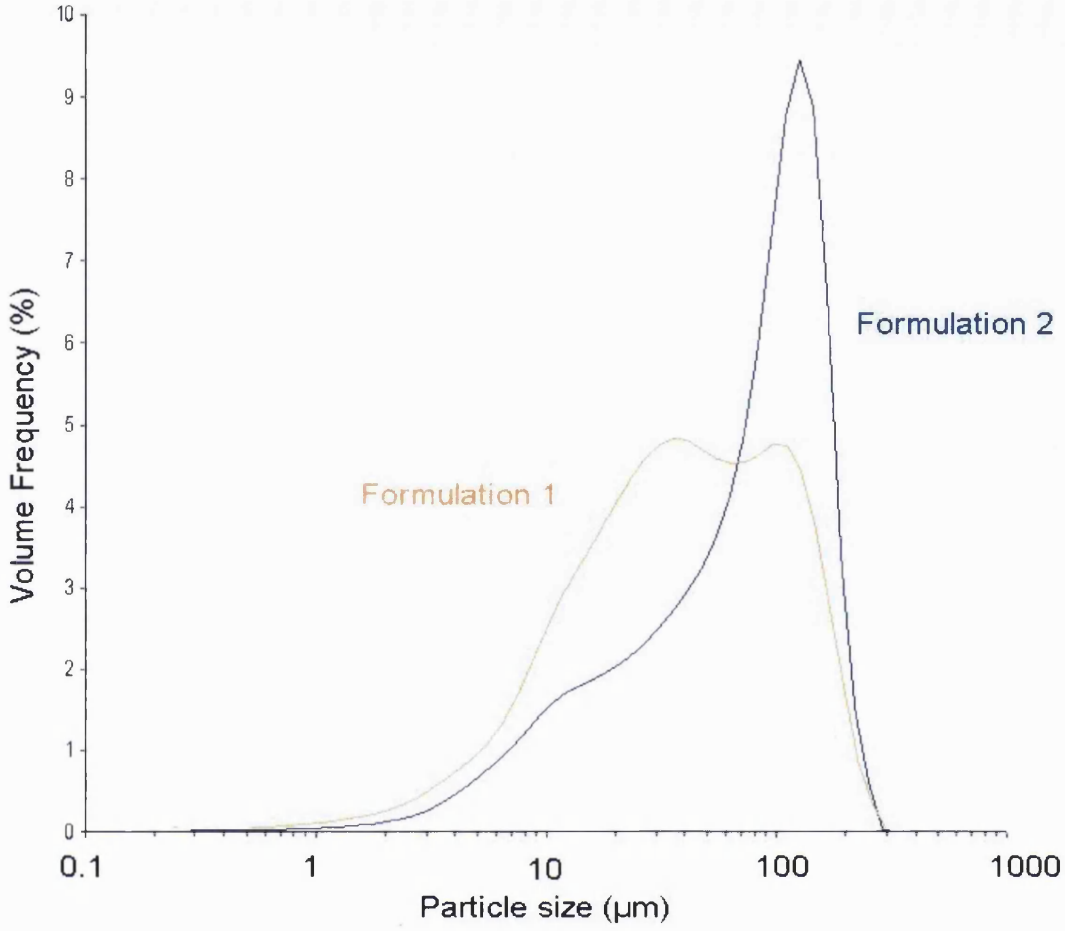

8.4.3.b) High speed video

Examples of images captured from the high speed video are shown in Figure 8.10. The pressure within the device forced out a plug of powder, which then dispersed in air into a fine plume.

Figure 8.10 Selected frames from a high speed video capture of a Uni-Dose DP™ actuating formulation F2. The frames illustrate the sequence of aerosol generation and dispersion.

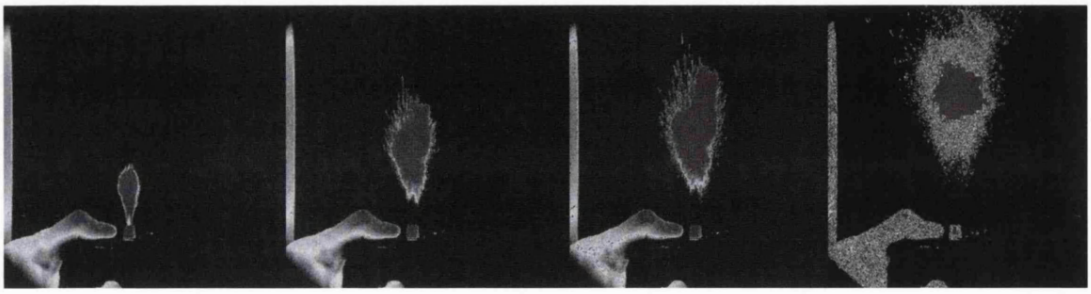

8.4.3.c) Nasal cast testing of basic formulations and blends with various excipients

Using the method described above to consistently fill the devices, it was clear that there were substantial differences in the achievable fill weights between different formulations. This is illustrated in Figure 8.11, where it can be seen that even between those formulations consisting of only spray-dried particles (F1, F2 and F1 + leucine), there were differences in the average fill weight. However, the largest difference was observed when F1 was blended with Respitose™, where the achievable fill weight was almost doubled, thereby allowing almost the same antibody dose to be delivered *per* device.

Figure 8.11 Average weight of powder that was loaded into each Uni-Dose DP™ nasal device for each formulation (n=4, mean + SD)

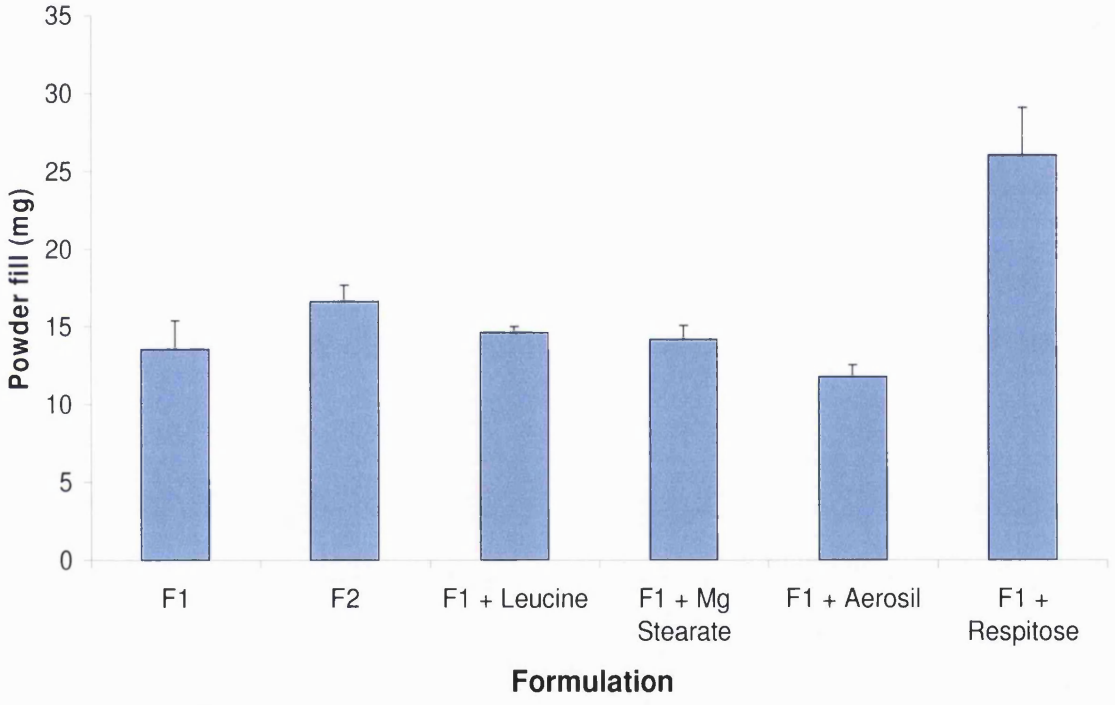

Figure 8.12 illustrates the data generated from weighing the devices used in the nasal cast experiment before and after actuation, in order to determine the percentage of the dose that had been actuated from the device. Based on these data, it can be seen that there was little variation between the formulations, and that the Uni-Dose DP™ was found to reproducibly eject 95-100% of the loaded dose.

Figure 8.12 Percentage of the loaded powder formulations that was actuated from the Uni-Dose DP™ devices used for the nasal cast experiments (n=4, mean + SD)

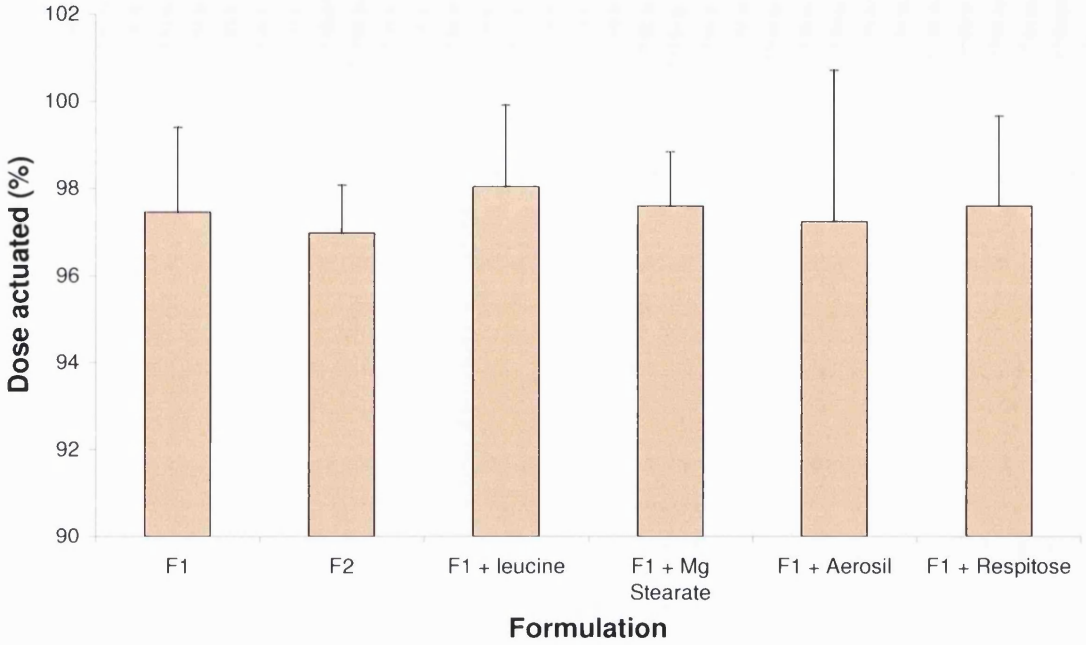

The nasal cast deposition data are given in Figure 8.13. For each formulation, the protein detected in each of the five compartments of the cast is given together with the calculated protein remaining in the device, and protein detected on the actuator surface, adaptor and filter. Based on the weight of formulation loaded into the devices used for each run, any protein that was unaccounted for was also calculated, and is shown in the Figure. It can be seen that majority of the protein (in most cases 50-65%) was deposited in the nasal vestibule. The two formulations with slightly lower deposition in this department were F2 and F1 + leucine. In the latter case, it appeared that this was compensated by a small increase in the deposition in deeper compartments of the nasal cavity. However, this was less clear for F2, and may be related to the larger amount of unaccounted protein for this formulation. In order to simplify these data, and highlight differences between formulations, Figure 8.14 illustrates the protein deposited beyond the nasal vestibule as a percentage of the delivered dose (see methodology Section 8.3.9). Here it can be seen that, whilst more than 30% of the dose reached these parts of the nasal cavity for all formulations, the leucine and Aerosil®-containing formulations had an even greater deposition (>40%).

Figure 8.13 Nasal cast deposition of protein in various formulations when actuated from Uni-Dose DP™ devices. One device was actuated into each nostril *per* run, two runs *per* formulation (mean, n=2).

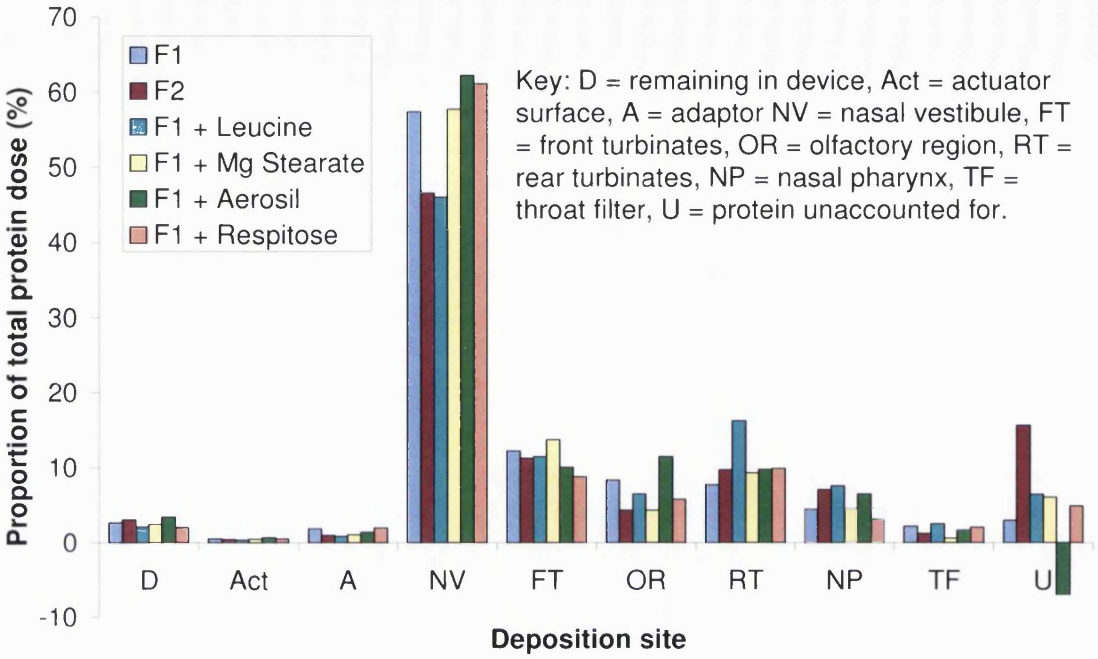

Figure 8.14 Delivery of protein in various formulations to the "bioavailable" regions of the nasal cast, when actuated from Uni-Dose DP™ devices. Values derived by summation of the dose in the front turbinates, olfactory region, rear turbinates and naso-pharynx, as a percentage of the delivered dose (i.e. the dose loaded in the devices, minus the dose remaining in the device, on the actuator and on the adaptor) (mean, n=2).

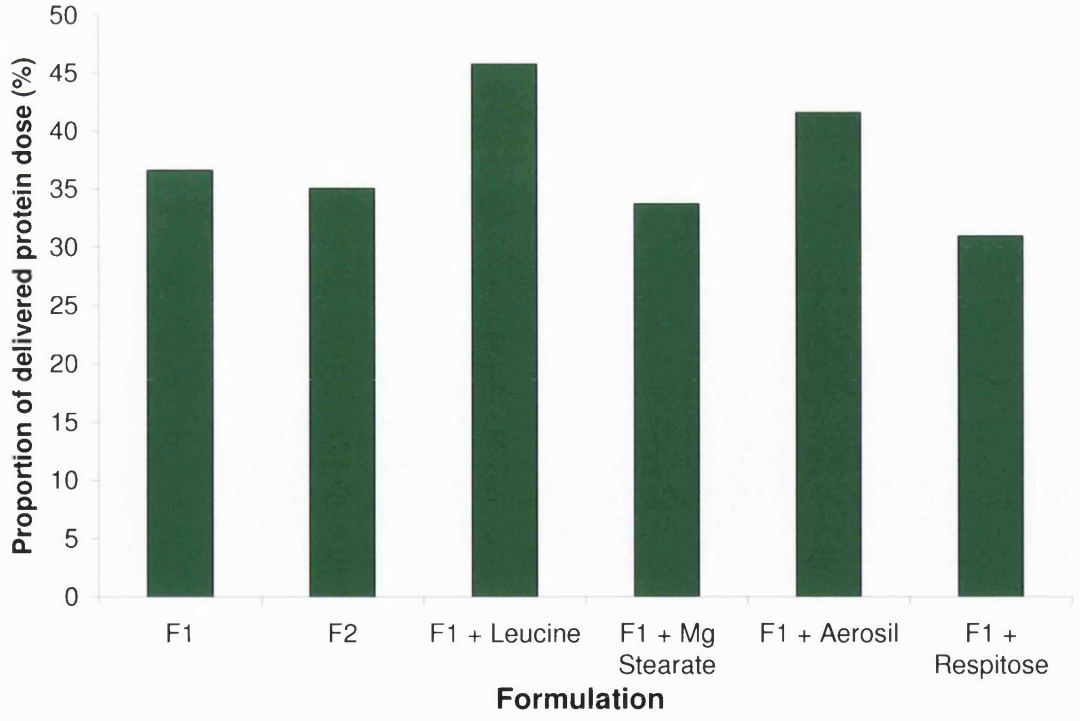

8.5 Discussion

8.5.1 Formulation development

The cyclone deposition experienced when spray-drying the IgG-sorbitol solution was thought to be due to the sorbitol's low glass transition temperature (T_g) (-3°C, Wang, 2000), and therefore 'sticky-point' temperature. Above a critical temperature (sticky-point), a phenomenon has been observed for some amorphous materials, in which their physical properties change to render them more adhesive. The sticky-point temperature of a material has been found to be related to its T_g (Ozmen and Langrish, 2002) (the temperature above which amorphous materials change from being in the glassy state to being in the rubbery state). When amorphous materials were heated beyond their sticky-point in the spray drier, the resultant particles were more likely to adhere to the cyclone walls as they passed through (Ozmen and Langrish, 2003). Static electricity may also have contributed to this effect (Maa *et al.*, 1998b). Unlike the spray drier collection vessel, which was relatively cool (almost room temperature), the cyclone was as hot as the outlet temperature of the spray drier [although other studies have adapted the spray-drier by adding a cooling jacket to the cyclone, e.g. Sebti & Amighi, 2006)]. Therefore, at the outlet temperatures required to properly dry the product (~80°C) the antibody was damaged, due to contact with the hot cyclone, as identified by the appearance of visible aggregates upon trying to dissolve the spray-dried powder in water. Regarding the double-emulsion, pulmonary formulations described in previous Chapters of this thesis, the volatile dichloromethane used in the emulsion, allowed lower outlet temperatures (~55°C) to be used to obtain a dry product, although there was appreciable cyclone deposition. As demonstrated in the previous Chapters, at outlet temperatures of ~55°C, antibody stability was not compromised, with emulsion formulations. Increasing the protein-to-sorbitol ratio by the addition of BSA, possibly raised the sticky-point temperature of the overall formulation, resulting in a decreased adherence to the cyclone wall.

At high concentrations, the feed was more viscous, and thus larger droplets were produced, given that the atomization energy remained constant (the atomisation airflow was held at 800 L/h) (Maury *et al.*, 2005b). This resulted in larger particles that did not dry, and so did not reach the final product, thereby reducing the yield. As mentioned in Chapter 4, the lab-scale spray drier (Büchi-191) used for the present work did not have the drying capacity to dry the larger droplets that would be required for these larger particles, without resulting in a substantial reduction in yield.

8.5.2 Formulation characterisation

Although larger particles of 10-20 μm diameter were considered optimal for nasal delivery, i.e. large enough to not pass out of the nasopharynx and into the lungs, yet small enough to be inhaled past the nostrils, the measured 1-10 μm mean diameter distribution of the optimised formulations could have been deposited within the nasal cavity, depending on the airflow conditions (Hinchcliffe and Illum, 1999). Also, it was postulated that the device would not be able to fully de-agglomerate the powder into primary particles, and thus agglomerates of the appropriate mean diameter may well have been formed.

The crystals observed on the particle surfaces of F1 were likely to have been sodium chloride (NaCl) crystals, as previously found by Chan *et al.* (1997), when they used NaCl in their microparticulate formulation. They anticipated that it was the presence of these crystals that enhanced their formulations' aerosolisation properties, measured in terms of fine particle fraction, since the uneven surfaces on the particles prevented agglomeration. For this application, such an effect may have enhanced the nasal deposition properties of the powder, perhaps requiring less inspiratory energy to disperse the powder into individual microparticles. The absence of such visible crystals on the surface of F2 was possibly due to the less amount of NaCl in this formulation. This suggested that somewhere between 12.5% m/m and 25% m/m was the minimum proportion of NaCl required in the formulation to produce this effect. The non-spherical morphology of the particles was typical of that observed by other researchers when spray-drying formulations containing a large proportion of protein at high temperatures. The morphology was possibly a combination of the 'dimpled' spheres observed when spray-drying pure antibody, and the raisin-shaped particles observed when spray-drying pure BSA (Maa *et al.*, 1997). Masters (1991) suggested that this deviation from sphericality was caused by a build up of vapour pressure within the spherical droplet as a result of high temperature, and the non-porous nature of an antibody-rich particle crust. The vapour pressure pushed on the crust, causing the particle to burst, and then collapse and 'dimple' (Maury, 2005).

X-ray powder diffraction was used to determine if the salt crystals, believed to be observed in the SEM images of F1, could be detected as a crystalline diffraction pattern. Spray-dried pharmaceutical excipients, such as sugars and polymers, are usually wholly amorphous, as the speed of solvent removal does not allow time for crystal formation. This is thought to benefit the stability of protein formulations due to the formation of a glassy matrix around the protein by the excipients (Wang *et al.*, 2007a). However, it

appeared that the crystalline nature of NaCl caused these formulations to show some crystallinity. The apparent greater crystalline content of F1 agreed with the observations of Chan *et al.* (1997), who found that crytallinity increased with NaCl content. However, F2 also contained detectable crystallinity despite the absence of visible crystals on the SEM image of the particle surfaces.

The water content of the formulations at less than 3% m/m was deemed acceptable for dry-powder inhalation, and was comparable with vacuum oven-dried, spray-dried, protein-carbohydrate powders (Maa *et al.*, 1998a). Although, the formulations generated in the present work were stored in a vacuum dessicator for several days before measuring, it was believed that the water content immediately after spray-drying was also very low, because laser diffraction sizing demonstrated that the powder microparticles were individually dispersible, and hence were dried thoroughly. The significantly higher water content of F2 (~3% m/m) (almost double the water content of F1) may have been due to the hydroscopic nature of lactose compared to NaCl. Higher water content may have disadvantages in terms of stability, as an aqueous environment would aid crystallisation of the amorphous content of the formulation, and aid chemical reactions that could compromise antibody activity (Wang, 2000).

Although it was clear from the SDS-PAGE results that spray-drying did not affect the molecular weight or aggregation status of the proteins, the impurities that were revealed with the BSA confused the picture slightly, since they overlapped with the antibody. However, it did appear that the formulation was an exact combination of the individual BSA and IgG samples, and that the spray-drying process had no impact on the appearance of the protein bands. The only aggregates detected by FFF were dimers, and these accounted for less than the 5% stipulated by the WHO as the aggregate limit for intravenous immunoglobulin formulations (Wang *et al.*, 2007a). The elution peaks of the formulation were again a simple combination of the IgG and albumin peaks, since they appeared when the two proteins were run separately. Therefore, some of the dimer peak may have actually consisted of the impurities found in the albumin. In addition, the MTT assay demonstrated that neither formulation of IgG caused a reduction in epithelial cell viability after exposure for 4 h.

8.5.3 Aerosolisation testing

The volume diameter distributions obtained, were acceptable based on Bespak's experience with the Uni-Dose DP™. It appeared that some of the dose was dispersed into individual microparticles, although as a function of total volume, most of the dose

was still in larger aggregates, thereby giving a bimodal peak for each distribution (Figure 8.9). It is important to note that these experiments relied on the pressure within the bellows of the device to provide the aerosolisation, not on any externally applied vacuum that would be essential for most dry-powder inhalers, which rely solely on the patient's inspiration to draw out the dose. In the case of this device, the patient's inspiration, if co-ordinated correctly, may have further enhanced the aerosolisation produced by the bellows.

For the 6 runs of each formulation in the experiment, it would appear that the F1 formulation powder was easiest to deagglomerate, suggesting that NaCl was superior to lactose in improving aerosolisation properties. Chan *et al.* (1997) proposed that NaCl crystals on the surface of microparticles reduced the surface contact between particles, thereby enabling them to flow more freely. In the field of oral tablet formulation, NaCl has been used as a lubricant (Palmieri *et al.*, 1986).

The high-speed videos captured sequence of events that took place when the Uni-Dose DP™ was actuated: a plug of powder was shot out from the device, which then dispersed into an aerosol cloud in air. However, there was a great deal of variability in the speed of the sequence, and in the distance the powder plug was shot, even when comparing devices filled with the same formulation. The primary cause for this variability appeared to be how the user depressed the bellows to actuate the device, in terms of the pressure used, and perhaps the speed that the pressure was applied (similarly reported by Guo and Doub, 2006). Other contributing factors may have been the device fill weight (this varied between formulations – see Figure 8.11), or how densely the powder was packed into the device.

As explained in the methodology, the Uni-Dose DP™ devices were filled by hand, loading the device perforator tube until completely full, and tapping the powder down as more was added. Therefore, differences in fill weight between formulations were related to their bulk densities. Respitose™, being composed of larger particles [10-150 μm, (DMV, 2007)], was likely to have a greater bulk density than a powder composed of microparticles (1-10 μm). Aerosil® had a density of only 50 g/L (Degussa, 2006), and hence this led to the decrease in powder fill weight, when it was blended with F1.

The powder deposition in the nasal cast had a similar pattern for all formulations. Approximately 95% of the dose was delivered to the nasal cavity, although the majority of it deposited no further than the nasal vestibule. The remaining 30-40% (exact value depending on the formulation) was deposited into deeper compartments of the nasal

cavity. Because there were no powder-based nasal formulations commercially available, and there are limited published data on nasal deposition, it was not clear whether this was an acceptable result. In-house experience at Bespak would suggest that with the Uni-Dose DP™ device, an acceptable formulation would achieve at least 15% dose deposition beyond the nasal vestibule. In terms of volume, the nasal vestibule was by far the largest compartment of the nasal cast. However, if the powder had been aerosolised completely into individual microparticles, the airflow should have carried them through the nasal vestibule without too much deposition. The work and data described in Appendix VII of this thesis, showed that the application of the 25 L/min airflow at the throat end of the model, to simulate a patient inspiring through the nose at the same time as using the device, did improve deposition in deeper compartments of the cast, and reduced nasal vestibule deposition (Kaye *et al.*, 2007). This was presumably due to enhanced aerosolisation, compared to purely relying on the force of compressed air within the device, to disperse and propel the powder into the nasal cavity. The amount of protein unaccounted for also decreased. This was probably due to the vacuum generated by the airflow, prevented powder falling back out of the nostrils. The airflow rate was a potentially important factor in determining whether those particles having diameters between 1 and 10 μm would have deposited in the nasal cavity (Hinchcliffe and Illum, 1999). An airflow of 25 L/min represented a deep inspiration by the patient. Other authors have demonstrated that this breathing pattern may be optimal for nasal deposition, since deposition was reduced if a cyclical, simulated-human, breathing pattern was applied (Häußermann *et al.*, 2002).

In terms of what would be clinically required, for the delivery of therapeutic antibodies against airborne infections, coverage across all regions of the nasal cavity, beyond the nasal vestibule, was likely to have produced the best clinical results. Antibody in the nasal vestibule was unlikely to be effective due to rapid clearance, and the limited surface area:volume ratio of this part of the nose. Also, the aerosolised pathogen being targeted would be more likely to deposit deeper in the nasal cavity. The aim of the delivery was not to achieve systemic absorption, and thus the turbinates did not need to be specifically targeted. Similarly deposition in the olfactory region, a potential route of delivery of small lipophilic drug molecules into the central nervous system (Graff and Pollack, 2005), was neither targeted nor avoided. Protein that was deposited in the filter, represented dose that would have been inhaled through the nasal cavity, into the lungs, or possibly ingested into the stomach.

The only difference in the deposition of the two basic formulations was the ~10%

decrease in nasal vestibule deposition of F2, despite the difference in particle diameter distribution of the aerosols, as determined by laser diffraction. Even this difference seemed to be offset by ~10% increase in undetected protein. Possible reasons for the lack of a complete mass balance could have been lack of precision of the Bradford assay, loss of powder out of the nostrils, incomplete dissolution of collected powder before sampling and/or adsorption of protein to the cast. The latter was found to be a problem with the metal model of the nasal cast. In Appendix VII of this thesis, it can be seen how protein recovery was reduced by up to 50% when the metal cast was used, compared to the nylon cast used here. The relatively small error bars in this work indicate that the variability in actuation observed during the high-speed video capture, did not translate into a drastic variation in nasal deposition.

Based on Figures 8.13 and 8.14, it would seem that the only additional excipients that showed any evidence of improving the formulation were leucine and Aerosil®. Respitose®, particulate lactose (10-150 μm), has been used as a carrier in most pulmonary dry-powder formulations (for a similar example to the formulations in this thesis see Chan *et al.*, 1997). Although the Respitose® particles were too large to be deposited beyond the nasal vestibule themselves, the hypothesis was that they would improve the flow and deagglommeration of the spray-dried microparticles, which would then detach from the lactose carrier once airborne. However, these data would suggest that unlike in the oropharynx, in the nasal cavity there was insufficient time for the many of the microparticles to detach themselves from the carrier, hence reduced deposition beyond the nasal vestibule resulted. It was also possible that this particular formulation adhered relatively strongly to the lactose due to strong Van der Waals forces, although Chan *et al.*, (1997) found that blending a similar formulation with a coarse lactose carrier improved aerosolisation in a pulmonary model. Magnesium stearate has been widely used in the pharmaceutical industry to improve powder flow. However, the data here would suggest that even if the flow was improved, this did not necessarily translate into to improved aerosolisation properties. Leucine is a hydrophobic amino acid that has been investigated for improving the aerosolisation properties of microparticulate powders, primarily by the reduction of interparticulate forces (Staniforth *et al.*, 2002; Li *et al.*, 2003; Najafabadi *et al.*, 2004; Rabbani and Seville, 2005; Learoyd *et al.*, 2008; Seville *et al.*, 2007). In agreement with the literature, leucine did appear to provide modest improvements to the aerosolisation of F1, as demonstrated by an increased delivery beyond the nasal vestibule (Figure 8.14). Aerosil® (anhydrous silicic acid), which was also found to modestly improve the nasal deposition pattern, has found many applications in improving the flow properties of

pharmaceutical powders, including Kawashima *et al.* (1998), who used it for the enhancement of the aerosolisation of formulations for inhalation. They found a clear improvement in fine particle fraction when using a 10% physical blend of Aerosil®. Of course in this work, each excipient was only investigated at a constant amount, and therefore, by employing different quantities other effects may have been observed with.

This work was carried out on nasal cast models that were constructed based on MRI scans of the nasal cavity of one person. Therefore, these results are specific to one particular example of a nasal cavity, and may well vary in other patients, particularly if they have very different nasal anatomies. For example, Bespak was in the process of developing another nasal cast based on a different subject. In this cast there was a clear line-of-sight to the turbinates from the nostrils, unlike the cast used in these experiments, where there was only a convoluted path through the nasal vestibule to reach the turbinates. Therefore, it could be envisaged that there will be some degree of variation in deposition pattern between the two models. Another inter-patient variable was the mucus. In this experiment, the cast was coated with artificial mucus composed of glycerol and ethanol [other researchers have used poly(ethylene oxide) solutions Shah *et al.*, 2005]. This was considered necessary to prevent the 'bouncing' of particles from their initial point of impact to a deposition site deeper within the nasal cavity. The work conducted in Appendix VII did not use mucus as a barrier layer, and it can be seen that the presence of mucus did indeed reduce deposition beyond the nasal vestibule. However, how this model would compare to the range of situations *in vivo* was unclear.

8.6 Conclusion

Both F1 and F2 are potential instant-release, dry-powder, nasal formulations of IgG antibody. They were produced at high yields, have been shown to protect the antibody during the solidification process, and appeared to have the required characteristics for nasal inhalation when actuated from an appropriate delivery device. Although most of their properties were similar, F1 may have some small advantages over F2 in terms of production yield, water content and aerosolisation properties, based on laser diffraction data. The addition of leucine to the F1 spray-drying solution, or a physical blend with Aerosil®, may have further enhanced the formulation's nasal deposition. The nasal cast model was an interesting technique for characterising nasal deposition, but more work was needed to establish the impact of variation in human nasal anatomy and mucus production. For optimal dose deposition, it will be important to control how the device is used in conjunction with the patient's breathing pattern.

9 GENERAL DISCUSSION AND CONCLUSIONS

9.1 Summary of findings

The aim of the work in this thesis was to develop formulations for the delivery of antibodies to the respiratory tract. Spray-drying was selected as an efficient method of producing dry powders that consisted of particles of a respirable diameter range (~1-5 μm). Such powders could theoretically be used in a portable, dry-powder inhaler device, for convenient self-administration. However, excipients were required, since spray-drying a solution of pure antibody was likely to have resulted in damage to the activity of the antibody, and potentially harmful aggregates (Maury *et al.*, 2005a; Arvinte, 2005). Therefore, where possible, excipients were selected that were biocompatible, and that were either approved, or potentially suitable, for use in pulmonary delivery to humans.

The experiments in Chapters 3-7 of this thesis developed and characterised formulations containing the biodegradable polymer poly(lactide-co-glycolide) (PLGA). The aim was to produce a modified-release (MR), pulmonary formulation of antibodies. The PLGA used had an estimated aqueous degradation period of 2-3 weeks. It was thought that by processes of surface-release, diffusion and degradation, the antibody would be released from the formulation over this time period. Because PLGA was not water soluble, a W/O/W double-emulsion was prepared, with the PLGA dissolved in dichloromethane. The antibody was located in the internal aqueous phase of the emulsion, such that droplets of antibody solution were dispersed within droplets of PLGA, prior to spray-drying. This was found to be important, since adding the antibody to the external aqueous phase of the double-emulsion, increased the proportion of antibody that was immediately released. Some of the work in Chapter 4 of this thesis further demonstrated that although microparticles were formed from the droplets generated by the spray drier, the properties of the emulsion, such as component location and parameters of the homogenisation process, also influenced microparticle characteristics. Dipalmitoylphophatidylcholine (DPPC), an endogenous component of human lung surfactant, was used to stabilise the emulsion. It was found to be superior to the more commonly employed emulsion stabiliser, poly(vinyl alcohol), in terms of improving antibody encapsulation efficiency, and reducing the immediate antibody burst-release, whilst being a more appropriate constituent for an inhaled formulation. However, the largest component of the formulation was lactose, since it prevented the melting of the PLGA during spray-drying, and possibly helped stabilise surface antibody.

The manufacturing process and components of the formulation were optimised by three separate factorial experiments (see Chapter 4 of this thesis). Factorial experimental design allowed many variables to be screened quickly and robustly. With the data produced, spray-drying yield was increased, IgG encapsulation efficiency was increased to ~100%, immediate IgG burst-release was reduced (<30% with 3.5% m/m IgG loading), and particle diameter range and particle morphology were improved. As a result of these experiments, it was found that a spray-drying outlet temperature of 50-60°C was critical for ensuring a dry product, without melting the formulation, or decreasing antibody activity. These experiments also showed that the proportion of antibody in the formulation was limited by the capacity of the polymer, such that high antibody loading resulted in a greater proportion of antibody being released instantly. The amount of each component in the formulation had appreciable effects on the particle morphology.

Laser diffraction sizing of the optimised formulation, using different dispersion media, led to an important discovery. Dispersion of the spray-dried formulation in cyclohexane produced a diameter distribution of 1-5 μm, which correlated with scanning electron micrograph images. This was the diameter of the whole, dry-powder particles (as they would be prior to delivery), and was thought to be a suitable diameter for inhalation into the lungs. However, laser diffraction sizing of the spray-dried powder once it had dispersed in aqueous media (following 2 h, 37°C incubation) produced a very different diameter distribution, consisting of particles ~400 nm. In this case the lactose in the formulation had dissolved, leaving insoluble PLGA nanoparticles, from which modified antibody release would have taken place. Given the correlation of these nanoparticle diameters, with the particle diameter of a freeze-dried double-emulsion of the same formulation, it appeared that the size of these constituent PLGA particles was determined by the PLGA droplet size within the double-emulsion. The generation of these nanoparticles upon dispersion of the formulation in aqueous media, was confirmed by photon correlation spectroscopy sizing, and transmission electron microscope imaging. This was considered a potentially beneficial property of the formulation, since microparticles of the required diameter for inhalation would transform into nanoparticles upon delivery to the respiratory tract. These nanoparticles were potentially small enough to avoid phagocytosis by pulmonary macrophages, enabling the entire antibody to be released.

The antibody release profile of the optimised formulation was investigated by the studies described in Chapter 5 of this thesis. As common to many reported MR

microparticulate protein formulations, when measuring the release profile in pH 7.4 phosphate-buffered saline (PBS), there was little extended antibody release following the initial burst, during the first day of such *in vitro* studies. This was thought to be due to readsorption of the released antibody onto the surface of the particles. Use of a pH 2.5 release media enabled almost complete antibody release to be observed over a period of 35 days. At this pH, the antibody presumably had a greater net charge, preventing aggregation and readsorption to the polymer, *via* a hydrophobic interaction. It was also thought that in an *in vivo* scenario, degradation of the polymer would generate an acidic microclimate, similar to the low-pH release media. Indeed it has previously been suggested that for a PLGA microparticulate protein formulation, the use of a pH 2.5 release media was more closely correlated with an *in vivo* paradigm, than a pH 7.4 release media (Jiang *et al.*, 2002). The uncapped 7 kDa PLGA used within the lead formulation described in this thesis, was found to achieve complete release more rapidly than 2 kDa poly(lactic acid), or end-capped versions of the PLGA. However, it was found that the addition of basic salts to the formulation could influence the amount of immediate antibody burst-release. Gel electrophoresis, enzyme-linked immunosorbent assay and field-flow fractionation, also found that the antibody released by 2 h was stable in terms of molecular weight and biological activity. The stability of subsequently released antibody was more difficult to determine, due to the stability and the concentration in the release media. However, there was some evidence that antibody released between 2 h and 7 days was stable in pH 2.5 release media.

The dry-powder dispersion work in Chapter 6 of this thesis demonstrated that the aerosolisation properties of the antibody formulation were comparable with other novel dry-powder formulations for inhalation. Therefore, in addition to having the MR, antibody stability and diameter transformation properties already demonstrated, the formulation could potentially be delivered deep into the respiratory tract by a dry-powder inhaler device. Small quantities (~1%) of magnesium stearate and leucine were found to further enhance dispersibility, as measured by pressure-diameter titration and fine particle fraction in the 'Andersen' cascade impactor.

Throughout the work described above, human normal immunoglobulin G was used as a model antibody. Having developed and characterised the formulation, this model was substituted for real therapeutic antibodies targeted against proteins of *Yersinia pestis*, which therefore had the potential for the treatment of plague. These antibodies were successfully purified from serum, and incorporated into the MR PLGA formulation, where they were shown by *in vitro* techniques to be stable relative to unformulated

antibody. *In vivo* studies attempted to demonstrate whether the formulated antibodies still had therapeutic activity. Formulations were administered intraperitoneally or intramuscularly to mice to protect against subsequent subcutaneous infection with *Y. pestis*. Unfortunately, these studies failed to demonstrate that the formulated antibody had any *in vivo* activity. However, given the IgG release profile of the formulation, and the limited effectiveness of an equivalent dose of unformulated antibody, this finding suggested that further work was required to establish the appropriate dose required to confer protection, rather than an incapability of the formulation to successfully deliver therapeutic antibodies.

Separate to the work described above, a more simple formulation was developed for the nasal delivery of antibodies (see Chapter 8 of this thesis). A model antibody was formulated by the spray-drying of an aqueous solution containing sorbitol, sodium chloride and albumin. This formulation contained 25% m/m IgG, and the spray-dried powder dissolved rapidly upon dissolution. This combination of excipients resulted in a high production yield, in the antibody remaining stable, and in a dry, microparticulate, powder. Potential deposition in the nasal cavity was demonstrated by the use of this formulation with a prototype nasal device, and actuation into a nasal cast model. Protein deposition into the turbinate regions of the nasal cavity was achieved with this formulation, and was possibly enhanced with the inclusion of both leucine and Aerosil®.

9.2 Further studies

This thesis has described the initial stages of formulation development. In terms of designing a potentially biocompatible system for the formulation of antibodies for delivery to the respiratory tract, the aims of this project have been achieved. The studies conducted thus far have suggested the developed formulations were capable of achieving modified-release of stable antibodies, and had the aerosolisation properties to enable their delivery as a dry-powder pulmonary inhalation. Obviously, much work still remains to bridge the sizable gap between what has been achieved thus far, and having a product ready for commercial use in the clinic. To execute the work remaining would require increased resources beyond a single PhD studentship of 3 years. However, from the data generated herein, there was little to suggest that there was any major factor that could prevent these formulations from being further developed and characterised, in order to make them viable for use in the clinic.

Had development of these formulations been continued beyond this particular PhD

studentship, there would have been a number of areas that would have benefited from further exploration. With regard to the MR PLGA formulation, the antibody release profile needed to be determined *in vivo*. A lung lavage-based method (similar to that performed by Dailey *et al.*, 2006) could possibly have been developed to measure cumulative antibody release in the lung. Further work would also have been required to establish whether the released antibody was stable and active, at all phases of the release profile. Ideally, an *in vitro* method could then have been developed to robustly replicate the data generated *in vivo*. With this information, it would have been easier to select an appropriate dose of the MR formulation for an *in vivo* efficacy study. The next stage of *in vivo* testing would have been to administer the formulation to the lungs, and determine the protection elicited against challenge with an aerosolised infection (as carried out by Hill *et al.*, 2006), since this would have been the relevant to the clinical paradigm for the formulation. Only with clinical studies could the dose deposition in the human lung have been fully characterised, and this would have been due to the aerosolisation properties of the formulation, and the choice of a specific delivery device.

The nasal formulation developed in the work described in Chapter 8 of this thesis could equally have been developed and tested as an instant-release formulation for pulmonary delivery, given the particle diameters produced by the Büchi-191 spray drier. 'Andersen' cascade impactor testing could have been used to further evaluate its aerosolisation potential when used in a pulmonary delivery device. Similar *in vivo* testing could also have been pursued. However, it would have potentially been very interesting to have had access to with a spray drier with a larger drying capacity, such that larger particles (10-15 μm) of this formulation could have been generated at high yield. Whilst particles of this diameter would have been small enough to be deposited in the turbinates, and surrounding regions, of the nasal cavity (without continuing through to the lungs), the smaller surface area would have made them less cohesive, possibly enhancing delivery efficiency.

10 REFERENCES

Aespira (2007) Aespira – Big Inhaler performance in a small package. From: www.aespira.com, Aespira Ltd., Israel.

Agu RU, Ugwoke MI, Armand M, Kinget R and Verbeke N (2001) The Lung As a Route for Systemic Delivery of Therapeutic Proteins and Peptides. *Respiratory Research* **2**:198-209.

Ahsan F, Rivas IP, Khan MA and Torres Suárez AI (2002) Targeting to Macrophages: Role of Physicochemical Properties of Particulate Carriers - Liposomes and Microspheres - on the Phagocytosis by Macrophages. *Journal of Controlled Release* **79**: 29-40.

Alouache AI, Kellaway IW and Taylor KM (2006) Pressurised Metered Dose Inhaler Solution Formulations to Generate Controlled Release Colloids. *Respiratory Drug Delivery* **3**: 853-856.

Alpar HO, Somavarapu S, Atuah KN and Bramwell VW (2005) Biodegradable Mucoadhesive Particulates for Nasal and Pulmonary Antigen and DNA Delivery. *Advanced Drug Delivery Reviews* **57**: 411-430.

Andya JD, Maa Y-F, Costantino HR, Nguyen P-A, Dasovich N, Sweeney TD, Hsu CC and Shire SJ (1999) The Effect of Formulation Excipients on Protein Stability and Aerosol Performance of Spray-Dried Powders of a Recombinant Humanized Anti-IgE Monoclonal Antibody. *Pharmaceutical Research* **16**: 350-358.

Annapragada AV, Swanson P and Muzzio F (1997) Biophysics of Inhaled Drug Particles, in *Inhalation Delivery of Therapeutic Peptides and Proteins* (Adjei AL and Gupta PK eds) pp 27-58, Marcel Dekker, New York.

Armstrong NA and James KC (1996) Pharmaceutical Experimental Design and Interpretation. Taylor and Francis, London, pp 131-168.

Arnold JJ, Ahsan F, Meezan E and Pillion DJ (2004) Correlation of Tetradecylmaltoside Induced Increases in Nasal Peptide Drug Delivery with Morphological Changes in Nasal Epithelial Cells. *Journal of Pharmaceutical Sciences* **93**: 2205-2213.

Arvinte T (2005) Concluding Remarks: Analytical Methods for Protein Formulations, in *Methods for Structural Analysis of Protein Pharmaceuticals* (Jiskoot W & Crommelin D eds) AAPS Press, Arlington, VA, pp 661-666.

Atkins PJ, Barker NP and Mathisen D (1992) Inhalation Drug Delivery Systems. In, *Pharmaceutical Inhalation Aerosol Technology* (Hickey AJ ed) Marcel Dekker, New York, pp 155-185.

Beck A, Bussat M-C, Zorn N, Robillard V, Klinguer-Hamour C, Chenu S, Goetsch L, Corvaïa N, Van Dorsselaer A and Haeuw JF (2005) Characterization by Liquid Chromatography Combined with Mass Spectrometry of Monoclonal Anti-IGF-1 Receptor Antibodies Produced in CHO and NS0 Cells. *Journal of Chromatography B* **819**:203-218.

Beuselinck L, Govers G, Poesen J, Degraer G and Froyen L (1998) Grain-Size Analysis by Laser Diffractometry:Comparison With the Sieve-Pipette Method. *Catena* **32**:193-208.

Bilati U, Allemann E and Doelker E (2005) Strategic Approaches for Overcoming Peptide and Protein Instability Within Biodegradable Nano- and Microparticles. *European Journal of Pharmaceutics and Biopharmaceutics* **59:** 375-388.

Binder P, Attre O, Boutin JP, Cavallo JD, Debord T, Jouan A and Vidal D (2003) Medical Management of Biological Warfare and Bioterrorism: Place of the Immunoprevention and the Immunotherapy. *Comparative Immunology, Microbiology & Infectious Diseases* **26**:401-421.

Blanco MD, Sastre RL, Teijón C, Olmo R and Teijón JM (2006) Degradation Behaviour of Microspheres Prepared by Spray-drying Poly(d,l-lactide) and Poly(d,l-lactide-co-glycolide) Polymers. *International Journal of Pharmaceutics* **326**: 139-147.

Blanco-Prieto MJ, Campanero MA, Besseghir K, Heimgatner F and Gander B (2004) Importance of Single or Blended Polymer Types for Controlled *in vitro* Release and Plasma Levels of a Somatostatin Analogue Entrapped in PLA/PLGA Microspheres. *Journal of Controlled Release* **96**:437-448.

Blasi P, D'Souza SS, Selmin F and DeLuca PP (2005) Plasticizing Effect of Water on Poly(lactide-co-glycolide). *Journal of Controlled Release* **108**: 1-9.

Bosquillon C, Lombry C, Préat V and Vanbever R (2001) Influence of Formulation Excipients and Physical Characteristics of Inhalation Dry Powders on Their Aersolization Performance. *Journal of Controlled Release* **70**: 329-339.

Bosquillon C, Préat V, and Vanbever R (2004a) Pulmonary Delivery of Growth Hormone Using Dry Powders and Visualisation of its Local Fate in Rats. *Journal of Controlled Release* **96**: 233-244.

Bosquillon C, Rouxhet PG, Ahimou F, Simon D, Culot C, Préat V and Vanbever R (2004b). Aerosolization Properties, Surface Composition and Physical State of Spray-Dried Protein Powders. *Journal of Controlled Release* **99**: 357-367.

Bot AI, Smith DJ, Bot S, Dellamary L, Tarara TE, Harders S, Philips W, Weers JG and Woods CM (2001) Receptor-Mediated Targeting of Spray-Dried Lipid Particles Coformulated With Immunoglobulin and Loaded With a Prototype Vaccine. *Pharmaceutical Research* **18**: 971-979.

Bot AI, Tarara TE, Smith DJ, Bot SR, Woods CM and Weers JG (2000) Novel Lipid-Based Hollow-Porous Microparticles as a Platform for Immunoglobulin Delivery to the Respiratory Tract. *Pharmaceutical Research* **17**:275-283.

Bradford, MM (1976) A Rapid and Sensitive Method for the Quantitation of Microgram Quantities of Protein Utilizing the Principle of Protein-dye Binding. *Analytical Biochemistry* **72**: 248-254.

Breedveld FC (2000) Therapeutic Monoclonal Antibodies. *The Lancet* **355**: 735-740.

British Pharmacopoeia (2001) Aerodynamic Assessment of Fine Particles – Fine Particle Dose and Particle Size Distribution: Apparatus D - ''Andersen'' Sizing Sampler. Appendix XII, pp A247-A250.

Brown L, Qin Y, Hogeland K, McGeehan J, Mason K, Jeannotte T, Fortier R and Moore E (2006) Water-Soluble Polymer Formation of Monodispersed Insulin Microspheres. In, *Polymeric Drug Delivery II*, ACS Symposium Series 924 (Svenson S ed), American Chemical Society, Washington DC, pp 329-339.

Bryan J (2004) Getting Systemic Treatments into the Bloodstream via the Nasal Mucosa. *Pharmaceutical Journal* **273**: 649-650.

Büchi Labortechnik AG (2002) Training Papers, Spray-Drying.
From: www.buchi.com.

Bustami RT, Chan H, Dehghani F and Foster NR (2000) Generation of Micro-Particles of Proteins for Aerosol Delivery Using High Pressure Modified Carbon Dioxide. *Pharmaceutical Research* **17**: 1360-1366.

Carrasquillo KG, Stanley AM, Aponte-Carro JC, De Jésus P, Costantino HR, Bosques CJ and Griebenow K (2001) Non-Aqueous Encapsulation of Excipient-Stabilized Spray-Freeze Dried BSA into Poly(lactide-*co*-glycolide) Microspheres Results in Release of Native Protein.
Journal of Controlled Release **76**: 199-208.

Chan H-K, Clark A, Gonda I, Mumenthaler M and Hsu C (1997) Spray Dried Powders and Powder Blends of Recombinant Human Deoxyribonuclease (rhDNase) for Aerosol Delivery. *Pharmaceutical Research* **14**: 431-437.

Chesko J, Kazzaz J, Ugozzoli M, O'Hagan DT and Singh M (2005) An Investigation of the Factors Controlling the Adsorption of Protein Antigens to Anionic PLG Microparticles. *Journal of Pharmaceutical Sciences* **94**: 2510-2519.

Clark AR and Egan M (1994) Modelling the Deposition of Inhaled Powdered Drug Aerosols. *Journal of Aerosol Science* **25**: 175-186.

Cole ML and Whateley TL (1997) Release Rate Profiles of Theophylline and Insulin from Stable Multiple W/O/W Emulsions. *Journal of Controlled Release* **49**: 51-58.

Copley (2007) 'Andersen' Cascade Impactor. From: www.copleyscientific.co.uk.

Criée CP, Meyer T, Petro W, Sommerer K and Zeising P (2006) *In Vitro* Comparison of Two Delivery Devices for Administering Formoterol: Foradil® P and Formoterol Ratiopharm Single-Dose Capsule Inhaler.
Journal of Aerosol Medicine **19**: 466-472.

Crotts G and Park TG (1995) Preparation of Porous and Nonporous Biodegradable Polymeric Hollow Microspheres. *Journal of Controlled Release* **35**: 91-105.

Dailey LA, Jekel N, Fink L, Gessler T, Schmehl T, Wittmar M, Kissel T and Seeger W (2006) Investigation of the Proinflammatory Potential of Biodegradable Nanoparticle Drug Delivery Systems in the Lung.
Toxicology and Applied Pharmacology **215**: 100-108.

Dale O, Nilsen T, Loftsson T, Hjorth Tønnesen H, Klepstad P, Kaasa S, Holand T and Djupesland PG (2006) Intranasal Midazolam: a Comparison of Two Delivery Devices in Human Volunteers.
Journal of Pharmacy & Pharmacology **58**: 1311-1318.

Dashevsky A (1998) Protein Loss by the Microencapsulation of an Enzyme (Lactase) in Alginate Beads. *International Journal of Pharmaceutics* **161**: 1-5.

Daugherty AL and Mrsny RJ (2006) Formulation and Delivery Issues for Monoclonal Antibody Therapeutics. *Advanced Drug Delivery Reviews* **58**: 686-706.

De Boer AH, Gjaltema D, Hagedoorn P and Frijlink HW (2002) Characterization of Inhalation Aerosols: a Critical Evaluation of Cascade Impactor Analysis and Laser Diffraction Technique.
International Journal of Pharmaceutics **249**: 219-231.

Degussa (2006) Safety Data Sheet for Aerosil 200® Pharma, Degussa GmbH.

Dellamary L, Smith DJ, Bloom A, Bot S, Guo G-R, Deshmuk H, Costello M and Bot A (2004) Rational Design of Solid Aerosols for Immunoglobulin Delivery by Modulation of Aerodynamic and Release Characteristics.
Journal of Controlled Release **95**:489-500.

Dellamary LA, Tarara TE, Smith DJ, Woelk CH, Adractas A, Costello ML, Gill H and Weers JG (2000) Hollow Porous Particles in Metered Dose Inhalers. *Pharmaceutical Research* **17**:168-174.

Delves PJ and Roitt IM (2000) The Immune System. First of Two Parts, *The New England Journal of Medicine* **343**: 37-49 and Second of Two Parts, 108-117.

DMV (2007) Certificate of analysis for Respitose ML001, DMV-Fonterra Excipients.

Domantis (2007) Domantis – Human Domain Antibody Therapeutics,
From: www.domantis.com, Domantis, GlaxoSmithkline, UK.

Duddu SP, Sisk SA, Walter YH, Tarara TE, Trimble KR, Clark AR, Eldon MA, Elton RC, Pickford M, Hirst PH, Newman SP and Weers JG (2002) Improved Lung Delivery from a Passive Dry Powder Inhaler Using an Engineered PulmoSphere® Powder. *Pharmaceutical Research* **19**: 689-695.

Dutta AS, Furr BJA, Hutchinson FG (1993) The Discovery and Development of Goserelin (Zoladex). *Pharmaceutical Medicine* **7**: 9-28.

Edris A and Bergnståhl B (2001) Encapsulation of Orange Oil in a Spray Dried Double Emulsion. *Nahrung/Food* **45**: 133-137.

Edwards DA, Ben-Jebria A, Langer R (1998) Recent Advances in Pulmonary Drug Delivery Using Large, Porous Inhaled Particles.
Journal of Applied Physiology **84**: 379-385.

Edwards DA, Hanes J, Caponetti G, Hrkach J, Ben-Jebria A, Eskew ML, Mintzes J, Deaver D, Lotan N and Langer R (1997) Large Porous Particles for Pulmonary Drug Delivery. *Science* **276**: 1868-1871.

Elversson J and Millqvist-Fureby A (2005) Particle Size and Density in Spray Drying – Effects of Carbohydrate Properties.
Journal of Pharmaceutical Sciences **94**: 2049-2060.

Elversson J, Millqvist-Fureby A, Alderborn G and Elofsson U (2003) Droplet and Particle Size Relationship and Shell Thickness of Inhalable Lactose Particles During Spray-Drying. *Journal of Pharmaceutical Sciences* **92**: 900–910.

European Pharmacopoeia 5 (2005) Preparations for Inhalation: Aerodynamic Assessment of Fine Particles, Apparatus D – "'Andersen'" sizing sampler 1: pp 250-253.

Evora C, Soriano I, Rogers RA, Shakesheff KM, Hanes J and Langer R (1998) Relating the Phagocytosis of Microparticles by Alveolar Macrophages to Surface Chemistry: the Effect of 1,2-Dipalmitoylphosphatidylcholine.
Journal of Controlled Release **51**:143-152.

Fiel SB (2001) History and Evolution of Aerosolized Therapeutics: Overview and Introduction. *Chest* **120**: 87S-88S.

Fineberg SE, Kawabata TT, Krasner AS and Fineberg NS (2007) Insulin Antibodies with Pulmonary Delivery of Insulin.
Diabetes Technology and Therapeutics **9**: Suppl. 1, S102-S110.

Fisher RA (1951) The Design of Experiments (sixth ed.). Oliver and Boyd, London, pp 91-106.

Fraunhofer W and Winter G (2004) The Use of Asymmetrical Flow Field-flow Fractionation in Pharmaceutics and Biopharmaceutics.
European Journal of Pharmaceutics and Biopharmaceutics **58**: 369-383.

Freiberg S and Zhu XX (2004) Polymer Microspheres for Controlled Drug Release. *International Journal of Pharmaceutics* **282**:1-18.

Freitas S, Merkle HP and Gander B (2005) Microencapsulation by Solvent Extraction/Evaporation: Reviewing the State of the Art of Microsphere Preparation Process Technology. *Journal of Controlled Release* **102**: 313-332.

Fu J, Fiegel J, Krauland E and Hanes J (2002) New Polymeric Carriers for Controlled Drug Delivery Following Inhalation or Injection. *Biomaterials* **23**: 4425-4433.

Fu K, Griebenow K, Hsieh L, Klibanov AM, Langer R (1999) FTIR Characterization of the Secondary Structure of Proteins Encapsulated within PLGA Microspheres. *Journal of Controlled Release* **58**: 357-366.

Fu K, Klibanov AM, Langer R (2000) Protein Stability in Controlled-Release Systems. *Nature Biotechnology* 18: 24-25.

Gabrielson JP, Brader ML, Pekar AH, Mathis KB, Winter G, Carpenter JF and Randolph TW (2007) Quantitation of Aggregate Levels in a Recombinant Humanized Monoclonal Antibody Formulation by Size-Exclusion Chromatography, Asymmetrical Flow Field Flow Fractionation, and Sedimentation Velocity. *Journal of Pharmaceutical Sciences* **96**: 268-279.

Garcia-Contreras L and Smyth HDC (2005) Liquid-Spray or Dry-Powder Systems for Inhaled Delivery of Peptide and Proteins?
American Journal of Drug Delivery **3**: 29-45.

Giddings JC (1993) Field-Flow Fractionation: Analysis of Macromolecular, Colloidal, and Particulate Materials. *Science* **260**: 1456-1465.

Gonda I (1992) Targeting by Deposition, in *Pharmaceutical Inhalation Aerosol Technology* (Hickey AJ ed), Marcel Dekker, New York, pp 61-82.

Gonda I (2000) The Ascent of Pulmonary Drug Delivery.
Journal of Pharmaceutical Sciences **89**: 940-945.

Graff CL and Pollack GM (2005) Nasal Drug Administration: Potential for Targeted Central Nervous System Delivery.
Journal of Pharmaceutical Sciences **94**: 1187-1195.

Grenha A, Seijo B and Remunan-Lopez C (2005) Microencapsulated Chitosan Nanoparticles for Lung Protein Delivery.
European Journal of Pharmaceutical Sciences **25**: 427-437.

Guo C and Doub WH (2006) The Influence of Actuation Parameters on *In Vitro* Testing of Nasal Spray Products. *Journal of Pharmaceutical Sciences* **95**: 2029-2040.

Gupta PK and Adjei AL (1997) Therapeutic inhalation aerosols, in *Inhalation Delivery of Therapeutic Peptides and Proteins* (Adjei AL and Gupta PK eds), Marcel Dekker, New York, pp 185-234.

Han W, Liebe D, Cooper J, Bruno A, Hovermale D, Mollica J, Billany M, Jones TM and Lund W (1986) Magnesium Stearate, in *Handbook of Pharmaceutical Excipients* (Rowe R C, Sheskey P J, Weller P J eds), 4th edition, The Pharmaceutical Press, London, pp 173-175.

Hardy JG, Chadwick TS (2000) Sustained Release Drug Delivery to the Lungs: An Option for the Future. *Clinical Pharmacokinetics* **39**: 1-4.

Häußermann S, Bailey AG, Bailey MR, Etherington G and Youngman M. (2002) The Influence of Breathing Patterns on Particle Deposition in a Nasal Replicate Cast. *Journal of Aerosol Science* **33**: 923-933.

Häussermann S, Acerbi D, Brand P, Herpich C, Poli G and Sommerer K (2007) Lung Deposition of Formoterol HFA (Atimos®/Forair®) in Healthy Volunteers, Asthmatic and COPD Patients. *Journal of Aerosol Medicince* **20**: 331-341.

Herberger J, Murphy K, Munyakazi L, Cordia J and Westhaus E (2003) Carbon Dioxide Extraction of Residual Solvents in Poly(lactide-co-glycolide) Microparticles. *Journal of Controlled Release* **90**: 181-195.

Heyder J (2004) Deposition of Inhaled Particles in the Human Respiratory Tract and Consequences for Regional Targeting in Respiratory Drug Delivery.
Proceedings of the American Thoracic Society **1**: 315-320.

Hickey AJ and Thompson DC (1992) Physiology of the Airways, in *Pharmaceutical Inhalation Aerosol Technology* (Hickey AJ ed), Marcel Dekker, New York, pp 1-27.

Hickey AJ, Concessio NM, Van Oort MM and Platz RM (1994) Factors Influencing the Dispersion of Dry Powders as Aerosols. *Pharmaceutical Technology* **18**: 58-64.

Hill J, Copse C, Leary S, Stagg AJ, Williamson ED and Titball RW (2003) Synergistic Protection of Mice against Plague with Monoclonal Antibodies Specific for the F1 and V Antigens of *Yersinia pestis*. *Infection and Immunity* **71**: 2234-2238.

Hill J, Eyles JE, Elvin SJ, Healey GD, Lukaszewski RA and Titball RW (2006) Administration of Antibody to the Lung Protects Mice against Pneumonic Plague. *Infection and Immunity* **74**: 3068-3070.

Hinchcliffe M and Illum L (1999) Intranasal Insulin Delivery and Therapy. *Advanced Drug Delivery Reviews* **35**: 199-234.

Holt LJ, Herring C, Jespers LS, Woolven BP and Tomlinson IM (2003) Domain Antibodies: Proteins for Therapy. *TRENDS in Biotechnology* **21**: 484-490.

Huang Y-Y, Chung T-W and Tzeng T-W (1999) A Method Using Biodegradable Polylactide/Polyethylene Glycol for Drug Release With Reduced Initial Burst. *International Journal of Pharmaceutics* **182**:93-100.

Hukkanen J, Pelkonen O, Hakkola J and Raunio H (2002) Expression and Regulation of Xenobiotic-Metabolizing Cytochrome P450 (CYP) Enzymes in Human Lung. *Critical Reviews in Toxicology* **32**: 391-411.

Hussain A, Arnold JJ, Khan MA and Ahsan F (2004) Absorption Enhancers in Pulmonary Protein Delivery. *Journal of Controlled Release* **94**: 15-24.

Illum L (2003) Nasal Drug Delivery – Possibilities, Problems and Solutions. *Journal of Controlled Release* **87**: 187-198.

Illum L and Fisher AN (1997) Intranasal delivery of peptides and proteins, in *Inhalation Delivery of Therapeutic Peptides and Proteins* (Adjei AL and Gupta PK eds), Marcel Dekker, New York.

Jakobovits A, Amado RG, Yang X, Roskos L and Schwab G (2007) From XenoMouse Technology to Panitumumab, the First Fully Human Antibody Product from Transgenic Mice. *Nature Biotechnology* **25**: 1134-1143.

Jiang G, Woo BH, Kang F, Singh J and DeLuca PP (2002) Assessment of Protein Release Kinetics, Stability and Protein Polymer Interaction of Lysozyme Encapsulated Poly(D,L-lactide-co-glycolide) Microspheres. *Journal of Controlled Release* **79**: 137-145.

Jones BE (2006) Two-piece Capsules for Dry Powder Inhalers. Published by www.qualicaps.com.

Jones BG, Dickinson PA, Gumbleton M and Kellaway IW (2002) The Inhibition of Phagocytosis of Respirable Microspheres by Alveolar and Peritoneal Macrophages. *International Journal of Pharmaceutics* **236**: 65-79.

Kawashima Y, Serigano T, Hino T, Yamamoto H and Takeuchi H (1998) Design of Inhalation Dry Powder of Pranlukast Hydrate to Improve Dispersibility by the Surface Modification with Light Anhydrous Silicic Acid (AEROSIL 200). *International Journal of Pharmaceutics* **173**: 243-251.

Kaye RS, Purewal TS and Alpar HO (2006a) Development of biocompatible formulations for the airway delivery of immunoglobulins. Abstracts from the Aerosol Society Drug Delivery to the Lungs XVI, *Journal of Aerosol Medicine* **19**: 231, A-28.

Kaye RS, Purewal TS and Alpar HO (2006b) The Effect of Manufacturing Parameters on the Properties of a Biocompatible Formulation for the Airway Delivery of Immunoglobulins. Abstracts from the Aerosol Society Drug Delivery to the Lungs XVI, *Journal of Aerosol Medicine* **19**: 231, A-29.

Kaye RS, Purewal TS and Alpar HO (2006c) Optimisation and Characterisation of Biocompatible, Microparticulate, Modified-Release Formulations, for the Pulmonary Delivery of Immunoglobulins. *Journal of Pharmacy and Pharmocology* **58** (S1): A-62, P167.

Kaye RS, Purewal TS and Alpar HO (2007) Development and testing of formulations for the nasal delivery of antibodies. Abstracts from the Aerosol Society Drug Delivery to the Lungs XVII, *Journal of Aerosol Medicine* **20:** 371, A-18.

Kelly JT, Asgharian B, Kimbell JS and Wong BA. (2004) Particle Deposition in Human Nasal Airway Replicas Manufactured by Different Methods. Part I: Inertial Regime Particles. *Aerosol Science & Technology* **38**: 1063-1071.

Kim CS and Folinsbee LJ (1997) Physiological and Biomechanical Factors Relevant to Inhaled Drug Therapy, in *Inhalation Delivery of Therapeutic Peptides and Proteins* (Adjei AL and Gupta PK eds), Marcel Dekker, New York, pp 3-25.

Kippax P (2005) Issues in the Appraisal of Laser Diffraction Particle Sizing Techniques. *Pharmaceutical Technology Europe,* January 32-39.

Kublik H and Vidgren MT (1998) Nasal Delivery Systems and Their Effect on Deposition and Absorption. *Advanced Drug Delivery Reviews* **29**: 157-177.

Kwon J-H, Lee B-H, Lee J-H and Kim C-W (2004) Insulin Microcrystal Suspension as a Long-Acting Formulation for Pulmonary Delivery. *European Journal of Pharmaceutical Sciences* **22**: 107-116.

Lalor CB and Hickey AJ (1997) Generation and Characterization of Aerosols for Drug Delivery to the Lung, in *Inhalation Delivery of Therapeutic Peptides and Proteins* (Adjei AL and Gupta PK eds), Marcel Dekker, New York, pp 235-276.

Lane ME, Brennan FS and Corrigan OI (2006) Influence of Post-Emulsification Drying Process on the Microencapsulation of Human Serum Albumin. *International Journal of Pharmaceutics* **307**: 16-22.

Laube BL (2005) The Expanding Role of Aerosols in Systemic Drug Delivery, Gene Therapy, and Vaccination. *Respiratory Care* **50**: 1161-1176.

Leach CL (2005) The CFC to HFA Transition and Its Impact on Pulmonary Drug Development. *Respiratory Care* **50**: 1201-1208.

Learoyd TP, Burrows JL, French E and Seville PC (2008) Chitosan-Based Spray-Dried Respirable Powders for Sustained Delivery of Terbutaline Sulfate. *European Journal of Pharmaceutics and Biopharmaceutics*, **68**: 224-234.

Li H, Neil H, Innocent R, Seville P, Williamson I and Birchall JC (2003) Enhanced Dispersibility and Deposition of Spray-Dried Powders for Pulmonary Gene Therapy. *Journal of Drug Targeting* **11**: 425-432.

Li W, Anderson KW, Mehta RC and DeLuca P (1995) Predicition of Solvent Removal Profile and Effect on Properties for Peptide-Loaded PLGA Microspheres Prepared by Solvent Extraction/Evaporation Method. *Journal of Controlled Release* **37**: 199-214.

Liang JF, Li YT and Yang VC (2000) Biomedical Application of Immobilized Enzymes. *Journal of Pharmaceutical Sciences* **89**: 979-990.

Litzén A, Walter JK, Krischolleck H, Wahlund K (1993) Separation and Quantitation of Monoclonal Antibody Aggregates by Asymmetrical Flow Field-Flow Fractionation and Comparison to Gel Permeation Chromotography. *Analytical Biochemistry* **212**: 469-480.

Louey MD and Garcia-Contreras L (2004) Controlled Release Products for Respiratory Delivery. *American Pharmaceutical Reviews* **7**: 82-87.

Lucas P, Andersen K and Staniforth JN (1998) Protein Deposition from Dry Powder Inhalers: Fine Particle Multiplets as Performance Modifiers. *Pharmaceutical Research* **15**: 562-569.

Lucas P, Anderson K, Potter UJ and Staniforth JN (1999) Enhancement of Small Particle Size Dry Powder Aerosol Formulations Using Ultra Low Density Additive. *Pharmaceutical Research* **16**: 1643-1647.

Maa YF, Costantino HR, Nguyen PA and Hsu CC. (1997) The Effect of Operating and Formulation Variables on the Morphology of Spray-dried Protein Particles. *Pharmaceutical Development & Technology* **2**: 213-223.

Maa YF, Nguyen PA, Andya JD, Dasovich N, Sweeney TD, Shire SJ and Hsu CC (1998a) Effect of Spray-drying and Subsequent Processing Conditions on Residual Moisture Content and Physical/Biochemical Stability of Protein Inhalation Powders. *Pharmaceutical Research* **15**: 768-775.

Maa YF, Nguyen PA, Sit K and Hsu CC. (1998b) Spray-drying Performance of a Bench-top Spray-Drier for Protein Aerosol Powder Preparation. *Biotechnology & Bioengineering* **60**: 301-309.

Maggio ET (2006) Intravail™: Highly Effective Intranasal Delivery of Peptide and Protein Drugs. *Expert Opinion on Drug Delivery* **3**: 529 539.

Manning MC, Patel K and Borchardt RT (1989) Stability of Protein Pharmaceuticals. *Pharmaceutical Research* **6**: 903-918.

Marks C and Marks JD (1996) Phage Libraries - a New Route to Clinically Useful Antibodies. *The New England Journal of Medicine* **335**:730-733.

Masters K (1991) *Spray-Drying Handbook,* 5th edition. Longman Scientific and Technical, UK.

Maury M (2005) Aggregation and Structural Changes in Spray-dried Immunoglobulins. PhD thesis, University of Erlangen-Nuremberg, Germany.

Maury M, Murphy K, Kumar S, Mauerer A and Lee G (2005a) Spray-Drying of Proteins: Effects of Sorbitol and Trehalose on Aggregation and FT-IR Amide I Spectrum of an Immunoglobulin G.
European Journal of Pharmaceutics and Biopharmaceutics **59**: 251-261.

Maury M, Murphy K, Kumar S, Shi L and Lee G (2005b) Effects of Process Variables on the Powder Yield of Spray-dried Trehalose on a Laboratory Spray-drier. *European Journal of Pharmaceutics & Biopharmaceutics* 59: 565-573.

McAllister SM, Alpar HO, Teitelbaum Z and Bennett DB (1996) Do Interactions With Phospholipids Contribute to the Prolonged Retention of Polypeptides Within the Lung? *Advanced Drug Delivery Reviews* **19**: 89-110.

McDonald KJ and Martin GP (2000) Transition to CFC-Free Metered Dose Inhalers - Into the New Millennium. *International Journal of Pharmaceutics* **201**: 89-107.

McGee JP, Davis SS and O'Hagan DT (1995) Zero Order Release of Protein from Poly(D,L-lactide-co-glycolide) Microparticles Prepared Using a Modified Phase Separation Technique. *Journal of Controlled Release* **34**: 77-86.

McGhee JR, Mestecky J, Dertzbaugh MT, Eldridge JH, Hirasawa M and Kiyono H (1992) The Mucosal Immune System: From Fundamental Concepts to Vaccine Development. *Vaccine* **10**:75-88.

McHugh MA and Krukonis VJ (1994) Supercritical Fluid Extraction: Principles & Practice. Butterworth-Heinemann, Boston.

Medina C, Santos-Martinez MJ, Radomski A, Corrigan OI and Radomski MW (2007) Nanoparticles: Pharmacological and Toxicological Significance.
British Journal of Pharmacology **150**: 552-558.

Michalovic M, Brust G, and Parrish D (1995) *Macrogalleria.* University of Southern Mississippi, Department of Polymer Science.

Molina MJ and Rowlands FS (1974) Stratospheric Sink for Chlorofluoromethanes: Chlorine Atom-Catalyzed Destruction of the Ozone. *Nature* **249**: 810-812.

Morita T, Saakamura Y, Horikiri Y, Suzuki T and Yoshino H (2000) Protein Encapsulation into Biodegradable Microspheres by a Novel S/O/W Emulsion Method Using Poly(ethylene glycol) as a Protein Micronization Adjuvant.
Journal of Controlled Release **69**: 435-444.

Mu L and Feng SS (2001) Fabrication, Characterization and *in vitro* Release of Paclitaxel (Taxol®) Loaded Poly (Lactic-Co-Glycolic Acid) Microspheres Prepared by Spray-drying Technique With Lipid/Cholesterol Emulsifiers. *Journal of Controlled Release* **76**:239-254.

Najafabadi AR, Gilani K, Barghi M and Rafiee-Tehrani M (2004) The Effect of Vehicle on Physical Properties and Aerosolisation Behaviour of Disodium Cromoglycate Microparticles Spray-dried Alone or with L-Leucine. *International Journal of Pharmaceutics* **285**: 97-108.

Newman SP (1997) Foreward, in *Inhalation Delivery of Therapeutic Peptides and Proteins* (Adjei AL and Gupta PK eds), Marcel Dekker, New York, pp xi-xii.

Newman S (2006) Respiratory Drug Delivery X. *Expert Opinion on Drug Delivery* **3**: 549-552.

Ng DK, Chow PY and Lam YY (2003) Administration of Aerosolized Medications. *The Education Bulletin of the Hong Kong Paediatric Society* **10**: 1-4.

Nightingale P and Martin P (2004) The Myth of the Biotech Revolution. *Trends in Biotechnology* **22**:564-569.

Noakes T (2002) Medical Aerosol Propellants. *Journal of Fluorine Chemistry* **118**: 35-45.

Novartis (2006) Foradil® Patient Information Leaflet. Novartis UK Ltd.

Ogawa Y, Yamamoto M, Okada H, Yahsiki T and Shimamoto T (1988) A New Technique to Efficiently Entrap Leuprolide Acetate into Microcapsules of Polylactic Acid or Coploy(Lactic/Glycolic) Acid. *Chemistry and Pharmacy Bulletin* **36**: 1095-1103.

Owen S C and Weller P J (2003). Polyvinyl Alcohol, in *Handbook of Pharmaceutical Excipients* (Rowe R C, Sheskey P J, Weller P J eds) 4th edition, Pharmaceutical Press, London, pp 491-492.

Ozmen L and Langrish T (2002) Comparison of Glass Transition Temperature and Sticky Point Temperature for Skim Milk Powder. *Drying Technology* **20**: 1177-1192.

Ozmen L and Langrish T (2003) An Experimental Investigation of the Wall Deposition of Milk Powder in a Pilot Scale Spray Drier. *Drying Technology* **21**: 1253-1272.

Palmieri A, Lipper RA and Wright P (1986) Sodium Chloride, in *Handbook of Pharmaceutical Excipients,* (Rowe R C, Sheskey P J, Weller P J eds), 4th edition, The Pharmaceutical Press, London, pp 266-268.

Panyam J, Dali MM, Sahoo SK, Ma W, Chakravarthi SS, Amidon GL, Levy RJ and Labhasetwar V (2003) Polymer Degradation and *In Vitro* Release of a Model Protein from Poly(D,L-lactide-*co*-glycolide) Nano- and Microparticles. *Journal of Controlled Release* **92**:173–187.

Patel J (2007) Bioadhesive Microspheres & Their Pharmaceutical Applications. *Drug Delivery Technology* **7**: 54-61.

Patton JS (1996) Mechanisms of Macromolecule Absorption by the Lungs. *Advanced Drug Delivery Reviews* **19**: 3-36.

Patton JS, Bukar J and Nagarajan S (1999) Inhaled Insulin. *Advanced Drug Delivery Reviews* **35**: 235-247.

Patton JS, Byron PR (2007) Inhaling Medicines: Delivering Drugs to the Body Through the Lungs. *Nature Reviews Drug Discovery* **6:** 67-74.

Poli MA, Rivera MA, Pitt ML and Vogal P (1996) Aerosolized Specific Antibody Protects Mice From Lung Injury Associated With Aerosolised Ricin Exposure. *Toxicon* **34**: 1037-1044.

Pollit MJ (2006) Protein Coating of Nanoparticles. PhD thesis, School of Pharmacy, University of London.

Porter WR (1997) Chemical and Physical Properties of Peptide and Protein Drugs, in *Inhalation Delivery of Therapeutic Peptides and Proteins* (Adjei AL and Gupta PK eds), Marcel Dekker, New York, pp 59-88.

Poyner EA, Alpar HO, Almeida AJ, Gamble MD and Brown MRW (1995) A Comparative Study on the Pulmonary Delivery of Tobramycin Encapsulated into Liposomes and PLA Microspheres Following Intravenous and Endotracheal Delivery. *Journal of Controlled Release* **35**: 41-48.

Qui Y, Gupta PK and Adjei AL (1997) Absorption and Bioavailability of Inhaled Peptides and Proteins, in *Inhalation Delivery of Therapeutic Peptides and Proteins* (Adjei AL and Gupta PK eds), Marcel Dekker, New York, pp 89-131.

Rabbani NR and Seville PC (2005) The Influence of Formulation Components on the Aerosolisation Properties of Spray-dried Powders. *Journal of Controlled Release* **110**: 130-140.

Rashba-Step J (2007) Efficient Pulmonary Delivery of Biological Molecules as PROMAXX Microspheres. *Drug Delivery Technology* **7**: 48-53.

Reff ME and Heard C (2001) A Review of Modifications to Recombinant Antibodies: Attempt to Increase Efficiency in Oncology Applications. *Critical Reviews in Oncology/Hematology* **40**: 25-35.

Ridder KB, Davies-Cutting CJ and Kellaway IW (2005) Surfactant Solubility and Aggregate Orientation in Hydrofluoroalkanes. *International Journal of Pharmaceutics* **295**: 57-65.

Rosevear A, Kennedy JF and Cabral JMS (1987) Immobilized Enzymes and Cells. IOP, Bristol.

Rouse JJ, Whateley TL, Thomas M and Eccleston GM (2007) Controlled Drug Delivery to the Lung: Influence of Hyaluronic Acid Solution Conformation on its Adsorption to Hydrophobic Drug Particles. *International Journal of Pharmaceutics* **330**: 175-182.

Sandor M, Riechel A, Kaplan I and Mathiowitz E (2002) Effect of Lecithin and $MgCO_3$ as Additives on the Enzymatic Activity of Carbonic Anhydrase Encapsulated in Poly(lactide-co-glycolide) (PLGA) microspheres.
Biochimica et Biophysica Acta **1570**: 63-74.

Schüle S, Frieß W, Bechtold-Peters K and Garidel P (2007) Conformational Analysis of Protein Secondary Structure during Spray-Drying of Antibody/Mannitol Formulations. *European Journal of Pharmaceutics and Biopharmaceutics* **65**: 1-9.

Schwach G, Oudry N, Delhomme S, Luck M, Linder H and Gurny R (2003) Biodegradable Microparticles for Sustained Releaseof a New GnRH Antagonist - Part I: Screening Commercial PLGA and Formulation Technologies.
European Journal of Pharmaceutics and Biopharmaceutics **56**: 327-336.

Schwendeman SP (2002) Recent Advances in the Stabilization of Proteins Encapsulated in Injectable PLGA Delivery Systems.
Critical Reviews in Therapeutic Drug Carrier Systems **19**: 73-98.

Scott TL, Brown LR, Riske FJ, Blizzard CD, and Rashba-Step J (2002) Sustained Release Microspheres. US Patent: 6,458,387 B1.

Sebti T and Amighi K (2006) Preparation and In Vitro Evaluation of Lipidic Carriers and Fillers for Inhalation.
European Journal of Pharmaceutics and Biopharmaceutics **63**: 51-58.

Seville PC, Learoyd TP, Li HY, Williamson IJ and Birchall JC (2007) Amino Acid-Modified Spray-Dried Powders with Enhanced Aerosolisation Properties for Pulmonary Drug Delivery. *Powder Technology* **178**: 40-50.

Shah S, Fung K, Brim S and Rubin BK (2005) An In Vitro Evaluation of the Effectiveness of Endotracheal Suction Catheters. *Chest* **128**: 3699-3704.

Shao PG and Bailey LC (1999) Stabilization of pH-Induced Degradation of Porcine Insulin in Biodegradable Polyester Microspheres.
Pharmaceutical Development and Technology **4**: 633-642.

Sharma R, Saxena D, Dwivedi AK and Misra A (2001) Inhalable Microparticles Containing Drug Combinations to Target Alveolar Macrophages for Treatment of Pulmonary Tuberculosis. *Pharmaceutical Research* **18**: 1405-1409.

Shekunov BY, Feeley JC, Chow AHL, Tong HHY and York P (2002) Physical Properties of Supercritically-Processed and Micronised Powders for Respiratory Drug Delivery. *KONA* **20**: 178-187.

Shüle S, Frieβ, Bechtold-Peters K and Garidel P (2007) Conformational analysis of protein secondary structure during spray-drying of antibody/mannitol formulations.
European Journal of Pharmaceutics and Biopharmaceutics **65**: 1-9.

Siiman O, Burshteyn A and Insausti ME (2001) Covalently Bound Antibody on Polystyrene Latex Beads: Formation, Stability, and Use in Analyses of White Blood Cell Populations. *Journal of Colloid and Interface Science* **234**: 44-58.

Sinha VR, Bansal K, Kaushik R, Kumria R and Trehan A (2004) Poly-ε-Caprolactone Microspheres and Nanospheres: an Overview. *International Journal of Pharmaceutics* **278**: 1-23.

Smith PK, Krohn RI, Hermanson GT, Mallia AK, Gartner FH, Provenzano MD, Fujimoto EK, Goeke NM, Olson BJ and Klenk DC (1985) Measurement of Protein Using Bicinchoninic Acid. *Analytical Biochemistry* **150**: 76-85.

Smith PL (1997) Peptide Delivery by the Pulmonary Route: a Valid Approach for Local and Systemic Delivery. *Journal of Controlled Release* **46**: 99-106.

Snell NJC (1997) Assessing Equivalence of Inhaled Products. *Journal of Pharmacy and Pharmacology* **49**(S3): 55-60.

Spiers ID, Eyles JE, Baillie LWJ, Williamson ED and Alpar HO (2000) Biodegradable Microparticles With Different Release Profiles: Effect on the Immune Response After a Single Administration Via Intranasal and Intramuscular Routes. *Journal of Pharmacy and Pharmacology* **52**: 1195-1201.

Staniforth JN (2002) Powders Comprising Anti-adherant Materials for Use in Dry Powder Inhalers. USA patent 6,475,523, Vectura Ltd.

Stein SW and Stefely JS (2003) Reinventing Metered Dose Inhalers: From Poorly Efficient CFC MDIs to Highly Efficient HFA MDIs. *Drug Delivery Technology* **3**: January/February (accessed on-line).

Sturesson C, Artursson P, Ghaderi R, Johansen K, Mirazimi A, Uhnood I, Svenssonc L, Albertssona AC and Carlfors J (1999) Encapsulation of Rotavirus into Poly(lactide-co-glycolide) Microspheres. *Journal of Controlled Release* **59**: 377–389.

Takada S, Uda Y, Toguchi H and Ogawa Y (1995) Application of a Spray Drying Technique in the Production of TRH-Containing Injectable Sustained-Release Microparticles of Biodegradable Polymers. *PDA Journal of Pharmaceutical Science & Technology* **49**: 180-184.

Takeuchi H, Yamamoto H, Toyoda T, Toyobuku H, Hino T, Kawashima Y (1998) Physical Stability of Size Controlled Small Unilameller Liposomes Coated with a Modified Polyvinyl Alcohol. *International Journal of Pharmaceutics* **164**:103–111.

Tamber H, Johansen P, Merkle H and Gander B (2005) Formulation Aspects of Biodegradable Polymeric Microspheres for Antigen Delivery. *Advanced Drug Delivery Reviews* **57**: 357-376.

Tang X and Pikal MJ (2004) Design of Freeze-Drying Processes for Pharmaceuticals: Practical Advice. *Pharmaceutical Research* **21**: 191-200.

Tsapis N, Bennett D, Jackson B, Weitz DA, and Edwards DA (2002) Trojan Particles: Large Porous Carriers of Nanoparticles for Drug Delivery. *Proceedings of the National Academy of Sciences of the United States of America* **99**: 12001-12005.

Tuovinen L, Peltonen S, Liikola M, Hotakainen M, Lahtela-Kakkonen M, Poso A and Järvinen K (2004) Drug Release From Starch-Acetate Microparticles and Films With and Without Incorporated α-Amylase. *Biomaterials* **25**: 4355-4362.

US Pharmacopoeia 29 (2006) <601> Aerosols, Nasal Sprays, Metered-Dose Inhalers, and Dry Powder Inhalers – Particle Size, pp 2622-2636.

Usmani OS, Biddiscombe MF and Barnes PJ (2005) Regional Lung Deposition and Bronchodilator Response as a Function of β_2-Agonist Particle Size. *American Journal of Respiratory and Critical Care Medicine* **172**: 1497-1504.

Vanbever R, Ben-Jebria A, Mintzes JD, Langer R and Edwards DA (1999a) Sustained Release of Insulin From Insoluble Inhaled Particles. *Drug Development Research* **48**: 178-185.

Vanbever R, Mintzes JD, Wang J, Nice J, Chen D, Batycky R, Langer R, Edwards DA (1999b) Formulation and Characterisation of Large Porous Particles for Inhalation. *Pharmaceutical Research* **16**: 1735-1742.

Vasir JK, Tambwekar K and Garg S (2003) Bioadhesive Microspheres As a Controlled Drug Delivery System. *International Journal of Pharmaceutics* **255**: 13-32.

Wang A-J, Lu Y-P, Sun R-X (2007a) Recent Progress on the Fabrication of Hollow Microspheres. *Materials Science and Engineering A* **460-461**: 1-6.

Wang J, Chau KM and Wang C (2004) Stabilization and Encapsulation of Human Immunoglobulin G into Biodegradable Microspheres. *Journal of Colloid and Interface Science* **271**: 92-101.

Wang W (1999) Instability, Stabilization, and Formulations of Liquid Protein Pharmaceuticals. *International Journal of Pharmaceutics* **185**: 129-188.

Wang W (2000) Lyophilization and Development of Solid Protein Pharmaceuticals. *International Journal of Pharmaceutics* **203**:1-60.

Wang W (2005) Protein Aggregation and its Inhibition in Biopharmaceutics. *International Journal of Pharmaceutics* **289**: 1-30.

Wang W, Singh S, Zeng DL, King K and Nema S (2007b) Antibody Structure, Instability and Formulation. *Journal of Pharmaceutical Sciences* **96**: 1-26.

Watts PJ, Davies MC and Melia CD (1990) Microencapsulation Using Emulsification/Solvent Evaporation: An Overview of Techniques and Applications. *Critical Reviews in Therapeutic Drug Carrier Systems* **7**: 235-259.

Weers JG, Tarara TE and Clark AR (2007) Design of Fine Particles for Pulmonary Drug Delivery. *Expert Opinion in Drug Delivery* **4**: 297-313.

Wichert B and Rohdewald P (1993) Low Molecular Weight PLA: a Suitable Polymer for Pulmomary Administered Microparticles? *Journal of Microencapsulation* **10**: 195-207.

Williams III RO and Liu J (1998) Formulation of a Protein with Propellant HFA 134a for aerosol delivery. *European Journal of Pharmaceutical Sciences* **7**: 137-144.

Williamson ED, Flick-Smith HC, LeButt C, Rowland CA, Jones SM, Waters EL, Gwyther RJ, Miller J, Packer PJ and Irving M (2005) Human Immune Response to a Plague Vaccine Comprising Recombinant F1 and V Antigens. *Infection & Immunity* **73**: 3598-3608.

Williamson ED, Flick-Smith HC, Waters E, Miller J, Hodgson I, Le Butt CS, Hill J (2007) Immunogenicity of the rF1+rV Vaccine for Plague with Identification of Potential Immune Correlates. *Microbial Pathogenesis* **42**: 11-21.

Witschi C and Doelker E (1998a) Peptide Degradation During Preparation and In Vitro Release Testing of Poly(lactic acid) and Poly(DL-lactic-co-glycolic acid) Microparticles. *International Journal of Pharmaceutics* **171**: 1-18.

Witschi C and Doelker E (1998b) Influence of the Microencapsulation Method and Peptide Loading on Poly(lactic acid) and Poly(lactic-co-glycolic acid) Degradation During In Vivo Testing. *Journal of Controlled Release* **51**: 327-341.

Wu C, Ying H, Grinnell C, Bryant S, Miller R, Clabbers A, Bose S, McCarthy D, Zhu R-R, Santora L, Davis-Taber R, Kunes Y, Fung E, Schwartz A, Sakorafas P, Gu J, Tarcsa E, Murtaza A and Ghayur T (2007) Simultaneous Targeting of Multiple Disease Mediators by a Dual-Variable-Domain Immunoglobulin. *Nature Biotechnology,* In Press doi:10.1038/nbt1345.

Yang J and Cleland JL (1997) Factors Affecting the in Vitro Release of Recombinant Human Interferon-γ (rhIFN-γ) from PLGA Microspheres. *Journal of Pharmaceutical Sciences* **86**: 908-914.

Yang Y-Y, Chung T-S and Ng NP (2001) Morphology, Drug Distribution, and *In Vitro* Release Profiles of Biodegradable Polymeric Microspheres Containing Protein Fabricated by Double-Emulsion Solvent Extraction/Evaporation Method. *Biomaterials* **22**: 231-241.

Yang Y-Y, Chung T-S, Bai X-L and Chan W-K (2000) Effect of Preparation Conditions on Morphology and Release Profiles of Biodegradable Polymeric Microspheres Containing Protein Fabricated by Double-Emulsion Method. *Chemical Engineering Science* **55**: 2223-2236.

Yun YH, Goetz DJ, Yellen P and Chen W (2004) Hyaluronan Microspheres for Sustained Gene Delivery and Site-Specific Targeting. *Biomaterials* **25**: 147-157.

Zeng XM, Martin GP, Tee S-K and Marriott C (1998) The Role of Fine Particle Lactose on the Dispersion and Deaggregation of Salbutamol Sulphate in an Air Stream in Vitro. *International Journal of Pharmaceutics* **176**: 99-110.

Zhang Y, Gilbertson K and Finlay WH (2007) In Vivo-In Vitro Comparison of Deposition in Three Mouth-Throat Models with Qvar® and Turbohaler® inhalers. *Journal of Aerosol Medicine* **20**: 227-235.

Zheng JY and Janis LJ (2006) Influence of pH, Buffer Species, and Storage Temperature on Physicochemical Stability of a Humanized Monoclonal Antibody LA298. *International Journal of Pharmaceutics* **308**: 46-51.

Zhu G, Mallery SR and Schwendeman SP (2000) Stabilization of Proteins Encapsulated in Injectable Poly(lactide-co-glycolide). *Nature Biotechnology* **18**: 52-57.

11 APPENDICES

11.1 Appendix I – Dilutions for the preparation of assay standards

Table I Standard concentrations for the Bradford assay.

Concentrationof standard (μg/mL)	*Volume 200 μg/mL solution (μL)*	*Volume 0.5 M NaOH (μL)*
150	750	250
100	500	500
80	400	600
60	300	700
40	200	800
20	100	900
0	0	1000

Table II Standard concentrations for the poly(vinyl alcohol) (PVA) assay.

Concentration of standard (mg/mL)	*Volume 10 mg/mL standard (μL)*	*Volume 0.5 M NaOH (μL)*
5	25	25
2.5	12.5	37.5
1	5	45
0.5	2.5	47.5
0.2	1	49
0.1	0.5	49.5
0	0	50

11.2 Appendix II – Calibration graphs

Figure I Example calibration curve for IgG absorbance, using the Bradford assay.
This graph was purposely produced against convention, with the measured values of absorbance appearing on the *X*-axis. Mathematically there is no problem with doing this, and it allows an easier calculation of the concentrations of unknown samples, by simply substituting their average absorbencies for *x* into the quadratic equation of the curve, and solving *y*. Plotted in the opposite configuration, a complicated rearrangement of the quadratic equation would be required to solve an unknown concentration, *x*. N.B. The Bradford reagent had an intrinsic absorbance of ~0.5 units.

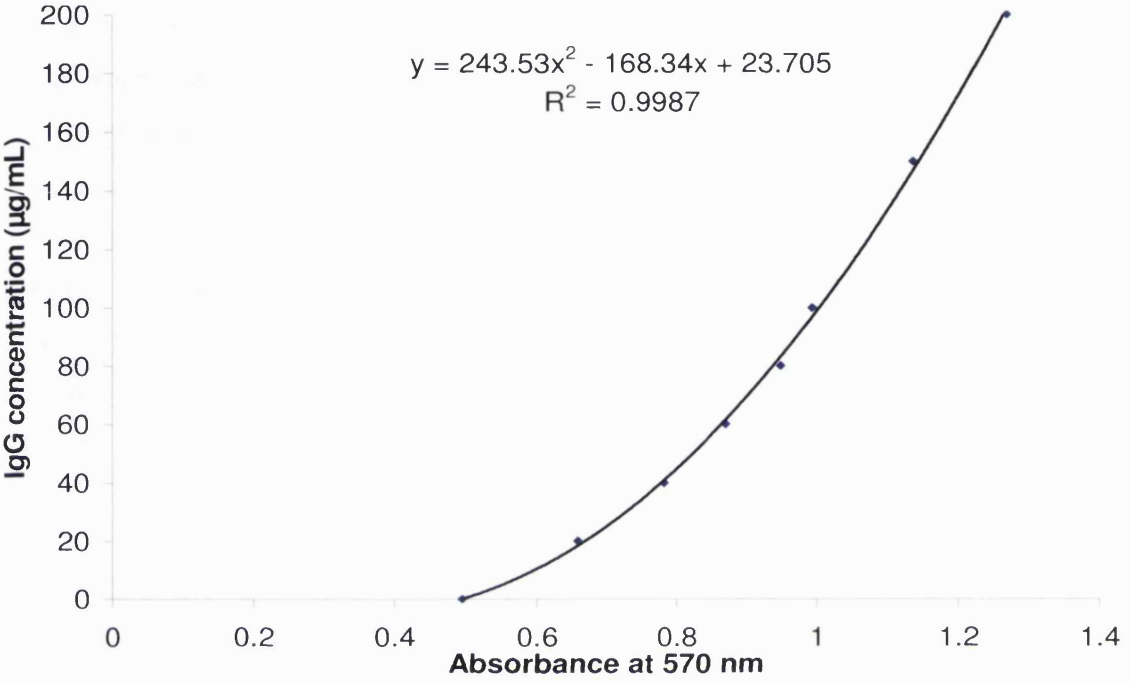

Figure II Calibration line for PVA assay (each point is an average of five absorbance readings).

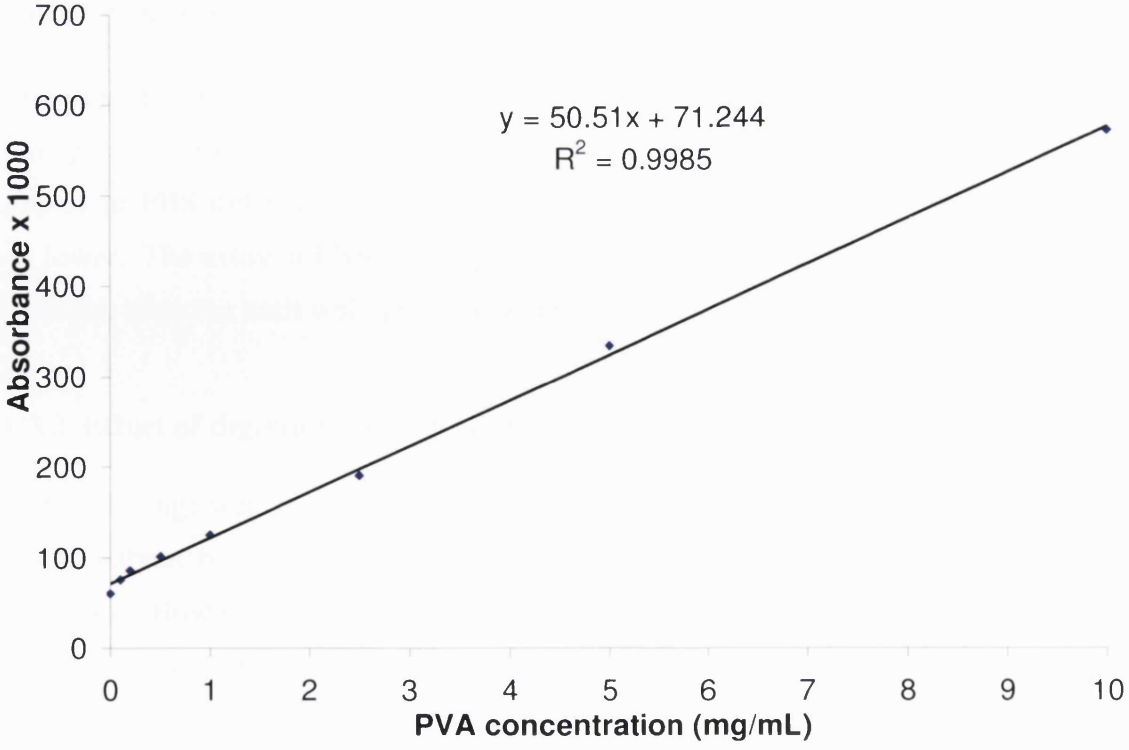

11.3 Appendix III – Development of the Bradford assay protocol

11.3.1 Development of a micro-plate method for the Bradford assay

It was preferable to perform assays such as the Bradford assay on a micro-well plate, since this allowed many samples (including multiple repeats) to be analysed simultaneously. However, the literature supplied with the Bradford reagent did not contain such a protocol for the protein concentration range of interest (0-200 μg/mL). This range was based on the sodium hydroxide (NaOH) method of particle digestion, where 5 mg of particles (loaded with up to 4% m/m of protein) were dissolved in 1 mL 0.5 M NaOH. One reason why such large concentration ranges were avoided in the supplied literature was that the Bradford assay only performed linearly over very small ranges. This was because the cationic (unbound) and anionic (bound) species both contributed to the absorbance reading to varying extents. However, it was found that over a larger protein concentration range, the curve produced closely fitted a quadratic equation (second order curve) (see Figure II, Appendix II).

The method was developed using different volume ratios of standard samples to reagent, and measuring the absorbance at 570 nm and 630 nm. The chosen method was the one that produced a standard curve with the largest absorption range between the most concentrated and least concentrated samples, and that gave an acceptable correlation coefficient (r^2) with a second order curve. Samples were prepared in both 0.5 M NaOH, as they would be for a total-loading assay, and in phosphate-buffered saline (PBS), as would be used for an *in vitro* release study.

It was found that the best results were generated by using 50 μL of sample with 250 μL of reagent, in each well, and measuring absorbance at 570 nm. Unlike in NaOH, samples in PBS did not reach an endpoint immediately, and the endpoint absorbance was lower. The assay in PBS was improved by substituting 50 μL reagent for 50 μL 0.5 M NaOH, added to each well, prior to the reagent.

11.3.2 Effect of digestion time on results from Bradford assay

Samples (5 mg) were incubated in 1 mL 0.5 M NaOH in order to digest the particles before analysis by the Bradford assay. Protein standards were treated with the same conditions. However, the time allowed for this process was found to affect the results obtained. Previously, it was noticed that incubating standards overnight at 37°C, gave a slightly lower concentration reading than incubating at room temperature overnight,

which in turn was lower than using freshly prepared standards. Similarly, digesting the samples for 16 h (overnight) at room temperature, gave lower absorbance readings than for the same batch digested for 8 h during the day. This would not necessarily be a problem, except that the rate of deterioration of the samples was greater than for the standards. Although the change in absorbance was small (usually just 0.1 to 0.2 absorbance units), this had appreciable consequences on the calculated encapsulation efficiency (EE). For example, digesting a sample overnight at 37°C resulted in an EE value of ~20% less than the value obtained after 5 h at room temperature. Even a reduction in digestion time from 5 h to 2 h increased the calculated EE by 5%. Typically, long digestion times have been used in order to fully break-down a high molecular weight PLGA, used in preliminary experiments. However, because only a low molecular weight PLGA was used for the work presented in this thesis, a shorter digestion time would probably have been sufficient.

It was therefore decided to investigate this problem of digestion time affecting absorbance by determining the optimum digestion time for a low molecular weight PLGA formulation. Two batches were used: one with a known high EE, and one with a low EE. For each time point (ranging from 1-6 h), calibration standards were used that had also been incubated for the same time period. For each time point, four samples of each batch were used, and two were centrifuged before use, in order to identify whether any insoluble material present (although there was none visibly present) made a difference to the absorbance value. The results obtained are illustrated in Figure III. (The calculation of EE, which is directly influenced by the measured protein concentration, was derived from the sample absorbance, as detailed in Section 2.3.2).

It was clearly observed that after 4 h of digestion, the measured concentration began to decrease relative to the calibration standards. One possible explanation for this was the accumulation over time of break-down products of other excipients present in the test samples, could have interfered with the Bradford reaction. The standards did not contain these excipients, and so were not subject to the same rate of time-dependent decline. From the data obtained, it was decided to use a digestion time of 2 h, given that this was quite a short time for digesting samples, but yet achieved EEs not appreciably different from digestion lasting 3 or 4 h. It was also established by the data obtained, that centrifugation of the samples before incubation was unnecessary.

Figure III Measured encapsulation efficiency (EE) of microparticulate formulations using the Bradford assay. Samples of a known high EE (batch 1) and samples of a known low EE (batch 2) were incubated in 0.5 M NaOH for a range of durations of disgestion before being analysed. It can be seen that after 4 h of digestion there was a clear decline in the EE in all 4 of the tested samples (mean, n=2).

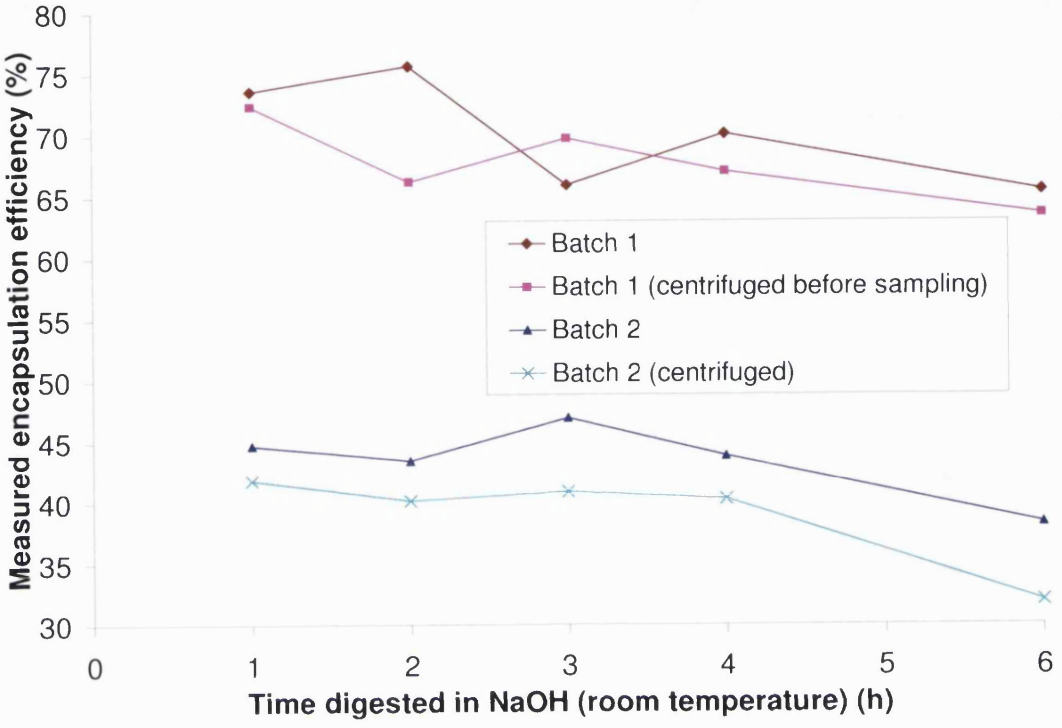

11.4 Appendix IV – Data collected from factorial experiments

Table III Summary of results for factorial experiment to optimise spray-drying parameters. Encapsulation efficiency (EE) data were measured in triplicate, where possible, material permitting. In these cases the standard deviation is given. Volume median particle diameter (D50%) was measured by laser diffractometry.

Batch	*Outlet T (°C)*	*Yield (%)*	*EE ± SD (%)*	*D50% (μm)*
1	50	2.3	55.9	6.49
2	32	1.3	53.0	2.34
3	47	18.2	61.7 ± 4.4	6.50
4	28	12.8	87.6 ± 6.0	2.90
5	53	1.2	76.5	4.18
6	33	0.8	62.2	3.92
7	52	35.6	84.4 ± 2.5	1.31
8	32	14.6	44.1 ± 2.8	3.20
9	85	10.7	41.5 ± 0.9	2.48
10	69	9.6	73.2 ± 5.4	1.67
11	78	32.8	77.0 ± 2.5	1.78
12	59	27.5	74.2 ± 1.0	0.95
13	97	5.6	71.3 ± 2.2	9.95
14	68	10.3	97.5 ± 6.5	1.84
15	89	48.0	61.6 ± 2.6	3.04
16	75	44.2	80.3 ± 4.6	2.44
17	61	13.8	46.2 ± 0.8	1.04
18	54	19.5	49.9 ± 2.3	1.26
19	57	19.4	50.4 ± 1.2	2.83

Table IV Summary of results for factorial experiment to optimise homogenisation time and external phase volume. Particle diameter was measured in cyclohexane (dry) and following 2 h (37°C) incubation in water +0.02% v/v Tween 20 (wet), and recorded as the modal diameter, median diameter (D50%), and the diameter that 90% of the volume of particles were smaller than (D90%). (For the encapsulation efficiency and burst-release within 2 h data, n=3 ± SD).

Batch	*Yield (%)*	*EE (%)*	*2 h burst-release (%)*	*Dry diameter mode (μm)*	*Dry D50% (μm)*	*Dry D90% (μm)*	*Wet mode (μm)*	*Wet D50% (μm)*
1	41.5	75.1 ± 1.2	40.9 ± 0.2	3.82	3.93	10.59	2.96	3.24
2	44.3	72.5 ± 1.1	40.6 ± 0.9	4.52	4.63	8.89	1.41	1.41
3	47.0	87.9 ± 2.6	29.2 ± 3.0	8.08	6.43	16.27	3.05	3.09
4	44.6	73.6 ± 3.8	18.8 ± 1.5	4.54	4.64	9.30	2.72	2.50
5	48.4	85.8 ± 3.8	17.2 ± 0.8	4.62	4.59	12.84	0.73	0.88
6	40.9	85.6 ± 1.1	20.2 ± 2.1	3.57	3.75	9.46	0.75	1.04
7	41.5	102.2 ± 4.9	21.5 ± 0.7	5.83	5.06	10.08	0.75	0.97
8	41.7	97.0 ± 5.6	15.1 ± 0.9	4.36	4.34	6.08	0.97	1.05
9	37.6	89.3 ± 5.1	33.9 ± 1.5	3.85	4.15	13.22	0.75	1.06
10	37.3	106.3 ± 2.7	38.8 ± 1.7	3.68	3.86	10.83	3.22	2.84
11	39.1	90.6 ± 3.9	56.0 ± 1.7	4.01	4.57	15.25	4.43	4.13

Table V Summary of data collected from the factorial experiment to optimise the formulation components. Particle diameter was measured in cyclohexane (dry) and following 2 h (37°C) incubation in water +0.02% v/v Tween 20 (wet), and recorded as the modal diameter, median diameter (D50%), and the diameter that 90% of the volume of particles were smaller than (D90%). (Where available encapsulation efficiency (EE) and the 2 h burst-release data are n=3 ± SD) (SEM rating refers to the grading of particle morphological quality attributed to each batch based, on scanning electron micrograph (SEM) images).

Batch	*Yield (%)*	*EE (%)*	*2 h burst-release (%)*	*D50% (μm)*	*D90% (μm)*	*D50% water (μm)*	*SEM rating*
1	12.9	84.5 ± 3.1	20.1	2.74	5.31	2.56	2
2	31.4	83.8 ± 2.6	5.0 ± 0.6	9.92	19.30	7.52	0
3	42.7	75.0 ± 0.9	10.4 ± 0.7	3.71	8.97	2.90	3
4	43.6	66.4 ± 2.6	4.1 ± 1.0	4.74	13.06	3.51	1
5	5.0	88.8 ± 1.5	29.3	2.91	5.73	2.08	2
6	26.0	91.7 ± 1.7	9.7 ± 0.6	5.18	14.02	1.66	2
7	34.5	68.6 ± 2.4	18.9 ± 1.2	2.81	4.56	7.14	3
8	37.8	75.2 ± 4.3	18.7 ± 2.3	3.90	7.86	2.78	2
9	31.8	72.1 ± 0.9	37.2 ± 1.6	5.76	10.56	3.48	1
10	35.7	91.0 ± 1.3	56.1 ± 2.0	6.61	11.04	3.57	0
11	43.4	87.2 ± 1.7	59.9 ± 4.5	4.35	11.69	7.52	2
12	43.7	79.3 ± 3.6	42.7	4.76	8.93	3.33	1
13	22.5	85.4 ± 2.9	37.2 ± 0.3	5.88	14.84	30.60	2
14	30.8	85.2 ± 4.2	53.3 ± 2.4	5.55	10.22	0.86	3
15	29.4	87.8 ± 5.4	51.4 ± 13.9	4.17	11.61	12.40	2
16	27.4	72.8 ± 4.1	55.3 ± 2.0	2.38	4.27	0.84	1
17	39.6	85.0 ± 3.1	32.0 ± 2.2	4.20	10.91	1.31	3
18	37.6	82.0 ± 1.6	45.0 ± 0.6	4.14	9.21	0.78	3
19	30.1	86.8 ± 4.5	45.3 ± 1.3	3.86	9.94	1.16	3

11.5 Appendix V – Outlet temperature results as an example of the factorial data analysis

Table VI presents the initial factorial fit data for outlet temperature. It can be seen from the probability values (p), that only pump speed and inlet temperature had a statistically significant effect on outlet temperature ($p<0.05$). None of the parameter interactions were statistically significant. The magnitude and direction of the effect is given in the "*Effect*" column, with larger magnitudes decreasing the probability that the effect was due to chance.

Table VI Factorial fit data for outlet temperature, using all experimental terms.

Estimated Effects and Coefficients for Outlet Temperature (coded units).

Term	*Effect*	*Coef*	*T*	*p*
Constant	59.188	0.8780		0.000
Pump Speed (%)	-19.375	-9.688	-11.03	0.008
Spray Flow (L/h)	-3.375	-1.687	-1.92	0.195
Aspiration (%)	6.375	3.187	3.63	0.068
Inlet Temperature (°C)	36.625	18.312	20.86	0.002
Pump Speed (%)*Spray Flow (L/h)	1.375	0.687	0.78	0.516
Pump Speed (%)*Aspiration (%)	-1.375	-0.687	-0.78	0.516
Pump Speed (%)*Inlet Temperature (°C)	-0.125	-0.062	-0.07	0.950
Spray Flow (L/h)*Aspiration (%)	2.625	1.312	1.49	0.274
Spray Flow (L/h)*Inlet Temp.	-1.125	-0.562	-0.64	0.587
Aspiration (%)*Inlet Temperature (°C)	3.125	1.563	1.78	0.217
Pump Speed (%)*Spray Flow*Aspiration	2.375	1.188	1.35	0.309
Pump Speed (%)*Spray Flow*Inlet Temp	1.625	0.813	0.93	0.452
Pump Speed (%)*Aspiration*Inlet Temp	-0.62	-0.312	-0.36	0.756
Spray Flow*Aspiration*Inlet Temp	1.375	0.687	0.78	0.516
Inlet Temp*Pump Speed*Spray Flow *Aspiration	2.125	1.063	1.21	0.350

The Pareto chart (Figure IV) graphically illustrates the absolute effect of each term in order of magnitude, with the red reference line indicating the minimum value of standardised effect required for statistical significance (this minimum value for statistical significance was dependant on which terms were included in the model). The normal probability plot (Figure V) identified the significant factors, and the direction of their effects. Terms with no significant effect would fall close to the blue line. It can be seen that inlet temperature statistically significantly increased outlet temperature, whilst pump speed statistically significantly decreased outlet temperature.

Figure IV Pareto chart of the 15 standardised effects included in the model. It can be seen that factors A and D individually statistically significantly affected outlet temperature ($p<0.05$). For this model the minimum value for statistical significance was 4.30.

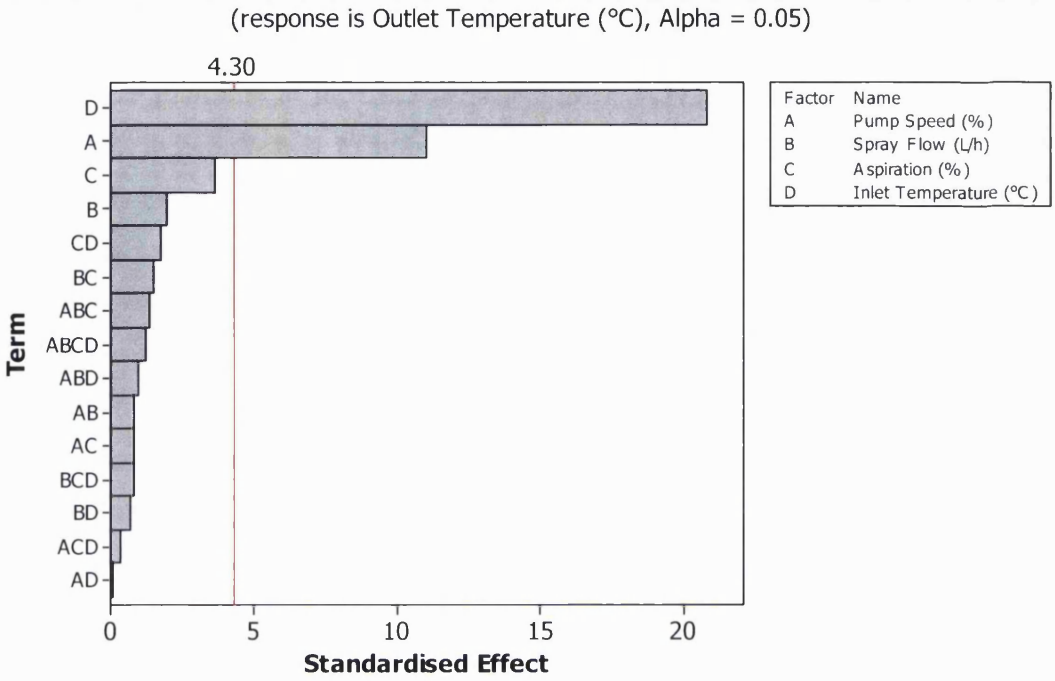

Figure V Normal probability plot of the 15 standardised effects included in the model (see Figure IV). It can be seen that increasing factors A and D statistically significantly decreased and increased outlet temperature, respectively ($p<0.05$), whilst the other 13 factors had no statistically significant effect on outlet temperature.

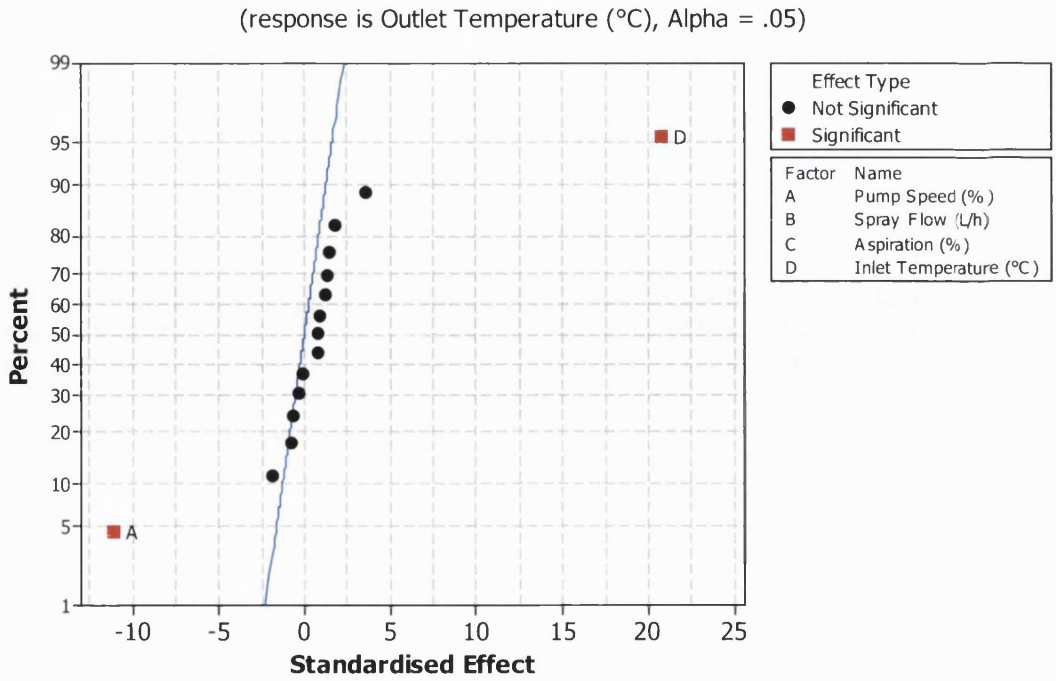

However, the initial model attempted to measure an effect for all of the terms. In this experiment, such a model was not appropriate, since only the centre-point batches had been replicated. Unimportant terms (rather than being tested for a significant effect), contributed to the background variance, thereby increasing the degrees of freedom, and therefore, the reliability of the model (Fisher, 1951). By removing them, the reliability of the model was expected to improve. However, removal of a term meant that its effect was not detected, and therefore, terms, which may become significant in a new model, were lost. Traditionally, the higher-order terms, such as third and fourth level interactions, would not be considered. However, with the software available, terms were removed more selectively by using the Pareto chart to identify the least important terms from the initial model. Generally, only those terms that appeared significant from this screening exercise were first tried in a new model. However, it can be seen from Figure IV that the aspiration level could also have been an important factor, despite not being statistically significant in the screening model. Therefore, this term was also retained in the new model. Several models were tried, and the best one was chosen based on several indicators, explained below. In this case, the best model was achieved by removing only the three least important factors: AD, ACD and BD.

The analysis was re-run without these three terms. It can be seen from the factorial fit data in Table VII, that (in addition to pump speed and inlet temperature) spray flow rate and aspiration now also had statistically significant effects. This was confirmed by new Pareto and normal plots (Figures VI and VII, respectively).

Table VII Factorial fit data, using optimised statistical model.

Estimated Effects and Coefficients for Outlet Temperature (°C) (coded units)

Term	Effect	Coef	T	p
Constant		59.188	94.54	0.000
Pump Speed (%)	-19.375	-9.688	-15.47	0.000
Spray Flow (L/h)	-3.375	-1.687	-2.70	0.043
Aspiration (%)	6.375	3.187	5.09	0.004
Inlet Temperature (°C)	36.63	18.312	29.25	0.000
Pump Speed (%)*Spray Flow (L/h)	1.375	0.687	1.10	0.322
Pump Speed (%)*Aspiration (%)	-1.375	-0.687	-1.10	0.322
Spray Flow (L/h)*Aspiration (%)	2.625	1.312	2.10	0.090
Aspiration (%)*Inlet Temperature (°C)	3.125	1.563	2.50	0.055
Pump Speed (%)*Spray Flow*Aspiration	2.375	1.188	1.90	0.116
Pump Speed (%)*Spray Flow*Inlet Temp	1.625	0.813	1.30	0.251
Spray Flow*Aspiration (%)*Inlet Temp	1.375	0.687	1.10	0.322
Pump Speed (%)*Spray Flow (L/h)* Aspiration (%)*Inlet Temperature (°C)	2.125	1.063	1.70	0.150

Figure VI Pareto chart of the 12 standardised effects, included in the optimal statistical model. This model omitted the 3 three standardised effects AD, ACD and BD. It can be seen that factors A, B, C and D statistically significantly affected outlet temperature ($p<0.05$). For this model the minimum value for statistical significance was 2.57.

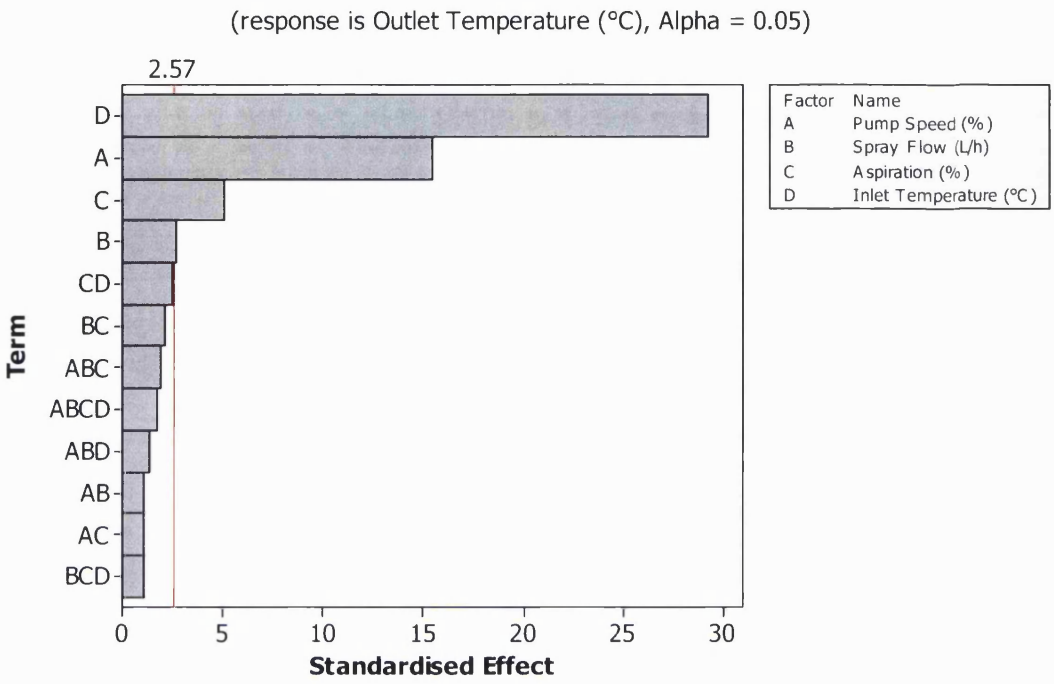

Figure VII Normal probability plot of the 12 standardised effects, included in the optimised statistical model (see Figure VI). It can be seen that increasing factors A and B statistically significantly decreased outlet temperature, and factors C and D statistically significantly increased outlet temperature ($p<0.05$), whilst the other 8 standardised effects caused no statistically significant changes. This graph also shows that the effects of A and D were greater than B and C.

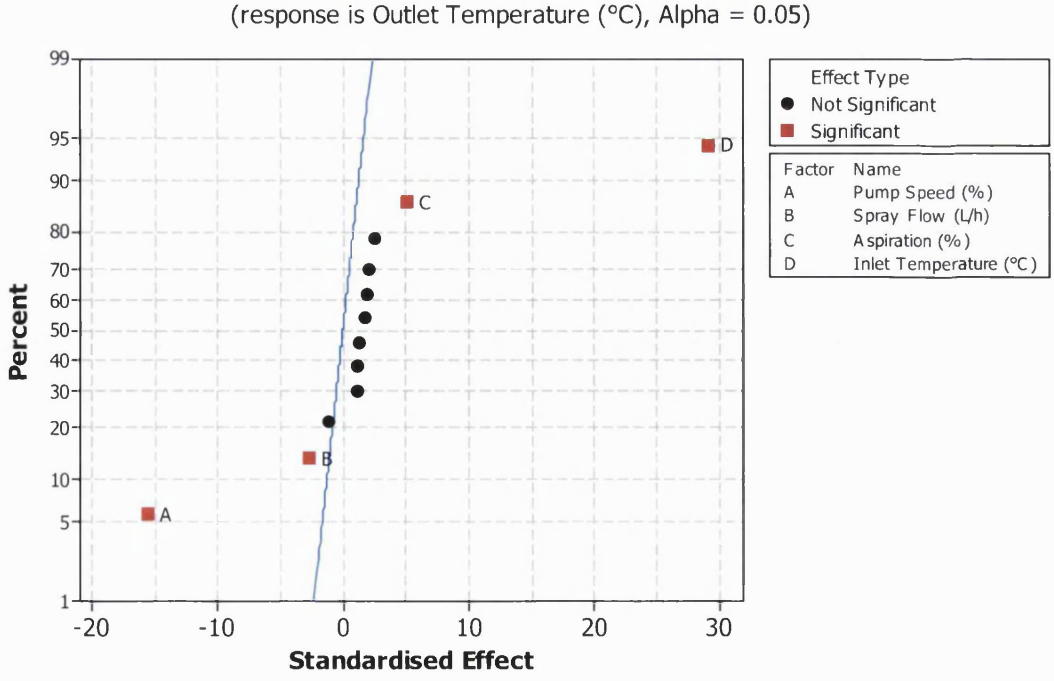

The fit of the model was first assessed by observing the ANOVA summary in Table VIII:

Table VIII Analysis of Variance for Outlet Temperature (°C). These data summarise the outcomes and fit of the optimised statistical model. The low probability value (p) for main effects indicated that individual spray-drying parameters had a statistically significant effect on outlet temperature. The high p-value for lack of fit, and the high R^2 values, demonstrated that the statistical model was a good fit for the data.

Source	DF	Seq SS	Adj SS	Adj MS	F	P
Main Effects	4	7075.25	7075.25	1768.81	282.07	**0.000**
2-Way Interactions	4	81.75	81.75	20.44	3.26	0.114
3-Way Interactions	3	40.69	40.69	13.56	2.16	0.211
4-Way Interactions	1	18.06	18.06	18.06	2.88	0.150
Curvature	1	5.53	5.53	5.53	0.88	0.391
Residual Error	5	31.35	31.35	6.27		
Lack of Fit	3	6.69	6.69	2.23	0.18	**0.901**
Pure Error	2	24.67	24.67	12.33		
Total	18	7252.63				

S = 2.50416 **R^2 = 99.57%** **R^2(adj) = 98.44%**

Again, Table VIII confirmed there were significant main effects, but no statistically significant interactions in the data. The p-value for the lack of fit (0.901) was highest with this model. This suggested that the model was a good fit for the data, since it was unlikely that the correlation between the model and the data was due to chance. The R^2 values refer to the percentage of the response data that could have been explained by the terms in the model. It can be seen that for this model, these values were very high.

Figure VIII is a set of four residual graphs that were used to further assess the quality of the model. The most important graph is the normal probability graph, which plots the residuals against their expected values from the model. The residual was the difference between the measured value and the value predicted by the model. Therefore, it was important to check the residual values were reasonably small. In this case they were all <±4°C, which was acceptable considering outlet temperature values varied from 28-97°C. The residuals should be normally distributed, and thus be evenly distributed along the straight line on this graph. Deviation from the line suggested non-normality of the data or outlying points, which would indicate a poorly fitting model. The other residual graphs confirm the fit. The histogram shows the residuals formed a bell-shaped normal distribution, and the fitted value and order graphs confirmed a random pattern of residuals across the data.

Figure VIII Residual plots for outlet temperature (°C). These graphs indicated the acceptable fit of the statistical model, since the residuals (differences between the measured values and the values predicted by the model) were small, fitted a normal distribution and were randomly ordered. The residuals were all <±4°C, which was a relatively small value, given that the measured outlet temperature ranged from 28-97°C. In these diagrams, the range of interest has been focused to magnify the values of the residuals (-4 to +4°C) in order to identify patterns within them. The graphs on the left-hand side indicated that the value of the residuals were evenly distributed, and fitted a normal distribution. The upper diagram on the right-hand side is a plot of the residual values against the corresponding outlet temperature values, as estimated by the statistical model for each experiment. The lower diagram on the right-hand side plots each residual value against where in the order the series of experiments that particular residual was generated. For both of these plots an acceptable model was suggested by the random distribution of residuals, with no clear trends.

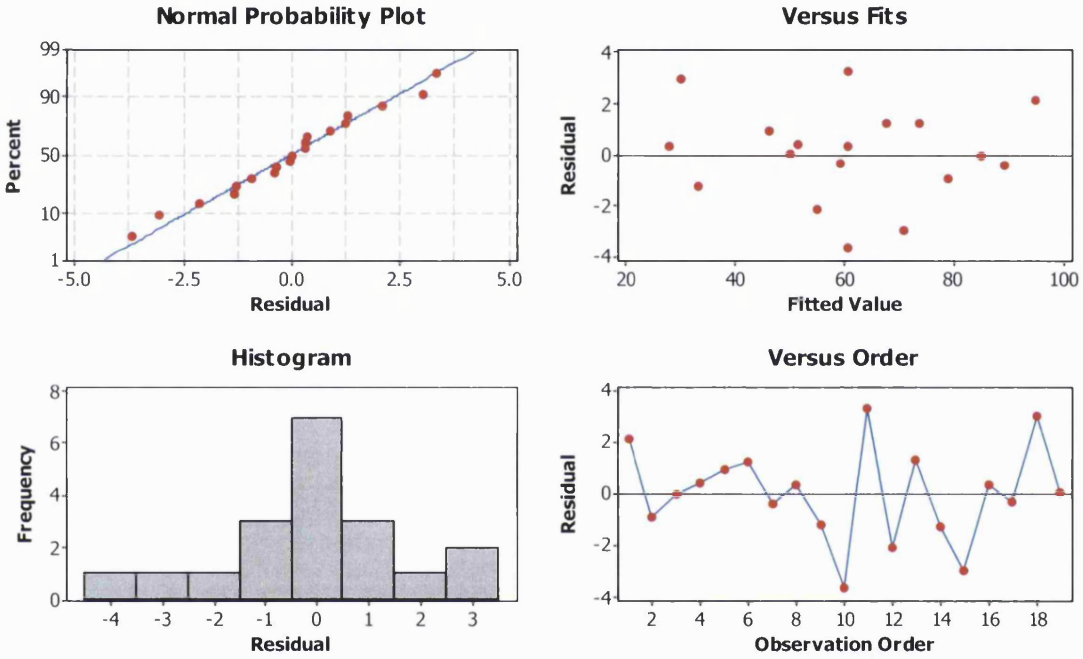

11.6 Appendix VI – Example figures from factorial data analysis

Part A: Example figures from the factorial experiment to optimise the spray-drying parameters (Chapter 4, Section 4.3)

Figure IX Normal probability plot of the 11 standardised effects of spray-drying parameters (included in the model) on product yield. This graph indicates that the spray-drying variables shown in red statistically significantly (ANOVA, $p<0.05$) affected the spray-drying yield of the IgG formulation, with spray-flow (B) having the greatest effect. The statistically significant interactions (e.g. spray flow with aspiration (BC)) are also shown. The other 4 standardised effects had no statistically significant influence on the spray-drying yield.

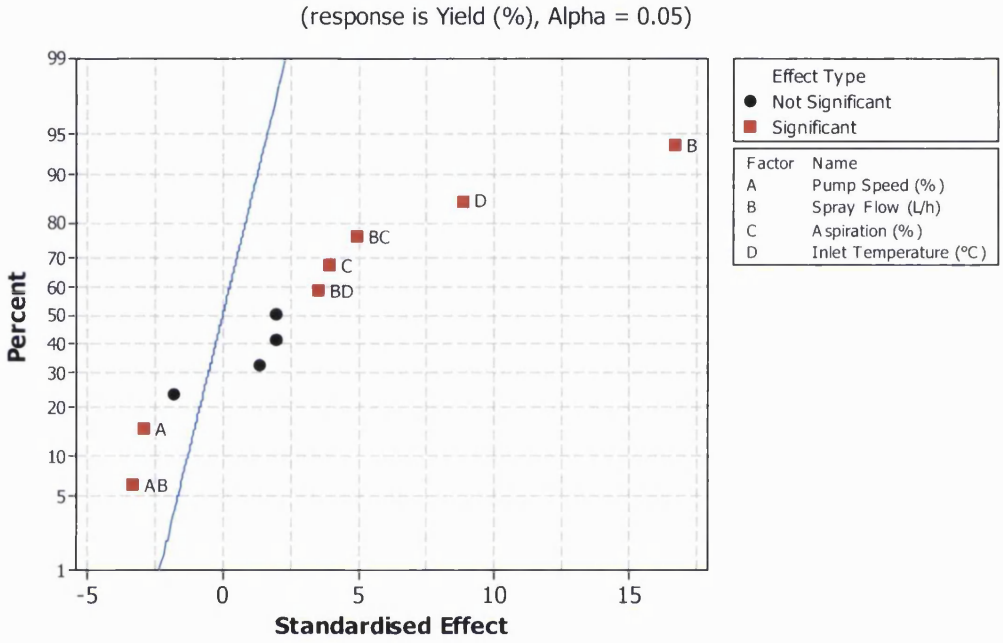

Figure X Normal probability plot of the 12 standardised effects of spray-drying parameters (included in the model) on IgG encapsulation efficiency (EE). This graph indicates that the spray-drying variables shown in red statistically significantly (ANOVA, $p<0.05$) affected the EE of IgG in the formulation, with the interaction of spray-flow and aspiration (BC) having the greatest effect. The other 4 standardised effects had no statistically significant influence on IgG EE.

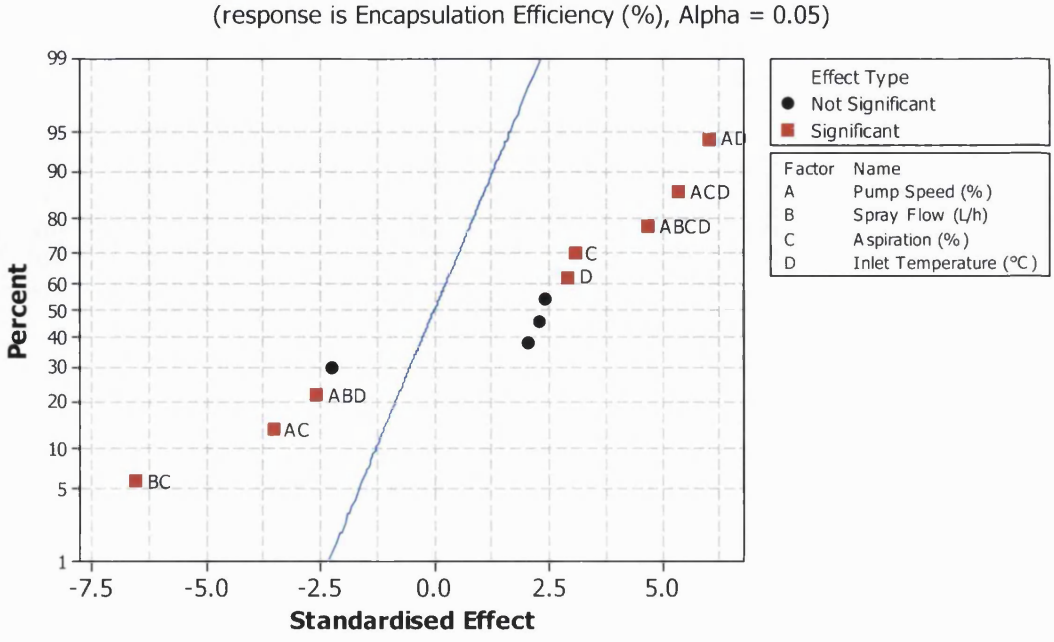

Part B: Example figures from the factorial experiment to investigate the formulation composition (Chapter 4, Section 4.5)

Figure XI Normal probability plot of the 8 standardised effects of excipient quantities (included in the model) on spray-drying yield. This graph indicates that the variables shown in red, statistically significantly (ANOVA, $p<0.05$) affected the spray-drying yield of the IgG formulation, with the quantity of lactose (B) having the greatest effect. The statistically significant interactions (e.g. poly(lactide-co-glycolide) (PLGA) with lactose (AB)) are also shown. The other 2 standardised effects had no statistically significant influence on spray-drying yield.

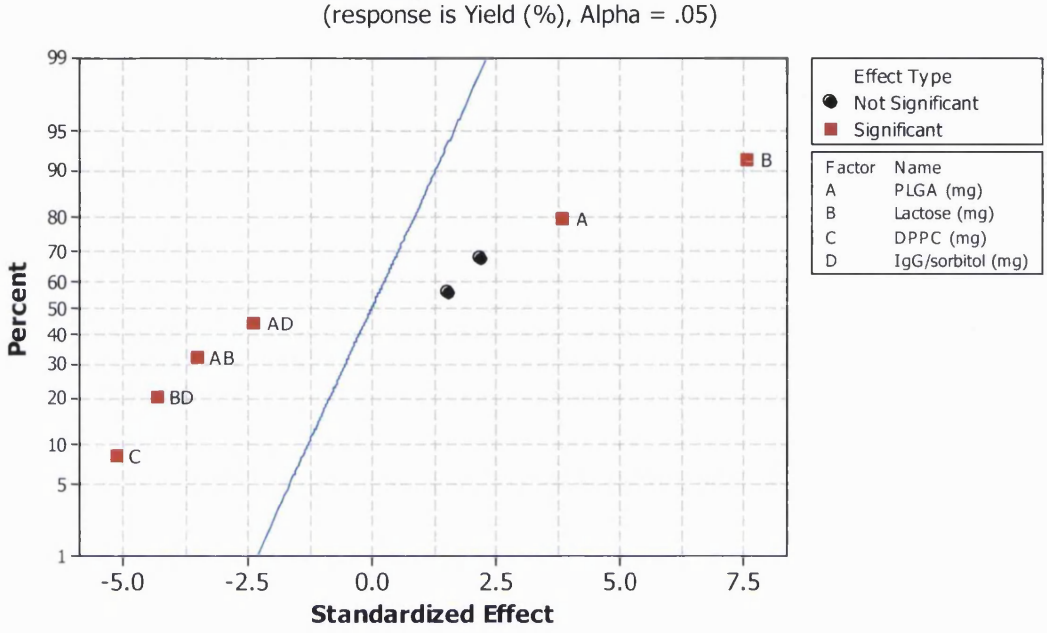

Figure XII Normal probability plot of the 11 standardised effects of excipient quantities (included in the model) on IgG encapsulation efficiency (EE). This graph indicates that the variables shown in red statistically significantly (ANOVA, $p<0.05$) affected the IgG EE of the formulation, with lactose (B) having the greatest effect. The statistically significant interactions (e.g. lactose with IgG (BD)) are also shown. The other 3 standardised effects had no statistically significant influence on IgG EE.

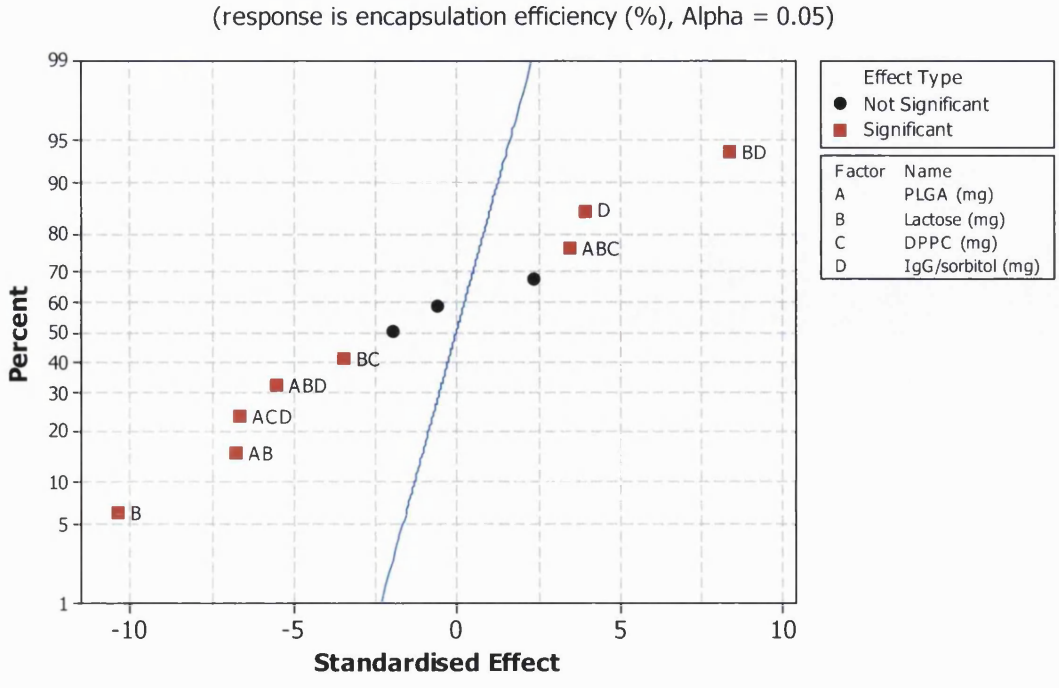

Figure XIII Normal probability plot of the 12 standardised effects of excipient quantities (included in the model) on particle volume median diameter (D50%) in cyclohexane. This graph indicates that the variables shown in red, statistically significantly (ANOVA, $p<0.05$) affected the D50% of the IgG formulation, with the quantity of lactose (B) having the greatest effect. The statistically significant interactions (e.g. poly(lactide-co-glycolide (PLGA) with IgG (AD)) are also shown. The other 2 standardised effects had no statistically significant influence on the particle D50% in cyclohexane.

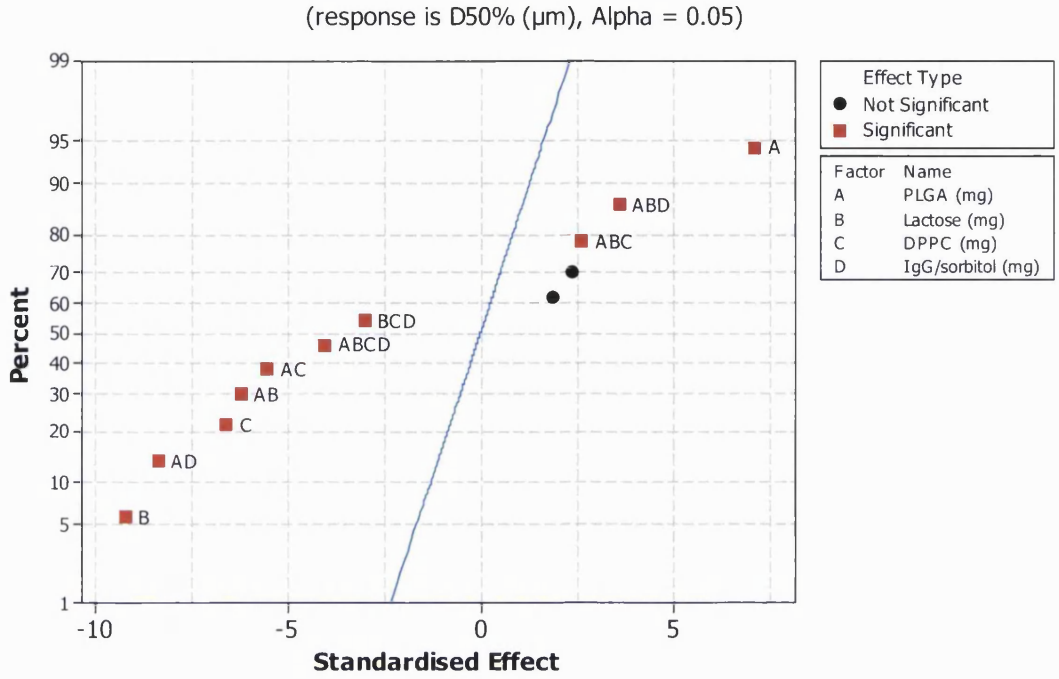

Figure XIV Normal probability plot of the 12 standardised effects of excipient quantities (included in the model) on particle volume median diameter (D50%) in water. This graph indicates that the variables shown in red statistically significantly (ANOVA, $p<0.05$) affected the D50% in water of the IgG formulation, with the quantity of poly(lactide-co-glycolide (PLGA) (A) having the greatest effect. The statistically significant interactions (e.g. PLGA with dipalmitoylphosphatidylcholine (DPPC) (AC)) are also shown. The other 5 standardised effects had no statistically significant influence on the particle D50% in water.

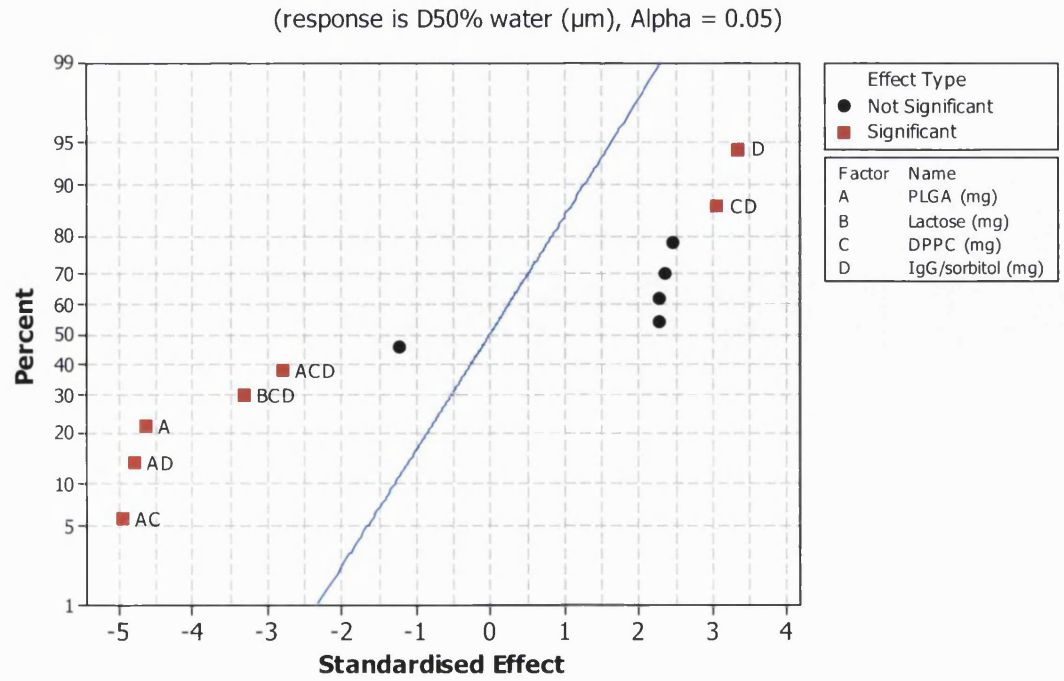

Figure XV Normal probability plot of the 9 standardised effects of excipient quantities (included in the model) on particle morphology. Morphology was measured on a quality rating based on scanning electron micrograph images, where 0 = Individual particles are not clearly defined, 1 = Defined particles, but aggregated, 2 = Non-aggregated, but irregular shape and 3 = Non-aggregated, spherical particles. This graph indicates that the variables shown in red statistically significantly (ANOVA, $p<0.05$) affected the quality of the particle morphology of the IgG formulations, with the quantities of poly(lactide-co-glycolide (PLGA) (A) and DPPC (C) both having the greatest effects. The statistically significant interactions (e.g. PLGA with dipalmitoylphosphatidylcholine (DPPC) (AC)) are also shown. The other 5 standardised effects had no statistically significant influence on particle morphology.

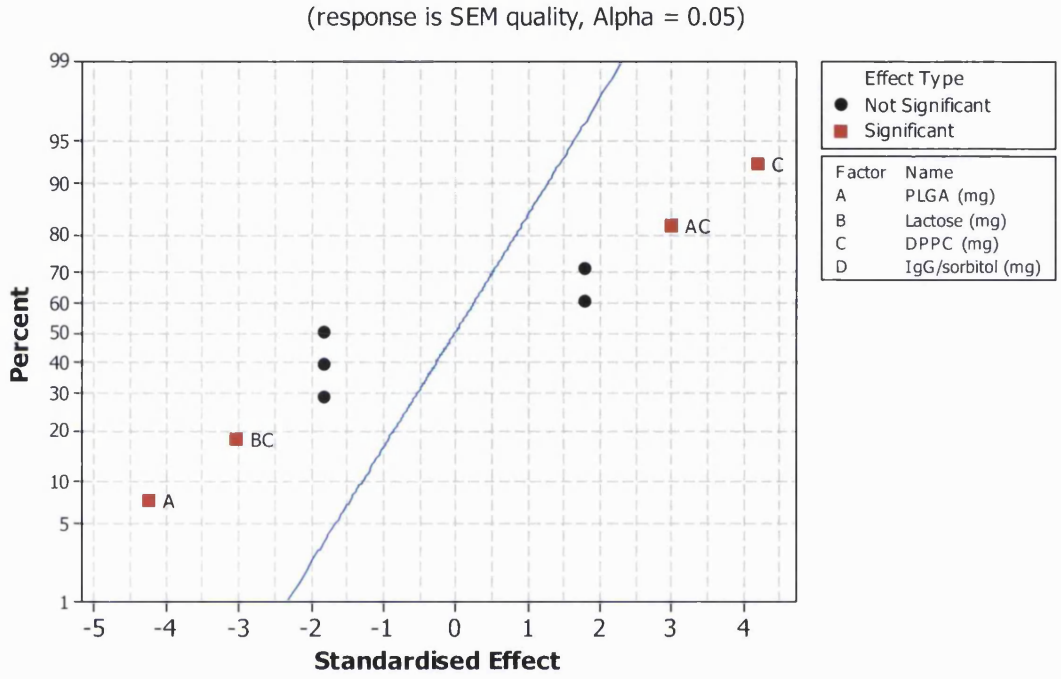

11.7 Appendix VII – Preliminary experiments with the nasal cast

11.7.1 Comparison of metal and nylon cast models

Figure XVI compares the deposition of formulation F1 (see Chapter 8 of this thesis for details) in the metal and nylon nasal cast models. It can be seen from the percentage of protein dose unaccounted for, that there was a lower dose recovery from the metal cast. This attributed to protein adsorption onto the surface of the cast. Therefore, the nylon cast was used for further experiments.

Figure XVI Protein deposition in the metal and nylon nasal cast when formulations were actuated from Uni-Dose DP™ devices. One device was actuated into each nostril per run, with three runs per formulation. Key: D: remaining in device, NV: nasal vestibule, FT: front turbinates, OR: olfactory region, RT: rear turbinates, NP: nasal pharynx, TF: throat filter, U = protein unaccounted for (n=3, mean + SD).

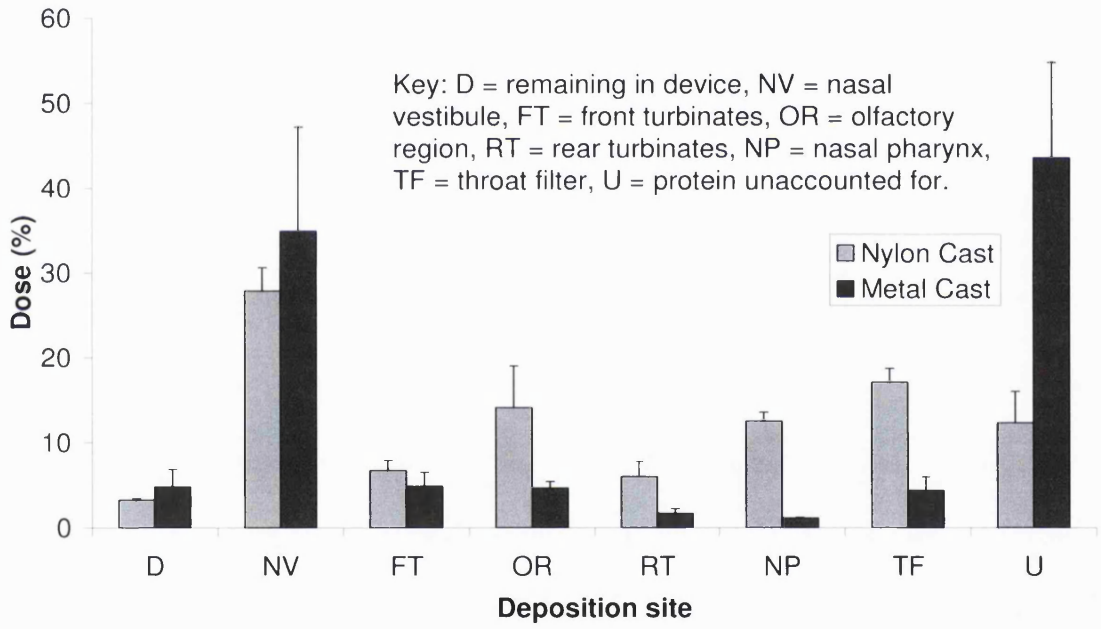

11.7.2 Comparison of nasal cast deposition with and without airflow

Figure XVII compares the deposition of formulation F1 (see Chapter 8 of this thesis for details) in the nylon nasal cast when either no airflow, or 25 L/min inspiratory airflow, was applied to the throat end of the model. Although the Uni-Dose DP™ had its own pressurised bellows to provide the force for powder aerosolisation, the inspiratory airflow appeared to further disperse the powder, since a larger proportion of the protein dose (~55%) was deposited in regions beyond the nasal vestibule (Kaye *et al.*, 2007). It was also likely that the airflow prevented deposited powder falling back out through the nostrils. This airflow can be related to a patient inspiring while actuating the dose. It should also be noted that artificial mucus was not used in these experiments (c.f.

Chapter 8). This resulted in higher deposition in regions beyond the nasal vestibule, since mucus prevented powder particles from 'bouncing' into deeper regions of the nasal cast model.

Figure XVII Nylon nasal cast deposition of formulated IgG when actuated from Uni-Dose DP™ devices, with or without 25 L/min inspiratory airflow. One device was actuated into each nostril per run, with three runs per formulation. Key: D: remaining in device, NV: nasal vestibule, FT: front turbinates, OR: olfactory region, RT: rear turbinates, NP: nasal pharynx, TF: throat filter, U = protein unaccounted for (n=3, mean + SD).